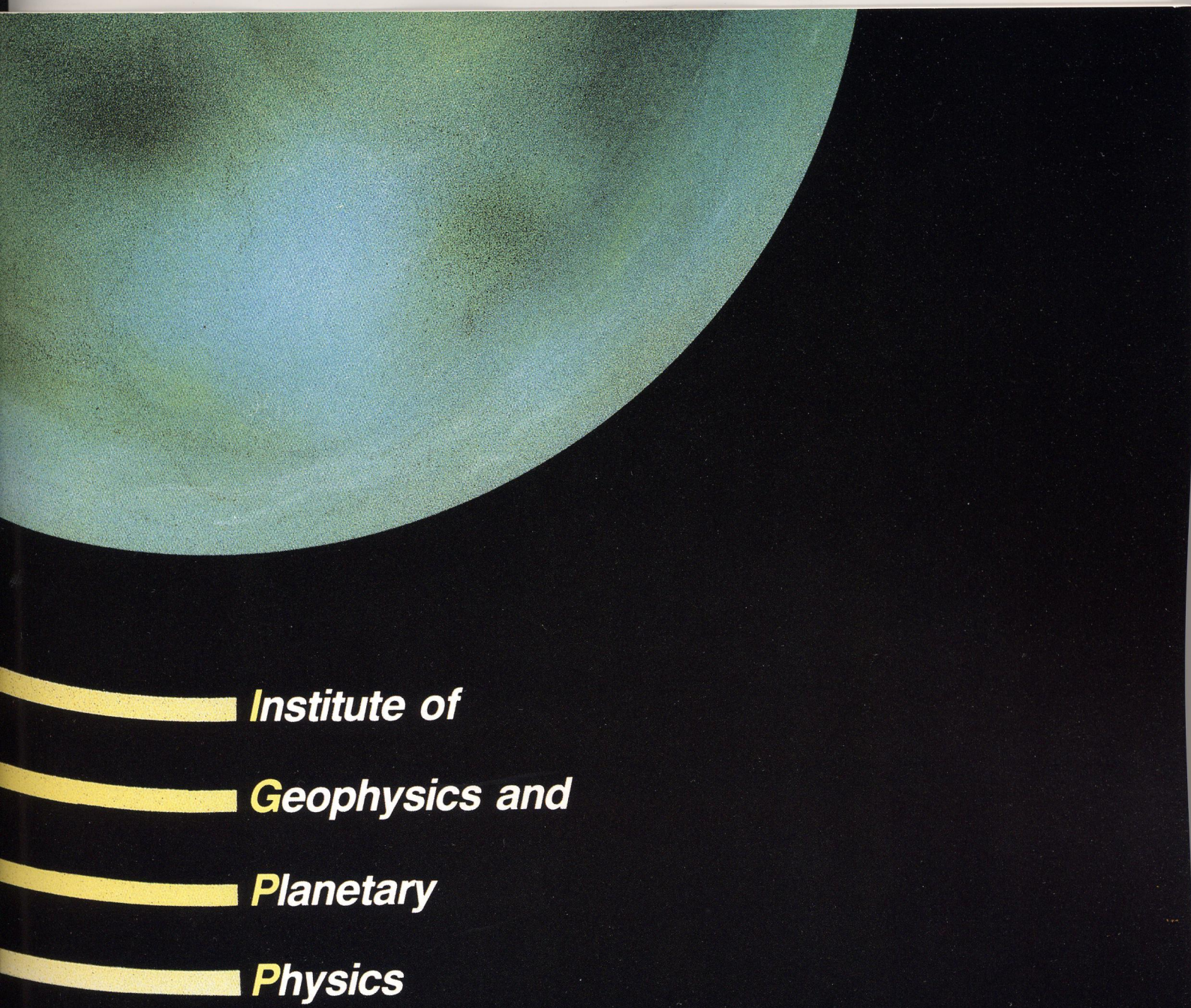

Institute of Geophysics and Planetary Physics

1999 – 2000 Annual Report

Frederick J. Ryerson, Kem H. Cook, and Brooke L. Hitchcock, editors

Manuscript date: January 27, 2003

UCRL-53809 -99/00

Lawrence Livermore National Laboratory University of California

This work was performed under the auspices of the U.S. Department of Energy by the University of California, Lawrence Livermore National Laboratory under Contract No. W-7405-Eng-48..

UCRL-53809-99/00

Geosciences

Section I. Overview

The Institute of Geophysics and Planetary Physics (IGPP) is a Multicampus Research Unit of the University of California (UC). IGPP was founded in 1946 at UC Los Angeles with a charter to further research in the earth and planetary sciences and related fields. The Institute now has branches at UC campuses in Irvine, Los Angeles, San Diego, Santa Cruz and Riverside, and at Los Alamos National Laboratory and Lawrence Livermore National Laboratory.

The University-wide IGPP has played an important role in establishing interdisciplinary research in the earth and planetary sciences. For example, IGPP was instrumental in founding the fields of physical oceanography and space physics, which at the time fell between the cracks of established university departments.

Because of its multicampus orientation, IGPP has sponsored important inter-institutional consortia in the earth and planetary sciences. Each of the seven branches has a somewhat different intellectual emphasis as a result of the interplay between strengths of campus departments and Laboratory programs.

The IGPP branch at Lawrence Livermore National Laboratory (LLNL) was approved by the Regents of the University of California in 1982. IGPP–LLNL emphasizes research in tectonics, geochemistry, and astrophysics. It provides a venue for studying the fundamental aspects of these fields, thereby complementing LLNL programs that pursue applications of these disciplines in national security and energy research.

IGPP–LLNL was directed by Charles Alcock during this period and was originally organized into three centers: Geosciences, stressing seismology; High-Pressure Physics, stressing experiments using the two-stage light-gas gun at LLNL; and Astrophysics, stressing theoretical and computational astrophysics. In 1994, the activities of the Center for High-Pressure Physics were merged with those of the Center for Geosciences.

The Center for Geosciences, headed by Frederick Ryerson, focuses on research in geophysics and geochemistry. The Astrophysics Research Center, headed by Kem Cook, provides a home for theoretical and observational astrophysics and serves as an interface with the Physics Directorate's astrophysics efforts. At the end of the period covered by this report, Alcock left for the University of Pennsylvania. Cook became Acting Director of IGPP, the Physics Direcorate merged with portions of the old Lasers Direcorate to become Physics and Advanced Technologies. Energy Programs and Earth and Environmental Sciences Directorate became Energy and Environment Sciences Directorate.

The IGPP branch at LLNL (as well as the branch at Los Alamos) also facilitates scientific collaborations between researchers at the UC campuses and those at the national laboratories in areas related to earth science, planetary science, and astrophysics. It does this by sponsoring the University Collaborative Research Program (UCRP), which provides funds to UC campus scientists for joint research projects with LLNL. Additional information regarding IGPP-LLNL projects and people may be found at http://www-igpp.llnl.gov/.

The goals of the UCRP are to enrich research opportunities for UC campus scientists by making available to them some of LLNL's unique facilities and expertise, and to broaden the scientific program at LLNL through collaborative or interdisciplinary work with UC campus researchers.

UCRP funds (provided jointly by the Regents of the University of California and by the Director of LLNL) are awarded annually on the basis of brief proposals, which are reviewed by a committee of scientists from UC campuses, LLNL programs, and external universities and research organizations. Typical annual funding for a collaborative research project ranges from $5,000 to

$30,000. Funds are used for a variety of purposes, such as salary support for UC graduate students, postdoctoral fellows; and costs for experimental facilities.

A statistical overview of IGPP–LLNL's UCRP (colloquially known as the mini-grant program) is presented in Figures 1 and 2. Figure 1 shows the distribution of UCRP awards among the UC campuses, by total amount awarded and by number of proposals funded. Figure 2 shows the distribution of awards by center.

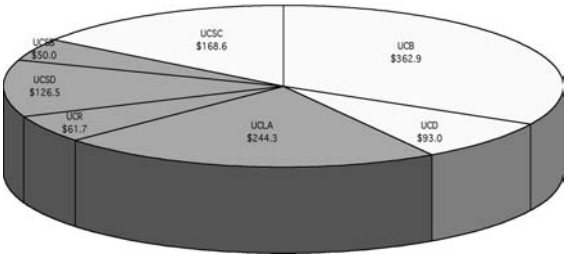

Figure 1a. Distribution of FY 1999-2000 UCRP awards to UC campuses from IGPP–LLNL by total amount awarded.

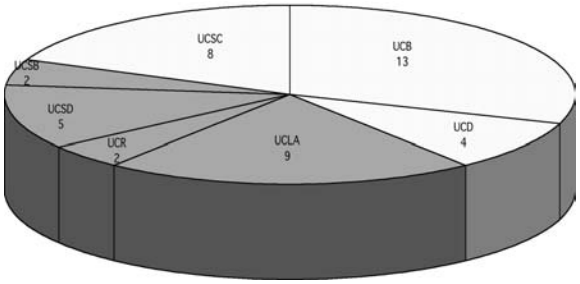

Figure 1b. Distribution of FY 1999-2000 UCRP awards to UC campuses from IGPP–LLNL by number of proposals funded.

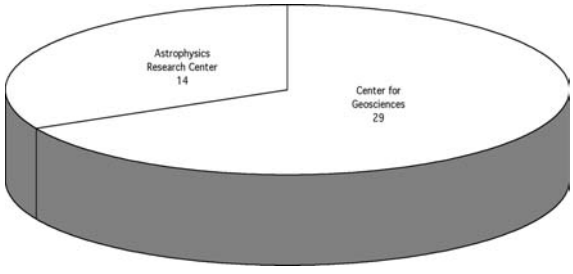

Figure 2. Distribution of awards by IGPP-LLNL center.

Although the permanent LLNL staff assigned to IGPP is relatively small (presently about 8 full-time equivalents), IGPP's research centers have become vital research organizations. This growth has been possible because of IGPP support for a substantial group of resident postdoctoral fellows; because of the 20 or more UCRP projects funded each year; and because IGPP hosts a variety of visitors, guests, and faculty members (from both UC and other institutions).

To focus attention on areas of topical interest in the geosciences and astrophysics, IGPP–LLNL hosts conferences and workshops and also organizes seminars in astrophysics and geosciences. Section IV lists the seminars given in FY 1999-2000.

Since FY 1988, IGPP–LLNL has maintained a bibliography of published research papers resulting from UCRP projects and from research by the IGPP's staff, postdoctoral fellows, and consultants. These lists are published each year in the annual report. Section V gives the bibliography for FY 1999-2000. As a measure of research productivity, the results are gratifying. The abundance of publications from IGPP collaborative projects is a measure of the significance of the results obtained in these projects. The refereed-journal publication rate for IGPP-related projects corresponds to more than 1 paper per year for each faculty member, 2 papers per year for each IGPP postdoctoral fellow, and 2 papers per year for each IGPP staff member.

Figure 3 compares the total papers published in refereed journals or conferences for the last five years. (Note: Because of the extensive peer-review process for most scientific journals, several papers submitted by the principal investigators are still in progress. Therefore, we cannot give an accurate total of 1999-2000 papers published until we receive formal notification from the journals and authors. Final 1999-2000 totals will be available in our 2001 report.)

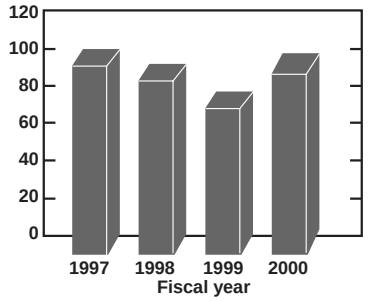

Figure 3. Total number of papers published in refereed journals and conference proceedings from 1994–1998.

Section II. Highlights of Fiscal Years 1999-2000

Astrophysics Research Center

INTRODUCTION

Lawrence Livermore National Laboratory (LLNL) is operated by the University of California (UC) under U.S. Department of Energy Contract No. W-7405-ENG-48. The primary missions of the Laboratory involve national defense and energy problems; in addition, basic research in a number of areas is supported full time. Most research in astrophysics is carried out in two closely affiliated groups-the Institute of Geophysics and Planetary Physics and V-Division within the newly created Physics and Advanced Technologies (PAT) Directorate and, on a part-time basis, by about 22 other scientists who have additional responsibilities in large LLNL programs. There is a growing emphasis on laboratory astrophysics and high energy laser experiments, in particular, of relevance to astrophysics. Since 1983, the LLNL branch of the University of California's Institute of Geophysics and Planetary Physics (IGPP) has acted as the focus of most astrophysics activities at LLNL. Until the end of August 2000 C. Alcock was the Director of the LLNL branch of IGPP, which is organized into two centers led by K. Cook (Astrophysics) and F. Ryerson (Geosciences). The current Acting Director is K. Cook (Acting). The goals of the IGPP branch at LLNL (http://www.llnl.gov/urp/IGPP/) are to make available to UC researchers some of LLNL's unique facilities and expertise, and to provide a forum for seminars, workshops, etc. This year, IGPP awarded small research grants totaling more than $600,000 to UC campus faculty and staff members, enabling 23 collaborative projects.

The senior staff at the Astrophysics Research Center of IGPP consisted of C. Alcock, K. Cook, and W. van Breugel. In addition, B. Macintosh and S. Marshall are staff members and there are several full-time postdoctoral fellows and researchers: S. Blais-Ouellette, A. Drake, W. de Vries, M. Hammergren, M. Lacy, S. Laurent-Muehleisen, J. Patience, and P. Popowski. C. Max (director of the University Relations Program) and S. Gibbard are LLNL staff closely associated with IGPP. IGPP also hosts a large number of faculty and student visitors from the UC campuses. Among these, R. Becker, M. Gregg, A. Stanford, and B. Holden (UC Davis) spend a considerable portion of their time in the IGPP.

The Physics and Advanced Technologies Directorate at LLNL has a strong interest in atomic, molecular, and plasma physics, and considerable theoretical and experimental expertise in these areas. The Astrophysics Group has been established in V-Division of PAT in order to channel LLNL expertise in advanced instrumentation, as well as large-scale computing, into astrophysics applications. The Astrophysics Group, led by K. Cook, is presently developing astronomical instruments for X-ray spectroscopy, gamma-ray spectroscopy and imaging, gamma-ray burst follow-up, multi-object optical spectroscopy and imaging Fourier transform spectroscopy. A significant new program, led by D. Dearborn, to develop a 3-D stellar evolution code running on massively parallel computing systems has been started. The Astrophysics Group is also involved in a variety of astrophysical investigations including astronomical observations, theoretical modeling, and laboratory measurements. V Division astrophysicists were C. Bennett, K. Cook, W. Craig, D. Dearborn, C. Mauche, H.-S. Park, E. Wishnow, and R. Wurtz.

RESEARCH

MACHO Microlensing Survey

The Massive Compact Halo Objects (MACHO)Project is an experimental search for

the dark matter, which makes up at least 90% of the mass of our Galaxy. It was initiated at LLNL and involves C. Alcock, K. Cook, A. Drake, S. Marshall, C. Nelson, and P. Popowski (LLNL); R. Allsman, T. Axelrod, K. Freeman, and B. Peterson (Mt. Stromlo Obs., Australia); A. Becker, C. Stubbs, and A. Tomaney (CfPA at U/Washington); K. Griest and T. Vandehei (CfPA at UC San Diego); D. Alves (STScI); D. Bennett (Notre Dame); M. Geha (UC Santa Cruz); M. Lehner (U/Sheffield); D. Minniti (P. Universidad Catolica, Chile); P. Quinn (European Southern Obs., Germany); W. Sutherland (Oxford University); and D. Welch (McMaster University).

The Milky Way's dark matter is thought to be distributed in a large, spherical halo. Its constitution is unknown, because it emits no detectable radiation. Most hypotheses for its constitution before the Project involved speculations from particle physics. This experiment searches for planets, brown dwarfs, and black holes or any other massive objects (MACHOs) having a mass range of $10^{-7} M_{Sun} < M < 30 M_{Sun}$.

If the dark matter consists of MACHOs, it will occasionally magnify light from extragalactic stars by the gravitational lensing effect. An event can be recognized by fitting a theoretical light curve to the observations (a four-parameter fit) and by its lack of color variation (achromaticity). Unambiguous recognition of microlensing requires an adequate number of data points on the light curve and measurements in at least two filter bands. To detect events, one must monitor millions of stars for several years because the probability of a microlensing event is very low. The experiment operated for eight years and collected last data in December 1999.

The MACHO Project used the 130-cm reflecting telescope of the Mt. Stromlo Observatory, near Canberra, Australia. Operating at prime focus with an innovative optical system gave a field of view 1 deg in diameter. MACHO used a dichroic filter for simultaneous imaging in a blue and a red spectral band, doubling the effective exposure rate.

The MACHO Project has been monitoring fields in two satellite galaxies of the Milky Way, the Large and Small Magellanic Clouds (LMC; SMC), as well as fields toward the center of the Milky Way. The Project has accumulated almost 8 TBytes of image data and about 600 Gbytes of photometry on about 70 million stars. Data were reduced in near real time, and microlensing events were often identified well before their peak.

The Project sent out alert announcements to the world, which were also posted on its web site http://darkstar.astro.washington.edu/. These alert announcements were used by different groups throughout the world to search for planets and to study ongoing microlensing events in detail.

Ongoing microlensing has also been used to study the source star in greater detail than possible without the magnification. Members of the Project have obtained high S/N Keck echelle spectra of main sequence stars in the bulge of the Milky Way for detailed abundance calculations, getting scheduled time during the bulge season knowing that there would be ongoing microlensing events with main sequence source stars (Minniti et al. 1998, ApJ, 499, L175).

The MACHO project released a few milestone analyses last year. They reported on the search for microlensing towards the LMC (Alcock et al. 2000, ApJ, 542, 281). Analysis of 5.7 years of photometry on 11.9 million stars in the LMC reveals 13 - 17 microlensing events depending upon the selection criteria. A detailed treatment of the detection efficiency shows that this is significantly more than the ~ 2 to 4 events expected from lensing by known stellar populations. They estimate the microlensing optical depth towards the LMC to be $\tau_{LMC} = 1.2 \pm 0.35 \times 10^{-7}$, with an additional 20% to 30% of systematic error. The optical depth is essentially the instantaneous probability that a star in the LMC is being lensed. The spatial distribution of events is mildly inconsistent with LMC/LMC disk self-lensing, but is consistent with an extended lens distribution such as a Milky Way or LMC halo. Interpreted in the context of a Galactic dark matter halo, consisting partially of compact objects, a maximum likelihood analysis

gives a MACHO halo fraction of 20% for a typical halo model with a 95% confidence interval of 8% to 50%. A 100% MACHO halo is ruled out at the 95% C.L. for all except the most extreme halo model. Interpreted as a Galactic halo population, the most likely MACHO mass is between $0.15M_{\rm Sun}$ and $0.9M_{\rm Sun}$, depending on the halo model, and the total mass in MACHOs in the halo out to the distance of the LMC is found to be $9 \pm 3.5 \times 10^{10} M_{\rm Sun}$, independent of the halo model. These results are marginally consistent with the previous MACHO results (Alcock et al. 1997, ApJ, 486, 697), but are lower by about a factor of two. This is mostly due to Poisson noise because with 3.4 times more exposure and increased sensitivity to long timescale events, the Project did not find the expected factor of ~4 more events. Besides a larger data set, this work also includes an improved efficiency determination, improved likelihood analysis, and more thorough testing of systematic errors, especially with respect to the treatment of potential backgrounds to microlensing. One important source of background are supernovae (SNe) in galaxies behind the LMC.

On another front, the MACHO Collaboration made substantial progress toward analyzing a few hundred events toward the Galactic bulge. Previous analyses by three, different teams indicated a very high microlensing optical depth, which was inconsistent with other measurements and Galactic models.

MACHO presented the microlensing optical depth towards the Galactic bulge based on the detection of 99 events found in their Difference Image Analysis (DIA) survey (Alcock et al. 2000, ApJ, 541, 734). This analysis encompasses three years of data, covering ~ 17 million stars in ~ 4 deg^2. The DIA technique improves the quality of photometry in crowded fields, and allows the MACHO Collaboration to detect more microlensing events with faint source stars. They find this method increases the number of detected events by 85% compared with the standard analysis technique. The total microlensing optical depth is estimated to be $\tau_{\rm total} = 2.43 \pm 0.385 \times 10^{-6}$ averaged over 8 fields centered at $(l, b) = (2.^\circ 68 - 3.^\circ 35)$. For the bulge component they find $\tau_{\rm bulge} = 3.23 \pm 0.51 \times 10^{-6}$ assuming a 25% stellar contribution from disk sources. These optical depths are in good agreement with the past determinations of the MACHO (Alcock et al. 1997) and OGLE (Udalski et al. 1994) groups, and are higher than predicted by contemporary Galactic models. The Project shows that the observed event timescale distribution is consistent with the distribution expected from normal mass stars, if one adopts the stellar mass function of Scalo (1986) as the lens mass function. However, they note that other mass functions are not excluded by this analysis.

The first results from a new, expanded analysis of the MACHO bulge microlensing events with clump giants as sources were reported by Popowski et al. (2000; astro-ph/0005466). This class of events allows one to obtain robust conclusions because relatively bright clump stars are not strongly affected by blending effects. MACHO gives the preliminary average optical depth of $\tau_{\rm bulge} = (2.0 \pm 0.4) \times 10^{-6}$ at $(l, b) = (3.^\circ 9 - 3.^\circ 8)$ which is somewhat lower than the previously derived values, and so in lesser conflict with other observational and theoretical constraints. The analyses of the spatial distribution of the bulge optical depth and the mass function of the lenses are underway. Using a standard frequency detection algorithm MACHO analyzed over 1300 variables classified provisionally as first-overtone RR Lyrae pulsators in the MACHO variable-star database of the LMC (Alcock et al. 2000, ApJ, 542, 257). They find that 70% of the total population is monoperiodic. Several types of RR Lyrae pulsational behavior are clearly identified for the first time from this sample. This study increased the number of known double-mode stars in the LMC to 181. The Project also discovered two additional types of multifrequency pulsators with low occurrence rates of 2% for each. In one of these types, the frequency components are closely spaced and symmetric relative to the central component. None of the current theoretical models are able to explain the observed close frequency components

without invoking non-radial pulsation components in these stars.

In a related work, MACHO has detected 90 objects with periods and light-curve structures similar to those of field δ-Scuti stars (Alcock et al. 2000, ApJ, 536, 798). The majority of these objects lie in or near the Galactic bulge. One of these objects may be an evolved non-radial pulsator. The amplitude distribution of these sources lies between those of low- and high-amplitude δ-Scuti stars, which suggests that they may be an intermediate population. The majority of these objects are evolved stars pulsating in fundamental or first overtone radial modes.

P. Popowski & C. Alcock (LLNL) investigated a problem of correcting parameters of events based on the "entropy" of a microlensing ensemble. They show how the fact that a group is more than just a collection of individuals reveals itself in the case of microlensing. They derive formulae for correcting the distribution of the dimensionless impact parameters of events, $u_{\rm min}$. They refer to the case when undetected biases in the $u_{\rm min}$-distribution can be alleviated by multiplication by a common constant factor, and in this case the general maximum likelihood problem of solving an infinite number of equations reduces to two constraints, and they find an analytic solution. Under the above assumptions, this solution represents a state in which the "entropy" of a microlensing ensemble is at its maximum, that is, the distribution of $u_{\rm min}$ resembles a specific box-like distribution to the highest possible extent. This technique, however, does not allow one to correct the parameters of individual events on the event by event basis independently from each other.

An important yardstick for measuring the size of the universe is the distance to the Large Magellanic Cloud. Continuing his work on the distance scale, P. Popowski (LLNL) explored the consequences of making the RR Lyrae and clump giant distance scales consistent in the solar neighborhood, Galactic bulge and LMC. He employed two major assumptions: 1) that the absolute magnitude - metallicity, $M_{\rm V}(RR)$ - [Fe/H], relation for RR Lyrae stars is universal, and 2) that absolute *I*-magnitudes of clump giants in Baade's Window are known (e.g., can be inferred from the local Hipparcos-based calibration or theoretical modeling). A comparison between the solar neighborhood and Baade's Window sets $M_{\rm V}(RR)$ at [Fe/H] = -1.6 in the range (0.59 ± 0.05,0.70 ± 0.05), somewhat brighter than the statistical parallax solution. More luminous RR Lyrae stars imply younger ages of globular cluster, which would be in better agreement with the conclusions from the currently favored stellar evolution and cosmological models. A comparison between Baade's Window and the LMC sets a limited range for the absolute brightness of clump giants in the LMC, which, in turn, sets a limited range of possible LMC distances. Popowski finds this distance to be in the range of 44 kpc - 49 kpc (152,000 light years). This range does *not* depend on the adopted value of the dereddened LMC clump magnitude. Popowski argues that the currently available information is insufficient to select the correct distance scale with high confidence.

C. Nelson, K. Cook, P. Popowski (LLNL), and D. Alves (STScI) presented UBV photometry of the eclipsing binary Harvard Variable 2274 in the LMC (Nelson et al 2000). The stellar parameters of this binary system were recently calculated by Guinan et al. (1989), who gave both a reddening toward HV 2274 of $E(B-V)=0.083 \pm 0.006$ and a distance to the LMC of 48 kpc . The reddening of this system was also determined by Udalski et al. (1998), who found $E(B-V)=.0149 \pm 0.015$. With Udalski et al. (1998) B and V photometry, Guinan et al. (1998) obtained $E(B-V)=0.12 \pm 0.009$ and a distance of 46 kpc. Using their UBV photometry, Nelson and collaborators derive a reddening of $E(B-V)=0.088 \pm 0.023$, consistent with the original value of Guinan et al. and supporting the slightly larger distance to the LMC of 48 kpc. Nelson et al. stress the uncertainties inherent in ground-based UBV photometry and the concomitant uncertainties in determining distances based upon such photometry.

Kuiper Belt Objects

C. Alcock, K. Cook, S. Marshall, and R. Porrata (LLNL) in collaboration with I. de Pater, C. Liang, and J. Rice (UC Berkeley), J. Lissauer (NASA/Ames), T. Axelrod (MSSSO, Australia), S. King, T. Lee, A. Wang and C.-Y. Wen (Academia Sinica, Taiwan), W.-P. Chen, and W.-S. Tsay (National Central U., Taiwan), and Y.-I. Byun (Yonsei University, Korea) are working on the Taiwan-American Occultation Survey (TAOS). TAOS will perform a census of small objects (>2 km) in the Kuiper Belt by searching for the brief occultations of stars by these objects. The occultations will be observed with four small telescopes to be located in the Yu Shan National Park in Taiwan. The first TAOS telescope was installed on Lulin peak in March 2000. The remaining telescopes are being integrated with the TAOS cameras and other elements of the control system at LLNL while development of power and network infrastructure continues at Lulin peak. The full four telescope system will be established at Lulin during the first half of 2001.

Asteroids

K. Cook (LLNL), C. Stubbs and A. Diercks (U/Wash.), and T. Bowell and B. Koehn (Lowell Obs., Arizona) have completed an innovative 2048 by 4096 pixel scanning CCD camera, which operates at prime focus on an 18-in. Schmidt telescope on Anderson Mesa in Arizona. This system is the heart of the Lowell Observatory Near-Earth Object Survey (LONEOS), and allows about 1000 square degrees per night to be triple-scanned to detect near-Earth objects through their rapid apparent motion. The LONEOS system began taking data with the newly refurbished Schmidt telescope in 1997. It was decided, however, that the corrector and field flattener that were being used needed to be refabricated. These elements was reinstalled during the winter of 1998, and the system has been operational since that time. It discovered its first NEO 1998 MQ in June, 1998. The survey has discovered a total of 17 new Near Earth Objects and 6 new comets.

M. Hammergren (LLNL) reported the results of an extensive spectroscopic survey of near-Earth objects, in a talk given at the 1999 Asteroids Comets Meteors Conference in Cornell, NY. After removing observational biases and selection effects, it is seen that the near-Earth object population is dominated in both apparent and real numbers by the relatively bright, silicate-rich S-type asteroids, with a substantial minority being the darker, carbon-rich C-types. This distribution of types is very similar to that seen for asteroids in the inner main belt, which on theoretical grounds has long been considered the primary source region for near-Earth objects.

M. Hammergren (LLNL) has examined the shapes and rotation rates of more than 850 asteroids, and concluded that the more elongated objects have a lower maximum limit on spin rates than the more spherical ones. In a presentation at the 1999 American Astronomical Society conference in Chicago, IL, Hammergren showed that such a shape-dependent limit is consistent with most asteroids being “rubble piles”, or essentially strengthless objects bound together by their self-gravity. Hammergren is also investigating the structural properties of “rubble pile” asteroids under the explicit assumption that they are composed of granular, and not fluid, material. Some preliminary models show that the rotational deformation of such objects proceeds catastrophically via landslides or avalanches, and results in shapes which are significantly different from ellipsoidal figures of equilibrium. Furthermore, there exists a maximum rotation rate for elongated objects, beyond which rotational deformation must result in mass shedding. This behavior may help explain the phenomenon of comet nucleus splitting, and the existence of asteroid satellites.

M. Hammergren (LLNL) continued his studies of solar system objects as an external collaborator in the Solar System working group of the Sloan Digital Sky Survey (SDSS). Hammergren has produced a theoretical asteroid taxonomy based on synthetic five-color SDSS photometry, and has shown that early results from SDSS commissioning data demonstrate the potential for pro-

ducing good taxonomic information on tens of thousands of asteroids which will be observed during the course of the survey.

Gamma Ray Bursts

S. Marshall (LLNL) in collaboration with C. Akerlof, R. Kehoe, B. Lee, and T. Mckay (U/Michigan), R. Balsano, J. Bloch, D. Casperson, S. Fletcher, G. Gisler, J. Hills, W. Priedhorsky, J. Szymanski, T. Vestrand and J. Wren (LANL) continued his work on the ROTSE (Robotic Optical Transient Search Experiment) collaboration. ROTSE is an experimental program to search for astrophysical optical transients on time scales of a fraction of a second to a few hours. This is an area of astronomical science that has been relatively unexplored until now. The primary incentive for this research is to find the optical counterparts of gamma-ray bursts (GRBs). These mysterious events are manifested by brief (~10 seconds) intense flashes of gamma-rays with typical photon energies of the order of 1 MeV.

The first phase of this project, ROTSE-I, comprises a 2x2 array of wide field cameras with 200 mm, f/1.8, telephoto lenses on a fast slewing mount. The 16 degree field of view has a limiting visual magnitude of approximately 15 for nominal 5 second images. This system is installed at the Los Alamos National Laboratory at a temporary site east of the LAMPF accelerator. Automated operation began in early 1998. The system operates in an all sky survey mode while it waits for the occasional gamma-ray burst trigger signal. On January 23, 1999 the system detected the first known prompt optical counterpart to a GRB. This burst counterpart, reached 9th magnitude at its observed peak and was detected 7 times over ~10 minutes down to a magnitude of 14.5 (Akerlof et al. 1999). More recently a search for gamma ray burst optical counterparts for six bursts covered by ROTSE-I was published by Akerlof et al. (2000). No optical counterparts were observed, implying that optical and gamma ray emission are not strongly correlated.

3--D Simulations of Stellar Structure and Evolution

D. Dearborn, with G. Bazan, K. Cook, D. Dossa, P. Eggleton, P. Eltgroth, R. Eastman, S. Murray, C. Nelson, I. Otero, B.S. Pudliner and A. Taylor (LLNL) have begun a significant program ("Djehuty") to develop a 3-D stellar evolution code running on massively parallel computing systems. Stars provide the fundamental metric for studying the universe: its size, age and composition. Three dimensional (3-D) phenomena are important in all stars, but to date these effects have been modeled through coarse approximation. LLNL's massively parallel computer systems coupled with the intense ASCI coding efforts has uniquely situated the Lab to improve our physical understanding of stellar properties by providing a quantitative capability to study three dimensional phenomena. Under an Laboratory Directed Research and Development (LDRD) sponsored Strategic Initiative they have commenced a cooperative effort between Defence and Nuclear Technologies (DNT), Physics and Advanced Technologies, and the Center for Applied Scientific Computing (CASC) to begin development of Djehuty as unique tool to study global 3-D processes in stellar structure and evolution. It will operate on massively parallel machines with the best available physical data (opacities, equations of state, etc.) as well as new algorithms tailored specifically for the MPP environment.

In the first year of operation, the recruitment of the core team has been completed, and it has taken the first steps in developing Djehuty. An analytic equation of state, consistent with the best LLNL tabulations, and an elementary gravity routine has been combined with other components to form the basic framework. A small 3-D stellar model (1.6 million zones) was generated and successfully executed a hydrodynamic simulation of this model on the TC2K computer system at LLNL. Additional tests are being made to ensure the accuracy of the simulations, and to develop methodologies for efficiently performing and analyzing 3-D stellar structure calculations. The experience gathered implementing an astrophysical

equation of state facilitates the addition of other physics, including astrophysical opacities and nuclear energy generation. Work has also begun to include diffusive energy transport. When this is complete, the first calculations will be made aimed at studying the long standing problem of convective core overshoot.

In a related effort C. Nelson, P. Eggleton and D. Dossa (LLNL) are investigating the link between the initial and final configurations of binary stars. Using the power of the LC TeraCluster with standard 1-D approximations they have completed a survey that exceeds all the computation ever done on this subject. Analysis of these results will provide insight into the most interesting binary problems for Djehuty. The ability to distort the structure for modeling non-spherical (binary) objects should be included over the next year.

Stellar High Energy Astrophysics

C. Mauche (LLNL) and J. Raymond (CfA) analyzed photometric and spectroscopic observations with the Extreme Ultraviolet Explorer (EUVE), taken over a period of three days in March 1997, of the eclipsing SU UMa-type dwarf nova OY Carinae when it was in superoutburst. Because of the longer time on source, the larger number of eclipses observed, and the higher count rate in the detector, they were able to significantly strengthen previous reports that there is little or no eclipse by the secondary of the EUV emission region of OY Car in superoutburst. The EUVE spectrum extends from 70 to 190 Angstroms and contains broad (FWHM ~ 1 Angstrom) emission lines of N V, O V-VI, Ne V-VII, Mg IV-VI, Fe VI-VIII, and possibly Fe XXIII. Good fits of the observed spectrum were obtained with a model (similar to that of Seyfert 2 galaxies) wherein radiation from the boundary layer and accretion disk is scattered into the line of sight by the system's photoionized accretion disk wind. Because radiation pressure alone falls an order of magnitude short of driving such a wind, it appears that magnetic forces must also play a role in driving the wind of OY Car in superoutburst.

C. Mauche (LLNL), R. Hynes (Univ. of Southampton), C. Haswell, S. Chaty (Open Univ.), C. Shrader (GSFC), and W. Cui (MIT) observed with the Extreme Ultraviolet Explorer (EUVE) the newly discovered X-ray transient XTE J1118+480 during the rising phase of the source's 2000 April outburst. These were the first EUV photometric and spectroscopic observations of an X-ray transient, made possible by XTE J1118's unusual high Galactic latitude and very low absorption line of sight. Together with Rossi X-ray Timing Explorer (2-100 keV), Hubble Space Telescope (1150-10000 Angstrom), United Kingdom Infrared Telescope (JHKL'M'), and radio telescope data, they obtained unprecedented spectral coverage of an X-ray transient. The flat IR-UV continuum appears to be a combination of optically thick accretion disk and possibly synchrotron emission, while at higher energies a typical low hard state power law was seen. EUVE observations reveal no periodic modulation, suggesting an inclination low enough that no obstruction by the disk rim occurs. They concluded that the outburst of XTE J1118 was more akin to the minioutbursts seen in GRO J0422+32 than to a normal X-ray transient outburst.

Normal Galaxies and Galaxy Formation

M. Gregg (UC Davis, and LLNL) and M. West (U. St. Mary's Halifax) reported the discovery of several large low surface brightness structures in the Coma galaxy cluster. The LSB features were found in deep broad band CCD images obtained with the Kitt Peak Burrell Schmidt telescope. The most striking is a plume-like feature about 130 kpc in length and 10-20 kpc long. These objects are interpreted as tidally disrupted galaxies or parts of galaxies which will disperse in a few dynamical timescales, augmenting the intracluster population of stars and gas or augmenting the haloes of the giant ellipticals which dominate the center of the cluster. If this is a typical moment in the history of Coma, such disrupted objects can account for

most of the light in the haloes of the central galaxies.

M. Gregg (UC Davis, and LLNL) and D. Minniti (U. Catolica, Chile, and LLNL), in collaboration with H. Ferguson (STScI), N. Tanvir (IofA, Cambridge), R. Catchpole (RGO), and S. Hughes (IofA, Cambridge) used the Hubble Space Telescope infrared camera (NICMOS) to obtain J and H band images of the halo of NGC3379, the nearest prototypical elliptical. The images clearly resolve individual red giants, permitting the first ever color-magnitude diagram of stars in a completely normal, luminous elliptical galaxy. The results will be used to estimate the metallicity of the halo of NGC3379, providing constraints for modeling the stellar population and chemical evolution of elliptical galaxies. By dividing the imaging into two epochs several months apart, the images have also detected a variable stars which may be indicative of an intermediate age population.

Galaxies and Clusters of Galaxies

S.A. Stanford (UC Davis, and LLNL) has been working on a near-IR mosaic made with HST/NICMOS of the Hubble Deep Field. In collaboration with M. Dickinson (STScI), he has identified a morphologically selected sample of early-type galaxies reaching to faint magnitudes and high redshifts. The color, luminosity, and redshift distributions of this sample has been compared with the predictions of passive luminosity evolution models for standard cosmologies. These models provide poor fits to the properties of the early-type galaxies, indicating that elliptical galaxies in HDF may not have formed monolithically at high redshift. An alternative theory based on hierarchical merging and cold dark matter scenario for structure formation is being investigated with R. Somerville (Cambridge University).

S. Blais-Ouellette (LLNL), C. Carignan (U of Montreal, Canada), P. Amram (LAM, France) and S.Cote (HIA, Canada) have studied the precise kinematics of late type spiral galaxies. They found that rotation curves of the smaller galaxies are rising too slowly when compared to the prediction of cold dark matter simulations. The slope of the inner density profile, χ, is lower than 0.6 for galaxies with maximum rotational velocity below 100 km/s, compared to χ for CDM simulations. They are now completing the study with a larger sample, extended to cover a wide span of morphological types.

S.A. Stanford and graduate student J. Whalen (UC Davis, and LLNL) searched for high redshift galaxy clusters using bent double radio sources selected from the FIRST (Faint Images of the Radio Sky at Twenty Centimeters) survey by R. Becker and M. Gregg (UC Davis, and LLNL). Optical imaging was carried out at the Lick 3 m telescope in two runs and IR imaging at the MDM observatory on Kitt Peak in one run. Combining these data, several moderate redshift cluster candidates have been identified for spectroscopic followup.

S.A. Stanford and B. Holden (UC Davis, and LLNL) obtained deep X-ray images of three high redshift clusters using the Chandra Observatory. These data were analyzed to determine the temperature of the hot gas in two of the clusters and the morphologies of all three. The results were presented by Stanford at a galaxy clusters conference in Paris, and two papers are being prepared. S.A. Stanford and B. Holden also continued a program in collaboration with P. Rosati (ESO) and P. Eisenhardt (JPL) of identifying high redshift cluster from an X-ray survey by obtaining spectroscopy of candidates at the Keck Observatory. These observations found 5 new clusters at redshifts between 0.5 and 1. Based on this sample, a proposal was submitted and approved to obtain deep X-ray data with the Chandra Observatory.

Active Galaxies and Quasars

R. Becker, S. Laurent-Muehleisen, and M. Gregg (UC Davis, and LLNL) in collaboration with R. White (STScI) and D. Helfand (Columbia Univ.) continued to collect and analyze new VLA observations for the FIRST survey imaging the radio sky at 1400 MHz. During the past year

approximately 300 hours of VLA time were awarded to expand the survey area to ~ 8000 sq. degrees. Most of the new area was between 8 and 17 hours Right Ascension and 5 to 20 degrees Declination. This same team, in collaboration with M. Brotherton (NOAO) also completed a bright quasar survey over the initial 3000 square degrees of the FIRST survey. A paper was published presenting spectra of the ~ 600 quasars found in the program by White et al (2000). In a related paper, the radio properties of the 30 broad absorpteion line (BAL) quasars in the sample were discussed (Becker et al 2000).

In 2000, R. Becker (UC Davis) in collaboration with R. White (STScI) and D. Helfand (Columbia) initiated a radio survey of the Galactic plane at 1400 MHz using the VLA. In the first year of the project, the longitude range between 19-32 degrees will be imaged using the B-, C-, and D-configurations of the VLA.

S. Blais-Ouellette (LLNL), M. Reuland (LLNL, Leiden Observatory, UC Davis) and W. van Breugel (LLNL) are investigating the possible presence of giant Ly-α halos around powerful radio galaxies using the Taurus Tunable Filter on the Anglo Australian Telescope (Australia). Preliminary results have shown many Ly-α emitters around MRC 0943-242 at a distance reaching 50 kpc. Using the great versatility of the tunable filter technology, they are now extending observations to a representative sample of powerful radio galaxies.

G. Canalizo (U Hawaii, and LLNL) and A. Stockton (U Hawaii) have estimated ages for the stellar populations of low-redshift quasar host galaxies that have infrared characteristics similar to those of ultraluminous infrared galaxies (ULIRGs). There is a clear connection between interactions, starbursts, and quasar activity in these objects, and their youth suggests that they represent a short-lived transition phase between ultra-luminous infrared galaxies and classical quasars.

C. De Breuck (LLNL graduate student guest, and Leiden Observatory), W. van Breugel (LLNL) and Leiden Observatory colleagues H. Rottgering and G.K. Miley constructed a large sample (669 sources) of very high redshift radio galaxy candidates. The sources were taken from the recently completed Westerbork Northern Sky Survey (WENSS), the Faint Images of the Radio Sky at Twenty cm survey (FIRST), the NRAO Very Large Array (VLA) Sky Survey (NVSS), and other surveys, using Ultra Steep Spectrum (USS) selection. The total sample contains 669 sources with a 20 cm flux density larger than 10 mJy and covers virtually the entire sky outside the Galactic plane. The sample forms the basis for an intensive campaign to obtain a large sample of high redshift ($z > 3$), massive forming galaxies that is selected in a way that does not suffer from dust extinction or any other optical bias. The success of this method was illustrated by the discovery of the most distant radio galaxy known, TN J0924--2201 at $z = 5.19$.

C. De Breuck (LLNL graduate student guest, and Leiden Observatory), W. van Breugel (LLNL) and Leiden Observatory colleagues (H. Rottgering, G.K. Miley and P. Best) compiled a sample of 165 radio galaxies from the literature to study the properties of the extended emission line regions and their interaction with the radio source over a large range of redshift ($0 < z < 5.2$). Using various radio and optical spectroscopic parameters they find several significant correlations. A correlation between redshift and absorption line asymetry is interpreted as an increase in the amount of HI around radio galaxies at $z > 3$. The almost exclusive occurrence of HI absorption in small radio sources could indicate a denser surrounding medium or an unpressurized, low density region. Other correlations provide evidence for a common energy source for the radio power and total emission line luminosity, as also found in flux density-limited ss to examine the ionization mechanism in the radio galaxies it was found that both AGN photo-ionization and shock ionization must be present. The latter is indicated by the CII/CIII ratios, which are closer to high velocity shock model predictions than to the line ratio's expected for pure AGN photoionization. It was found that

shock dominated ionization seems to occur mostly in the smallest radio sources.

W. de Vries (LLNL), P. Barthel (Univ. of Groningen, The Netherlands), and C. O'Dea (STScI) continued their research on galaxy hosts of compact radio sources. Utilizing the high angular resolution of HST, both in the optical (WFPC2, R band, narrow band LRF) and the near-IR (NICMOS, J and K bands), significant inroads to the nature and evolution of these radio sources have already been made. Furthermore, cycle 8 Hubble Space Telescope (HST) observations will be used to study the kinematic and physical properties of the emission line gas interacting with the expanding radio plasma. These data, combined with existing observations, will yield robust constraints on the evolution of powerful radio sources.

M.D. Gregg, in collaboration with R. Becker (UC Davis), M. Brotherton (NOAO), S. Laurent-Muehleisen (UC Davis), M. Lacy (LLNL, and UC Davis), and R. White (STScI) discovered a remarkable quasar, FIRST J101614.3+520916 (Gregg et al. 2000). Its optical spectrum shows unambiguous broad absorption lines (BALs) while its double-lobed radio morphology and luminosity clearly indicate a classic Fanaroff-Riley Type II (FR-II)radio source, a combination once thought never to occur. Its radio luminosity places it at the extreme of the recently established class of radio-loud broad absorption line quasars (Becker et al. 2000). Its hybrid nature may indicate that FIRST J101614.3+520916 is a typical FR-II quasar which has been rejuvenated as a broad absorption line (BAL) quasar. When combined with the evidence presented by Becker et al. (2000) for a sample of 29 BAL quasars, the implication is that, contrary to most “unification by orientation” schemes for understanding quasar properties, no preferred viewing orientation is necessary to observe BAL systems in a quasar's spectrum. This, and the probable young nature of the radio source in FIRST J101614.3+520916, leads naturally to the alternate picture in which the BAL phenomenon is an early evolutionary stage in the lives of quasars.

D. Proctor (LLNL) used pattern recognition techniques to automate selection of bent-double sources from the FIRST survey database. Such sources may then be used as tracers for clusters of galaxies (Blanton, et al., 2000). The task is complicated by the low resolution (in a pattern recognition sense) of the images, chance superposition of sources, the ambiguous nature of visual classifications and considerable variation in bent morphology. Decision tree and artificial neural network methods are compared and show substantially equivalent results. Resulting classifiers provide well-defined samples for future studies.

M. Lacy (LLNL and UC Davis) has begun a program to study the clustering of radio galaxies at moderate redshifts. Radio galaxies, which are found associated almost exclusively in giant elliptical galaxies and typically in poor cluster environments, should make excellent tracers of large-scale structure at high redshift. The pilot stage of this project, involving taking spectra for ~30 radio galaxies at Lick Observatory and the Nordic Optical Telescope has been completed. This has resulted in the first detection of radio galaxy clustering at $z \sim 0.3$.

M. Lacy (LLNL and UC Davis), in collaboration with A. Bunker (IoA, Cambridge, UK) and S. Ridgway (Johns Hopkins University), has completed a near-infrared study of high redshift radio galaxies from the 7C3 sample, a sample significantly fainter in radio flux than most previously-studied samples of powerful radio sources. This allows the redshift-luminosity correlation present in all single flux-limited samples to be broken. Only a weak dependence of radio luminosity on host galaxy mass is found, and hosts of radio galaxies continue to be massive elliptical galaxies out to $z \sim 2$. This is consistent with a supermassive, billion solar mass black hole, and a correspondingly massive host galaxy, being necessary to produce powerful radio jets. Beyond $z \sim 2.5$ there is evidence for evolution in the population, consistent with results from studies at sub--mm wavebands, and detailed morphological studies of high redshift radio galaxies. It is suggested that the hosts of radio galaxies may form early due to the

high baryon densities at the centers of the most massive dark halos in the early Universe.

M. Lacy (LLNL, and UC Davis), in collaboration with M. Wold (Stockholm), P.B. Lilje (Oslo) and S. Serjeant (Imperial College, UK) has continued a program to study the cluster environments of quasars at $0.5 < z < 0.8$. It is found that the environments of radio-quiet and radio-loud quasars are indistinguishable, with both being found in environments ranging from isolated to moderately-rich clusters. The typical environment is an Abell Class 0 cluster. This is consistent with recent HST-based studies of the hosts and environments of luminous quasars at low redshifts, and suggests little evolution in quasar environments has taken place between $z \sim 0.7$ and the present day.

S.A. Stanford (UC Davis, and LLNL) continued a program with van Breugel (LLNL) of studying ultraluminous IR galaxies at high redshifts. The first phase survey results are in press (Stanford et al 2000). The second phase has begun, in collaboration with UC Berkeley graduate student E. Halderson and postdoctoral fellow G. Canalizo (LLNL), in which the expanded sample of FIRST radio sources was matched with the IRAS faint source catalog and then cross correlated with bright star catalogs to identify targets for adaptive optics imaging at Lick and Keck Observatories.

W. van Breugel (LLNL), in collaboration with G. Canalizo (U Hawaii, and LLNL), A. Stockton (U Hawaii), and M. S. Brotherton (NOAO) studied the z = 0.6344 post-starburst quasar UN J1025-0040 using Keck imaging and spectroscopy. Previous observations had shown that the quasar has an extremely bright post starburst population of age ~ 400 Myr. The new Keck data show that the quasar has also a nearby (4.2 arcseconds) companion galaxy at redshift z = 0.6341, with an estimated age of ~ 800 Myr for the dominant stellar population. The companion appears to be interacting with the quasar host galaxy, and this interaction may have triggered both the starburst and the quasar activity in UN J1025-0040.

W. van Breugel (LLNL), in collaboration with colleagues from Leiden Observatory (J.D. Kurk, H.J.A. Rottgering, L. Pentericci, and G.K. Miley), C.L. Carilli (NRAO), H. Ford and T. Heckman (Johns Hopkins University), P. McCarthy (OCIW) and A. Moorwood (ESO) imaged the powerful radio galaxy PKS 1138-262 at z = 2.156 and its surrounding 38 square arcminute field with the ESO Very Large Telescope in a broad band and a narrow band filter encompassing the redshifted Ly-α emission (Kurk et al 2000). Approximately 50 objects were detected with rest equivalent widths larger than 20 Angstrom, as well as a luminous, very extended Ly-α halo around the radio source. If the radio galaxy is at the center of a forming cluster, as observations at other wavelengths suggest, the Ly-α emitting objects are candidate cluster galaxies at the redshift of the radio galaxy. Subsequent spectroscopic observations of these objects (Pentericci et al 2000), also with the VLT, confirmed that 14 galaxies and one QSO are at approximately the same distance as the radio galaxy. All galaxies have redshifts in the range $2.14 < z < 2.18$, centered around the redshift of the radio galaxy, and are within a projected physical distance of 1.5 Mpc from it. The velocity distribution suggests that there are two galaxy subgroups having velocity dispersions of ~ 500 km/s and ~ 300 km/s and a relative velocity of 1800 km/s. If these are virialized structures, the estimated dynamical masses for the subgroups are ~ 9 and ~ 3×10^{13} M_{SUN} respectively, implying a total mass for the structure of more than 10^{14} M_{SUN}. The observations strongly suggest that the structure of galaxies around PKS 1138-262 is a forming cluster.

W. van Breugel (LLNL), in collaboration with M. Kishimoto and R. Antonucci (UC Santa Barbara), A. Cimatti (Arcetri Observatory), T. Hurt (UC Santa Barbara), A. Dey (NOA O) and H. Spinrad (UC Berkeley) used UV spectropolarimetry and far-UV spectroscopy with the Faint Object Spectrograph onboard the Hubble Space Telescope (HST) to search for evidence of hidden quasars and determine the nature of scattering regions in two low-redshift narrow-line radio galaxies (Kishimoto et al 2000). Spectropolarimetry of several Narrow Line Radio Galaxies (NLRGs) has

shown that they have hidden quasars, as inferred from the presence of scattered, polarized broad permitted lines. Imaging polarimetry has shown that NLRGs, including the two observed targets, often have large scattering regions of a few kpc to ~ 10 kpc scale. This poses a problem for understanding the nature of the scatterers in these radio galaxies. From the HST observations, when combined with previous optical/infrared polarimetry data, it was found that the scattering might be caused by opaque dust clouds in the NLRGs, and this would be a part of the reason for the apparently grey scattering. In high-redshift radio galaxies these opaque clouds could be the protogalactic subunits which may be seen in HST images. However, one can not rule out the possibility of electron scattering, which could imply the existence of large gas masses surrounding these radio galaxies.

W. van Breugel (LLNL), in collaboration with D. Stern and P. Eisenhardt (Caltech/IPAC), H. Spinrad and S. Dawson (UC Berkeley), A. Dey (NOAO), W. De Vries (LLNL) and S.A. Stanford (UC Davis, and LLNL) used deep near--IR and optical photometry with the Keck telescopes to show that the claimed z = 6.68 galaxy STIS 123627+621755 (Chen et al 1999, Nature 398, 586) is no longer the most distant galaxy. Instead they find that the object is most likely a low luminosity dwarf galaxy like the Small Magellanic Cloud (M(B) = -17) at a redshift z = 1.51 (Stern et al 2000).

Adaptive Optics: Systems Development

The Adaptive Optics (AO) system on the 10-m W.M. Keck II telescope, jointly constructed by LLNL and the California Association for Research in Astronomy, achieved first light in February 1999 and entered general scientific use in late 1999-early 2000. The Keck AO system routinely achieves resolutions of 0.04 arcsconds in H-band, the highest-resolution infrared imaging system in astronomical use (Wizinowich et al 2000). During 2000, LLNL engineers worked on understanding and improving Keck AO performance, in particular the deep AO point spread function for high-contrast imaging. The LLNL participation in the Keck AO effort is led by S. Olivier and C. Max.

LLNL also continued to refine the laser guide star (LGS) AO system on the 3-m Shane telescope at Lick Observatory. The Lick AO team is led by D. Gavel (LLNL). At 15-20 watts, this is the most powerful operational sodium laser beacon in the world, and has achieved the highest Strehl ratio (0.4) recorded for such a system. Improvements in 2000 focused on usability, improving the robustness of the Lick AO/LGS system to the point where it is an easily-operated facility-grade system, and reducing the manpower requirements for the laser system. In natural guide star (NGS) mode, the system requires a $V<13$ star within 30-40 arcseconds of the object in LGS mode, it only requires a $R<17$ star within 60 arcseconds. Many improvements to the laser were based on similar modifications to the laser delivered for the Keck AO system, which is expected to be tested in 2001.

In November 2000 the Center for Adaptive Optics began operating at UC Santa Cruz under the NSF Science and Technology Program. LLNL is a major participant in this Center, with C. Max (LLNL) serving as the Center's Associate Director for Advanced Adaptive Optics Technology, and S. Olivier (LLNL) leading the Center's project to develop micro-electro-mechanical technology for next-generation AO.

Speckle Imaging of Titan, Io, and Neptune

C. Max, D. Gavel, B. Macintosh, and S. Gibbard (LLNL), working with collaborators from UC Berkeley, NASA Ames, the Southwest Research Institute, and JPL, continued to observe solar system objects at very high spatial resolution using the technique of speckle imaging. Speckle imaging uses a series of very short exposures to “freeze” the turbulence of the Earth's atmosphere, which limits the resolution of most ground-based observations to 0.5 arcseconds. Near-infrared observations were obtained at the 10-meter W. M. Keck Telescope of Saturn's moon Titan, Jupiter's

volcanically-active moon Io, and Neptune. The speckle imaging technique allowed to obtain spatial resolution near the diffraction-limit of the telescope, 0.04 arcseconds at a wavelength of 2 microns.

Titan, Saturn's largest moon, is unique among planetary satellites in possessing a thick atmosphere. Seen in visible light, Titan is shrouded in a featureless, orange haze. This haze is believed to be composed of organic compounds produced by the photolysis of methane. Models suggest that this haze gradually settles to Titan's surface, and over long periods of time, could form oceans, lakes, or underground reservoirs of liquid. Excellent images of Titan's leading (brighter) hemisphere and the darker trailing hemisphere were obtained. The data were taken through the K' and H filters, which include both a strong methane absorption band, which provides data on Titan's atmospheric structure, and a window in the band through which we can see surface features on Titan. This technique allows one to obtain interesting information both about the surface and about previously unknown characteristics of Titan's atmosphere.

These data clearly show a continent-sized bright surface feature on Titan's leading hemisphere, which is consistent with icy or rocky highlands, as well as a very low albedo region that is consistent with the presence of liquid hydrocarbons on the surface. Titan's darker hemisphere has a very low albedo ($< < 0.05$) overall, with some brighter areas. If Titan's dark areas are liquid hydrocarbons, this would be the first detection of surface liquids on a solar system body other than the Earth.

Io, the innermost large moon of Jupiter, experiences tidal stresses and enough internal heating to create volcanoes on its surface. By observing Io in the infrared while the Sun is eclipsed by Jupiter, emission from individual volcanoes can be imaged or even resolved. These data may be used to determine the time variations, size, spacing, and number of volcanoes, which in turn yields information about the nature of these volcanoes, particularly the high-temperature events thought to be silicate volcanism. Seventeen individual volcanic features on Io's surface were resolved in observations during an eclipse in July 1998. The Keck observations of Io represent the highest resolution infrared measurements available to date.

Neptune is a very dynamically active planet of which little is known because of its small angular extent (2.5 arcseconds). Voyager 2 detected prominent dark and bright spots at visible wavelengths, as well as some bright wispy cloud features. These features change on timescales varying from hours to years. The goals in observing Neptune are to determine the altitude and composition of the material that makes up the infrared-bright features on the disk of Neptune; to determine the timescales over which these features evolve; to look for oscillations in spot size or shape; and, ultimately, to determine the contribution of these storms to Neptune's overall heat budget.

Neptune was observed in speckle mode at H band, and in conventional mode using infrared narrow bands. The latter probe different heights in Neptune's stratosphere. Using a model adapted from a Neptune radiative transfer code developed by K. Baines (JPL), it was possible to constrain the number density of Neptune's stratospheric haze layers and to verify that the infrared-bright storm features are, indeed, located in Neptune's stratosphere rather than lower down in the troposphere.

Solar System: AO Imaging

C. Max, B. Macintosh, S. Gibbard and D. Gavel (LLNL), along with UC Berkeley collaborators I. de Pater, H. Roe, and S. Martin (UC Berkeley), have been observing solar system objects at very high spatial resolution using the Keck AO system. During 2000 they observed and analyzed data from near-infrared observations of Saturn's largest moon Titan and the gas giant planets Uranus and Neptune.

Observations of Titan on 30 October 1999 showed a bright cloud band at 70 degrees latitude in two narrowband filters which probe the atmo-

sphere above the tropopause. The feature was spatially unresolved in latitude and extended over all visible longitudes. Furthermore a broad haze band was seen, extending over approximately 60 degrees of latitude centered slightly south of Titan's equator. The AO system achieved a spatial resolution at 1.158 microns of 0.032 arcseconds, or 190 km on Titan. Mid-infrared Long Wavelength Spectrometer (LWS) images from September and November 1999 with a resolution of 0.25 arcseconds clearly show east-west and north-south structure across the disk of Titan; the emission is probably thermal, from high-altitude haze layers.

The LLNL / UC Berkeley group also observed Neptune several times during the year, a project which culminated in June 2000 with a large coordinated effort (along with A. Ghez (UCLA) and M. Brown (Caltech) to track infrared-bright features over a 20-day period. The images are spectacular, revealing narrow zonal bands at 3-4 degree latitude spacings within bright regions and near the equator. There are three zones of latitude which contain bright features along zonal bands. The dimmest zone is located in the Northern hemisphere and extends from 20 degrees N to 40 degrees N. There are two bright zones located in the Southern hemisphere which extend from 20 degrees S to 50 degrees S, and from 60 degrees S to 70 degrees S. The zone near the South pole, a recently quiet region, contains a bright tear drop shaped feature which may be related to the Westerly jet previously observed by Voyager at a similar latitude.

The planet Uranus was observed with the recently commissioned AO/NIRSPEC system (Adaptive Optics system with the Near-Infrared echelle Spectrograph) on June 17 and 18, 2000. With this system images and spectra can be taken simultaneously. Excellent images were obtained of Uranus' ring system. Inside of the Epsilon ring at least three more, slightly resolved, rings are visible: from the outside inwards these are: 1) combined Delta, Gamma, Eta rings, 2) combined Beta, Alpha rings, and 3) combined 4,5,6 rings. On the planet itself at least eight different cloud features can be detected, five of which are in the Northern hemisphere (the hemisphere which just came into sunlight after being in complete darkness for ~40 years). Two features could be tracked over a 40-60 degree longitude range, and yield wind velocities of 175 +- 35 m/s at a latitude of 30 degrees, and of 120 +- 40 m/s at 40 degrees latitude. The data suggest that the wind profile is similar to that derived for Neptune, though at reduced velocities.

Extrasolar Planets

With the Keck AO system operational, it now becomes possible to directly detect infrared emission from young extrasolar planets. Keck AO is capable of detecting objects at contrast ratios of 10^6, sufficient to see a 1 Jupiter-mass planet in a 50 AU orbit around a star in the TW Hydra association. B. Macintosh (LLNL), B. Zuckerman and E. Becklin (UCLA) are beginning a large-scale search for such young planetary companions to field stars, with UCLA identifying new populations of young stars while LLNL works on improved techniques for high-contrast imaging. Adaptive Optics is currently the only technique that can detect planets in 20-100 AU orbits.

Active Galaxies and Starburst Systems

W. de Vries, W. van Breugel (LLNL), and A. Quirrenbach (UCSD), have begun a Keck AO imaging program of powerful radio galaxies and Ultraluminous Infrared Galaxies (ULIRGs). Observations of two radio galaxies and a ULIRG during a June 2000 NIRSPEC-AO run at the Keck telescope have provided unprecedented morphological resolution of components like nuclear dust-lanes, off-centered or binary nuclei, and merger induced starforming structures. All of these are key features in understanding galaxy formation and the onset of powerful radio emission. Furthermore, since the near-IR resolution of the AO images matches, or even surpasses, the optical resolution of HST, high resolution multi-wavelength images can be constructed by combining the AO and HST datasets. These maps provide an even better understanding of off-nuclear star for-

mation and obscuration properties of these merger induced structures. NIRSPEC-AO spectroscopic follow-up has been proposed to start a high resolution analysis project of these features in particular. AO can provide the high spectroscopic and spatial resolution essential to this program, which will contribute significantly to our understanding of black hole mass distribution among radio galaxies, galaxy mergers, and the triggering of powerful radio emission.

Instrumentation

W. van Breugel (LLNL) and J. Bland-Hawthorn (AAO) co-edited the proceedings of a major international conference on `Imaging the Universe in Three Dimensions: Astrophysics with Advanced Multi-Wavelength Imaging Devices'. This conference was held under the auspices of LLNL, in Walnut Creek, California, from March 29 - April 1, 1999. The purpose was to bring together instrumentation experts and observers to discuss the new opportunities afforded by the new class of advanced multi-wavelength imaging instruments that are currently being designed for major ground- and space-based observatories. The proceedings have been published in the Astronomical Society of the Pacific Conference Series Nr. 195. There were 18 invited review talks, covering scientific opportunities and instrumental challenges, 23 talks highlighting some of the first results obtained with 3-D instruments, 19 contributed talks, and 43 poster. The main topics covered by the science talks were related to galaxy formation and large scale structure, obscured galaxies, starbursts and AGN, outflows from stars, starbursts and active galaxies, and the evolution and environments of quasars. Nearly 90 papers are included in the proceedings, with more than 600 pages. The volume serves as an important reference work on advanced multi-wavelength imaging.

Center for Geosciences

The Geosciences Research Center was formed to promote collaborative research in the geosciences among LLNL, the various UC campuses, and other scientific organizations both within the U.S. and abroad. LLNL's mission-oriented programs in national security and in environmental and energy research employ many disciplines within the geosciences. IGPP draws upon these capabilities and expertise and acts as a focal point for research in the more fundamental aspects of the earth sciences. We hope to consolidate many unique talents and capabilities at LLNL and to provide an easily identifiable avenue for LLNL-UC collaborations. The Center for Geosciences is the focus of these interactions with visitors from academic (UC and other universities), industrial, and governmental research institutions. The Center's research emphasis is on the physics and geochemistry of the solid Earth, including seismology, geochemistry, experimental petrology, mineral physics, environmental geochemistry, hydrology, tectonics, and active tectonics. The Center is housed in the Geophysics and Global Security and Geosciences & Environmental Technologies divisions of LLNL's Energy and Environments Directorate (EED). It is involved with several programs within EED and also with the Analytical and Nuclear Chemistry Division of LLNL's Chemistry and Materials Science Directorate, which is a major contributor in the area of geochemical expertise and analytical facilities. The Center also has active collaborations with the staff of LLNL's Center for Accelerator Mass Spectrometry (CAMS).

The scientific staff of the Center include Rick Ryerson (Center Head), Henry Shaw, Marc Caffee, Bob Finkel, Ian Hutcheon, Dan Farber and Douglas Phinney. Postdoctoral fellows during FY99/FY00 included Adam Kent (Australian National University), Keith Putirka (Lamont-Doherty Geologic Observatory), Jerome Van der Woerd (Institut de Physique du Globe de Paris) and Lucilla Benedetti (Institut de Physique du Globe de Paris). Putirka is working on developing and applying methods of phase equilibria to constrain the relative effects of melting conditions and mantle composition on the chemical diversity of basaltic lavas. Van der Woerd is working on the tectonics of Northern Tibet using satellite image interpretation, field mapping, and cosmic-ray surface exposure dating. Adam Kent has been working on the diffusion of cations in carbonate minerals found in 'Martian' meteorites as a means of constraining the thermal history of these samples and the implications for past life on Mars. He has also been using the ion microprobe to analyze volatile constituents in glass inclusions in phenocrysts from various lava suites. Lucilla Benedetti is developing new paleoseismic methods based on the production of cosmogenic ^{36}Cl in exposed earthquake fault scarps. Kent and Putirka have left the lab to take positions at the Danish Lithosphere Center and Indiana University of Pennsylvania, respectively.

RESEARCH HIGHLIGHTS

The The Himalayas and the Tibetan Plateau, formed as a result of the collision of India and Asia, provide an excellent natural laboratory for the investigation of the mechanical response of the outer 100 km of the Earth (the lithosphere) to tectonic stress. Geophysicists are divided in their views on the nature of this response: one group advo-cates homogeneously distributed deformation in which the lithosphere deforms as a fluid continuum, while others contend that deformation is highly localized, with the lithosphere deforming as a system of rigid blocks. The latter group draws support from the high slip rates recently observed on strike-slip faults along the northern edge of the Plateau [e.g. the Altyn Tagh Fault (ATF)], coupled with seismic observations suggesting that these faults penetrate the entire lithosphere. These "lithospheric faults" define continental lithospheric plates and facilitate the eastward extrusion of the rigid central Tibet plate. If such extrusion occurs, then equivalent fea-tures must exist at its southern boundary, which must have slip rates similar to those in the north. Because the southern boundary of Tibet, defined by the Main Himalayan

Thrust (MHT), has no lateral component of motion, it is kinematically incompatible with motion in the north. However, a series of features to the north of the MHT - the Karakorum Fault, the Karakorum-Jiali Fracture Zone (KJFZ), the Jiali Fault, and the Red River Fault - may define the actual kinematic, southern boundary of this central Tibet plate. The LLNL group consisting of Rick Ryerson, Bob Finkel, Marc Caffee and Jerome van der Woerd in collaboration with Paul Tapponnier and Anne-Sophie Meriaux at Institut de Physique du Globe de Paris and Mike Taylor at UCLA are determining slip rates on these faults, along with those on the ATF in northern Tibet, using a combination of satellite image interpretation, field mapping, and cosmic-ray-exposure dating at LLNL's Center for Accelerator Mass Spectrometry (CAMS) to assess the kinematic compatibility of features in northern and southern Tibet. This investigation supports efforts to understand the structure and mechanical response of the Earth's crust-information that forms the basis for activities such as nuclear test monitoring and resource recovery. CAMS at LLNL is uniquely suited to surface exposure dating, allowing a number of cosmogenic isotopes to be measured.

Our results for the ATF indicate that the slip rate decreases from west to east as slip is transferred to associated strike-slip and thrust faults. The rate on the central ATF (now supported by our own radiocarbon dating at key sites) is as great as 35 mm/yr. Such a high rate supports the hypothesis that these large strike-slip faults play an important role in accommodating Indo-Asian convergence; therefore, the deformation is localized rather than distributed. Similar conclusions can be drawn from our preliminary analysis of the morphological offsets along the Karakorum Fault. Here we have observed what, based on morphological criteria, appear to be glacial deposits associated with the Last Glacial Maximum (~10,000 yrs ago) that have been offset by distances greater than 100 m, implying slip rates of greater than 10mm/yr. We are currently dating these samples using the beryllium-10 and aluminum-26 decay schemes to quantify both lateral and ver-tical slip rates. These data will allow us to assess the role of the Karakorum Fault in allowing eastward extrusion of central Tibet.

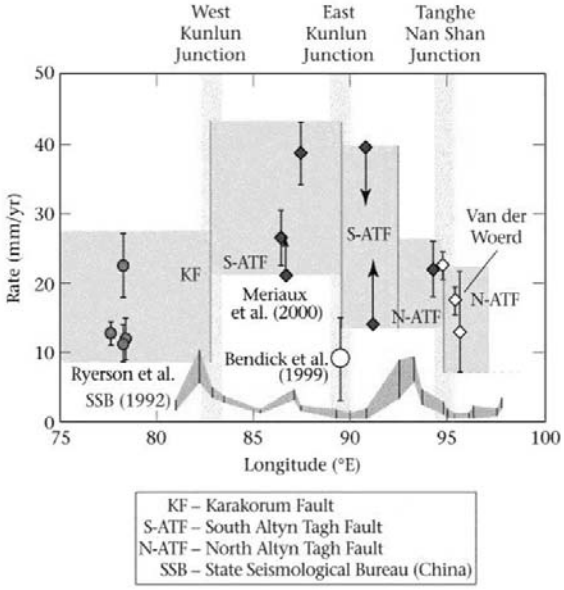

Longitudinal variation in slip-rate along the Altyn Tagh Fault from cosmogenic dating compared with GPS (Bendick et al., 1999) and previous Chinese results (SSB 1992). The decreasing rate indicates that slip on the ATF is transferred to other faults at its eastern terminus, causing uplift and plateau growth.

EARTHQUAKE TIME-SERIES DETERMINED FROM DIRECT COSMOGENIC DATING OF FAULT SCARPS

The simplest view of the process that creates earthquake scarps is that earthquakes repeat at regular intervals in the same place with about the same slip for each event. This concept of a “characteristic earthquake” now forms the basis for understanding earthquake hazard. But, is the characteristic earthquake concept a good approximation to the physics of the earthquake process? Historical information for the Mediterranean region suggests that the frequency of major events varies substantially with time. For small events, compilations, which comprise many thousands of earthquakes, have been shown to exhibit fractal characteristics in magnitude, space and time. Whether large seismic events are really part of the same fractal set is still undetermined. This is a crit-

ical question and can only be addressed by investigating magnitude-frequency characteristics for large earthquakes over millennial time scales.

This project, a collaboration between Lucilla Benedetti, Bob Finkel, Dan Farber and Rick Ryerson at IGPP, Geoffrey King, Rolando Armijo and Frederic Flerit at Institute de Physique du Globe de Paris and Dimitri Papanastassiou, National Observatory of Athens has developed a new method of direct dating of exhumed limestone fault scarp using cosmogenic ^{36}Cl surface exposure dating. The interactions between neutrons and muons from the cosmic rays and target elements such as ^{40}Ca produce cosmogenic isotopes such as ^{36}Cl. This production decreases exponentially with depth. Therefore, ^{36}Cl mostly accumulates while the rock at the surface. The addition of major earthquakes on a fault creates cumulative scarps. With each new earthquake, a new section of material will be exposed on the scarp (Figure 1). The samples highest on the scarp will have been exposed longest, and have the highest ^{36}Cl concentration. We can model this distribution for a scarp that was created by n events, with varying recurrence time. The position of nuclide concentration discontinuities and the nuclide concentrations values yield a magnitude-frequency spectrum for the fault.

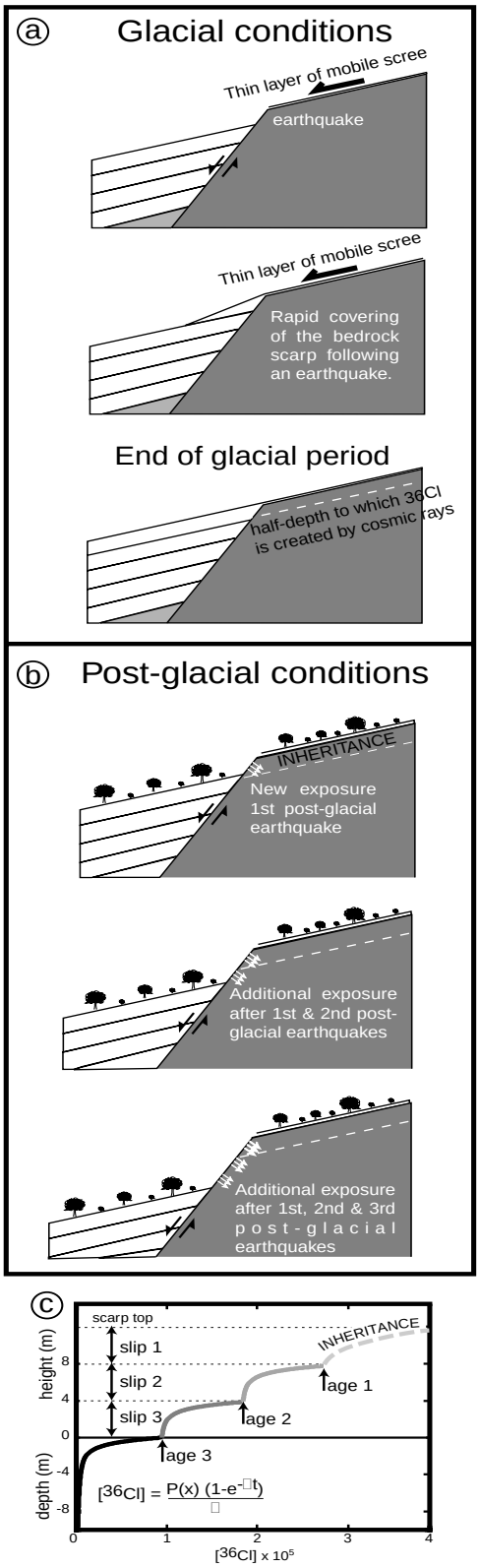

Figure 1: a. During the cold and dry climate, that prevailed during the last glaciation, slopes were unstable. Free-faces formed during repeated earthquakes were immediately buried Note layering in the hanging-wall, associated with this process. b. At the end of glaciation, the wet warm climate stabilized the slopes and earthquake slip began to accumulate and to form the present day escarpments. c. Synthetic profiles for a scarp created by three earthquakes with 4m of slip each at 5000 yr intervals. ^{36}Cl concentration is given by the equation with 1, the ^{36}Cl decay constant (2.27x10-6 yr^{-1}) and P(x) the ^{36}Cl production rate. P(x) decreases approximately exponentially with depth.

We sampled two continuous profiles at two different sites along the Sparta fault (Peloponnesus) in Greece (Figure 2). The fault cuts limestone bedrock to produce a 20-km-long, very well preserved normal fault scarp, which, in the central part, reaches a height of 10-12 m. On the best-preserved sections of this scarp we sampled two 6-8m vertical profiles separated by about 12km. We sampled continuous vertical profiles with a resolution of 10 cm. In the 66 and 82 samples collected at those two sites, the concentration of ^{36}Cl and of stable chlorine has been measured by accelerator mass spectrometry (AMS) at the LLNL-CAMS.

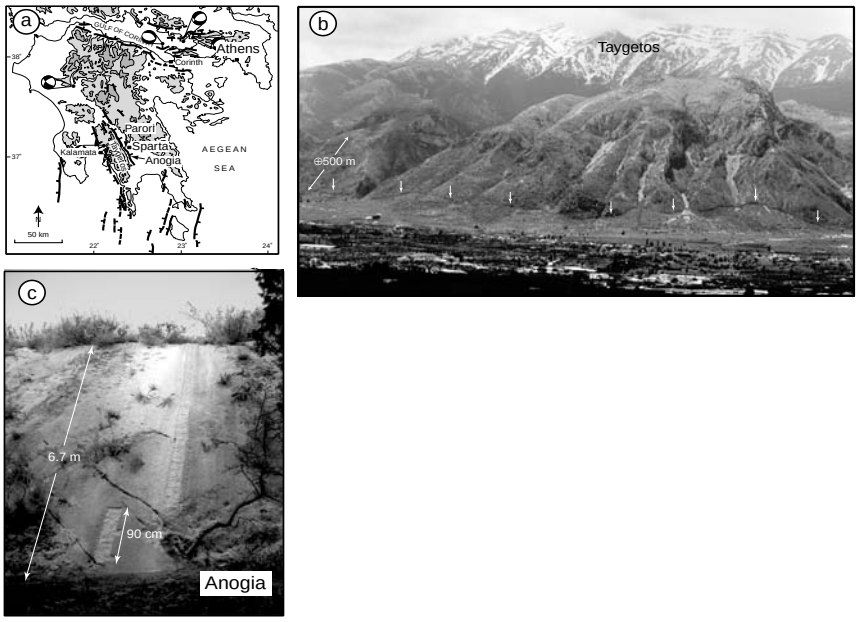

Benedetti_Figure 1

Figure 2: a) Map of active faults of southern Greece. b)The Sparta fault. The prominent triangular facets in this view are about 500 m high. Arrows outline the scarp trace. Note the regularity of scarp height and the continuity of the scarp along the range front. c-)Photograph of sampling site at Anogia. Samples are 15-20 cm wide, less than 2.5 cm deep. They were divided into 10cm blocks for measurement.

The last event on this fault occurred about 2500 yr ago in agreement with Armijo et al. (1991) who proposed that this fault is the source of the earthquake that destroyed Sparta in 464 BC. The seismic history is different at the two study sites which are located on two separated segments (Figure 3). Both segments record three earthquakes with two common events. Finally the figure shows an increase of the slip-rate on the Anoghia segment, this increase is coeval with the activation of the Parori segment.

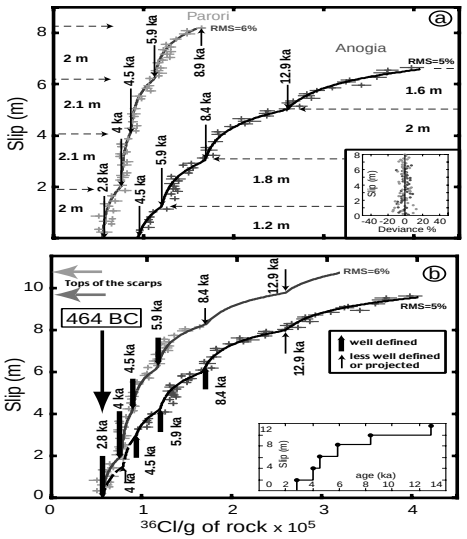

Figure 3: The ^{36}Cl data and the models. Crosses are ^{36}Cl concentrations per gram of rock for each sample with error (7% RMS for Parori and 4% RMS for Anogia, see details in supplementary material), lines are synthetic profiles. Green indicates Parori, red Anogia. a. Four earthquakes fit Parori and Anogia with 6% RMS at Parori and 5% at Anogia (see inset with deviance for details). b. Reconstructed profiles with 2.8 ka and 4 ka events added for Anogia and 12.9 ka event and inheritance added for Parori. Note that events at Parori now fit with the ones at Anogia. The RMS residuals are the same. Inset is time per slip of event deduced from the models.

This new methodology provides new, previously unattainable data on the earthquake history and on the slip distribution of a fault.

DIFFUSION IN MARTIAN CARBONATES

In 1996, scientists working for the National Aeronautics and Space Administration (NASA) announced the discovery of fossil life in Martian meteorite ALH 84001 and unleashed a firestorm of scientific controversy. Scientists around the world scrambled to test and assess these startling conclusions. Numerous stud-ies examined the composition and formation of ALH 84001, the meteorite containing the putative fossil remnants. In par-ticular, the carbonate minerals containing the microscopic, fossil-like structures have been subject to intense scrutiny. Much of this work has centered on the formation temperature of these minerals. Because terrestrial life is only viable over a relatively narrow and well-defined range of temperatures (0 to 150ºC), knowledge of the formation temperature and thermal history of the carbonate minerals in ALH 84001 would provide a direct constraint on the possibility that this meteorite hosts the fossil remains of ancient Martian biota. Adam Kent, Ian Hutcheon and Rick Ryerson have been working on a series of experiments designed to better constrain the thermal history of this meteorite, focusing on the carbonate minerals.

Previous studies by researchers at the University of Tennessee and NASA Johnson Space Center showed abrupt changes in the abundances of iron (Fe), magnesium (Mg), and calcium (Ca) within the ALH 84001 carbonates over distance scales as short as 1 tm. Over time, diffusion will act to homogenize such chemical zoning; therefore, because diffusion is a temperature-driven process, we can use cation diffusivities to constrain the temperature history of the car-bonate minerals.

We used LLNL's secondary ion mass spectrometer (SIMS) to measure the rates of change of Mg and Ca concentration as a function of depth below the surfaces of carbonate miner-als annealed at temperatures of 400 to 600ºC (Figure 4). The SIMS techniques developed in this study enabled us to determine diffusivities at much

lower temperatures (200ºC) than in any previous study and to avoid the pitfalls associated with large down-temperature extrapolations. Our data established the rates of chemical diffusion of Mg in calcite and Ca in magnesite and allow us to set stringent con-straints on the formation temperature and thermal history of carbonates in ALH 84001. We find that the diffusion of Mg in calcite at temperatures between 400 and 550ºC is substantially faster than predicted by the extrapolation of existing higher-temperature data, suggesting that different mechanisms govern Mg diffusion at temperatures above and below about 550ºC.

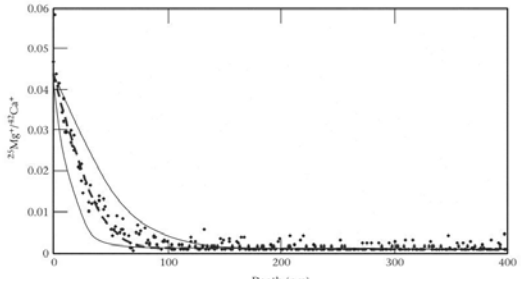

Figure 4. Measured diffusion gradient for chemical diffusion of Mg in calcite for an experiment annealed at 450°C for 152 days. Filled circles represent individual ion microprobe measurements of the $^{25}Mg/^{42}Ca$ ratio as a function of depth beneath the sample surface. The dashed line shows the error function fitted to these data and corresponds to a diffusion coefficient of 1.04 x 10^{-22} m_2/s. To emphasize the quality of the error function fitting procedure, the thin solid lines bounding the data show diffusion profiles calculated for a factor-of-2 variation in the diffusion coefficient.

These data can be used to model thermal histories that allow the micrometer-length scale variations in Ca-Mg composition in ALH 84001 carbonates to survive diffusive homogenization. For initial cooling rates between 0.1 and 1,000ºC/Ma, these results demonstrate that these Martian carbonates most plausibly formed at temperatures of less than 200ºC.

Our study excludes the possibility that the ALH 84001 carbonates formed by high-temperature fluid or melt-related (igneous) processes on Mars, as was previously believed. While not resolving the controversy over the possibility of fossil life, the low temperature derived from our results agrees well with data on oxygen-isotope compositions and leads to a self-consistent model of carbonate formation through metamorphic and/or hydrothermal processes, such as precipitation from saline fluids in the Martian crust.

Section III. Research Summaries of Collaborative Projects

Astrophysics

Speckle and Adaptive Optice Imaging of Planets and Satellites (99-AP001)

Principal Investigator: Imke de Pater (UC Berkeley)
LLNL Collaborators: Seran Gibbard, Claire Max, Bruce Macintosh, Don Gavel
Graduate Student: Henry Roe (UC Berkeley)

The purpose of this proposal was to image solar system objects with high (diffraction limited) spatial resolution using the speckle imaging and adaptive optics techniques developed at LLNL by C. Max and collaborators. Such observations enable us to study the weather and geological surface processes on other planets, studies which enable scientists ultimately to get a better understanding of the meteorology and geological processes on our own Earth. We concentrated on two principal targets: Saturn's largest moon Titan, and the planet Neptune. Titan possesses a substantial atmosphere overlying an unknown surface which may contain lakes or oceans of liquid hydrocarbons. High-resolution images at infrared wavelengths that probe through Titan's atmosphere to the surface have enabled us to produce a surface albedo map at 2 microns. This map has a higher spatial resolution and greater contrast than any other available Titan surface map. We have also investigated weather patterns and changes in the atmospheric structure on Neptune, and produced new diffraction-limited adaptive optics images of storms on the planet.

TITAN

We obtained excellent images of Titan in speckle imaging mode with the 10-m Keck telescope on Mauna Kea during the duration of this and previous grants.[5] In collaboration with researchers (C. McKay and E. Young) at NASA Ames we have developed a simple atmospheric radiative transfer model which we used to constrain atmospheric haze parameters and to separate surface and atmospheric contributions to light received from the satellite. This has allowed us to recover the surface albedo for each image of Titan taken over a total of 14 nights during the years 1996-1998. A full surface albedo map has now been constructed from these images (Fig. 1). The resolution of this map is close to the diffraction limit of the telescope (0.04"). The map shows clear bright and dark features, consistent with possible ice/rock “continent” and very dark regions that may be the elusive “ethane seas” predicted by photochemical models but never before observed.[8]

We observed Titan's atmosphere in several 10 μm bands where we mostly see emission from warm haze particles and trace atmospheric species. Understanding the presence and concentration of trace species is critical to understanding the processes that lead to haze formation and modification of the surface. We also obtained spectra of the satellite with NIRSPEC (1 - 2.5 μm), where we observe haze and surface in scattered and reflected sunlight. Student Henry Roe is analyzing the data and writing an in-depth atmospheric modeling code in collaboration with C. McKay at NASA Ames. This code will be more

detailed than the simple code we have used so far, and will eventually incorporate a Monte Carlo component in order to account correctly for geometry of Titan's atmosphere. (Titan's atmosphere extends a significant distance compared to its radius and thus plane-parallel approximations break down.) In the future we will obtain spectra of Titan with NIRSPEC coupled to adaptive optics, allowing us to map the surface and hazes at high spatial and spectral resolution.

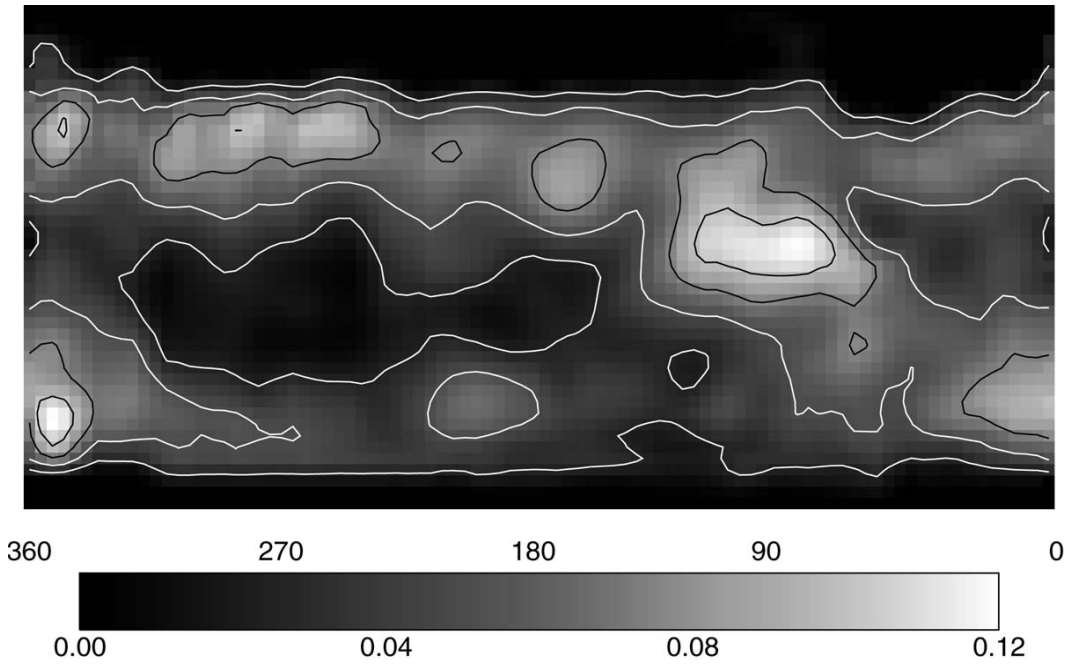

Figure 1: Surface albedo map of Titan at 2.1 microns (K band). Shown are latitude and longitude as well as a colorbar indicating the albedo.

NEPTUNE

We have used the NIRC speckle system at Keck the past few years to image Neptune at the diffraction limit of the telescope (0.04"). Some of our resulting images over a 3-year span are shown in Fig. 2. We have submitted a paper describing and analyzing the images from 1996 and 1997,[5] using both the high-resolution (0.04 arcsecond) broadband speckle imaging and conventional imaging with narrow-band filters. The speckle data enable us to track the size and shape of infrared-bright features (‘storms’) as they move across the disk. We determined rotation periods for latitudes -30° and -45°, which agreed very closely with previous observations. We have been using a model atmosphere program from Kevin Baines (JPL), which student Henry Roe debugged and modified/improved substantially: Henry updated the model with the most accurate representation of the methane absorption bands, through the use of H_2-broadened *k*-distribution coefficients.[6] He also replaced the hydrogen absorption code with the more recent H_2 collision induced absorption coefficients by Borysow and coworkers.[1,2,3,4,9] We also changed the temperature-pressure curve with that published by Lindal,[7] and extended it to higher altitudes. Henry used this model to constrain the altitude of Neptune's haze layers both in storm-free regions and within the storms.

We also used Keck's new NIRSPEC system to get spectra of the planet; these spectra have an extremely high signal-to-noise. Henry Roe has developed software to reduce these data, and most of it has been reduced. The signal-to-noise far exceeds that of any spectra published in the literature to date. The spectra we currently have are not with the adaptive optics system, and are thus at a

lower spatial resolution. Our current data set includes spectra of Northern polar streaks and a southern infrared-bright disturbance or 'storm'. Without adaptive optics we were unable to cleanly separate the very dark equatorial region from the nearby bright regions. In June we will use NIRSPEC coupled to the AO system to acquire high-spatial and high-spectral resolution spectra that will cleanly separate the different features observed on Neptune, including the extremely dark equatorial region. These new data, combined with modeling work by Henry Roe, will allow us to more accurately constrain the particle properties of the clouds, storms, and hazes, as well as their vertical and horizontal extent.

Figure 2: Speckle images of Neptune from the Keck Telescope, taken in (from left to right): September 1996, October 1997, and July 1998. The bright spots in the southern hemisphere may be associated with features similar to the "Great Dark Spot" seen by Voyager. Note also the northern limb brightening, probably due to a high-altitude haze layer. The scale is 2.33 arc-seconds across the disk of Neptune.

FIRST RESULTS FROM THE NEW KECK AO SYSTEM

We obtained several AO images of Titan, Neptune and Uranus taken by the Keck AO team during engineering/commissioning time. The performance of the AO system and the quality of the data are excellent. The Titan images are as good as our best speckle images (Fig. 3), whereas the Neptune AO images are far superior to speckle images (Fig. 4), because of the increased signal-to-noise resulting from the longer integration time on this relatively faint target. We have begun an analysis of these images using the Titan and Neptune radiative transfer codes described above; our analysis will be improved by the new radiative transfer code being developed by Henry Roe.

Figure 3: Adaptive optics image of Titan from the Keck Telescope.

Figure 4: An image of Neptune taken with adaptive optics. The image was taken at the Keck Telescope at H band (1.6 microns) in April 1999. Note the bright storm in the lower right; the streaky features at southern latitudes are much more clearly seen than in the speckle images (Fig. 2).

REFERENCES

1. Borysow, A., "Erratum to: rotovibrational collision-induced absorption spectra of H2-H2 pairs in the fundamental band 0 goes into 1 at temperatures from 20 to 300K," *Icarus*, 106, 614 (1993).

2. Borysow, A., "Modeling of collision-induced infrared absorption spectra of H2-H2 pairs in the fundamental band at temperatures from 20 to 300K," *Icarus*, 92, 273-279 (1991).

3. Borysow, A., and L. Frommhold, "Collision-induced infrared spectra of H2-He pairs at temperatures from 18 to 7000K II - overtone and hot bands," *Ap. J.*, 341, 549-555 (1991).

4. Borysow, A., L. Frommhold, and M. Moraldi, "Collision-induced infrared spectra of H2-He pairs involving 0-1 vibrational transitions and temperatures from 18 to 7000K," *Ap. J.*, 336, 495-503 (1989).

5. Gibbard, S.G. B. Macintosh, D. Gavel., C.E. Max, I. de Pater, A.M. Ghez, E.F. Young, and C.P. McKay, "Titan: High-Resolution Speckle Images from the Keck Telescope," *Icarus*,139, 189-201 (1999).

6. Irwin, P.G.J., S.B. Calcutt, F.W. Taylor, and A.L. Weir, "Calculated *k* distribution coefficients for hydrogen- and self-broadened methane in the range 2000-9500 cm^{-1} from exponential sum fitting to band-modelled spectra," *J. Geophys. Res.*, 101, 26137-26154 (1996).

7. Lindal, G.F., "The atmosphere of Neptune: An analysis of radio occultation data acquired with Voyager 2," *Astron. J.*, 103, 967-982 (1992).

8. Lunine, J.I., *Rev. Geophys. Space Phys*., 31, 133 (1993).

9. Zheng, C., and A. Borysow, "Modeling of collision-induced infrared absorption spectra of H2 pairs in the first overtone band at temperatures from 20 to 500 K," *Icarus*, 113, 84-90 (1995).

A Radio Selected Sample of Active Galactic Nuclei (99-AP007), (00-AP011)

Principal Investigator: Robert H. Becker (UC Davis)
LLNL Collaborator: Wil van Breugel
Graduate Students: Jerry Whalen and Trevor Price (UC Davis)

The FIRST survey has completed and released radio images and an associated catalog of radio sources for ~6000 square degrees of sky in the north Galactic cap. Additional observing time has been granted by the Very Large Array to expand thesky coverage to ~8000 square degrees. The survey is being used to create the FIRST Bright Quasar Survey (FBQS). Quasars found in the FBQS are at the heart of a number of research programs including searches for gravitational lens, studying the relationship between radio morphology and optical properties, detailed studies of broad absorption line (BAL) quasars, and defining the astrometric grid for a future NASA mission - the Space Interferometry Mission (SIM).

OBJECTIVES

The primary objective is the creation of a complete sample of radio-selected quasars. This new sample will be free of many of the selection effects from which optical quasars surveys suffer. The survey will be particularly powerful in finding large numbers of radio intermediate quasars which were too faint in the radio to turn up in previous radio-selected samples but too rare to occur in great numbers in optically selected samples.

PROGRESS

A number of ongoing scientific programs based on the FBQS are producing important results. The list of publications originating under this minigrant are listed below. The primary papers arise from the FBQS itself which is an ongoing attempt to create a large, uniformly selected sample of bright quasars over the entire area of the FIRST survey.[2,4] To date over 1000 quasars have been found and the sample is expected to double in size over the next two years. We are currently preparing a third paper which extends the survey a magnitude fainter over ~600 square degrees of sky in the southern Galactic cap.[4] By going fainter, we can study to what extent quasar properties depend on their optical luminosity.

The FBQS is turning out to be a starting point for a number of exciting projects. Two years in a row, we have been successful in winning Hubble Space Telescope observing time to search for small separation gravitational lenses. In total, we have been granted 600 snapshot images with STIS (approximately 15% of the snapshots available). In the first 4 months of this program, we have already identified a new lensed quasar. In a related program, we have been awarded a night of Keck time with a near infrared camera (NIRC) to search for lensed quasars. The HST program is now an international collaboration including scientists from Europe and Australia.

We have also been pursuing a vigorous program to study the nature of broad absorption line (BAL) quasars. Approximately 10% of quasars show high velocity outflows of varying degrees of ionization. The FBQS has been very successful at finding extreme examples of these objects. We have an aggressive program of observations using Keck Observatory to gather both high resolution spectra of the absorption lines as well as spectropolarimetric data to measure the polarization signature of the scattered light. These data are revealing results which are in conflict with the

standard model from BAL quasars. In particular, we have concluded that these objects represent a short lived stage early in a quasar's life rather than quasars viewed at a special orientation.[1,4] Recently we have been awarded observing time with the Chandra X-ray telescope to measure the x-ray emission from the FBQS BAL quasars. These observations will better constrain the ionization state of the absorbing gas.

We have been using the Very Large Array to better define the radio properties of the FBQS quasars. In particular, we have been reobserving the quasars at several wavelengths to determine their radio spectral slopes. We have also made observations at higher angular resolution to separate the diffuse component of emission from that arising directly from the central engine.

The FBQS is also serving as a source of bright quasars for improving the astrometric grid for NASA's Space Interferomery Mission (SIM). SIM needs ~300 bright quasars to tie the reference frame determined from ~3000 grid stars to an extragalactic inertial reference frame. We have already been funded for a one year pilot project to assist the SIM project.

Two University of California at Davis graduate students (Jerry Whalen and Trevor Price) have come to IGPP/LLNL this year to work on their PhD using data from the FIRST survey. Trevor's funding comes directly from this minigrant.

REFERENCES

1. Gregg, M., Becker, R., *et. al.*, "The Discovery of a FIRST FR II Radio-Loud BAL Quasar", *ApJ* submitted (2000).
2. Schecter, P.L., Gregg, M.D., Becker, R.H., Helfand, D.J., White, R.L., "The First FIRST Gravitationally Lensed Quasar: FBQ 0951+2635", *AJ*, 115, 1371 (1997).
3. White, R.L., Becker, R.H., Helfand, D.J., Gregg, M.D., "A Catalog of 1.4 GHz Radio Sources from the FIRST Survey", *ApJ*, 475, 479 (1997).
4. White, R.L., Becker, R.H., *et. al.*, "The FIRST Bright Quasar Survey II. 60 Nights and 1200 Spectra Later", *ApJSupp*, in press (2000).

Detection of Occultations (99-AP012)/(00-AP-006)

Principal Investigator: John A. Rice (UC Berkeley)
LLNL Collaborators: Charles Alcock and Stuart Marshall
Other Collaborator: Imke de Pater (UC Berkeley)
Graduate Student: Chyng-Lan Liang (UC Berkeley)

A rich population of "comets" in the flattened annulus beyond Neptune, known as the Kuiper Belt, has been inferred and more than three hundred of its larger members have been directly observed to date.[1] The Taiwanese American Occultation Survey (TAOS), a collaboration between the Lawrence Livermore National Laboratories (LLNL), Academia Sinica and National Central University, will estimate directly the number of comets in the Kuiper Belt, by measuring the rate of occultations of stars by these objects, using an array of three to four, 0.5-m, wide-field robotic telescopes. Some 3,000 stars will be monitored, resulting in about 300 million photometric measurements per night. Since the size distribution of these comets is unknown for cometary radii < 20 km, estimated event rates range from 10 to 4000 a year. The TAOS survey will help characterize the Kuiper Belt, which is useful to constrain theories regarding the origin of our Solar System. To optimize the success of TAOS, we have used elaborate simulations and statistical methods to investigate opposing methods of gathering and processing the data, resulting in different detection schemes, with the aim of maxmizing the detection rate.

THE DATA

The telescopes are equipped with CCD arrays. The CCD columns will be aligned with the Right Ascension direction so that stars will travel across the frame during the exposure, if left untracked. We currently plan to track the stars and rapidly shift the counts in each pixel across the CCD, by a set number of pixels, at set intervals of time. The "star trail" would then resemble a zipper, with clusters of counts at spaced intervals. A potential advantage of this mode of operation is reduced shutter activity and wear. Operation, in this mode, is governed by various parameters; flexibility regarding these parameters makes it necessary to investigate, using simulations, the various different observing modes.

OBJECTIVES

To find the ideal detection algorithm, we have to understand the nature of the signal and noise. Characterization of the stochastic structure of the noise and signal allows us to generate simulated data and these may be used to develop optimal tests. The primary goal of this proposal was to design optimal detection algorithms, guided by theoretical arguments, simulations and by real test images. Our calculations will be used to guide the choice of the various operational parameters, determining the mode of actual observation, when the telescopes begin operating robotically, in the fall of the year 2001. We require from our system a false alarm probability per measurement of $\sim 10^{-12}$. The algorithm must run in real time under varying sky conditions, processing about 10^6 measurements per exposure. Both statistical and computational efficiency are therefore important.

PROGRESS

We have generated star occultations in simulated CCD images, using the USNO catalogue, in order to develop and optimize observational procedures to maximize the detection rate. We have made the 'observations' as realistic as possible by including various sources of noise in the CCD

images, such as Poisson counting fluctuations, image motion due to atmospheric turbulence, partial overlap of images from different stars, scintillation and CCD electronics. A model, based on current theories regarding the Kuiper Belt population, was used to generate fake occultations in our simulated images.

We studied in particular the effects of various changes in parameters on the detection rate, such as using different star fields, changes in the angle of observation and the level of sky background. We also simulated the potential improvement in detection rates from upgrades in the CCD camera. Some of these results are shown in Figure 1; this graph may also be used to determine the cut-off magnitude of the stars to be monitored. We noticed that the detection rate may improve by adjusting both the cut-off magnitude of stars and our detection scheme depending on the observing conditions.

Not all dimmings of stars ("flags") are due to occultations. Noise in the data may result in false alarms. We considered how, with one year's worth of data, we might estimate the number of detections actually due to an occultation from the total number of flags. A level α test controls the probability of false alarm at α and the number of flags and the proportion of real detections will vary with the level of the test. Figure 2 shows the mean and estimated 95% confidence interval for the estimate for the number of real detections, π versus the level of the test, α, for 350 occultations in 1×10^{10} photometric measurements, with 200 repetitions.

We have used simulations to determine the "best" mode of the TAOS operation, from the detection scheme on down to the operation of the CCD. Using the computational and time constraints set by the experiment, simulations allowed us to investigate more quantitively the advantages of upgrading the cameras, to determine which stars to monitor (in a certain field for a certain brightness of sky) and which angle to observe at. We also investigated various methods to estimate the number of real detections versus false alarms.

Although we learned much from our simulations, we note that it is crucial to carefully analyze actual test images taken under varying circumstances. In particular, their features must be compared to the simulator and the latter modified as necessary. This process may lead to modifications in the detection algorithm.

The work described above has been carried out by graduate student Chyng Liang for her Ph.D. thesis, and as supervised jointly by Professors. John Rice, Imke de Pater and Charles Alcock.

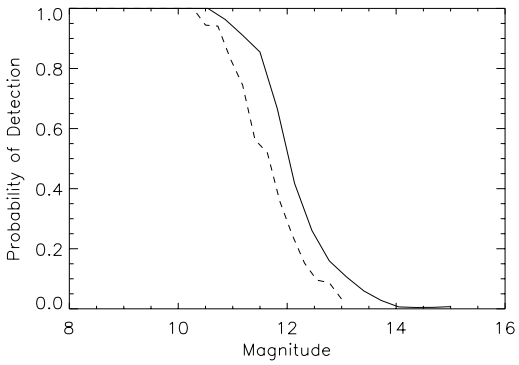

Figure 1: Graph Shows the Probability of Detection for the New CCD (Unbroken) and the Old CCD (Dashed), with Sky Level of Magnitude 20 and angle of observation near quadrature.

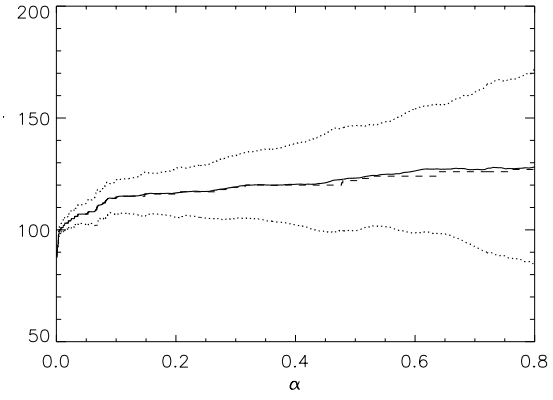

Figure 2: Graph Shows the Number of Real Detections (Dashed), the Mean (Unbroken) and Estimated 95% Confidence Interval (Dotted) for the Estimate for the Number of Real Detections in 200 Repetitions, for 350 Occultations in 1×10^{10} Tests.

REFERENCES

1. Jewitt, D., “Kuiper Belt Objects”, *Annual Review of Earth and Planetary Sciences*, 27, 287-312 (1999).

Collective Absorption Properties of Neutrinos in Supernovae (99-AP017)

Principal Investigator: John M. Dawson (UC Los Angeles)
LLNL Collaborator: H. E. Dalhed
Postdoc: Luis Silva (UC Los Angeles)
Graduate Student: John Tonge (UC Los Angeles)

This is a UCLA-LLNL collaboration to investigate the influence of collective interactions between the intense neutrino flux from the core of a supernova and the plasma of its surrounding stellar envelope. The mechanism is similar to the Forward Raman Instability that occurs when intense laser light interacts with plasma through the generation of electron plasma waves. In the neutrino case, the instability is much weaker due to the weakness of the neutrino elctron interaction. Nevertheless, recent work at UCLA has shown that because of the extrme conditions that exist in a supernova, the forward Raman instability goes. The neutrinos carry away most of the energy of the supernova. Models of supenova have problems explaining how a supernova explodes if so much energy is carried by neutrinos with additonal energy expended in dissociating iron and other heavy nuclei. Compter simulations at LLNL have shown that explosions can be made to occur if a few percent of the neutrino energy is deposited in the stellar envelope. The forward Raman instability appears to be strong enough to do this. At UCLA we are developing techniques for computing the transport of the neutrinos through the stellar plasma and the resulting energy transfer when collective interactions are included. This involves two quasi linear plasma waves. The quasi linear equation for the neutrinos describes the evolution of the neutrino spectrum due to their interaction with the plasma waves. The plasma wave equation computes the spectrum of plasma waves produced by the neutrinos and includes damping by electrons and the resultant flow of energy from neutrons to electrons. The quasi linear equation for electrons describes the evolution of the electron distribution function. These equations must be solved numerically; this work is carried out in collaboration W. L. Kruer. Once we can solve these equations as functions of space and time, we will incorporate them in the supernova codes of Dalhed by computing effective electron heating rates and neutino scattering rates; this will be done in collaboration with Dalhed. The effects on the neutrino energy distribution will be calculated to explore possible detectable signatures of the process.

PROGRESS

Neutrino transport in supernovas represents a key issue of the theory of supernovae cxplosions and neutron star formation. Most of the energy (99%) in a supernovae explosion is released as neutrinos, and understanding how some of this energy can be deposited in the outer layers of the exploding star is a fundamental issue to determine the main features of the explosion, and neutrino signal signatures.

Recently, it was shown that collective neurtino-plasma interactions could lead to anomalous energy deposition of the successful ejection of the neutrinos and thus,[1] provide the necessary plasma heating for a successful ejection of the overlying layers of the star and the production of a visible supernovae explosion.

In the last year, we have developed the theoretical framework for collective neutrino-plasma interactions based on a kinetic theory for the neu-

trinos coupled with the background electrons.[2] We have shown that neutrino driven instabilities (Forward Raman Scattering) can grow in conditions relevant for supernovae evolution models.

The kinetic theory of the neutrinos represents a first step towards the incorporation of collective neutrino-plasma processes in the neutrino transport component of LLNL supernovae code. Based on our set of kinetic equations, we have derived a set of quasi-linear equations describing the evolution of the neutrino spectrum and the electron distribution function on a slow time scale (of the order of the plasma heating rate). These two equations are coupled with an equation for the evolution of the plasma waves spectrum. Preliminary numerical results indicate electron heating rates of the order of 10 Mev/s/electron for neutrino luminosities of 10^{52} erg/s, at 300 km from the core of the star.[3] The quasi-linear model describes two central issues: (1) the saturation mechanism of neutrino dirven instabilities and (2) the plasma heating process and associated rates. The latter is the parameter to be included in the LLNL supernovae code; it will allow evaluation of the impact of collective neutrino-plasma interactions on supernovae dynamics.

As part of ths project, we are developing a Particle-in-Cell code for the neutrinos (the neutrinos are treated as particles with a distribution function in energy and direction) and the neutrino plasma interaction; this effort is in its early stages. This will be a crucial tool not only to understand the nonlinear features of the neutrino driven instabilites, but it will also provide a more complete description of the plasma heating mechanism. We have constructed such a code. It is possible to treat photon plasma interactions by an identical code. We are testing our methods for the photon (light) plasma case and comparing the results with ones from Electromagnetic PIC models. The results look very promising and particle photon code reproduces many of the results obtained from the full electromagnetic code.

REFERENCES

1. R. Bingham, J. M. Dawson, J. J. Su, H. A. Bethe, "Collective interactions between neutrinos and dense plasmas," *Physics Lett.*, A193, 278 (1994).

2. P. K. Shukla, L. O. Silva, H. Bethe, R. Bingham, J. M. Dawson, L. Stenflo, J. T. Mendonca, S. Dalhed, *Plasma Phys. and Cont. Fursion*, 41, A699-707 (1999).

3. L. O. Silva, R. Bingham, J. M. Dawson, H. E. Dalhed, J. T. Mendonca, P. K. Shukla, presented at the *APS Centennial*, Atlanta (1999).

First Extragalactic Astronomy with Laser Guide Star Adaptive Optics (99-AP020)

Principal Investigator: Andreas Quirrenbach (UC San Diego)
LLNL Collaborators: Claire Max, Don Gavel,
Bruce Macintosh, Scot Olivier
Postdoc: David Mitchell (UC San Diego)

We have started observations of extragalactic objects with the adaptive optics systems at UC's 3m Shane and 10m KeckII telescopes in natural guide star mode. Keck observations of the Seyfert galaxies NGC1068 and NGC7469 reveal detailed structure in the 3" *star forming ring in NGC7469, and an elongation of the nucleus in NGC1068. A few radio galaxies that happen to have nearby bright guide stars were observed with the Shane telescope at Lick observatory. Data obtained on the barred spiral galaxy UGC1347 in the cluster Abell262 as part of an observing program at the 3.5m telescope on Calar Alto are the first observations of an extragalactic object with laser guide star adaptive optics.*

OBJECTIVES:

Adaptive optics (AO) and laser guide star (LGS) technologies are key technical objectives for observational astronomy, because they will enable astronomers to image as clearly from the ground as with telescopes located in space. This opens an enormous potential for observations of faint objects in the early Universe. In the past few years the improvements in angular resolution brought about by the Hubble Space Telescope, and the exquisite sensitivity of UC's 10-meter Keck Telescopes, have lead to major advances in understanding the formation of galaxies in the young Universe. Adaptive optics will allow UC, via its Keck and Lick Observatories, to take the next important step in this field by bringing together high resolution and large collecting area simultaneously. The LGS systems developed and built by LLNL are a crucial component of these instruments, because they allow access to a large fraction of the sky independent of bright natural guide stars.

AO observations are still very challenging in many respects, and observing extragalactic objects pushes the capabilities of the present systems to their limits. The goal of this project was therefore twofold: to develop the observing procedures and data reduction tools necessary to observe faint and fuzzy objects, and to initiate the first scientifically meaningful observations of external galaxies with laser guide star adaptive optics.

PROGRESS:

Two observing runs at Lick Observatory were plagued by bad weather conditions, so that the data quality was poor, and we could not operate the laser guide star system altogether. However, we could use the observing time to test the procedures required to perform observations with natural guide stars at large off-axis angles. This mode of operation is needed for faint targets, and had not been tried at Lick before. We did indeed find a few problems that had been overlooked in the design of the system, which were then fixed for the second run. During the last observing night we could finally obtain a fairly good set of observations on a few radio galaxies that happen to be projected near bright stars at separations of < 20 arcseconds. We are currently in the process of analyzing the data from this night.

The AO system at the Keck,II telescope was commissioned and extensively tested in the course of 1999, and is now routinely used for a variety of scientific programs. The Keck LGS system was delivered from LLNL to Hawaii and assembled at the headquarters of Keck Observatory (located in Waimea), but it has not yet been installed at the telescope. Therefore we had to start our Keck observing program with natural guide star AO. During the science verification phase of the Keck II AO system, we observed the nuclear regions of the Seyfert Galaxies NGC1068 and NGC7469.[1] Individual knots within the star-forming ring (3 arcsec diameter) of NGC7469 are clearly resolved in our H-band images. Comparison with other high-resolution data sets shows that information near the diffraction limit of the telescope can be reliably obtained. The main goal of the observations of NGC1068 was to determine the compactness of the nucleus at infrared wavelengths. Great care has to be exercised with this type of observation, since the behavior of the adaptive optics system is different for extended objects than for point sources. The wavefront sensor operates at visible wavelengths, where the nucleus of NGC1068 is fairly diffuse; this can give rise to artifacts that can be mistaken for structures within the central arcsecond. Therefore we took images at different angles of the image rotator to separate artifacts from real structure. In this way we could measure a faint extension of the nucleus at position angle ~20º; this result is consistent with speckle data in the literature. The first observations of extragalactic objects with laser guide star adaptive optics were carried out with ALFA at the 3.5m telescope on Calar Alto;[2] A. Quirrenbach had been responsible for designing and building that LGS system. The target for these observations was the barred spiral galaxy UGC1347 in the cluster Abell 262. These observations were part of a larger program in which high angular resolution near-infrared data on three galaxy clusters at different redshifts were obtained using adaptive optics. The three clusters are well suited for high resolution investigations since bright field stars for tip-tilt or wavefront sensing are located close to the line of sight to cluster galaxies. In summary our high angular resolution NIR data combined with other information clearly indicates star formation activity or interaction between cluster members at all three redshifts. For two barred galaxies in the Abell 262 cluster, UGC1344 and UGC1347, we can interpret our NIR imaging results in combination with published radio, far-infrared, and Hα data in the framework of a star formation model. In addition to the star-forming resolved NIR nucleus in UGC1347 we found a bright and compact region of recent and enhanced star formation at one tip of the bar. The ratio of 2.1μ to Lyman-χ luminosity as well as the V-K color of that region imply a starburst that happened about 10^7 years ago. For UGC,1344 we find that the overall star formation activity is low and that the system is deficient in fuel for star formation.

The importance of star formation in galaxy clusters is also supported by a comparison of seeing-corrected nuclear bulge sizes of a sample of spiral galaxies within and outside the central HI deficient zone of the Abell 262 and Abell 1367 clusters. The galaxies inside the Abell radii of both clusters show a tendency for more compact bulges than those outside. This phenomenon could be due to increased star formation activity triggered by interactions of cluster members inside the Abell radius.

The star formation activity in the two higher redshift clusters J1836.3CR and PKS 0743-006 is determined via comparison to stellar population models in near-infrared two-color-diagrams. While J1836.3CR is consistent with an evolved cluster, objects in the field of PKS 0743-006 show indications of more recent star formation activity. The central object in J1836.3CR shows a radial intensity profile that is indicative for cD galaxies in a rich cluster environment. Extended wings in its light distribution may be consistent with recent or ongoing galaxy-galaxy interaction in this cluster.

We intend to continue the UCSD / LLNL collaboration on adaptive optics observations of extragalactic sources, initially with natural guide stars, and then with the Keck LGS system. Observing time has already been allocated for observations of Seyfert galaxies (Max and Quirrenbach), and for a sample of high-redshift radio galaxies (van Breugel and Quirrenbach).

REFERENCES:

1. Quirrenbach, A., Lai, O., Larkin, J., Neugebauer, G., Weinberger, A., & Wizinowich, P., "Keck Adaptive Optics Observation of Seyfert Nuclei," *BAAS*, 31, 93.04 (1999).

2. Hackenberg, W., Eckart, A., Davies, R., Rabien, S., Ott, T., Kasper, M., Hippler, S., & Quirrenbach, A., "Near-Infrared Adaptive Optics Observations of Galaxy Clusters: Abell 262 at z = 0.0157, J 1836.3,CR at z = 0.414, and PKS 0734-006 at z = 0.994," *ApJ*, submitted (2000).

A Full Determination of the MACHO Microlensing Detection Efficiency Toward the LMC, SMC, and Bulge

(99-AP023) (00-AP-028)

Principal Investigator: Kim Griest (UC San Diego)
LLNL Collaborator: Stuart Marshall
Graduate Student: Thor Vandehei (UC San Diego)

The most important scientific result of the MACHO microlensing survey is the optical depth for microlensing towards the Large Magellanic Cloud (LMC). This number determines whether or not the dark matter in the Milky Way consists of compact objects. A key ingredient in determining this number is the efficiency with which the microlensing survey detects microlensing. We determined this quantity by adding artificial stars into actual LMC images, adding simulated microlensing events into actual lightcurves, and analyzing these with the same software we use to detect actual microlensing events. Our determination is the best of any microlensing collaboration and helps make the MACHO collaboration dark matter results the world's best.

Thor Vandehei took the lead in writing and running the software needed to determine the MACHO collaboration microlensing efficiency for the 5.7-year LMC data set. He and Kim Griest played key roles the event selection and background rejection for the analysis of the 5.7-year results. He, with much assistance from Stuart Marshall, designed and implemented software to add artificial stars into MACHO images over a wide range of observing conditions and source star magnifications.

The MACHO photometry code was run on these stars and the accuracy with which the input magnification was recovered was determined. In total, more than 1 million artificial stars with V magnitudes between 16.5 and 24.5 were added to images taken from 10 fields, each over roughly 70 observing conditions. The resulting photometry was organized into a Photometric Response Data Base (PRDB), which had a total size of 10.4 Gbytes. This compares with the 5.7-year LMC data set that contained photometry of 12 million stars in 30 fields with an average of 720 images of each field.

The PRDB was used to add simulated microlensing events into a large random sample of MACHO lightcurves, and these simulated events were processed using the same software as used on the survey data. The resulting statistical characterizations of the lightcurves were processed with the same selection criteria that were used to select the 14-17 LMC microlensing events found in the 5.7 year data.[1] Thus microlensing detection efficiency was found as the fraction of simulated microlensing events that the software recovered as a function of event duration, event magnification, and source star magnitude. The resulting efficiency function is shown in Figure 1. While the above procedure sounds simple, the size of the project required substantial programming and computational effort, and there were a large number of subtleties that had to be carefully handled. The procedure we developed ensures that all the important effects are taken into account, including bad weather and uneven time sampling, variable seeing and sky, telescope slips, uneven field crowding, differing sensitivity on different magnitude and color source stars, blending, etc. Our determination of the MACHO efficiency is the best done by any microlensing survey in the world. One example of a subtlety is the treatment of the luminosity function of the LMC. Many of the objects monitored actually consist of blends of several stars. The number of stars being monitored is therefore substantially larger than the number

photometric objects. The faint blended stars increase microlensing optical depth because any one of them can be lensed. However, the chance of detecting microlensing on a very faint blended star is small, lowering the detection efficiency. Thus we used HST images to carefully calibrate the ratio of actual stars to photometric objects, and were careful to understand the probability of detecting microlensing on faint blended stars. Another example of a subtlety is the change in event duration that blending causes. The optical depth depends upon the measured duration of events, and we made a careful correction to the event duration to allow for this effect.

A major publication resulted,[2] and much greater detail about the procedures and results can be found there, as well in the UCSD PhD thesis of Thor Vandehei.

In related work, the efficiency pipeline was used on the 5-year bulge data set to find the efficiency of detecting microlensing on our sample of bulge clump giant stars. This will allow a determination of the microlensing optical depth as a function of bulge field, which can be compared to galactic models to determine the distribution of stellar populations of the Milky Way disk and bulge.

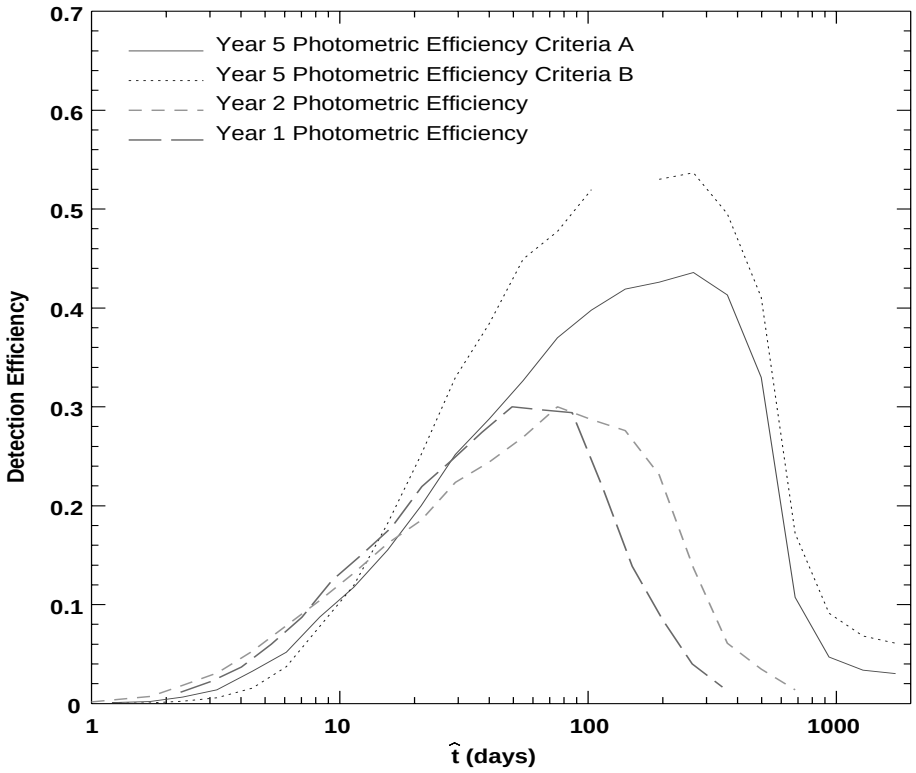

Microlensing detection efficiency for the 5.7-year LMC data set, as a function of event duration, ^ t . The solid line shows the efficiency computed for selection criteria set A, which gave 13 microlensing candidates, while the dotted line shows the efficiency for selection criteria set B, which gave 17 microlensing candidates. The other two curves show previous efficiency determinations for previous MACHO collaboration data sets.

REFERENCES

1. C. Alcock, *et. al.*,"The MACHO Project: Microlensing Results from 5.7 Years of LMC Observation," *ApJ*, 542, 281 (2000).
2. C. Alcock, *et. al.*, "The MACHO Project: Microlensing Detection Efficiency,"*to appear in ApJ Supp. (*2000).

A Search for Red Quasars: The Radio-Loud Quasar Population at $z \geq 3$ (99-AP026)

Principal Investigator: Hyron Spinrad (UC Berkeley)
LLNL Collaborator: Wil van Breugel
Graduate Student: Daniel Stern (UC Berkeley)

With support from IGPP-LLNL, we have pursued a systematic search for high-redshift, radio-loud quasars. The quasars are selected using the1.4 GHz VLA FIRST survey in conjunction with the (second generation) digitized Palomar Observatory Sky Survey.[1,2] Considering optical counterparts to FIRST radio sources, we select unresolved optical identifications with colors consistent with distant quasars. High-redshift quasars provide some of the earliest glimpses we have of the Universe, constrain models of structure formation, and are valuable probes of the intervening intergalactic medium. Our technique is successful: during this project, we discovered six quasars at redshift z > 3.8, including three at z > 4. These are among the most distant sources identified from the FIRST survey and are a significant fraction of the highest-redshift, radio-selected sources known. As part of this project, Stern also studied the radio properties of optically-selected quasars at z > 4, finding no evolution in the radio-loud fraction between z ~ 2 and z > 4.

OBJECTIVES

The primary objective is to create a census of the high-redshift, radio-loud quasars. Previous studies focussed on flat-spectrum sources with flux densities 1 - 3 orders of magnitude greater than the FIRST survey limit and confirmed the decrease in the space density of radio-loud quasars at high redshift.[3,4] Our sample probes a new regime of parameter space: low radio flux density, high-redshift quasars regardless of radio spectral index. This last point is by necessity since no large-area radio survey of comparable depth exists at a frequency different from FIRST. This work will be valuable for constraining the faint end of the radio quasar luminosity function at high redshift, and provides a useful sample of and to the distant Universe. Possible obscuration and absorption processes in quasars imply that radio is an ideal search wavelength for quasars, less prone to selection effects than optical (grism) surveys.

PROGRESS

Our technique is efficient at identifying high-redshift, radio-loud quasars. We have discovered six quasars at $z > 3.8$, including three at $z > 4$ (Fig. 1). These are among the most distant sources identified from the FIRST survey thus far. Our work until now emphasized developing techniques and code to efficiently select spectroscopic candidates from the immense catalogs considered. Stern headed these efforts, which have necessitated close collaboration with the DPOSS working team (Steve Odewahn, Roy Gal, S.G. Djorgovski). Spectroscopy of the sample was obtained at the 3-meter Shane Telescope at Lick Observatory. Preliminary results were presented at the Summer 1998 AAS meeting in San Diego.[5] This work comprised a significant portion of Stern's thesis at UC-Berkeley (completed in October 1999). We are currently modifying portions of the thesis to compose a paper for submission to the Astonomical Journal.[8]

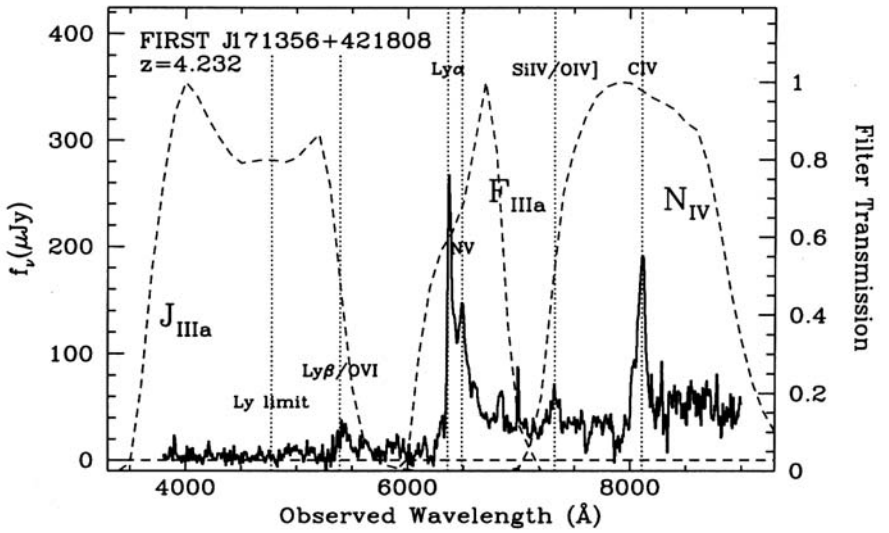

Figure 1: Response of POSS-II JFN filters (dashed lines), with spectrum of a high-redshift quasar plotted for comparison (solid line). Selecting objects with red J - F color and relatively flat F - N color is a robust technique to identify high-redshift quasars. The Lymana forest causes the bluest passband to drop-out, or disappear.

As an offshoot of this project, Stern also analyzed the radio properties of optically-selected $z >$ 4 quasars. This project was useful for addressing differential evolution between the radio-loud and radio-quiet quasar populations. Though it has long been accepted that both radio-loud and radio-quiet quasar co-moving space densities decrease at high redshift, the relation between the decline in the two populations has been poorly quantified. Differential evolution between the populations would be a fascinating result, helping shape our understanding of the different types of active galaxies. For many models of AGN, a lag in the appearance of radio-loud quasars is expected relative to the more common radio-quiet quasars. The results of this research, which comprised a portion of Stern's thesis and appeared in Stern *et. al.*,[7] show no evidence of redshift-dependence in the radio-loud fraction between $z \sim 2$ and $z > 4$ (see Fig. 2).

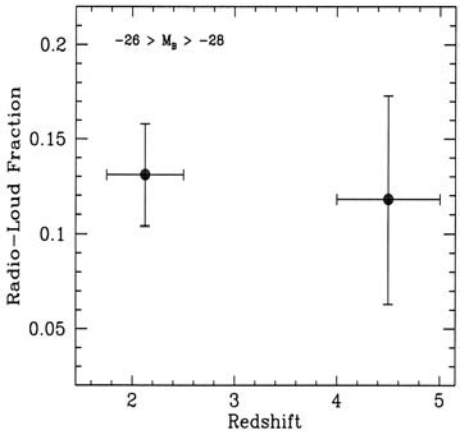

Figure 2: Fraction of radio-loud quasars as function of redshift. Two redshift ranges are plotted, with 1s errors. No redshift dependence in the radio-loud fraction is evident.

REFERENCES

1. Becker, R.H., White, R.L., and Helfand, D.J., "The FIRST Survey: Faint Images of the Radio Sky at Twenty Centimeters," *Astrophys. J.*, 450, 559 (1995).

2. Djorgovski, S.G., de Carvalho, R.R., Gal, R.R., Pahre, M.A., Scaramella, R., and Longo, G., "Cataloging of the Digitized POSS-II, and Some Initial Scientific Results From It," astro-ph/9612108 (1996).

3. Hook, I.M. and McMahon, R.G., "Discovery of Radio-Loud Quasars at $z = 4.72$ and $z = 4.010$," *MNRS*, 294, 7 (1998).

4. Shaver, P.A., Hook, I.M., Jackson, C.A., Wall, J.V., and Kellerman, K.I., "The Redshift Cutoff and the Quasar Epoch," astro-ph/9801211 (1998).

5. Stern, D., Spinrad, H., van Breugel, W., Djorgovski, S.G., Odewahn, S., Gal, R., and de Carvalho, R., "Correlating FIRST with DPOSS: A Search for Radio-Loud Quasars at $z \sim 4$," *BAAS*, 192, #55.20 (1998).

6. Stern, D., "Probing the Dark Ages: Observations of the High-Redshift Universe," Ph.D. thesis (1999)

7. Stern, D., Djorgovski, S.G., Perley, R.A., de Carvalho, R., and Wall, J.V., "Radio Properties of $z > 4$ Optically-Selected Quasars," *Asron. J.*, 132, 1526 (2000).

8. Stern, D., Spinrad, H., van Breugel, W., Djorgovski, S.G., Odewahn, S., Gal, R., and de Carvalho, R., "Correlating FIRST with DPOSS: A Search for Radio-Loud Quasars at $z \sim 4$," in preparation (2002).

High Resolution Imaging and Spectroscopy of Neptune and Titan (00-AP009)

Principal Investigator: Imke de Pater (UC Berkeley)
LLNL Collaborator: Seran Gibbard
Graduate Students: Shuleen Martin and Henry Roe (UC Berkeley)

The purpose of this proposal was to image solar system objects with high (diffraction limited) spatial resolution using the speckle imaging and adaptive optics techniques developed at LLNL by C. Max and collaborators. Such observations allow us to study the weather and geological surface processes on other planets, studies which enable scientists ultimately to get a better understanding of the meteorology and geological processes on our own Earth. We concentrated on two principal targets: Saturn's largest moon Titan, and the planets Neptune and Uranus. Titan possesses a substantial atmosphere overlying an unknown surface which may contain lakes or oceans of liquid hydrocarbons. High-resolution images at infrared wavelengths that probe through Titan's atmosphere to the surface have enabled us to produce a complete surface albedo map at 2 microns. This map has a higher spatial resolution and greater contrast than any other available Titan surface map. We started a detailed study of the hazes in Titan's atmosphere, which show an interesting dawn-dusk asymmetry and a bright ring near Titan's south pole. We obtained excellent adaptive optics images of Neptune and Uranus, which we used to investigate weather patterns and changes in the atmospheric structure on these planets, and to derive ring particle albedos.

TITAN

We obtained excellent images of Titan in speckle imaging mode with the 10-mKeck telescope on Mauna Kea during the duration of previous grants,[2] which were synthesized into a complete surface albedo map at 2 μm during the past year.[4] The resolution of this map (Fig. 1) is close to the diffraction limit of the telescope(0.04"). The map shows clear bright and dark features,consistent with possible ice/rock “continents” and very dark regions thatmay be the elusive “ethane seas” predicted by photochemical models butnever before observed.[7] Over the past year we have observed Titan in the near-infrared (1-2μm) with the W.M. Keck Observatory Adaptive Optics (AO) system and inthe mid-infrared (8-13 μm) with the Keck Long Wave Spectometer(LWS). Most notable were our narrow band images (Oct. 30, 1999) in two filters (each ~1% bandwidth centered on 1.158μm and 1.702μm) which probe the atmosphere above the tropopause (Fig. 2). From measurements of a star, the AO system achieved a spatial resolution at 1.158 μm of 0.032", or 190 km on Titan. We observed a broad haze band extending overapproximately 60° of latitude centered slightly south of Titan's equator. This band has a prominent dawn-dusk asymmetry, which we now believe is a geometrical viewing (Sun-Titan-Earth) effect rather than intrinsic to Titan. Even more remarkable was the detection of a narrowbright ring at a latitude near 70°S; this feature was spatially unresolved in latitude and extended over all visible longitudes. Titan was reobserved in August 2000, and showed a similar structure. The bright ring near the satellite's south pole could be similar to the C_4N_2-ice seen by Samuelson *et. al.*[9] in Voyager spectra around the north pole during northern spring. Our observations were obtained during southern spring. Mid-infrared LWS images from the fall of 1999 and 2000 with a resolution of~0.25" clearly show east-west and north-south structure across thedisk of

Titan. We believe that this emission is thermal emission fromhigh-altitude haze layers. Spectra obtained in the fall of 2000 show numerous C_2H_6 lines. Graduate student Henry Roe has reduced all the data and made much progress in the analysis. To aid in the analysis, Henry developed a first-order radiative transfer model (DISORT) for Titan, which includes opacity by methane gas (using correlated-k data [5]), as well as scattering by hazes. He will now be able to use this model to interpret the data more qualitatively.

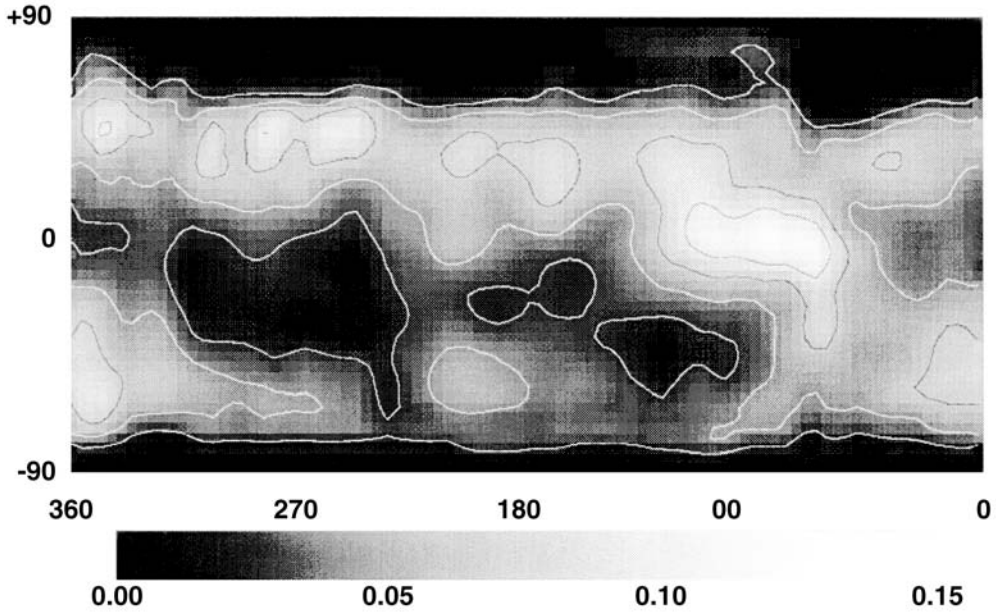

Figure 1: Surface albedo map of Titan at 2.1 microns (K band). Shown are latitude and longitude as well as a ``colorbar'' indicating the albedo.

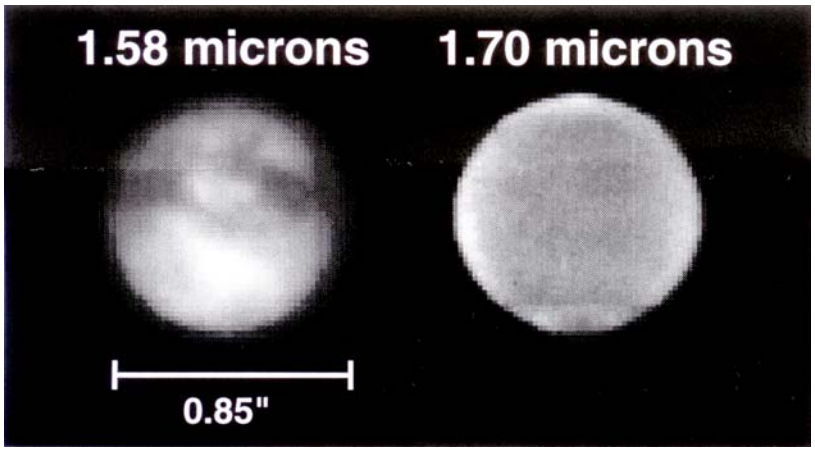

Figure 2: Adaptive optics images of Titan from the Keck Telescope. The image on the left (1.58 microns) probes Titan's surface; the image on the right (1.70 microns) probes only the haze layers in Titan's upper atmosphere.

NEPTUNE

We have used the NIRC speckle system at Keck in previous years to image Neptune at the diffraction limit of the telescope (0.04"). These data have been submitted for publication.[3] For the interpretation of the data we have been using a model atmosphere program from Kevin Baines (JPL), which student Henry Roe debugged and modified/improved substantially.

Our group observed Neptune with the AO system on the Keck II telescope several times during the year, a project which culminated in June 2000 with a large coordinated effort of tracking clouds over a 20-day period (we collaborated with Andrea Ghez at UCLA and Mike Brown at Caltech to extend the imaging baseline out to 20 days). During this period we took near-infrared images of Neptune with the slit-viewing camera SCAM on the AO/NIRSPEC system. During some of the sessions we obtained spectra of some of the brighter storm systems simultaneously with the images; these spectra have not yet been reduced, however. The images are spectacular (Fig. 3),revealing narrow zonal bands at 3-4 degree latitude spacings within bright regions and near the equator. There are three zones of latitude which contain bright features along zonal bands. The dimmest zone is located in the Northern hemisphere and extends from 20°N to 40°N. There are two bright zones located in the Southern hemisphere which extend from 20°S to 50°S, and from 60°S to 70°S. The zone near the South pole (a recently quiet region), contains a bright teardrop shaped feature which may be related to the Westerly jet observed by Voyager and reported by Limaye and Sromovsky[6] at a similar latitude. Analysis of these images, with .07" seeing, will lead to a detailed characterization ofthe morphology and time-evolution of the cloud features and of atmosphericwaves. This level of detail at these wavelengths was not possible before the advent of AO imaging. Such information may provide understanding ofthe mode of propagation and possibly of the origin of storm features on Neptune. Shuleen Martin is working on these data, which will form part of her Ph.D. research.

Henry Roe developed software to reduce NIRSPEC data. He applied this software to conventional NIRSPEC data on Neptune obtained by the NIRSPEC team, and submitted the results for publication.[8] He showed in a very elegant way from the spectra (conventional, i.e., low spatial resolution) that the cloud tops of Neptune's 'storm' are located near (just below) the tropopause. Shuleen will use the same algorithms to analyze theAO/NIRSPEC spectra obtained in June 2000.

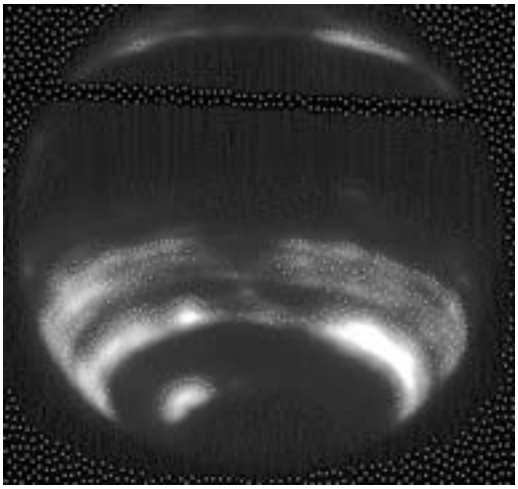

Figure 3: A Keck adaptive optics image of Neptune obtained in June 2000. The scale is ~2.5 arcseconds across the disk of Neptune.

URANUS

We observed Uranus with the AO/NIRSPEC system on the 10-m W.M. Keck telescope, UT June 17 and 18, 2000, at wavelengths between 1 and 2.4 μm. The angular resolution of the imagesis ~ 0.06-0.09". We identified eight small cloud features on Uranus's disk, four of which were in the northern hemisphere. The latter features are ~ 1000 - 2000 km in extent, and located in the uppertroposphere, above the methane cloud, at pressures between 1 and 0.5 bar. The motion of the clouds across Uranus's disk yield a wind velocity(prograde) of 166 $\pm$ 26 m/s at latitude +28°. The features at southern latitudes are invisible in the K' filter; we estimate these features to be at pressure levels of ~ 1.1-1.2 bar. We derived a wind velocity of 41$\pm$ 11 m/s at -27°, in good agreement with previous(Voyager/HST) results. Our images

further show Uranus's entire ring system (Fig. 4): the asymmetric ε ring, as well as the three groups of inner rings (outwards from Uranus): the rings 6,5 and 4, the α and β rings, and the η, γ and δ rings.

During the data reduction and analysis process we learned much about point spread functions (PSFs) in AO observations. We noticed that images where the AO loop was closed on Uranus (3.6" diameter) produce a secondary peak in the PSF, which created ring-loops in Uranus's ring system. As a first step we removed the artifacts by a simple cleaning procedure, where we assumed the rings to be symmetric about peri/apoapse.[1] We determined a PSF profile from observations of stars and Uranus's moon Miranda (for Miranda we closed the loop on Uranus). We noticed that, despite the fact that Uranus (mag=5.7) on the wavefront sensor was expected to be similar to a star of mag. 9-10, it displays a PSF profile in the core like that of a star with mag. ~11-11.5, and that the Strehl ratio is even lower, so that the halo is much more pronounced (we used the Miranda profile to simulate the halo). To determine ring particle albedos, we matched 1D scans through artificial rings to a 1D profile through the observations; we simulated the PSF by convolving model rings with images of stars and Miranda. Our derived ring albedos agree quite well with HST observations for the combined ringlets. We derived the equivalent width and ring particle reflectivity for each individual ringlet. It was not possible to resolve the ringlets with HST data because it had lower spatial resolution than Keck AO. Typical particle albedos are ~ 0.04-0.05, in good agreement with HST data at 0.9 m. The innermost rings appear to be somewhat darker. A paper detailing the results has been submitted.[1] This work was completed in close collaboration with graduate student Henry Roe and LLNL collaborator Bruce Macintosh.

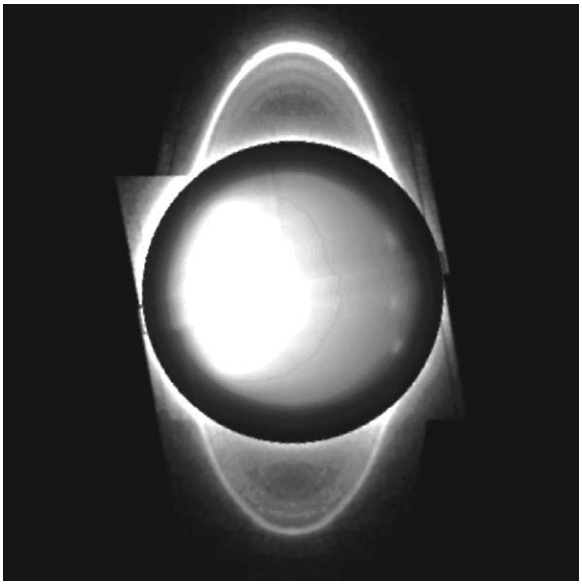

Figure 4: Keck adaptive optics image of Uranus and its rings at 2 micron, taken in June 2000. This image has been processed and rotated so that the rings are oriented north-south on the picture. The planet itself was darkened by a factor ~20 so both the rings (note the three fainter rings interior to the bright \epsilon ring) and details on the planet (note the south polar cap and the three northern cloud features) could be made visible in the same picture. (The disk of Uranus is 3.65'' across)

REFERENCES

1. de Pater, I., B. Macintosh, H. Roe, D. Gavel, S.G. Gibbard, and C.E. Max, *Icarus*, submitted (2000).

2. Gibbard, S.G. B. Macintosh, D. Gavel., C.E. Max, I. de Pater, A.M. Ghez, E.F. Young, and C.P. McKay, "Titan: High-Resolution Speckle Images from the Keck Telescope," *Icarus*, 139, 189-201 (1999).

3. Gibbard, S.G., I. de Pater, H. Roe, B. Macintosh, D. Gavel C.E. Max, K. H. Baines, and A. Ghez, "Lightning on Neptune," *Icarus*, submitted (1999).

4. Gibbard, S.G., B. Macintosh, D. Gavel, C.E. Max, I. de Pater, H. Roe, A.M. Ghez, E.F. Young and C.P. McKay, *Icarus*, submitted (2000).

5. Irwin, P.G.J., S.B. Calcutt, F.W. Taylor, and A.L. Weir, *J. Geophys. Res*. 101, 26137-26154 (1996).

6. Limaye, S.S., and L.A. Sromovsky, L.A., *J. Geophys. Res. Suppl.*, 96, 18,941-18,960 (1991).

7. Lunine, J.I., *Rev. Geophys. Space Phys.*, 31, 133 (1993).

8. Roe, H.G., J.R. Graham, I.A. McLean, I. de Pater, E.E. Becklin, D.F. Figer, A.M. Gilbert, J.E. Larkin, N.A. Levenson, H.I. Teplitz, and M.K. Wilcox, "The Altitude of an Infrared-bright Cloud Feature on Neptune from Near-Infrared Spectroscopy," *Astron. J.*, Submitted (2000).

9. Samuelson, R.E., L.A. Mayo, M.A. Knuckles, and R.J. Khanna, "C_4N_2 ice in Titan's north polar stratosphere," *Plan. Sp. Sci.*, 45, 941-948 (1997).

Direct Detection of Massive Planetary Companions to Young Stars (00-AP019)

Principal Investigator: Ben Zuckerman (UC Los Angeles)
LLNL Collaborator: Bruce Macintosh
Other Collaborators: Eric Becklin (UC Los Angeles)
Graduate Student: Denise Kaisler (UC Los Angeles)

Once its adaptive optics (AO) system became operational, the 10-m W. M. Keck II telescope became the most powerful instrument available for direct imaging of faint companions close to bright stars. We have used this AO system to search ~70 nearby young stars for substellar companions - brown dwarfs and massive planets. Two imaged objects appear to be brown dwarfs (masses in the range 15 to 75 times the mass of Jupiter). Another object, initially detected with the infrared camera on the Hubble Space Telescope, if confirmed with AO to be a companion to a very young star, would have a mass only about twice that of Jupiter.

OBJECTIVES

The past five years has seen the discovery of numerous giant planets in very close orbits around solar-type stars. These planets have been found indirectly through detection of the reflex motion of the star in response to the gravitational attraction of the planet. The objective of our project is, rather, to directly image giant planets that orbit further from their stars - specifically at distances comparable to or greater than the distances at which the giant planets orbit the Sun. In this way, we will help to elucidate whether our planetary system is ordinary or unusual. Our technique is to look for infrared emission at 1-2 microns wavelength emitted by warm young planets. The planet/star contrast for such planets is much more favorable than it is for cold planets that orbit around old stars. Indeed, the latter are not detectable with current AO sensitivities.

PROGRESS

The first step in our AO search for substellar companions was preparation of a list of young dwarf stars (age < 100 million years) within 80 pc of the Sun. We estimate that substellar (brown dwarf and massive planetary) companions would have near-infrared fluxes within a million times that of the stars about which they orbit.[1] This would be detectable with the Keck AO system at separations of 1-3" (see Figure for one representative example).

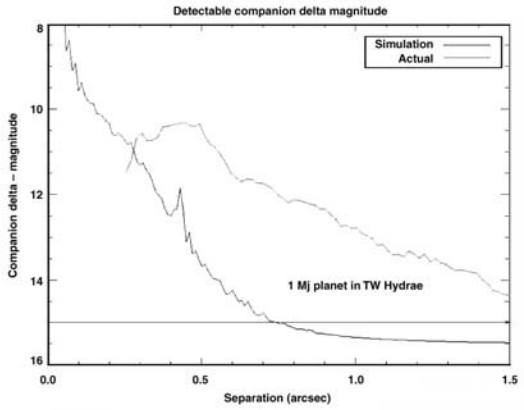

The figure shows the sensitivity of the Keck AO system to faint companions to stars. The heavy (lower) curve is the sensitivity our calculations (simulations) suggested would be achieved with the AO system when it became operational. The lighter curve above the simulation curve is what has actually been achieved. The LLNL group analyzed the actual performance and determined that irregularities in the Keck mirror segments have, so far, prevented us from reaching the simulated sensitivities. Even so, as the horizontal (1 Jupiter mass - Mj) line at delta-magnitude = 15 indicates, the actual sensitivity is sufficient to detect planets with masses as low as 1-2 Jupiter masses beyond an arc second from stars in the TW Hydrae Association.

We identified our target stars primarily on the basis of their space motions in a survey of the Hipparcos catalog. For example, one of our procedures involved calculation of the 3-dimensional space motions of the roughly 16000 Hipparcos stars with measured radial velocities and identifying those that have motions in the narrow range defined by Zuckerman & Webb[4] as representative of young stars in various nearby associations.

In addition, we supplemented our master list with stars derived from literature searches. We regarded large X-ray (ROSAT) fluxes in dwarfs later than F5, large lithium abundances, and H-alpha emission as indicators of youth. Our initial list comprises some 200 stars, but more will surely be added as we learn more about which stars near the Sun are, in fact, very young.

We previewed more than 100 of these stars at near-infrared wavelengths using the AO system installed on the Shane 3-m telescope at Lick Observatory. The main purpose of this Lick study was to identify, and reject, stars that have stellar companions with separations 1-2". Although substellar companions could exist in such systems, the radii of stable orbits would either fall below the Keck AO resolution limit (0.1"), or exceed the Keck AO field of view (4.5").[2] Thus, such binary pairs are unsuitable for our survey.

To date, we have observed 69 of our target stars with the Keck AO system, using the KCAM and NIRSPEC (SCAM) cameras. We have confirmed that a candidate companion to TWA5 is indeed associated with the primary star;[3] thus the secondary is a brown dwarf of some 30 Jupter masses. Another interesting candidate is in the field of GJ 559.1, its colors are consistent with an M dwarf spectrum. Given the age of the system, this would place its mass somewhere near the hydrogen burning limit (~75 Jupiter masses). Perhaps the most interesting object we have examined to date is a potential 2 Jupiter mass companion to a very young star (TWA6) in the TW Hydrae association. This object was detected initially with the NICMOS camera on the Hubble Space Telescope. We should be able to determine this year whether or not the object is a planetary-mass companion located about 100 Astronomical Units from TWA6.

REFERENCES:

1. Burrows, A., Marley, M., Hubbard, W. B., Lunine, J. I., Guillot, T., Saumon, D., Freedman, R.; Sudarsky, D., Sharp, C., "A Nongray Theory of Extrasolar Giant Planets and Brown Dwarfs", *Astrophys. J.*, 491, 856-875 (1997).

2. Holman, M.J. & Weigert, P.A., "Long-term Stability of Planets in Binary Systems", *Astronom. J.*, 117, 621-628 (1999).

3. Lowrance, P.J. et al., "A Candidate Substellar Companion to CD-337795 (TWA5)", *Astrophys. J.*, 512, L69-72 (1999).

4. Zuckerman, B. & Webb, R.A, "Identification of a nearby Stellar Association in the Hipparcos Catalog: Implications for recent local star formation," *Astrophys. J.*, 535, 959-964 (2000).

Neutrinos, the Baryon Loading Problem in Gamma-Ray Burst Models, and the Dynamics of Massive Objects (00-AP029)

Principal Investigator: George M. Fuller (UC San Diego)
LLNL Collaborators: James R. Wilson, Jay Salmonson
Graduate Students: Jason Pruet (UCSD) and Kev Abazajian (UCSD)

We have studied two problems possibly associated with the mysterious Gamma-Ray Burst (GRB) phenomenon. First, we discovered and are investigating a surprising connection between GRB fireball energetics, the baryon loading problem, and the weak interaction. Namely, we have found that the amount of energy required in the fireball to produce a given Lorentz factor in the final flow depends on the isospin of the baryons, i.e., on whether they are neutrons or protons. A significant neutron excess not only eases energy demands but can also lead to neutron decoupling in the relativistic flow and a host of secondary effects which could have distinctive observational signatures. Second, we have investigated the physics of stellar collisions, especially for neutron star mergers in dense clusters and related issues.

OBJECTIVES

Our objectives for this project were: (1) to investigate whether the baryon loading problem in GRB models depended in anyway on whether the baryons were neutrons or protons; and (2) to investigate the physics of stellar mergers, especially those mergers/collisions associated with large star cluster collapse and involving neutron stars. We realized a few years ago that isospin effects in the GRB environment had not been explored. The relatively small cross sections characteristic of the interactions of neutrons with the electron/positron/photon component of the GRB fireball plasma suggested to us that neutrons might decouple and afford an interesting solution to the baryon loading problem. The Lorentz factors of GRB fireballs, as inferred from observations, are large, of order a thousand, so that if significant numbers of baryons were moving with the flow the energy requirements are prodigious. But suppose the protons in the fireball are turned into neutrons. Does this help alleviate this baryon loading problem? What other implications would a neutron excess have for the GRB event? We also sought other explanations for the GRB energetics. In particular, could a collapsing cluster of stars give rise to many collisions and a significant Gamma-Ray flux?

PROGRESS AND CONCLUSIONS

We have made considerable progress on several aspects of the projects listed above and we are continuing to collaborate in an attempt to resolve key problems. This work will be the basis of UCSD graduate student Jason Pruet's PhD thesis and it will make up some of UCSD student Kev Abazajian's thesis. (Pruet will likely graduate during the next academic year; Abazajian will graduate this year and already he has accepted a postdoctoral position with the Fermilab Astrophysics Group starting August 2001.)

We have discovered a rich connection between neutrinos, neutrons, and the energetics/morphology of GRB fireballs. The beginnings of this work are written up in Fuller, Pruet, and Abazajian.[4] What if neutrons were truly noninteracting? Imagine that protons inertially tether an electron/positron/photon plasma via Thomson drag on electrons (or positrons). The drag on electrons/positrons influences protons through Coulomb interactions. If these protons were suddenly converted to noninteracting "neutrons," then the

fireball would expand relativistically, leaving behind the baryonic component! Real neutrons can approximate this limit, as they interact with the electron/positron/photon plasma only via the neutron magnetic dipole moment. (Electron-neutron scattering has a typical cross section some seven orders of magnitude smaller than the Thomson cross section, which is about 1 barn; while the neutron-photon scattering cross section is down from Thomson by twelve orders of magnitude.) Our calculations have shown, however, that the real limit on the efficacy of this mechanism is strong interaction neutron-proton scattering. This will dominate the energy transfer between neutrons and the plasma when conversion of protons to neutrons is incomplete.

Interestingly, Wilson and Salmonson, in a series of works, have shown that at least one venue suggested as a GRB central engine, neutron star mergers, can be extremely neutron-rich. Also, many compact object environments suggested as GRB central engines are dominated by neutrinos. We have worked out how the neutron/proton ratio in these environments can be influenced by matter-enhanced neutrino flavor transformation. Likewise, in these scenarios it is possible to produce extreme neutron excesses (with electron fractions < 0.1).

Once the neutrons have decoupled, they are left out of the subsequent acceleration of the fireball, while the residual protons are not. Pruet is developing a simple transport calculation to follow the evolution of both the neutron and proton (and electron/positron/photon) components of the plasma as the fireball accelerates. If the above scenario holds true then it is clear that we could have high momentum transfer collisions between energetic protons flowing with the bulk of the relativistic plasma and slower neutrons. This could result in the production of pions which could, in turn, alter the neutrino and electromagnetic signals of the GRB.

Additionally, such high momentum transfer neutron-proton collisions could result in the production of a slow proton component. Pruet, Abazajian, and Fuller have shown that under some circumstances the re-thermalization (re-acceleration) timescale for these slow protons could exceed the fireball evolution time.[2] In other words, a component of slow protons decouples. If this effect stands up, then the energy requirement for producing a GRB fireball with a given Lorentz factor would be even further reduced, potentially by orders of magnitude. (Essentially, only a small fraction of the protons would be moving with the highest Lorentz factors.) However, it is not at all clear that this effect will survive when collective plasma mode re-coupling processes are adequately modeled.

For example, a large dispersion in the velocities of the proton component could be subject to erasure through instabilities associated with charge neutrality/Compton scattering and with anisotropy-driven electromagnetic collisionless processes. We are continuing to try to model these effects. Wilson and Salmonson are attempting to modify their hydrodynamic neutron-star-merger code to see simple neutron decoupling as discussed above. We are also working together to estimate the effectiveness of plasma instabilities as outlined above.

We have made surveys of star cluster collapse parameters and Salmonson and Wilson and other LLNL collaborators have simulated Gamma-Ray production in relativistic stellar encounters. So far it is clear to us that the most favorable situation is the merger of two neutron stars. This is by far the most efficient generator of Gamma-Rays. The role of the dense star cluster may be to facilitate one or a few such events. We are continuing this study.

It is important to note that Abazajian, Pruet, Fuller and Salmonson and Wilson have made a number of trips to facilitate this collaboration (Abazajian and Pruet to LLNL once; Salmonson and Wilson to UCSD twice). More collaboration trips are planned. We are working on writing up our exploration of star clusters and collisions,[3] and we are continuing or joint study of baryon decoupling in GRB fireballs and eventually we hope to write a joint paper on this work as well.

REFERENCES

1. G. M. Fuller, J. Pruet, and K. Abazajian, "Can a Large Neutron Excess Help Solve the Baryon Loading Problem in Gamma-Ray Burst Fireballs?" *Phys. Rev. Lett.*, 85, 2673 (2000).

2. J. Pruet, K. Abazajian, and G. M. Fuller, "A New Connection between Central Engine Weak Physics and the Dynamics of Gamma-Ray Burst Fireballs," *Phys. Rev. D*, submitted (2001).

3. J. Salmonson, J. R. Wilson, K. Abazajian, and G. M. Fuller, "Colliding Stars and Gamma-Ray Bursts," in preparation (2001).

4. K. Abazajian, J. Pruet, and G. M. Fuller, "The Link between Neutrons, the Weak Interaction, and the Gamma-Ray Burst Baryon Loading Problem," Jan. 7 ,2001, *Bul. Am. Astron. Soc.*, in press.

Optical and Infrared Photon-Counting Nanobolometry with Potential On-Chip Refrigeration (00-AP032)

Principal Investigator: Andrew Cleland (UC Santa Barbara)
LLNL Collaborator: Simon Labov
Other Collaborator: Philip Lubin (UC Santa Barbara)
Postdoctoral Fellow: Joel Ullom

This project is aimed at developing mechanically suspendednanometer-scale bolometers, with the potential for on-chip electronic refrigeration. The approach we are pursuing is to fabricate normal metal-insulator-superconductor (NIS) tunnel junctions for use as thermistors and refrigerators, and to incorporate these on top of a nanopatterned block of insulator or semiconductor. The project plan was to first develop techniques to fabricate a single device, and then proceed with electronic tests at cryogenic temperatures to understand the thermal and electronic properties of these novel devices. Additional support for this project has been provided by NASA under their Explorer Technology funding series.

OBJECTIVES

The integrated nanostructure should provide an environment with a very weakly coupled thermal link to the external environment, where both the electronic and phonon coupling are strongly reduced from the bulk values, due to the reduction in geometric cross-section. We have spent the one-year funding period of this project (funding was received in October of 1999) developing a suitable fabrication scheme. We had previously demonstrated the ability to make mechanically suspended single crystal structures, and demonstrated the ability to separately fabricate SIS tunnel junctions. Integrating these two separate capablities proved to be much more challenging than was intially anticipated, mostly due to issues relating to materials incompatibility during different process stages.

PROGRESS

After much effort, we have succesfully developed a fabrication recipe that involves the use of a suspended PMMA resist bridge, patterned by e-beam lithography with excellent alignment to the pattern for the mechanically suspended structure. The resist bridge is fabricated using a bilayer resist consisting of a copolymer (MMA-MAA) underlayer, with high electron-beam dosage sensitivity, and a top layer of PMMA with high pattern resolution. The tunnel junctions are then fabricated by successive angled evaporations with an intermediate oxidation step.

An SEM micrograph showing a double SINIS tunnel junction structure before and after nanopatterning the substrate is shown in Figure 1 and Figure 2. Using this technique we have also fabricated nanometer scale Al-Al oxide-Al tunnel junctions, with lateral dimensions of 0.1x 0.1 μm^2 and tunnel resistances in the range of 100-200 k. These have identical appearance to those shown in Fig. 1 but are difficult to view in an SEM due to the low scattering cross-section of electrons from the thin Al layers.

The successful fabrication approach is as follows:

1. Nanopatterning, anisotropic etching, and physical suspension of structures based single-crystal GaAs. These structures have minimum lateral dimensions of 0.1 μm, and thicknesses of 0.2 μm. Patterning is accomplished by a combination of photolithography and electron beam lithography, and the anisotropic etching accomplished through the use of chlorine-based reactive ion

beam etching. The substrates we are using include a buried sacrificial AlGaAs layer. This buried layer is removed through the use of a wet etchant which selectively removes it; we use hydrochloric acid for the AlGaAs layer, an etch which is timed to allow release of the suspended structure but insufficient for full liftoff of the top layer of the wafer.

2. The devices include gold leads for large-area wire-bond contacts for electrical transport measurements, and to couple microwave radiation; these are seperately patterned by photolithography and aligned with roughly 0.5 μm accuracy to the nanopatterned suspended structure.

3. The NIS tunnel junctions are fabricated using an e-beam patterned layer positioned with 0.05 μm accuracy to the pattern for the suspended structure. We use Al as the superconducting material, and Cu as the normal metal, with a junction fabrication technique based on successive metal evaporation, oxidation and evaporation in a single vacuum pumpdown. This approach to junction fabrication is highly reliable and in general produces tunnel junctions with 10% uniformity in critical current density and tunnel resistance-capacitance (RC) product. The single-pumpdown approach is usually accomplished by using suspended PMMA resist bridges as shadow masks.

Figure 1. Integrated double NIS tunnel junctions with suspended nanostructure. Large finger pattern allows DC and infrared electrical coupling to the device in center of micrograph. Substrate is single crystal GaAs. Scale bar is 10 microns.

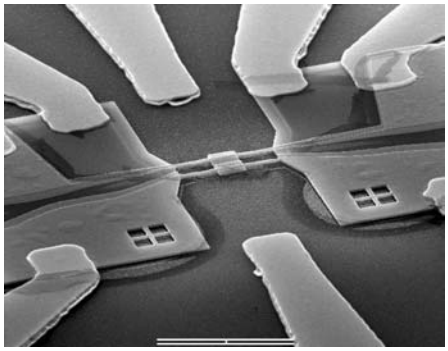

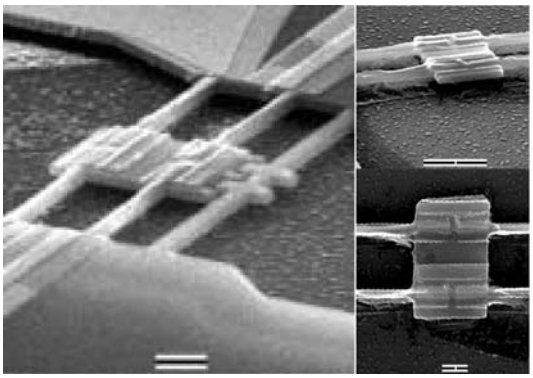

Figure. 2. Suspended double NIS tunnel junctions with geometry similar to that shown in Fig. 1. Three views are shown of two different geometries. Junctions are Cu-Al oxide-Al. Scale bars are 1 micron. Substrates are single-crystal GaAs.

Electrical and cryogenic tests are performed on a ^{3}He-^{4}He dilution refrigerator with a base temperature of 20 mK. We use a conventional bias circuit applying a control voltage across the combination SINIS junction, and measure the current through the device using room temperature amplifiers. The input noise of the amplifier generates an estimated 10^{-20} W of power in the device. A resistance-bias voltage characteristic is shown in Figure 3; in Figure 4 we display the zero-bias conductance as a function of temperature, along with a fit from BCS theory. We find that the zero-bias conductance can be well explained by BCS theory with the addition of a small gap smearing of 5% of the superconducting gap, typical for these thin-film devices.

We can estimate the noise-equivalent power for this device, using the estimated heat capacity for the suspended structure as well as the electrical noise in the readout thermistor. A plot comparing our existing device with other devices is shown in Figure 5. A second version is being worked on which should show improvement over that in the figure.

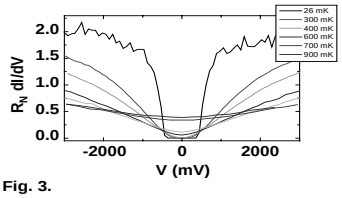

Fig. 3.

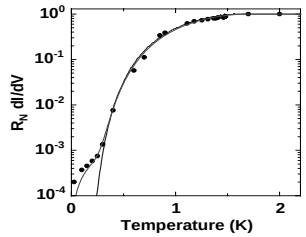

Fig. 4.

Figure 3. Thermistor resistance as a function of bias resistance. The exponential dependence at low bias voltage is used to extract electron temperatTemperature (K)

Figure 4. Thermistor conductance as a function of temperature. The solid line is the fit to BCS tunneling theory.

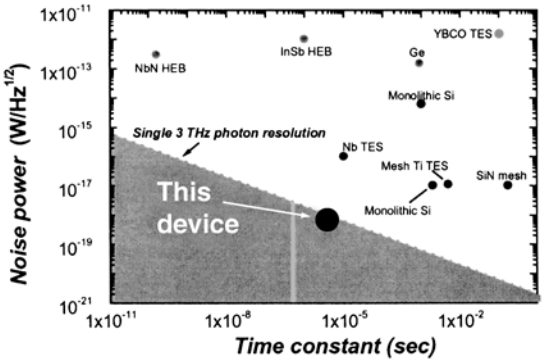

Figure 5. Estimate of the electrical noise-equivalent power for this device, compared to a number of existing bolometer designs. This device is competitive with the state-of-the-art, and future developments now under way should lead to a factor of 10 improvement in performance.

We are also interested in on-chip cooling using electronic refrigeration. At this point we have not completely understood the thermal circuit or electrical issues that will allow us to explore this. Our next device design should allow us to measure this.

In summary. we have succesfully fabricated a prototype device which shows state-of-the-art noise performance. Further device developments, as well as optical tests, are underway using other funds. Figure 5. Estimate of the electrical noise-equivalent power for this device, compared to a number of existing bolometer designs. This device is competitive with the state-of-the-art, and future developments now under way should lead to a factor of 10 improvement in performance.

Initiation Age and Rate of E-W Extension in Northern Tibet: Implications for the Dynamic Cause of Tibetan Uplift (99-GS-005)

Principal Investigators: A. Yin and T. Mark Harrison (UC Los Angeles)
LLNL Collaborator: F. J. Ryerson
Student: M. H. Taylor (UC Los Angeles)

In order to evaluate the role of east-west extension within the Tibetan plateau, detailed geologic mapping was conducted to constrain the geometry and kinematics of active extensional fault systems in central Tibet. The results of this research suggest that north-south trending rifts in Tibet are linked with conjugate strike-slip faults. In North Tibet, active NE-striking left-slip faults are dominant in its southern part, which are in turn linked with north-south normal faults in its northern part. In South Tibet, however, strike-slip faults are right-slip and NW-trending. They are dominant in the north and are linked with a series of north-south trending normal faults in the south. The two strike-slip fault systems merge along the Bangong-Nujiang suture zone, which separates the North and South Tibet blocks. Surface mapping along the Mayer Kangri fault in North Tibet suggests that its left- slip magnitudes 11-I 6 km) and slip rates (2-3 mm/yr) are similar to those of its conjugate right-slip fault in South Tibet. This suggests that North Tibet is not a rigid block extruding eastward as a whole. Instead, it has been undergoing distributed eastward spreading via both conjugate strike-slip faulting and east-west extension in the Cenozoic. More accurate determination of slip rates along strike-slip faults both in North and South Tibet is being currently conducted at UCLA and LLNL.

OBJECTIVE

The active deformation in the interior of the Tibetan plateau is characterized by east-west extension based on earthquake focal mechanisms and interpretations of satellite imagery. In South Tibet, the east-west extension has been interpreted to be expressed by the development of both strike-slip and normal faults. However, whether North Tibet is extending at all and how E-W extension and strike-slip faulting are linked were not clear, due to the lack of direct field observations. Because of this, the importance of extrusion tectonics of North Tibet as a rigid block remained unconstrained. This led to a 2-month geologic expedition in the summer of 1999 along the Mayer Kangri fault system, a prominent rift in North Tibet.

PROGRESS

From northeast to southwest, the Mayer Kangri fault system consists of three distinctive segments (Figure 1): (1) the Northeast Segment is a 90-km long left-slip fault, which trends N35°E and is linked with a pull-apart basin in the Central Segment to the south; (2) the Central Segment is a 13 0-km long and 50-km wide pull-apart basin, which is bounded by a west-dipping normal fault system trending N 1 0°E at its eastern side and is linked with a left-slip fault system in the Southwest Segment in the south, and (3) the Southwest Segment is a 120-km long, N65°E-trending fault zone, which is linked with the Central Segment in the north and terminates near the Bangong-Nujiang suture in the south.

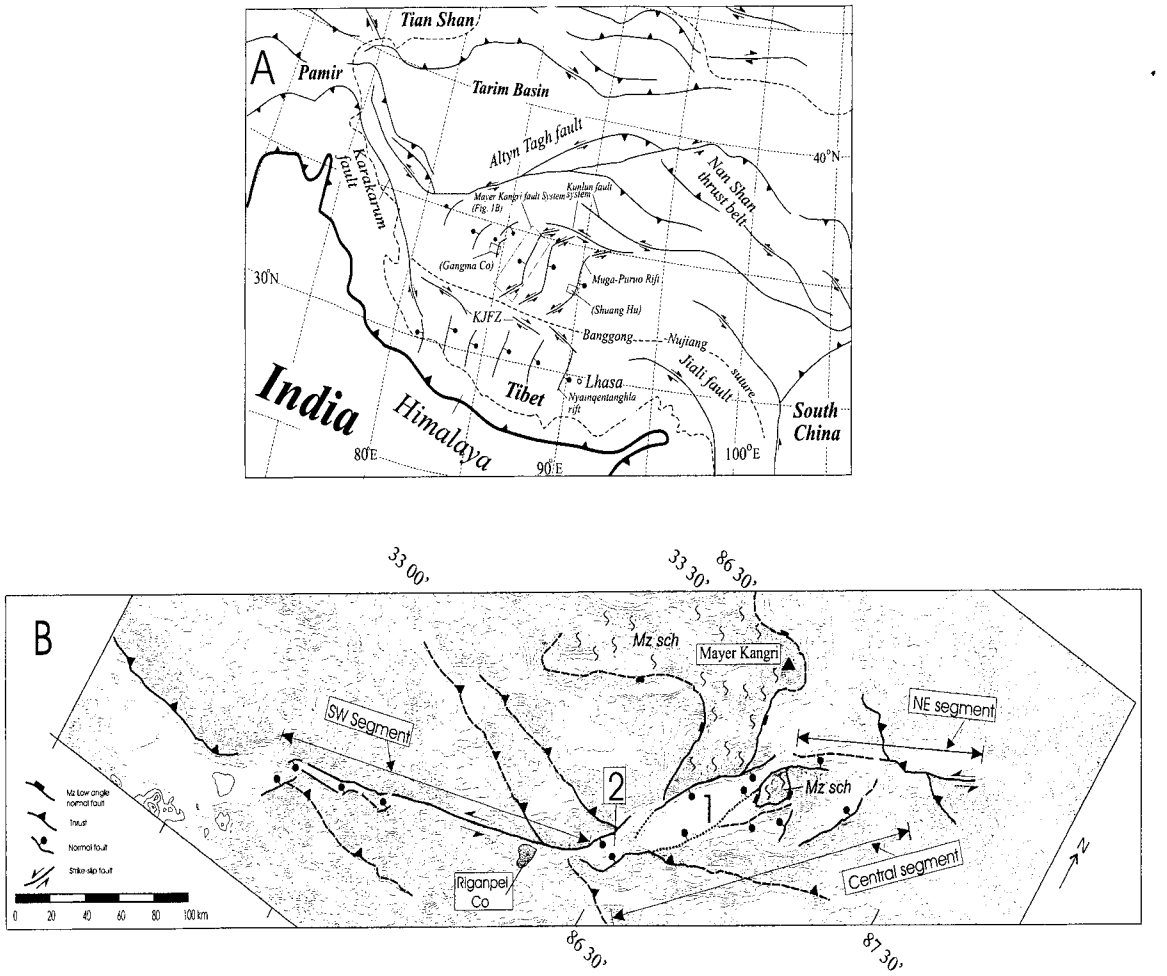

A. Regional tectonic map of the tibetan plateau and its neighboring regions. The Mayer Kangri fault system lies between the Gangma Co and Shuang u rifts. KJFZ is the Karakorum-Jiali fault zone. B. Simplified gologic map of the Mayer Kangri falut system. The system is topographically defined and consists of three distinct segments. 1, Zaga basin; 2. Ringanpei Co pull-apart basin; Msz sch, Mesozoic schist; Contour interval = 100 m.

Northeast Segment

A thrust juxtaposing Paleozoic carbonate strata over shallow-dipping Tertiary red beds is systematically offset left laterally by the Mayer Kangri fault system into three segments. On the west side of the Mayer Kangri fault, the thrust changes its strike westward, from N90°E in the east to N30°E in the west. The dip of the strata become subvertical as they approach the fault due to oroclinal bending. The thrust is offset by a left-slip fault for - 5 km to the west. This central segment of the thrust is in turn offset left laterally by another left slip fault to the west for ii km (Figure 1). Thus, a total amount of -16 km left-lateral separation is indicated by the offset of this distinctive thrust. Kinematic indicators observed on fault surfaces that truncate the thrust display dominantly subhorizontal striations with a slight normal-slip component. Left slip along the NNE trending faults in the Mayer Kangri fault system is also indicated by offsets of stream channels varying in magnitude from ~300 m to ~1500 m.

Central Segment

The Central Segment of the Mayer Kangri system is characterized by a broad basin that links

with the Northeast Segment left-slip fault in the north and Southwest Segment left-slip fault in the south. This basin is formed as a dilational stepover between the two left-slip faults (Figure 1). Kinematic indicators

along basin-bounding faults in this nearly N-S trending segment of the Mayer Kangri system suggest it is dominated by normal faulting and east-west extension. In particular, its west-dipping normal fault system along its eastern margin has resulted in a broad east-dipping section of strata in its hanging wall.

Southwest Segment

Estimates of fault offsets (separations) along the Southwest Segment of the left-slip Mayer Kangri system (northeast of Riganpei Co) (Figure 1) are possible by correlating a system of south-directed thrusts which are offset by the strike-slip fault in a similar manner to the Northeast Segment in the north. South-directed thrusts are characterized by juxtaposition of massive Permian limestone in the hanging wall over Tertiary red beds in the foot-wall. Thrusts themselves are commonly tightly folded into E-W trending antiformal structures, with erosional windows exposing the thrust contacts. A correlation of similar stratigraphic relationships and the south-directed thrusts across the Mayer Kangri fault yields an estimate of 11-16 km left-lateral separation. As kinematic indicators collected on fault surfaces suggest sinistral motion with a slight normal component, the observed left-lateral separation of thrusts reflects closely the magnitude of left slip motion along the Southwest Segment of the Mayer Kangri fault system.

INITIATION AGE OF THE MAYER KANGRI RIFT SYSTEM

Northeast of Riganpei Co at the northern end of the Southwest Segment, a morphologically defined small pull apart basin with dimensions of-4 km x 4 km was mapped. Incision by a modem drainage perpendicular to two active normal fault traces reveals their cross-sectional geometry. The continuous extent of the faults on map view is -1500 m, which displays normal offsets of Quaternary fan surfaces. The faults strike N25°E and dip 70°SE. Two topographic profiles were measured from each fault scarp, which are used to determine the oldest possible age of the fault scarp using the linear diffusion model of Avouac (1993).

$$\tan\theta = a/(\pi\tau)^{1/2-} + b$$

where θ is the maximum slope angle of the fault scarp, a is half the scarp offset, and b is the regional slope angle. We use a fault dip angle of S to be 60° and the total slip of S can be calculated as $S = 2a/\sin\delta$ The characteristic time for diffusion is τ; defined as $\tau = \kappa\tau$ (κ is the coefficient of mass diffusivity, and τ is the age of the fault scarp). We use the κ value from southern Tarim as a lower bound in central Tibet,[3,8] due to the higher altitude and permafrost setting.[6] Averaging the two scarp profiles results in ~8 m offset of the alluvial fan surface. This yields ~2 ka for the oldest age of the scarp and 3 mm yr' for its minimum slip rate. If we assume a 10 km of total normal slip across the normal fault bounding the pull-apart basin as required by the magnitude of the kinematically linked left-slip fault in the south, the initiation age of the pull apart basin may be inferred to be ~3.2 Ma. This age is similar to that estimated for the Shuang Hu rift,[7,8] some 200 km to the east (Figure 1).

SUMMARY

Recent field studies were conducted in three rifts in North Tibet, spanning an east-west distance of - 500 km. They are the Shuang flu ,[4,8] Gangma Co,[5,8] and the newly discovered left-slip transtensional Mayer-Kangri (this study) rift systems (Figure 1). The widely distributed rifts in North Tibet suggest that eastward extrusion of rigid North Tibet via the Karakoram-Jiali fault zone is an inadequate kinematic description of Late Cenozoic deformation within the Tibetan plateau. Instead,[1,2] the presence of widespread extensional

structures and kinematically linked NE-trending left-slip faults in North Tibet and the NW-striking right-slip faults in South Tibet suggests that active deformation is Tibet is distributed over its entire region. This conjugate-fault relationship implies that the Tibetan plateau is currently undergoing eastward spreading via distributed strike-slip faulting and kinematically linked normal faults. Deformation of Tibet is best characterized by contrictional strain with relatively uniform east-west extension and coeval north-south compression. The conjugate-strike-slip interpretation requires that the slip magnitudes and slip rates along the left-slip fault in North Tibet and right-slip faults in South Tibet are comparable. This prediction is being currently tested via cosmogenic dating at LLNL and by further field mapping in the coming summer.

REFERENCES

1. Armijo, R., Tapponnier, P., Mercier, J. L., and Han, T.-L., 1986, "Quaternary extension in southern Tibet: Field observations and tectonic implications," *Geophys. Res.*, 91, 13803-13872.

2. Armijo, R., Tapponnier, P., and Tonglin, H., 1989, "Late Cenozoic right-lateral strike-slip faulting in southern Tibet," *Geophys. Res.*, 94, 2787-2838.

3. Avouac, J. P.., and Peltzer, G., 1993, "Active tectonics of the southern Xinjiang, China: Analysis of terrace risers and normal fault scarp degradation along the Hotan-Qira fault system," *Geophys. Res.*, 98, 21.1773-21,807.

4. Blisniuk, P. M., Siwen, S., Kuchel, 0., and Ratschbacher, L., 1998, "Late Neogene extension in the Shuang Hu graben, central Tibet," EOS (Transactions, American Geophysical Union), 79, 794.

5. Kapp, P., Yin, A., Manning, C. E., Murphy, M., Harrison, T. M., and Spurlin, M., 2000, "Blueschist-bearing metamorphic core complexes in the Qiangtang block reveal deep crustal structure of northern Tibet," *Geology.*

6. Liao, K., 1990, Atlas of the Qinghai-Xizang Plateau: Beijing, Institute of Geography, Science Publishing House, 237

7. Siwen, B., Blisniuk, P., Hacker, B., Glodny, J., Ryerson, R., and L., R., 1999, "Timing of Late Neogene extension in central Tibet," *EOS Trans.*, 80, 46, F1015.

8. Yin, A., Kapp, P. A., Murphy, M. A., Harrison, T. M., Grove, M., Ding, L., Deng, X., and Wu, C., 1999, "Significant late Neogene east-west extension in northern Tibet," *Geology*, 27, 9, 787-790.

The Isotopic and Chemical Composition of Carbonaceous Matter Produced by Serpentinization—An Exploration of a Potential Fischer-Tropsch Type Reaction Process (99-GS-006)

Principal Investigators: Stephen J. Mojzsis and Craig E. Manning (UC Los Angeles)
LLNL Collaborator: Kevin Knauss
Graduate Student: Alice A. Ormsbee (UC Los Angeles)

Carbon isotope distributions have long been used to identify, and make inferences about, the role of life in the geochemical cycling of carbon between the atmosphere, hydrosphere and lithosphere (Wickman, 1952). The kinetics of metabolic processing of carbon discriminates against the heavy isotope (^{13}C) to form "light" bioorganic matter, and provides what is considered a unique signature of life from isotopic measurements of the residues of biological processes. Hence, based on interpretations of the isotopic compostions of reduced organic carbon (C_{org}) in sediments, practically all organic matter preserved in the geologic record is held to be of biological origin. However, several experimental attempts have been made to test inorganic means of producing isotopically fractionated C_{org} of the maginitude and sign characteristic of metabolic cycling, with uncertain and conflicting results (e.g. Lancet and Anders, 1970; Yuen et al., 1986). Recent studies by Berndt et al. (1996) have shown that the serpentinization of olivine (Fo_{88}) under experimental hydrothermal conditions (300^o C and 500 bar) produces a host of "amorphous carbon particles" throughout the olivine reaction medium, via the purported reduction of CO_2 from the reation CO_2 goes to C + O_2, and at high (~75%) yield (although other reation paths are possible). The collaborative work here between UCLA and LLNL will 1) seeks to reproduce the products of this reaction scheme under conditions mimicking the pervasive hydrothermal alteration of oceanic crust, 2) explore the range of variable (fO_2, pCO_2, pCH_4, water/rock ratio etc.) conditional to the proposed experiment, and observed in nature, and 3) analyze the carbon isotopice fractionization between reactanct CO_2 and product C($\Delta\delta^{13}C$) as the reaction proceeds, by both conventional mass spectometry and in situ isotope compositional analysis of individual carbon particles using an ion microprobe. We will test the hypothesis that efficient production of reduced carbon by serpentinization may play a role in the inventory of reduced carbon in the crust at present. Furthermore, if significant amounts of reduced carbon are produced which are also isotopically fractionated to a degree that mimics the activity of life, then the presence of such material in the geologic record must be interpreted with caution. The impact of the Fischer-Tropsch process during metamorphism on the problems of the golobal carbon cycle, the origin of life, and early Earth condidtions must be addressed.

Timing of Late Quaternary Slaciation in the Hunza Valley, Karakoram Mountains, Northern Pakistan (99-GS-008)

Principal Investigator: Lewis A. Owen (UC Riverside)
LLNL Collaborators: Robert Finkel and Marc Caffee
Post-doctoral Researchers: Lyn Gualtieri and Joel Q. Spencer (UC Riverside)

Landforms and sediments that record multiple glaciations in the Hunza Valley, Karakoram Mountains, Northern Pakistan and in the Lahul Himalaya, Northern India were examined during two field seasons. Samples were collected for ^{10}Be and ^{26}Al cosmogenic radionuclide and optically stimulated luminescence dating to constrain the timing of glaciation. The data shows that glaciations in these regions reflect changes in the mid-latitude westerlies that are broadly synchronous with changes in the Northern Hemisphere ice sheets and oceans.

OBJECTIVES

Glacial landforms and sediments in the Hunza Valley of Northern Pakistan provide one of the best records of glacial fluctuations within the Himalayan-Tibetan region. At least eight glacial advances of varying magnitude during Late Quaternary times have been recognised, yet previous attempts to date these events have failed because of the lack of organic material for radiocarbon dating. However, cosmogenic radionuclide and optically stimulated luminescence (OSL) dating provide methods for dating these landforms and sediments. Constraining the ages of these glacial phases will provide the most detailed record for Late Quaternary glaciation in the high mountains of Central Asia. This is important for quantifying the rates and magnitudes of earth surface processes to help formulate and test geologic and climatic models for the evolution of the high mountains of Central Asia.

PROGRESS

Owen, Finkel, Caffee and Spencer undertook fieldwork in the Hunza valley during May-June 1998 to examine the glacial sediments and landforms, and to collect samples for cosmogenic and OSL dating. Owen and Gualtieri were able to extend the scope of the project by undertaking fieldwork in August 1998 in the Lahul Himalaya of Northern India. During this fieldwork they examined the glacial history of the region and collected samples for cosmogenic dating. At the LLNL, Gualtieri, Finkel and Caffee measured the ^{10}Be and ^{26}Al cosmogenic radionuclides in the samples collected from both Hunza and Lahul. The dates obtained are shown in Figures 1 and 2. Spencer dated 12 sediment samples from Hunza in the new OSL laboratory at UCR (Table 1).

The cosmogenic and OSL dates from Hunza show that at least six, and probably seven, of the glacial advances in this region occurred during the last glacial cycle (Figure 1). These glacial advances have a periodicity that is in the order of ~ 10 ka and they are likely to be coincident with Bond cycles that reflect fluctuations in the Northern Hemisphere ice sheets and oceans (Figure 1). In the Lahul Himalaya, the cosmogenic radionuclide dates constrain the timing of deglaciation of two glacial stages, the Batal and Kulti Glacial Stages, to ~13-17 ka and ~9-12 ka, respectively (Figure 2). Deglaciation at the end of the Batal Glacial Stage was probably synchronous with the Late Glacial Interstadial. This was followed by a short period (~1000 years) when glaciers of the Kulti Glacial Stage advanced ~10 km beyond their current positions. This advance was probably synchronous with the Younger Dryas Stade. Deglaciation of the Kulti Stage occurred towards the end of the Younger Dryas Stage and during the early

Holocene. Both sets of data show that glacier oscillations these high mountains at the SW margin of the Tibetan Plateau probably reflect changes in the mid-latitude westerlies that are broadly synchronous with changes in the Northern Hemisphere ice sheets and oceans. We are now extending this work as part of a new IGPP/LLNL grant by dating glacial successions at the NE and South Central margins of the Tibet Plateau. This will test if glaciation is synchronous across the Tibetan Plateau.

The dates obtained in this project are the first comprehensive set of data for any region of the Himalayan and Tibetan region. A paper on the Lahul results has been submitted to Geology and we are preparing a paper for Nature describing the Hunza results. .

Sample #	Glacial Stage	IRSL dates (ka)	GSL dates (ka)
Hunza 24	t8	11.9±1.2; 9.1±0.7	
Hunza 22	t7	15.4±1.7; 21.8±1.9	
Hunza 20	t6	13.7±1.8; 13.5±1.2	
Hunza 17	Below t6	42.1±6.1; 50.8±5.6	
Hunza 27		75.7±8.9; 66.3±7.6	8.2±0.9; 27.8±3.0; 30.6±3.5; 54.5±5.9
Hunza 11		45.6±3.5	
Hunza 4	Above t5	8.7±1.0	
Hunza 18	t5	11.5±1.9	
Hunza 38	Below t5	70.3±6.6	
Hunza 32	t4	47.9±6.2; 63.1±6.6	24.2±3.0; 35.0±3.7; 39.9±4.2; 47.7±5.1
Hunza 8	Below t4	44.0±5.2	
Hunza 30	t3	124.6±8.1;157.7±20.0	

Table 1. OSL dates for samples from Hunza. IRSL – infrared stimulated luminescence on coarse grained feldspar fractions; GSL –green light stimulated luminescence on coarse-grained quartz.

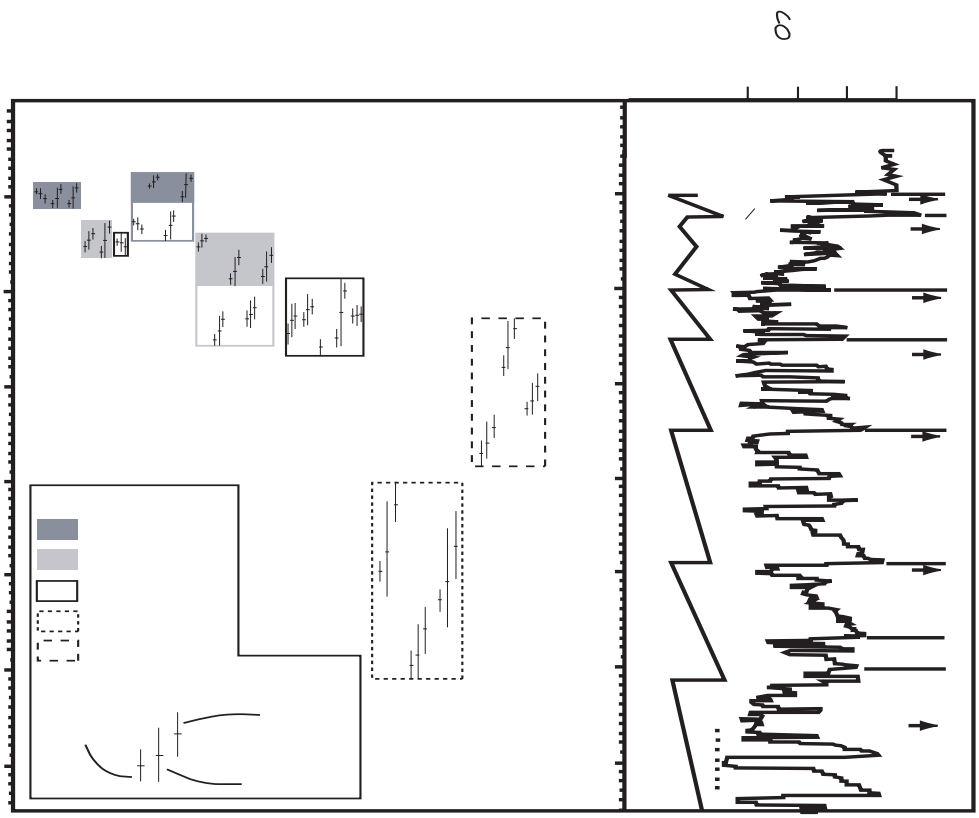

Figure 1. Cosmogenic radionuclide dates for the Hunza valley compared with the oxygen isotope data from Summit Ice Core in Greenland and Heinrich events (H1-H5) that are proxies for oscillations in the northern Hemisphere ice sheets and oceans (1 & 2).

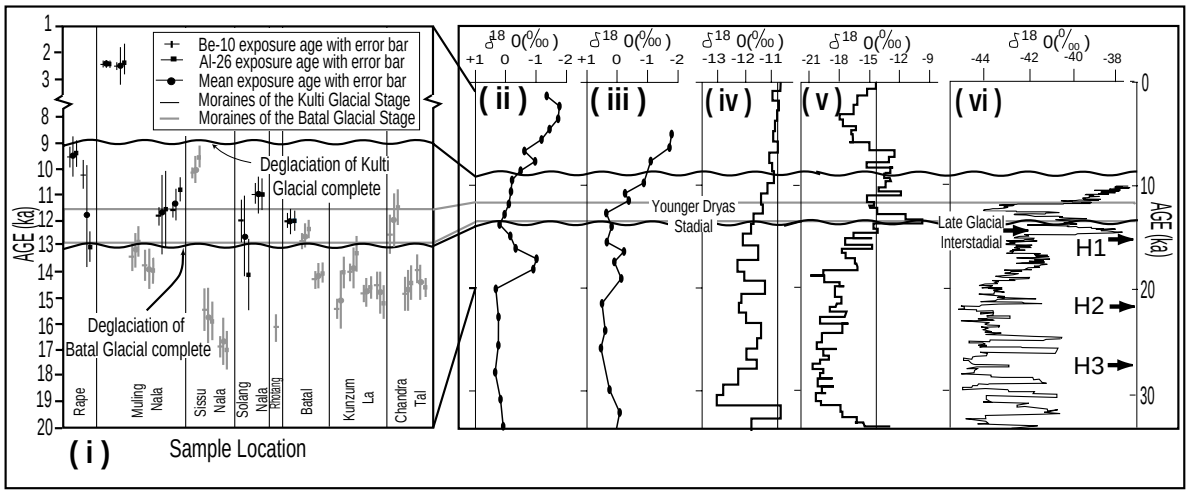

Figure 2. Comparison of the cosmogenic radionuclide dates for deglaciation in the Lahul Himalaya (i) with d18O data from (ii) Globigerinoides sacculifer in core SK-20-185 from the East Arabian Sea (3), (iii) Globigerinoides sacculifer in core CD-17-30 off the coast of the Oman (1), (iv) the Dunde Ice Cap core in Tibet (4), (v) the Guliya Ice cap core in Tibet (5) and (vi) the Summit Ice Core in Greenland (1). The gray horizon band show the duration of the Younger Dryas Stade. H1, H2 and H3 in part (vi) show the timing of Heinrich events between during the last 30 ka (2).

REFERENCES

1. Dansgaard, W., Johnson, S.J., Clausen, A.B., Dahl-Jensen, D., Gundestrup, N.S., Hammer, C.U., Avidberg, C.S., Steffensen, J.P., Sveinbjornsdottir, A.E., Jouzel, J. and Bond, G., 1993, "Evidence for general instability of past climate from a 250-kyr ice-core record," *Nature*, 364, 218-220.

2. Bond, G., Heinrich, H., Broecker, W., Labeyrie, L., McManus, J., Andrews, J., Huon, S., Jantschik, R., Clasen, S., Simet, C., Tedesco, K., Klas, M., Bonani, G. and Ivy, S., 1992, "Evidence for massive discharges of icebergs into the North Atlantic during the last glacial period," *Nature*, 360, 245-249.

3. Sarkar, A., Ramesh, R., Battacharya, S.K. and Rajgopalan, G., 1990, "Oxygen isotope evidence for a stronger winter monsoon current during the last glaciation," *Nature*, 343, 549-551.

4. Thompson, L.G., Thompson, E.M, Davies, M.E., Bolzn, J.F., Dai, J., Gunderstrup, N., Wu, X., Klein, L. and Xie, Z., 1989, "Holocene-Late Pleistocene climatic ice core records from the Qinghai-Tibet Plateau," *Science*, 246, 474-477.

5. Thompson, L.G., Yao, T., Davis, M.E., Henderson, K.A., Mosley-Thompson, E., lin, P.-N., Beer, J., Synal, H.A., Cole-Dai, J. and Bolzan, J.F., 1997, "Tropical climate instability: the Last Glacial Cycle from a Qinghai-Tibetan Ice Core," *Science*, 276, 1821-1825.

3D Modeling of Structure in D" (99-GS-013)

Principal Investigator: Barbara Romanowicz (UC Berkeley)
LLNL Collaborator: Shawn Larsen
Graduate Student: Ludovic Breger (UC Berkeley)
Postdoc: Hrvoje Tkalvcic (UC Berkeley

We have analyzed the effects of the heterogeneous D" on PKP differential travel timeresiduals, traditionally used to probe the bulk of the inner core. PKP(AB-DF) travel times are very sensitive to mantle structure, and can almost be solely explained by D" heterogeneity. PKP(BC-DF) differential travel time residuals exhibit some systematic lateral variations that could again be explained by extreme mantle velocity anomalies. They also preclude any simple inner core structure, such as a homogeneous axisymmetric anisotropy. Finally, we have shown that P'P' absolute and differential travel time residuals were inconsistent with a strong (~3.5%) anisotropy in the inner core.Our results suggest that the effects of complex structure in the deep mantleshould be carefully considered in order to reliably estimate the anisotropic structure of the inner core, and that the contamination of differential residual ssuch as PKP(AB-DF) and PKP(BC-DF) by strong D" heterogeneity could have been so far severely underestimated.

OBJECTIVES

Fifteen years ago, Poupinet *et. al.* showed that waves turning in the inner core and travelling parallel to the Earth rotation axis were on average 1 to 2s faster than those propagating along the equatorial plane.[9] Those observations were later interpreted in term of inner core anisotropy,[8] which could simulteanously explained the anomalous splitting of inner core modes.[11] This pioneer work was followed by a subsequent number of modes and travel time residuals analysis, and although the existence of an axisymetric anisotropy of 3 to 3.5% in the inner core seems now reasonably well accepted, there is yet no concensus as to what its exact structure is. The D" region, at the base of the mantle, is on the other hand thought to play a critical role in the dynamic of the earth. We had documented in several recent studies the strong heterogeneity of D" (see GS98-14). In the light of those results, the objective of this ongoing project was to analyze the effect of deep mantle structure on some of the observables which have been used to study the structure of the inner core, namely PKP(AB-DF) and PKP(BC-DF) differential travel time residuals.

RESULTS

We have analyzed a dataset of several hundred hand-picked differential travel times residuals, composed of our own measurements as well as residuals reported by Vinnik *et. al.*[10] PKP(AB-DF) differential residuals show a significant dispersion ($\pm$ 2s), and some large scale patterns. Most of the trends observed are consistent with predictions made using recent tomographic results. In particular, residuals corresponding to Fiji Islands earthquakes present a smaller scale azimuthal and angular pattern which is well explained the presence of particularly slow velocities and possibly Ultra Low Velocity Zones at the bottom of the mantle. We observed the largest PKP(AB-DF) residuals (more than 4s) for PKPab waves sampling this large African anomaly, and PKPdf propagating through a normal to fast mantle, and showed that those observations could be explained by a differential effect of the mantle, and that they do not necessarily require strong anisotropy (~3%) in the bulk of the inner core.

We performed a more detailed analysis of residuals corresponding to quasi-polar paths beneath Africa and the eastern Atlantic Ocean, and showed, using simple arguments, that mantle heterogeneity has to be responsible for at least 3s out of the 4s generally observed for those paths (Fig. 1). This suggests an upper bound of about 1 to 1.5% for the average central inner core anisotropy.

We have simultaneously analysed PKPbc and PKPdf absolute ISC travel time residuals for earthquakes in the South Sandwich Islands region recorded in Eurasia and North America, and earthquakes in Alaska recorded in Antartica. For those three paths, we showed that, when the station is fixed, PKP(BC-DF) residuals depend strongly upon the position of the earthquake and can vary from zero to several seconds. The observations are compatible with a constant anisotropy model of at most 1.5% in the outer 400 km of the inner core (Fig. 2). A very complex inner core structure, where the iron crystal alignment changes abruptly from perfect to random over distances of several hundreds of kilometers, would have to be invoked in order to explain the extreme observed variations in term of an inner core effect on DF. We showed that the complex behaviour of BC-DF residuals correlates with the presence of strong heterogeneity in D'', and proposed that it would probably be better explained by short scales (<500km) deep mantle structure.

We finally investigated the possibility of using P'P' to further constrain possible inner core structures.We measured absolute P'P'df and differential P'P'bc-P'P'df and P'P'ab-P'P'df travel time residuals for earthquakes in the Aleutians and the Kurile Islands recorded in Scandinavia. For such paths, P'P'df samples two regions of the inner core which have been identified as strongly anisotropic (~ 3.5%), respectively beneath the Central Pacific and Africa, and should arrive some ~6s earlier than predicted by a standard model. The observed P'P'bc - P'P'df are however no larger than about 1 to 2s. A very complex texture and/or heterogeneity of the top ~400km of the inner core, or a significant contribution from the strongly heterogeneous D'', could explain this discrepancy. These results are consistent with our analysis of PKP(bc-df) differential travel time residuals.

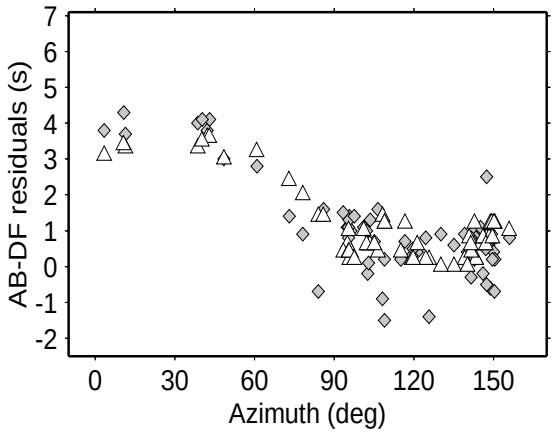

Figure 1: Comparison between observed differnetial travel time residuals(gray diamonds) and our estimate of the effect of the mantle (white triangles). Here, we have compiled PKP(ab-df) high-quality hand-picked differential travel time residuals from Creager [1999], Vinnik et al. [1994], McSweeney et al. [1997], and Breger et al. [2000], and selected the paths that correspond to earthquakes in the South Sandwich Islands and stations in Eurasia. Residuals are computed with respect to reference model ak135 [Kennett et al. 1995], and plotted a function of the azimuth. Note how most of the variations can be explained by mantle structure, which suggests a maximum possible (~ 1%) inner core anisotropy on the order of 1%.

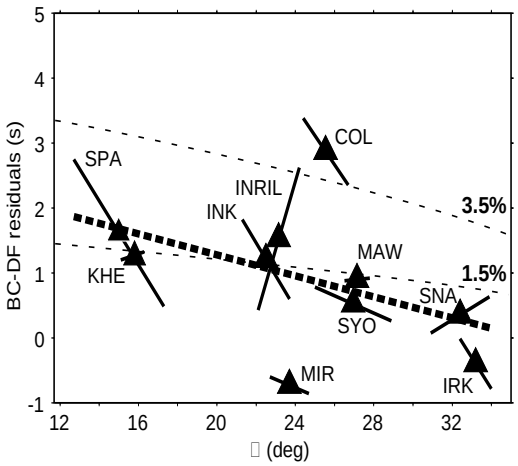

Figure 2: Summary of the estimated variations of PKP(bc-df) travel time residuals for several polar paths. Residuals are computed with respect to reference model ak135 [Kennett et al., 1995], and plotted a function of the angle ξ between the PKPdf ray at its turning point and the earth's spin axis. Triangles represent the mean values of the extrapolated residuals for a given station, and the thick black lines their variations as a function of ξ. The thick dashed line represents the average observed linear trend, and is compared with the predictions for 3.5% and 1.5% anisotropy (thin dashed lines) at 148º epicentral distance.

REFERENCES

1. Breger, L., Romanowicz, B, & Tkalvcic, H.. "PKP(BC-DF) travel time residuals and short scale heterogeneity in the deep earth," *Geophys. Res. Lett.,* 26, 3169-3172, 1999.

2. Breger, L., H. Tkalvcic, and B. Romanowicz, "The effect of D" on PKP(AB-DF) travel time residuals and possible implications for inner core structure," *Earth Planet. Sci. Lett.,* 175, 133-143, 2000.

3. Breger, L., B. Romanowicz, and S. Rousset, "New constraints on the structure of the inner core from P'P'," Submitted to *Geophys. Res. Lett*., 2000.

4. Breger, L., B. Romanowicz, C. Ng, and H. Tkalvcic, "The effect of deep mantle heterogeneity on PKP(ab-df) travel times," In preparation, 2000.

5. Creager, K.C., "Large-scale variations of inner core anisotropy," *J. Geophys. Res*., 104}, 23127-23139, 1999.

6. Kennett, B.L.N., E.R. Engdahl, and R. Buland, "Constraints on seismicvelocities in the Earth from travel times," *Geophys. J. Int.*, 122, 108-124, 1995.

7. McSweeney, T.J., K.C. Creager, and R.T. Merrill, "Depth extent of inner-core anisotropy and implications for geomagnetism," *Phys. Earth Planet. Int.*, 101,131-156, 1997.

8. Morelli, A., A.M. Dziewonski, and J.H. Woodhouse, "Anisotropy of the core inferred fromPKIKP travel times," *Geophys. Res. Lett*., 13, 1545-1548, 1986.

9. Poupinet, G., R. Pillet, and A. Souriau, "Possible heterogeneity of the Earth's core deduced from PKIKP travel times," *Nature*, 305, 204-206, 1983.

10. Vinnik, L., B. Romanowicz, and L. Breger, "Anisotropy in the central part of the inner core," *Geophys. Res. Lett*., 21, 1671-1674, 1994.

11. Woodhouse, J.H., D. Giardini, and X.-D. Li, "Evidence for inner core anisotropy from splitting in free oscillation data," *Geophys. Res. Lett.*, 13, 1549-1552, 1986.

High-Resolution Study of Inner-Core Rotation (99-GS-015)

Principal Investigator: John Vidale (UC Los Angeles)
LLNL Collaborator: Doug Dodge
Other Collaborator: Paul S. Earle
Graduate Student: Fei Xu

Recent studies have disagreed whether the inner core moves with respect to the mantle. The detection of scattering in the inner core enables a simple test for inner core motion.[10] We compare scattered waves recorded at LASA from two nearby nuclear tests at Novaya Zemlya in 1971 and 1974. The coda shows small but coherent changes. We observe that waves scattered in the inner core to the west of the great circle path are up to 0.1 s earlier in 1974 than 1971. The opposite trend appears for scattering from the east. This pattern suggests an inner-core rotation rate of 0.15° per year.

OBJECTIVES

The announcement that the inner core may be rotating faster than the mantle has been of wide interest.[7] The reported signal is subtle, about a tenth of a second change per decade in the separation of two compressional seismic waves with differing paths through the core. Subsequent studies of similar data have generally supported the initial conclusions.[3,5,6] However, the difficulty locating the older earthquakes coupled with strong lateral variations in the structure near the core-mantle boundary have caused questions about the reality of the proposed inner core motion.[1,8] In addition, analysis of free oscillations suggests a fixed inner core.[4] The seismic tests were motivated by outer core convection research suggesting the possibility of inner-core rotation. Consideration of the interaction of inner-core-boundary topography and mantle-induced irregularity in the gravity field, however, could lock the inner core to the mantle.[2] The detection of scattering in the inner core enables a simple test for inner core motion.[10] We compare scattered waves recorded in Montana from two nearly co-located nuclear tests at Novaya Zemlya in 1971 and 1974.

PROGRESS

We use LASA (Large Aperture Seismic Array) for this study. Although in operation almost three decades ago, it provides an unparalleled number and density of short-period seismometers, all buried 70-m underground. We examine LASA recordings of two large nuclear explosions three years apart (Table 1). The blasts were similar in size and were separated by less than 1 km. These were two of the four nuclear tests in the dataset of 16 events used to identify inner-core scattering.[10]

In order to build a consistent set of seismograms, we discarded any stations that did not record both explosions. This resulted in the elimination of the E and F outer rings of the LASA array, which were turned off before the 1974 blast.

Inner-core scattering (ICS) is clearest near one Hz;[10] other phases are stronger at longer periods and the seismograms contain little teleseismic signal above 2-3 Hz. Therefor, we bandpass-filter the data to keep only 1-2 Hz motion. In order to eliminate noisy traces, we cross-correlated the initial 3 s of the P wave for each station between the two events. We discarded the 21 stations with correlation coefficients less than 0.9, leaving 184 stations.

Our analysis hinges on interpreting the variation in the ICS waves in terms of relative inner-core rotation. Our geometry may be approximated by considering explosions on the North Pole and the array in its true location in Montana. We only see the outermost quarter of the inner core with ICS because of its strong attenuation. If the inner core rotates faster than the mantle, then the struc-

tures in the inner core to the west of LASA will come nearer over time. Structures in the region to the east will recede. Thus, inner core rotation would lead to earlier scattered arrivals from the west in 1974 compared to 1971, and later scattered arrivals from the east.

We observe this pattern of advancing arrivals from the west and delayed arrivals from the east. Between 1971 and 1974, there is a change of more than 0.1 s in the arrival times of the ICS as a function of transverse slowness. An alternative we must consider is the possibility that the spatial separation of the two explosions causes the observed variation in the ICS waves. To this end, we compared all three phases that have traversed the core; ICS, PKKP, and P'P'.

Our calculation assumes Born single scattering and uniformly distributed 1.2% variations in the moduli and density with a 2-km wavelength,[10] attenuation Qp of 360, and traces rays through PREM. The results are not sensitive to these choices. We assume differential rotation about the same pole as the rotation of the Earth. Movement of the inner core would change the scattered wavefield two ways; focusing and interference patterns would change, and the arrival times of the scattered energy would shift in time. We ignore the former effect, which would not lead to systematic time shifts, and calculate the latter, which would.

To calculate the average arrival-time shift of the scattered wavetrain, we assume all points within the inner-core contribute to the observed ICS. The time shift resulting from a given amount of differential rotation for a given scatterer (point in the inner-core) is calculated by finding the difference between the travel-time to the scatter before and after the rotation. This delay is weighted by its amplitude contribution to the entire ICS wavetrain. The amplitude contribution for a particular scatter is effected by geometrical spreading, inner-core attenuation, scattering angle, and the contrast in elastic properties.

The predicted amplitude and time delay patterns resulting from an inner-core rotation of 0.45°, given our scattering model, match the observations well. The observed time delay of ±0.1 s accrued over three years determines that the inner core was rotating 0.15° per year faster than the mantle.

We confirm the inner-core rotates as first claimed in 1996 but at a considerably slower rate,[7] 0.15 °/yr compared to 0.5 to 1.1 °/yr. Our estimate falls within the bounds of 0 ± 0.2 °/yr set by measurement of normal modes.[4] Future studies of ICS waves can be used to search for time-dependence in the differential inner-core rotation as well as test the assumption that the differential rotation is about the Earth's north-south axis. We have submitted a manuscript with more details.[10]

Table 1:

Date	Time	Lat. (N)	Lon. (E)	Depth (km)	Distance
09/27/71	05:59:55.75	73.393	54.929	0	59.5°
08/29/74	09:59:56.15	73.397	54.914	0	59.5°

REFERENCES

1. Breger, L., and B. Romanowicz, "Three-dimensional structure at the base of the mantle beneath the central Pacific," *Science*, 282, 718-720, 1998.

2. Buffett, B.A., "Geodynamic estimates of the viscosity of the Earth's inner core," *Nature*, 388, 571-573, 1997.

3. Creager, K.C., "Inner core rotation rate from small-scale heterogeneity and time-varying travel times," *Science*, 278, 1284-1288, 1997.

4. Laske, G., and T.G. Masters, "Rotation of the inner core from a new analysis of free oscillations," *Nature*, 402, 3397-3400, 1999.

5. Song, X., "Joint inversion for inner core rotation, inner core anisotropy, and mantle heterogeneity," *J. Geophys. Res.*, in press.

6. Song, X., and A. Li, "Support for differential inner core superrotation from earthquakes in Alaska recorded at South Pole station," *J. Geophys. Res.*, 105, 623-630, 2000.

7. Song, X.D., and P.G. Richards, "Seismological evidence for differential rotation of the Earth's inner core," *Nature*, 382, 221-224, 1996.

8. Souriau, A., P. Roudil, and B. Moynot, "Inner core differential rotation: Facts and artefacts," *Geophys. Res. Lett.*, 24, 2103-2106, 1997.

9. Vidale, J.E., D.A. Dodge, and P.S. Earle, "Slow differential inner-core rotation inferred from changes in scattering over time," *Nature*, submitted.

10. Vidale, J.E., and P.S. Earle, "Fine-scale heterogeneity in the Earth's inner core," *Nature*, in press.

Ultra-High Pressure Melting Studies (99-GS-018)

Principal Investigator: Raymond Jeanolz (UC Berkeley)
LLNL Collaborator: Jagannadham Akella
Graduate Student: Wendy Panero (UC Berkeley)

We are carrying out high-temperature studies at ultrahigh pressures using the diamond-anvil cell with a combination of laser- and internal-resistance heating. The objective is to better control and characterize the temperature distribution achieved at ~50-120 GPa pressures and ~3000-5000 K temperatures, thereby yielding quantitative determinations of melting temperatures and associated properties such as thermal and electerical conductivity. The work would focus on the melting of iron in contact with oxides or inert pressure media, in order to better constrain temperatures and possible geochemical interactions taking place at the base of the Earth's mantle. The proposed research combines unique strengths in ultra-high P-T experimental capabilities at LLNL and UCB, addresses a significant problem in the geosciences, and develops methodologies that are critically needed for the LLNL's mission.

Cosmogenic Nuclide Systematics in Olivine and Calcite (99-GS-019)

Principle Investigator: Kunihiko Nishiizumi (UC Berkeley)
LLNL Collaborators: Robert C. Finkel and Marc W. Caffee
Postgraduate Researcher: Ping Kong (UC Berkeley)

We are attempting to develop a new method to date surface features and processes using in situ produced cosmogenic nuclides in olivine. In the method, pure olivine fractions were obtained by a combining physical separation with selective chemical leaching. Meteoric ^{10}Be was effectively removed by a sequential leaching procedure, which uses various chemical reagents. The Al concentration in the olivine fraction was reduced to a level that reflects only in situ Al in the olivine crystals. Using this method, we analyzed several olivine samples with different exposure histories. The results are preliminary and may necessitate a reevaluation of those processes pertaining to the extraction of materials at mantle hotspots.

OBJECTIVES

Surface exposure dating using cosmogenic nuclides has proven to be a valuable technique in tectonics, geomorphology, and paleoclimatology. Most of the applications have used ^{10}Be and ^{26}Al from quartz or ^{36}Cl from whole rock or mineral separates. In many geological settings, however, quartz is not available. Extending the *in situ* produced cosmogenic nuclide technique to other minerals would greatly expand the range of problems to which the technique could be applied. Olivine and calcite are abundant in many geological environments where quartz is rare. A significant benefit of olivine is that it potentially allows the detection of numerous *in situ* produced radionuclides (^{14}C, ^{41}Ca, ^{36}Cl, ^{26}Al, ^{10}Be, and ^{53}Mn) and stable nuclides (^{3}He and ^{21}Ne). Accordingly, the goal of this work is to extend the application of the *in situ* produced cosmogenic nuclide technique to olivine- and calcite-containing rocks.

PROGRESS

During this period we focussed on olivine. Removal of meteoric ^{10}Be and reducing intrinsic Al (for ^{26}Al measurement), Ca (for ^{41}Ca), and Mn (for ^{53}Mn) levels in the olivine are critical components of this work. Olivine was isolated from igneous rocks first using a Frantz magnetic separator, then by the heavy liquid, methylene iodide. With XRD and an electron microprobe, it was found that the isolated olivine contains numerous µm-size chromite and glass inclusions. The glass inclusions are enriched relative to the olivine itself in Al and Ca. Since the inclusions are too small to be separated by finer crushing, we have therefore developed a chemical method, which is able to selectively leach these constituents out of the olivine. After a series of experimental tests, we found that NaOH effectively removes Al-rich minerals, which are aggregated with olivine crystals. We also found that olivine is about 10 times more soluble in dilute HCl and HNO_3 than augite, chromite and feldspathic glass which may co-exist as inclusions inside olivine. A selective chemical leaching method was employed that combined the advantages of NaOH and dilute HCl or HNO_3. This technique brought the Al concentrations in the leached olivine in line with the Al concentration of the olivine as determined by an electron microprobe.

Because the olivine crystal structure is not as tight as that of quartz, removal of meteoric ^{10}Be is more difficult and considerable effort has been devoted to removing meteoric ^{10}Be from the olivine fraction. After testing a wide range of chemi-

cal reagents, a procedure was developed by which the concentration of meteoric ^{10}Be could be reduced by a factor of 1000. Analysis of an olivine sample separated from long-term exposed beach sands from Kauai, Hawaii, give ^{26}Al and ^{10}Be concentrations which appear to be derive from *in situ* production. More precise experiments (using a low ^{10}Be carrier) are being conducted in order to elucidate the evolutionary history of the Kauai beach sand.

In order to verify that meteoric ^{10}Be can be totally removed, we have applied the developed procedures to a young volcanic lava sample from Kilauea, Hawaii, erupted in 1840. The expected *in situ* produced ^{10}Be and ^{26}Al for this sample is 650 atoms/g olivine and 2000 atoms/g olivine, respectively. Surprisingly we obtained a ^{10}Be concentration of 1.6×10^5 atoms/g olivine, which is much higher than expected from *in situ* production. There are two possibilities for the high ^{10}Be: 1) meteoric ^{10}Be has diffused into the olivine crystal and has not been removed by our leaching procedures; 2) contaminant ^{10}Be, i.e. ^{10}Be not produced in-situ by cosmic rays, has been incorporated into the olivine crystal during crystallization. Conceivably this contaminant could have been scavenged from local rock during the emplacement of the basalt. If the latter is the case, it may imply alteration of the upwelling melts during Hawaii volcanic activity. To further investigate this observation ^{10}Be from various sources encompassing a wider range geologic settings will be investigated. Similar tests on procedures for removal of meteoric ^{10}Be from calcite will also be conducted.

Experimental Constraints on the Chemical Evolution of Icy Satellites (99-GS-021), (00-GS-036)

Principal Investigator: Quentin Williams (UC Santa Cruz)
LLNL Collaborator: F. J. Ryerson
Graduate Student: Henry Scott (UC Santa Cruz)

We derive experimental constraints on the interior structure and mineralogy of large icy satellites by reacting material of chondritic chemistry with water at a pressure of 1.5 GPa, temperatures between 300°C and 800°C and a range of oxygen fugacities. Our results document the existence of three chemical processes that probably occur in large icy satellites as a result of high pressure hydrothermal processing: (1) the formation of low-density hydrated silicates. (2) alloying of iron and sulfur to form FeS-dominated cores, and (3) the instability of organic material relative to carbonates. Models of the thermal and structural state of Ganymede's interior based on these data suggest that the magnetic field of this body arises from convection within a mostly iron sulfide core. Simple thermochemical calculations are conducted to further explore the likely effects of composition and oxygen fugacity on the high pressure chemistry undergone by organic material within icy satellites. Both experimental and calculated results show that primordial organics are likely to have been largely oxidized to carbonates through hydrothermal processing early in Ganymede's history, potentially sterilizing Ganymede's H_20 layer

OBJECTIVES

Jupiter's icy satellites Ganymede and Callisto and Saturn's Titan are similar in size to Mercury (with radii greater than 2,400 km), and have mean densities between 1,800 - 2,000 kg/m^3. Compositional and structural models of these large icy satellites typically incorporate density stratified layers (with the possible exception of Callisto), and contain approximately 50-80% silicate minerals and iron alloy by weight, with H_20-ice constituting most of the remaining mass. These ice-rich satellites are likely to contain signif-icant quantities of organic molecules, either through accretion of primordial organic compounds (as demonstrated by the abundance of organics within carbonaceous chondrites and the observation of organic material on the surfaces of Ganyniede and Callisto) or through their subsequent produc-tion, as on Titan.

During accretion and differentiation (which could be ongoing), and perhaps from tidal heating generated by orbital resonances, the silicate and organic complements of the large satellites are expected to have interacted with aqueous fluids at moderate to high temperatures (200°C to >800°C) and pressures (>1 GPa). There are a number of scenarios under which rock would have interacted with hot water during this time. In approximate tem-poral sequence: 1) rapid heating of a rock-ice aggregate through a large impact or catastrophic differentiation; 2) incorporation of hydrous silicates (common in primitive carbonaceous chondrites) during accretion and their subsequent dewatering at depth within an interior heated by accretion, differentiation, or radiogenic activity; 3) pervasive hydrothermal circulation within a porous (and possibly heavily fractured) silicate mantle.

The ice-rock interface in icy satellites may also present the most likely habitats for extraterrestrial life in the solar system; however, it is not known whether organic material is stable with respect to high-pressure hydrothermal processing (at the base of a 500-1,000 km layer of H_20, the

pressure will be on the order of 1 GPa, even for low mean density bodies). Similar hydrothermal processing has been theoretically investigated at modest pressures for volatile species, but at pressures substantially below those likely to occur at the water-rock interface in Ganymede. Such hydrothermal interactions could con-trol the interior mineralogy of the silicate fraction.

We have designed and conducted reconnaissance experiments to address the uncertainties in internal mineralogy and the stability of organic material within large icy satellites. We combine experiments at simultaneous high pres-sures and temperatures with internal modeling of the bulk structure of these satellites to produce experimentally and observationally consistent models of their internal structure and chemistry.

PROGRESS

We assume that icy satellites accreted from material similar to carbonaceous chondrites, with their primary difference relative to chondrites (and each other) being the amount of additional volatile material accreted. For our experiments, we synthesized a model carbonaceous chondrite with the chemistry of the Orgueil meteorite, and allowed it to react with excess H2O (~20 wt%) within a piston-cylinder apparatus for three to ten days. We conducted these experiments at a pressure of 1.5 GPa (approximately the pressure at the ice-rock interface in Ganymede), and temperatures between 300 and 800°C, over a range of oxygen fugacities. These temperatures span a range compatible with the cooling of these bodies following the genesis of a molten iron alloy core during accretion/differentiation. X-ray diffraction, infrared spectroscopy and electron microprobe observations were used to analyze our run products. A summary of our phase equilibria data is shown in the Figure. Specifically, these data address three key issues in icy satellites: the formation conditions of different hydrated ferromagnesian silicates and iron-sulfur alloys and the stability of organic carbon.

The most important general observation derived from our experiments is that the chondrite-water system is dominated by hydrous, rather than anhydrous silicates over the entire range of P-T conditions investigated. Below 400°C the silicate portion of the assemblage is composed of serpentine (antigorite) and talc; above 400°C serpentine is replaced by chlorite (clinochlore). The phase assemblage observed is not particularly sensitive to oxygen fugacity; more oxidizing conditions appear to weakly increase the abundance of talc relative to clinochlore at T> 400°C. The weak dependence on oxygen fugacity is likely a result of the low iron concentration in the silicate phases.

Our results provide experimental confirmation that hydration can readily occur, and constrain the temperature dependence of mineralogy (and thus density) in the chondrite-water system. The existence of serpentine, talc and chlorite imply significant changes in the inferred internal structure of icy satellites relative to models with anhydrous silicate layers. The shift in inferred internal structure associated with hydration is simply a consequence of the low density of these silicates (~2,700 kg/m3) relative to anhydrous silicates (~3,000 kg/m3).

Our results further demonstrate that iron and sulfur readily alloy under even modest temperatures (<450°C) in this sulfur-rich system, and that the formation of pyrrhotite-dominated (Fe_1-xS) cores is likely: indeed, pyrrhotite is the sole high-density iron-rich phase observed in these experimental charges. Pyrrhotite has a lower density (~5,500 kg/m3) than iron (~8,000 kg/m3), thus the stability of pyrrhotite relative to iron in this system indicates a markedly lower core density for these icy satellites. Furthermore, pyrrhotite remains the dominant iron-bearing phase at oxygen fugacities varying from the Fe_2O_3:Fe_3O_4 to Ni:NiO buffer, implying that the formation of reduced sulfur species is robust over the full range of pressure and temperature conditions investigated.

Organic carbon (initially present as polyethylene) is unstable at high pressures above 450°C in the chondritic assemblage, and is oxidized to car-

bonate minerals. This oxidation occurs even under relatively reducing conditions, such as the Ni:NiO buffer. This observation has important astrobiological implications. Icy satellites possess large amounts of H_2O and presumably had a large initial budget of organic material (making them a popular locale for invoking the possibility of extraterrestrial life), yet any deep circulation of organics into their water / ice layers (particularly during an early, liquid stage) should irreversibly oxidize the organic material, thus creating carbonate veining or layering near their ice/rock interface. Therefore, organic material is unlikely to survive equilibration between water and silicates at high pressure and temperatures in large icy satellites. Accordingly, much of the accreted organic component of these bodies may not have survived the earliest stages of the satellite's history.

In conclusion, our results document: 1) the likely importance of hydration of silicates during accretion, differentiation and possibly the later evolution of large icy satellites; 2) the probability that the cores of the icy satellites are dominated by iron sulfide; and 3) the annihilation of organic compounds under conditions of high pressure hydrothermal processing. The hydration of silicates decreases the inferred density and rheology of the silicate portion of the interior of these bodies; the abundance of iron sulfide indicates that the solidifying cores of these bodies could lie on the FeS-rich side of the Fe-FeS eutectic system, and that cooling of an initially molten core may produce solidification at its top, rather than formation of a central solid inner core as on Earth; and the oxidation of organics to carbonates by deep water – rock interactions indicates that organic materials could be difficult to preserve in abundance on satellites with thick ice / water layers. Therefore, the ability to produce life from primordial organics on such bodies may be marginal.

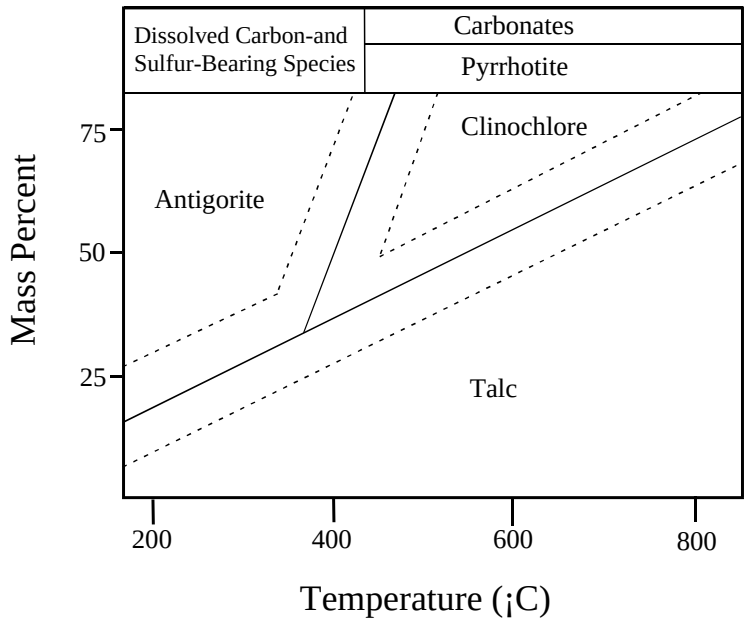

Estimated modal composition as a function of temperature for a hydrothermally processed carbonaceous chondrite at 1.5 GPa. Dashed lines represent variability in modal composition as a result of varying fO_2: the effect of changing fO_2 between the Ni:NiO and Fe_2O_3:Fe_3O_4 buffer on phase equilibria is to lower the temperature at which antigorite reacts to form talc and chlorite, and to weakly shift the boundary between talc and clinochlore upward. The reaction between antigorite and talc is likely augmented by uptake of magnesium from CO2 evolved from the oxidation of organic material through the reaction 2 $Mg_3Si_2O_5(OH)_4$ + 3 CO_2 $Mg_3Si_4O_{10}(OH)_2$ + 3 $MgCO_3$ + 3 H_2O. Talc is anticipated to dehydrate at temperatures of 800 – 850°C to a pyroxene-dominated assemblage.

Source Effects on Regional Seismic Discriminant Measurements (99-GS-022)

Principal Investigator: Thorne Lay (UC Santa Cruz)
LLNL Collaborator: William R. Walter
Researcher: Jiajun Zhang (UC Santa Cruz)

Three data sets are used to investigate radiation pattern and source depth effects on the observed scatter of regional seismic discriminant measurements of high-frequency P/S-type ratios. Each set comprises observations of one or more clusters of earthquakes located within 10 km from the center of the cluster. The first data set spans the range 250-300 km and involves LNN (Livermore NTS Network) observations of the 1992 Little Skull Mountain aftershock sequence, and the second data set spans the range 100-400 km and involves TERRAscope and BDSN (Berkeley Digital Seismic Network) observations of small earthquakes in Southern California.

The first two data sets are used to assess effects of source radiation pattern. Although predicted variations of P/S-type ratios using focal mechanism integrations correlate well with measurements on regional distance synthetics, the observed scatter proves to be poorly correlated with focal mechanism predictions, indicating that simple theoretical corrections are not viable for regional phases.

The third data set spans the range 100-1000 km and involves significantly more events in Southern California and stations throughout California than the second data set. This data set is used to assess effects of source depth and to determine the statistical variance in the measurements. For each event the observed Pn/Lg and Pg/Lg ratios are averaged over various stations to reduce the effects of source radiation pattern and wave propagation which vary among stations. The depth distribution of the station averaged measurements for events in each cluster is analyzed. For very shallow events (d < 1 km) Lg is strongly excited for events located in basin-like structures, in contrast with events located otherwise. For events with depths of a few km the Pn/Lg depth distributions are very complex, which is presumably caused by the sensitivity of the pPn and sPn energy to near-free surface structure. For most clusters the strongest Lg excitation relative to Pg and Pn is observed for events at depths between 3 and 5 km. This suggests that Lg excitation depends strongly on the distance between the event and the lower boundary of the shallow crust waveguide, given the fact that the most significant velocity jump for the Southern California crust occurrs at the depth of about 5 km.

OBJECTIVES

One major challenge confronting seismic monitoring and verification is the need for improved understanding of the variance in regional seismic discriminant measurements caused by earthquake source radiation pattern and source depth, as this may lead to more robust application of regional discriminants, enhancing our ability to seismically monitor a Comprehensive Test Ban Treaty (CTBT). Many efforts are being made to assess the performance of the measurements in nuclear test detection and discrimination. The Pg/Lg and Pn/Lg ratios for frequencies higher than 3 Hz have been demon-

strated to discriminate nuclear tests from earthquakes quite well at magnitude above 3.5, but there is significant overlap at lower magnitudes. The major obstacle to reliable source identification with these discriminants is the scatter in the two events populations, which results in the observed overlap at smaller magnitudes, and possibly overlap at larger magnitudes if more earthquake signals were available.

The scatter in the earthquake population is not well-understood. It is well-recognized that there are very significant wave propagation effects. Near-source effects have also been observed for events recorded on nearly identical paths with regional discriminants showing significant scatter. The objective of this research effort is to quantify near-source effects to regional P/S-type seismic measurements.

PROGRESS

In this year we significantly expanded the data sets from an initial project by collecting seismograms recorded at eleven BDSN and seven TERRAscope stations from about 350 earthquakes in Southern California. We analyzed three data sets. The first and second data sets involve waveforms for the Little Skull Mountain aftershocks and Southern California earthquakes, respectively, which were collected in our previous study. The third data set involves the newly collected waveforms.

The focal mechanisms of the events in the first and second data sets have been determined previously. We constructed regional distance synthetics for various source/receiver geometries using the range in source depths and focal mechanisms of the events for the two data sets. This allows us to define radiation pattern integration criteria to better reflect the actual contributions from phases for different source depths. Then we found ranges of radiation pattern integrations that provide reasonably good predictions of the observed relative amplitudes in the Pn, Pg, and Lg windows. This guided us to incorporate sPn contributions to the Pn window for shallow events and Sg contributions to the Pg window (S waves that come out from the source, convert to P and then arrive in the Pg window).

Our predicted variations of short-period Pn/Lg and Pg/Lg ratios using focal mechanism integrations correlate well with the measurements on regional distance synthetics. However, the observed scatter proves to be poorly correlated with focal mechanism predictions. It presumably does reflect some remarkable complexities of the effects of wave propagation due to the crust waveguide.

The third data set is used to determine the statistical variance in the measurements and to assess effects of source depth on the observed scatter of the measurements. Figure 1 (top panel) shows locations of various clusters for the data set, with each cluster including 40-70 earthquakes. Some clusters are closely located and named with similar identifications; events in A-clusters are associated with the earthquake sequence of Northridge of 17 January 1994 (M_w=6.7); B-clusters for the Joshua Tree sequence of 23 April 1992 (M_w=6.1) and Landers sequence of 28 June 1992 (M_w=7.3); C-clusters for the Big Bear sequence of 28 June, 1992 (M_w=6.2).

For waveforms recorded at a given station we calculated Pn/Lg and Pg/Lg spectral amplitude ratios for various frequency bands (0.5-1, 1-2, 2-4, 4-6, 6-8, and 8-10 Hz). With the exception of Pn/Lg measurements for cluster A1 events, most of the Pn/Lg and Pg/Lg measurements normalized with the average value for all the events in a cluster are within the range from -0.5 and 0.5 in the 10 base logarithm.

Figure 1a shows the Pg/Lg measurements for the 0.5-1 Hz passband as a function of source depth for clusters A1, B1, and C1 earthquakes recorded at station ISA, indicating little correlation between Pg/Lg measurements with source depth. Weak correlations of Pg/Lg and Pn/Lg measurements with source depth are also found for other passbands and for other stations, suggesting that the measurements are more sensitive to source radiation pattern or the precise location of each event than to source depth.

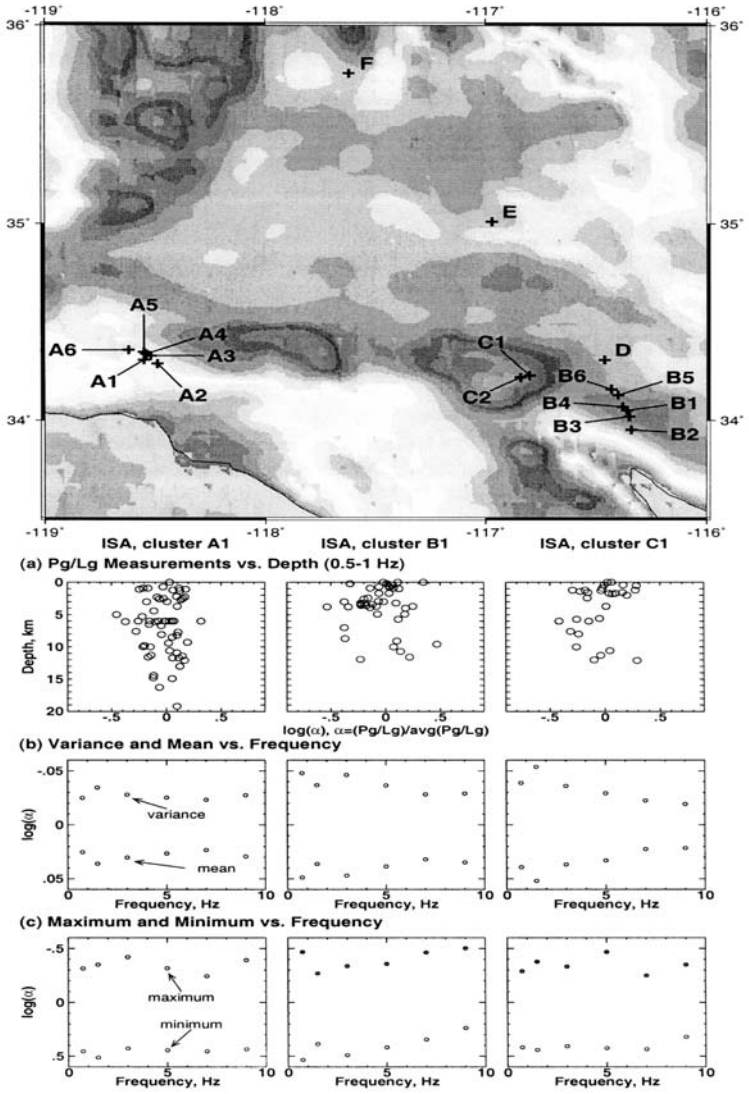

Figure 1. Map showing locations along with the identifications of the 17 clusters (crosses) for the third data set. (a, b, c) Characteristics of Pg/Lg measurements at station ISA for earthquakes in cluster A1 (left column), B1 (middle column), and C1 (right column) (From Zhang et al.).

We computed the variance, mean, minimum, and maximum of the amplitude ratios for all the events in a cluster to characterize the scatter of the Pn/Lg and Pg/Lg measurements at each station. The results for three clusters for station ISA are shown in Figures 1b and 1c, plotted against the center frequencies of various passbands. Note all the means are negative, and there are moderate variations for each parameter over the frequency passband used here.

To examine source depth effects on the observed scatter, we stacked (averaged) the ratios observed at various stations, with the expectation that effects of source radiation pattern and wave propagation can be reduced by stacking. Figure 2 shows the depth distributions of the station averaged Pg/Lg and Pn/Lg measurements for events in each cluster, which are plotted in logarithm against the depths of the events, normalized with the average value for all the events in the cluster.

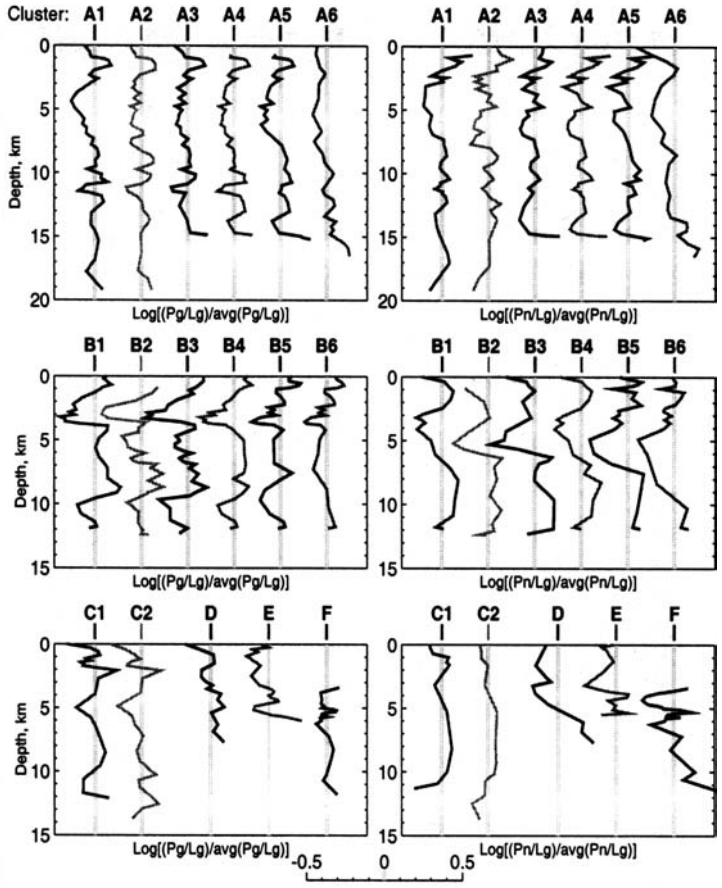

Figure 2. Pg/Lg (left column) and Pn/Lg (right column) measurements in the 0.5-1 Hz passband averaged over various stations, plotted as a function of source depth for events in various clusters. The cluster identification is shown above each curve and the zero reference line (dashed) (From Zhang et al.).

For A-cluster events, which comprise the largest event cluster used in this study, the negative logarithmic Pg/Lg ratios for events near the free surface indicate large Lg excitation relative to Pg in comparison with events in other depths; the logarithmic Pg/Lg and Pn/Lg have minima at depths between 3 and 5 km; below 5 km the overall trend of Pg/Lg and Pn/Lg is to increase with depth.

Large Lg excitations for shallow events are also found for C- and D-cluster events, but not for B-cluster events. Since the events in A-, C-, and D-clusters occurred in basin-like structures in contrast with B-cluster events (Figure 1), the large Lg excitations may be caused by surface geology and/or topography associated with the basin structures.

The overall trend of increasing Pg/Lg and Pn/Lg for depths below 5 km is also found for events in clusters B, D, and F, which suggests that deep events excite stronger Pg and Pn waves and weaker Lg waves than shallow events. The Pg/Lg and Pn/Lg minima at depths between 3 and 5 km are found for most clusters, which may correspond to large Lg excitations in comparison with events at other depths. The minima may be associated with discontinuities of material properties of the Southern California crust

There is much similarity between the depth distributions for events in clusters A and B, while the depth distributions for events in clusters C to F differ significantly. This may reflect the fact that our events sets for C to F clusters are much smaller

than for A and B clusters and that the effects of source depth on the observed Pg/Lg and Pn/Lg ratio are better resolved for events in A and B clusters than for other clusters.

Since the largest velocity jump in the Southern California crust occurs at the depth of about 5 km, the depth distributions of station averaged Pg/Lg and Pn/Lg suggest some deterministic effects of the velocity structure, with large Lg excitations associated with sources located in the lower part of the shallow crust waveguide.

REFERENCES

1. Zhang, J., T. Lay, and W. R. Walter, "Source effects on regional seismic discriminant measurements at TERRAscope and BDSN stations for earthquakes in southern California," *Eos AGU*, 80(46), Fall Meet. Suppl., F658 (1999).
2. Zhang, J., T. Lay, and W. R. Walter, "Source Effects on Regional Seismic Discriminant Measurements in California," *Bull. Seism. Soc., Am.,* in preparation (2000).

Cosmogenic Exposure Age Dating of Glacial Deposits in the Cordellero Blanca, Peru: Toward a Detailed Record of Southern Tropical Climate Change (99-GS-025)

Principal Investigator: Robert S. Anderson (UC Santa Cruz)
LLNL Collaborators: Daniel Farber and Robert Finkel
Student: TBN

Well-dated terrestrial paleoclimate records are needed for the low-latitude regions of the Earth in order to understand more fully the climate response to orbital forcing. Understanding global climate change relies on precise and widespread documentation of past climatic fluctuations. We propose to date late Pleistocene to Holocene moraine complexes found in several valleys draining the western Cordillera Blanca, Peru, using in situ produced ^{10}Be and ^{26}Al. This range likely contains the most detailed moraine record of Pleistocene to recent glaciation in the southern tropics (e.g.Clapperton, 1981); however, quantitative dating of these deposits has thus far been largely by minimum-limiting ^{14}C dates. We seek to document more precisely the timing of glacial fluctuations by dating the extensive moraine complexes of this range using ^{10}Be and ^{26}Al. Changes in the glacial extent in the Cordillera Blanca primarily reflect variations in temperature (Lliboutry et al., 1977), allowing straightforward calculation of temperature depression associated with each moraine sequence. In addition, we wish to date a series of fluvial terraces that bound streams draining these same valleys. These dates will allow us to address quantiatively the response of these river systems to fluctuations in glacial extent in their headwaters; specifically, we will test for the synchroneity of terrace formation with glacial maxima, which is proposed to occur in many glacially derived fluvial systems. We will also compare directly two very different paleoclimate proxies: our detailed moraine chronolgy, and a high resolution isotopic record obtained from an ice core within the range (Thompson et al., 1995). Finally, this low-latitude (~10^{o}S) setting is ideal for calibration of ^{10}Be and ^{26}Al production rates. As part of our work, we will seek calibration sites where independent age control is possible (obtained from ^{14}C dates), providing important low-latitude constraints on cosmogenic nuclide production rates, which are presently based solely on mid-latitude sites.

Collaborative Seismic Investigation of South American Tectosphere (99-GS-027)

Principal Investigator: Justin Revenaugh (UC Santa Cruz)
LLNL Collaborator: Stephen Myers
Graduate Student: Emily Havens (UC Santa Cruz)

This report documents results of a collaborative seismic investigation of the crust and subcrustal tectosphere of South America using nearly 25 years of digitally recorded intermediate and deep seismicity in South and Central America, data from the recent BANJO and SEDA Passcal experiments, and several imaging methodologies. The majority of our effort was directed toward ScS reverberation mapping of the upper mantle and transition zone beneath South America. For these purposes, the data set was divided into 27 seismic corridors, each sampling a narrow swath of crust and mantle between sources and receivers. Using the combined waveform inversion/migration technique of Revenaugh and Jordan,[6,7] we obtained path-averaged shear-wave reflectivity profiles for each corridor. To extract precise information about mantle reflector depth and strength, these profiles were forward modeled. The resulting array of mantle discontinuities is familiar from previous work with ScS reverberations. The 410-km and 660-km discontinuities are observed in all 27 corridors, with mean depths of 407 and 655 km, very close to the global mean obtained from a variety of previous studies. Curiously, the 520-km discontinuity is observed in only two. Accompanying these two discontinuities are four additional reflectors whose spatial extent is limited and which occur in consistent suites. These are the H, G, L and X reflectors. H is seen primarily in continental lithosphere at depths up to 100 km, but suffers from strong interference with crustal reverberations. G marks an impedance decrease that we associate with the Lid/low-velocity zone transition. The depth of G increases to the east across the mantle wedge beneath the Andean margin, reaching nearly 200 km before fading in intensity to undetectable levels. L is restricted to continental lithosphere and ranges in depth from 180 to 270 km. G and L do not overlap geographically, with the latter confined to cratons and platforms of eastern South America. Lastly X marks an impedance increase at depths of 200 to 300 km. It appears limited to the deep mantle wedge and is usually associated with G. At present, there are no known mantle phase transitions capable of explaining our observations of X.

OBJECTIVE

Our objective in this study is to place constraints on the growth and stabilization mechanisms of continental tectosphere by imaging seismic reflectors within it. We approach this by combining ScS reverberation mapping with receiver function analysis, producing the tectospheric equivalent of a fence diagram where the high resolution vertical "point" profiles obtained from receiver functions are tied together by reverberation mapping. Unlike a true fence diagram, the ties are 1D. Nonetheless, the additional insight into geographic extent and detailed velocity structure of tectospheric reflectors we are garnering from this approach is significant. Continental tectosphere exhibits an alphabet soup of reflectors, in particular, the Hales (H), Lehmann (L), and X and W reflectors.[8] These reflectors have been mapped using ScS reverberations in Australia and China. More recently, similar features were

imaged in broadband receiver functions beneath the Slave craton in Canada.[3,4] The greater resolution of the Bostock study, coupled with the availability of nearly coincident Lithoprobe reflection lines, lent new insight into the origins of H, L, and X, casting the three in terms of slab accretion. This is in contrast to Revenaugh and Jordan,[8] whose more extensive coverage led them to propose mineral and rheological phase changes for H, L and X. If the reflectors observed by Bostock are indeed the H, L and X of Revenaugh and Jordan, then slab accretion is the primary means of tectospheric growth. South America offers an ideal opportunity to combine ScS reverberation mapping and receiver function analysis in one experiment designed to test this hypothesis.

PROGRESS

Reflectivity profiling with multiples ScS reverberations is essentially complete. The results are 27 modeled seismic corridors imaging shear-wave impedance structure in the upper ~1200 km of the mantle over much of western and central South America. Our work reveals details of transition zone and upper mantle discontinuity structure that have been overlooked or extensively smoothed by horizontal averaging in previous studies. In this brief summary, we wish to draw attention to just two aspects of this structure: (1) transition zone width across the Andean margin and (2) identification of a deep mantle-wedge reflector.

Figure 1 details a pseudo-tomographic reconstruction of the depths of the 410-km and 660-km discontinuities beneath the Altiplano of western South America. There is a clear broadening of the transition zone from west to east, increasing by ~19 km over a horizontal distance of roughly 250 km. Increasing separation of the exothermic 410-km and endothermic 660-km discontinuities is geographically consistent with slab impingement on the transition zone. Using thermodynamic quantities tabulated in Revenaugh and Jordan ,[7] we estimate a 200°C decrease in mean transition zone temperature across the subduction margin. Our observation of significant widening is in direct opposition to the results of Flanagan and Shearer who noted little topography.[5] It should be noted that the latter study had relatively sparse sampling of South America and was extensively smoothed.

Eighteen of twenty seven seismic corridors examined in this study contain evidence of an impedance increase at depths between 200 and 300 km. Common to these paths is extensive sampling of the deep mantle wedge arc ward of the subduction front. In the majority of these corridors, evidence of a shallower, but distinct, impedance increase can also be found. We refer to these two discontinuities as X and G, respectively. The latter is thought to mark the Lid/low-velocity zone transition. The arc-ward increase in depth is broadly consistent with thermodynamic modeling of subduction zones. The former discontinuity, X, is not easily explained. The X reflector has been seen in several back-arc settings, prompting Revenaugh and Jordan to explain it in terms of hydrous phase reactions.[8] Since then, it has been suggested that X arises due to changes in crystalline symmetry of clinoenstatite;[1,2] and that geographic patchiness of the reflector mimicks variations in composition, in particular the degree of basalt depletion. There are several flaws in this explanation. First, basalt depletion is expected to be most pronounced in the downgoing subcrustal lithosphere, not the mantle wedge. The results of this study, suggest that X is limited to the mantle wedge. Second, the mean impedance increase of the 18 observations of X (~3%) is an order of magnitude larger than that predicting for even the most pyroxene-rich mantle mineralogies (0.7%). Even if we account for an upward bias induced by the neglect of non-observations, the observed reflector remains far too strong.

Lacking a convincing phase transition or disassociation origin to X, we are forced to look elsewhere. A possible candidate, which we have only begun to investigate, is stishovite. It is possible that seismically fast stishovite crystallizes out of water-rich silicate melts percolating through the mantle wedge, forming a sill-like feature over

time. If so, the X reflector is limited to mantle wedge settings. Variations in depth would be dictated by the stability field of stishovite, and thus are sensitive to melt and mantle temperature and chemistry. Clearly much more work needs to be done to confirm or deny the feasibility of this hypothesis.

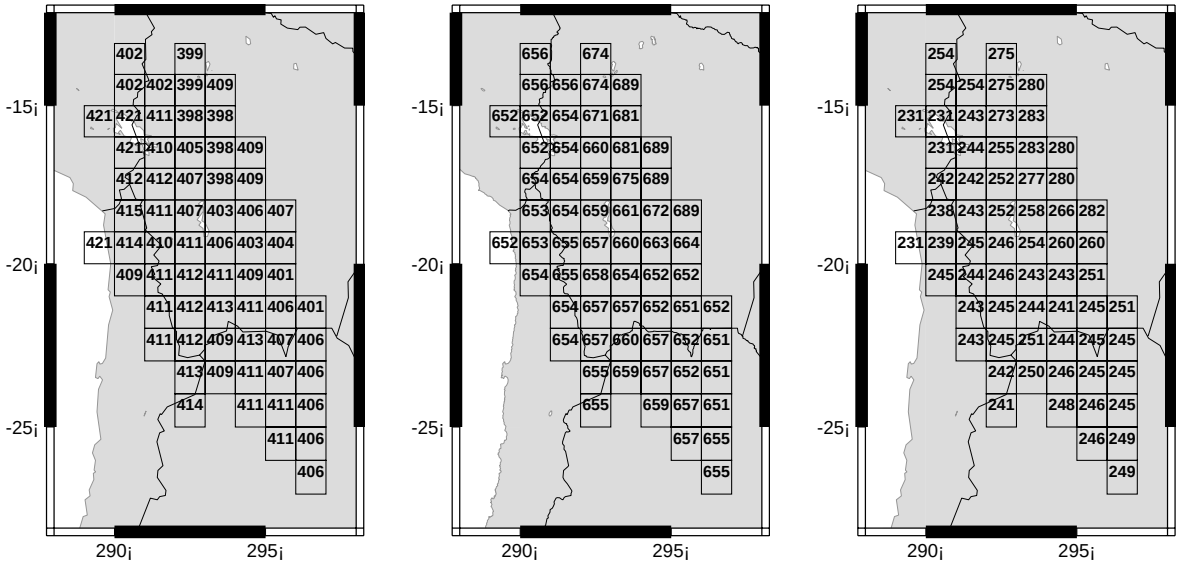

Figure 1. Pseudo-tomographic decomposition of path-averaged discontinuity depth estimates. T three panels show depth to the 410-km discontinuity (left), depth to the 660-km discontinuity (middle) and transition zone width (right). Note the general easterly increase in transition zone width.

REFERENCES

1. Angel, R.J., A. Chopelas, and N.L. Ross, "Stability of high-density clinoenstatite at upper mantle pressures," *Nature*, 358, 322–324, 1992.

2. Angel, R.J., and D.A. Hugh-Jones, "Equations of state and thermodynamic properties of enstatite pyroxenes," *J. Geophys. Res*., 99, 19,777–19,783, 1994.

3. Bostock, M.G., "A seismic image of the upper mantle beneath the North American craton", *Geophys. Res. Lett.*, 23, 1593–1596, 1996.

4. Bostock, M.G, "Anisotropic upper-mantle stratigraphy and architecture of the Slave craton," *Nature*, 390, 392–395, 1997.

5. Flanagan, M.P., and P.M. Shearer, "Global mapping of topography on transition zone discontinuities by stacking SS precursors," *J. Geophys. Res.*, 103, 2673–2692, 1998.

6. Revenaugh, J., and T. H. Jordan, "Mantle layering from ScS reverberations: 1. Waveform inversion of zeroth-order reverberations", *J. Geophys. Res.*, 96, 19,749–19,762, 1991a.

7. Revenaugh, J., and T. H. Jordan, "Mantle layering from ScS reverberations: 2. The transition zone," *J. Geophys. Res*., 96, 19,763–19,780, 1991b.

8. Revenaugh, J., and T. H. Jordan, "Mantle layering from ScS reverberations: 3. The upper mantle," *J. Geophys. Res*., 96, 19,781–19,810, 1991c.

Seismic Velocity Structure of the North and Central African Lithosphere from Upper Mantle P, PP, S, and SS Waveform Modeling (99-GS-028), (00-GS-039)

Principal Investigator: Susan Y. Schwartz (UC Santa Cruz)
LLNL Collaborator: Arthur Rodgers
Graduate Student: Sara Russell (UC Santa Cruz)

The Red Sea rift zone is the youngest and most tectonically active region in northeast Africa, however the seismic velocity structure of this and nearby geologic provinces are relatively unexplored due to the sparseness of African earthquakes and a historic lack of seismic arrays. We present results from an investigation of northeast Africa's lithospheric structure, concentrating on the Red Sea rift zone region. Our dataset consists of 3-component regional broadband data from 15 African earthquakes (M > 5.5) recorded at the KEG, ATD, EIL, and FURI stations of the MEDNET, GEOSCOPE, and IRIS seismic networks. The seismograms densely sample the Red Sea region and also include paths through the relatively undisturbed region to the west of the rift zone. We estimate lithospheric structure by modeling full waveforms using a grid-search approach. Our results are compared with previous research modeling the lithospheric structure beneath the Arabian-Nubian Peninsula.

OBJECTIVES

Our goal is to characterize the lithospheric structure of northern Africa by modeling seismic broadband waveforms to obtain models of the crust and upper-mantle velocity structure. We are specifically concentrating on the Red Sea region, which is the youngest and most tectonically active region in northeast Africa. These geological provinces are relatively seismically unexplored due to lack of arrays and dearth of earthquakes located inside the continent. Recent deployments of IRIS-GSN, MEDNET, and GEOSCOPE instrumentation in northern and central Africa make it possible to gather high-quality seismic data at regional distances.

This project is motivated by the need to characterize lithospheric structure as it influences wave propagation of regional phases that can be used for explosion discrimination. An accurate knowledge of the crustal and lithospheric structure beneath strategic areas is essential for successful seismic monitoring at regional distances. We are investigating the lateral variability in mantle structure and interpreting the resulting models in terms of tectonic continental evolution of north and east central Africa. Additionally, we compare the waveform results with previous research modeling the lithospheric structure beneath the Arabian-Nubian Peninsula.

PROGRESS

Our dataset includes 3-component regional broadband data from 15 African earthquakes (M > 5.5) recorded at the KEG, ATD, EIL, and FURI stations of the MEDNET, GEOSCOPE, and IRIS seismic networks. The epicentral distance range of our data is 14 - 29 degrees. Figure 1 illustrates our source to receiver geometry with the recordings at ATD, KEG, and EIL stations providing dense coverage of the Red Sea rift zone. Events were culled to insure data possess distinct compressional, shear, and surface wave arrivals. Preprocessing of the data includes deconvolution of the station response and bandpass filtering between 5-100 seconds.

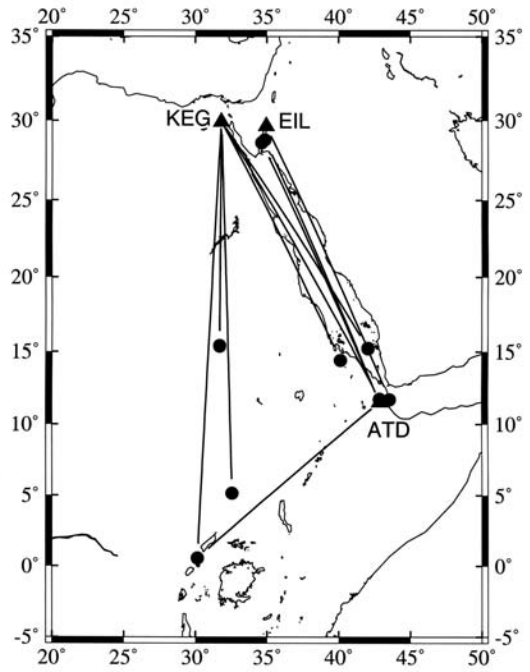

Figure 1. Map of northern Africa illustrating our source-receiver geometry. The earthquakes are denoted as circles and the stations are triangles. The most dense raypath coverage is located in the Red Sea rift zone.

We employ a grid-search algorithm to model both the surface and body waves in the period range 20-100 seconds. Using a range of velocity and layer thickness parameters, we create a suite of models and synthetic seismograms using a reflectivity code.[3] The best parameters are chosen by calculating a least-squares misfit between the data and synthetic components. During the first iteration we concentrate on constraining the crustal velocities and thickness through fitting the absolute timing and amplitude of the surface wave packet. Later iterations involve varying the lid and upper mantle thickness and gradients to fit the P and S bodywave arrivals and amplitudes. Data amplitudes are based on the earthquake's moment rather than scaled to the data.

We begin by modeling the six seismograms for events with focal mechanisms previously derived by Foster and Jackson.[1] Four of these seismograms traverse the shield through Sudan and Egypt (see Figure 2 for an example) and two sample the Red Sea rift zone. Although we find variations between the individual models in a region, there are dramatic differences between the rift and shield velocity structures. For the Red Sea paths, we find a 15-25 km thick crustal layer with Vp = 6.0-6.2 km/s and Vs = 3.4 - 3.6 km/s best fit the waveforms. The best-fit models also suggest that extremely slow mantle velocities are appropriate for the Red Sea region. For the shield paths, we find on average a 30-38 km thick crust with Vp = 6.0-6.4 km/s and Vs = 3.5-3.6 km/s and mantle velocities Vpn = 8.0-8.1 km/s and Vsn = 4.4-4.7 km/s best fit the data. At this stage of the modeling, velocities below approximately 100 km are not well-constrained.

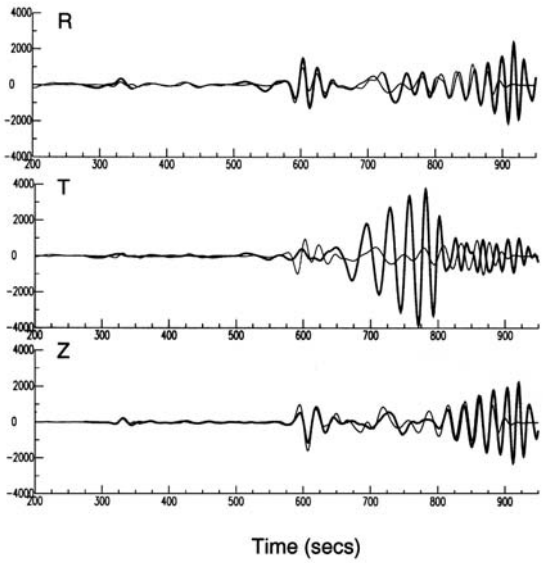

Figure 2. Data (thick line) and best-fit synthetic seismogram for M=5.2 African earthquake on March 29, 1991 sampling a shield path at epicentral distance 24.6 degrees.

Comparison with velocity models derived for other stable regions shows that our best-fit structure for the shield paths do not differ greatly from those models. The Arabian shield model and model S25,[4,2] although containing more crustal layers than our averaged one-layer crust, contain crustal and lid velocities that are similar to our shield model. Model GCA, developed for the rift zone in the Gulf of California by Walck appears to

be on average slightly faster than our best fit model for the Red Sea.[5]

We are working to model the remaining waveforms in the dataset that mainly traverse the Red Sea. This will augment the coverage through the rift zone and add further constraints to the velocity model. We also plan to improve the modeling through exploration of a model space with several crustal layers. In addition, the exceedingly slow upper mantle velocities in the Red Sea models could be biased by horizontal refraction, which we will examine through analysis of the surface wave polarizations.

REFERENCES

1. Foster, A.N., and J.A. Jackson, 1998. "Source parameters of large African earthquakes: implications for crustal rheology and regional kinematics," *Geophys. J. Intl.*,134, 422-448.

2. Lefevre, L.V., and D.V. Helmberger, 1989. "Upper mantle P velocity structure of the Canadian Shield," *J. Geophys. Res.*, 94, 17749-17765.

3. Randall, G., 1994. "Efficient calculation of complete differential seismograms for laterally homogeneous earth models," *Geophys. J. Intl.*, 118, 245-254.

4. Rodgers, A.J., Walter, W.R., Mellors, R.J., Al-Amri, A.M.S., and Y-S. Zhang, 1999. "Lithospheric structure of the Arabian Shield and Platform from complete regional waveform modeling and surface wave group velocities," *Geophys. J. Int.*, 138, 871-878.

5. Walck, M., 1983. "The P-wave upper mantle structure beneath an active spreading center: The Gulf of California," *Geophys. J. R.A.S.*, 76, 697-723.

Simulation of *In Situ* Production of Cosmogenic Nuclides (00-GS-01)

Principal Investigator: Kunihiko Nishiizumi (UC Berkeley)
LLNL Collaborator: Robert C. Finkel
Research Scholar: Jozef Masarik

Cosmogenic nuclide surface exposure dating has proven to be a valuable tool in tectonics, geomorphology, paleoclimatology and other fields. In order to use this technique, knowledge of the production rate for each nuclide as a function of rock composition, geographic location, site elevation, burial depth and exposure geometry is essential. The growing range of geologic settings in which in situ produced cosmogenic nuclides are being applied and the increasing demand for highly accurate interpretation, requires a more detailed understanding of the parameters which affect nuclide production than has been available. Developments in computing technology and in the understanding of the intermediate energy nuclear reactions which are important at the earth's surface form the basis for an investigation of cosmogenic nuclide production rates by computer simulation. The LLNL-ASCI supercomputer offers a platform which will greatly increase the speed of the computation-intensive Monte Carlo calculations on which these simulations are based. The goal of this work is to characterize, from numerical simulation, the basic dependencies of in situ nuclide production on the controlling parameters listed above. In addition, the contribution of nucleons and muons to the total production rate will be investigated separately. The method to be used allows tailoring the computation to the specific details a given field site and will thus be able to impact directly the interpreation of ongoing measurements programs at UCB and LLNL. One of the goals of this work is to compare theoretical predictions with experimental results to gain increased confidence in both approaches. This work is being carried out at the Space Science Laboratory at UCB and the Earth Science Division and Center for Accelerator Mass Spectrometry at LLNL.

InSAR Observations and Mechanical Modeling of Geothermal Systems (00-GS-002)

Principal Investigator: Roland Burgmann (UC Berkeley)
LLNL Collaborator: Bill Foxall
Postgraduate Researcher: Evelyn Price (UC San Diego)

Geothermal systems occur globally in regions where heat from deep-seated sources within the Earth's crust is transferred close to the surface by convecting fluids. The deformation associated with geothermal systems is highly variable in space and time,[6,9,3] and is modulated by geologic structures, seasonal effects, precipitation, industrial extraction and reinjection, and active volcanic and faulting processes. While geothermal energy is generally an environmentally advantageous and renewable source of power, a fuller understanding of the geothermal plumbing system will allow us to make the most efficient use of this resource. The spatial and temporal details of the surface deformation field associated with geothermal production areas include both localized deformations due to the transfer of fluid mass along zones of relatively high permeability and broad subsidence due to long-term pumping of fluids from reservoirs at depth. A single InSAR (Interferometric Synthetic Aperture Radar) image produced using data from existing SAR satellites (European Space Agency ERS-1 and ERS-2) is capable of mapping sub-centimeter displacements over areas of 100x100 km2 with a spatial sampling (pixel size) of 10-30m every 35 days. InSAR can recover both the short- and long-wavelength components of the complete, spatially variable surface deformation fields associated with geothermal systems.[10,11,5 ,2,4] The InSAR deformation field can be inverted, along with other geodetic measurements, for the displacements on complex planar and point sources in the Earth's crust. These displacements can be used in boundary element, thermo-elastic, and poro-elastic models of the geothermal system to predict the stresses acting on bulk volumes and across the complex fracture systems inherent in these crustal environments.[8] The result of these studies will complement our understanding of the interplay between forces and structure within geothermal systems.

OBJECTIVES

One goal of this project was to gain an improved understanding of the fluid flow, heat transfer and mechanical processes taking place within a geothermal system. We were particularly interested in understanding the details of the flow connectivity through geologic structures and the resultant implications for the mechanical processes that define the geothermal plumbing system. We wanted to deduce the relative importance of channeled and diffuse transfer of fluid mass within the geothermal system and determine how the poroelastic and thermoelastic stresses associated with geologic structures, seasons, precipitation, industrial extraction and reinjection, and active volcanic and faulting processes modulate the surface deformation field in space and time. We also intended to investigate the causes and interactions of earthquakes within geothermal systems associated with tectonic stress, thermal, and fluid-pressure changes. A further goal was to investigate similarities and differences among world-wide geothermal systems which have been shown to be highly variable in their structure, host rock, productivity, and surface deformation.

PROGRESS

This project supported the research of a post-doctoral investigator (Evelyn Price) for 9 months. The scientists involved completed numerous tasks directed towards the accomplishment of the proposed research goals. These included identification of possible research targets, development of enhanced InSAR capability at UC Berkeley, and working knowledge of inversion and boundary element modeling (BEM) routines. This development was used to generate results of a separate project funded by the Southern California Earthquake Center. These results gave insight into the interaction between the earthquakes that happened in 1992 near Landers, California and in 1999 near Hector Mine, California.[7]

The locations of possible research targets were limited by data availability. Geothermal areas considered for study were located in California including Casa Diablo, The Geysers, Coso, and Cerro Prieto; in Dixie Valley, Utah; and in Tibet. Data was obtained from the Western North America Interferometric Synthetic Aperture Radar Consortium (WInSAR) over the Coso geothermal field (Figure 1). This well-studied geothermal area in southern California is the site of more than 90 operating wells.

Preliminary phase and phase gradient analysis of a five-year interferogram over the Coso geothermal field (Figure 1) illustrates a number of interesting features. First, integrating the interferometric phase over the area of geothermal production gives approximately 15 cm of vertical displacement. Second, the pattern of subsidence is not strictly radially symmetric indicating that the surface displacements are a result of stresses induced by draw-down and re-injection in a complexly faulted stratum. Third, plotted with the seismicity in the region, the phase and phase gradient maps show approximately 28 mm of LOS displacement associated with an earthquake cluster to the southeast of the geothermal field containing three earthquakes with magnitude greater than 5. This analysis shows that we can indeed map the complex deformation field of a geothermal region using InSAR.

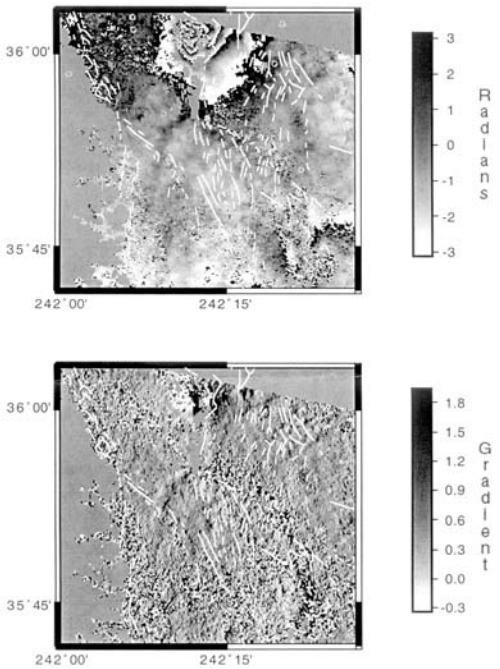

Figure 1. The ERS-1 and ERS-2 phase and phase gradient maps spanning 8/30/1993 to 10/22/1998. Each fringe in the interferogram represents 28 mm of LOS displacement. Major faults are plotted in white and circles are M 3-8 shocks.

The postdoctoral researcher gained familiarity with JPL's ROIPAC software and began to tailor it for geothermal applications. She also developed inversion tools in Matlab, aimed at inferring complex distributions of displacements on buried faults and point sources. These tools integrate different geodetic data types including GPS and InSAR displacements. In addition, she learned how to use BEM routines developed at Stanford for modeling of tectonic stress transfer. If the project had continued, the inversions would have allowed the researchers to obtain a kinematic view of the three-dimensional displacements within the geothermal fields while the BEM modeling would have allowed an assessment of the stress fields under realistic overburden and fault friction conditions. Also, if the project had continued, researchers at UC Berkeley and LLNL would have used the poroelastic and thermoelastic modeling codes under development at LLNL in conjunction with inversion and boundary element modeling to investigate poroelastic and thermoelastic effects on deformation of geothermal areas.[1]

REFERENCES

1. Bosl, W., "Computational studies of crustal fluids and seismicity, Ph.D. dissertation," *Stanford Univ.*, 1999.

2. Carnec et al., "Monitoring surface deformation with radar interferometry at the Cerro Prieto geothermal field (Mexico)", *Geotherm. Resources Council Trans*., 22, 297-301, 1998

3. Hatton, J.W., "Ground subsidence of a geothermal field during exploitation", *Geothermics*, special issue 2, 1294-1296, 1970.

4. Ikehara, M.E., Galloway, D.L., Fielding, E., Bürgmann, R., Lewis, S., and Ahmadi, B., "InSAR imagery reveals seasonal and longer-term land surface elevation changes influenced by ground -water levels and fault alignment in Santa Clara Valley, California" *EOS Trans. AGU*, 79 (45), 37, 1998.

5. Massonnet, D., Holzer, T., and Vadon, H., "Land subsidence caused by the East Mesa geothermal field, California, observed using SAR interferometry" *Geophys. Res. Lett*., 24, 901-904, 1997.

6. Mossop & Segall, "Subsidence at the Geysers geothermal field, N. California, from a comparison of GPS and leveling," *Geophys. Res. Lett*., 24, 1839-1842, 1997

7. Price, E.J., and R. Bürgmann, "Interactions between the Landers and Hector Mine earthquakes from space geodesy, boundary element modeling, and time-dependent friction," *Bull. Seism. Soc. Am*., submitted, 2000.

8. Segall & Fitzgerald, "A note on induced stress changes in hydrocarbon and geothermal reservoirs," *Tectonophysics*, 289, 117-128, 1998

9. Sorey, M.L., Farrar, C.D., Marshall, G.A., and Howle, J.F., "Effects of geothermal development on deformation in Long Valley caldera, eastern California, 1985-1994," *J. Geophys. Res.*, 100, 12,475-12,486, 1995.

10. Thatcher, W., and D. Massonnet, "Crustal deformation of Long Valley Caldera, eastern California, 1992-1996, inferred from satellite radar interferometry," *Geophys. Res. Lett*., 24, 2519-1522, 1997.

11. Webb, F.H., Simons, M., Hensley, S., Rosen, P. A., Chapin, E., and Shaffer, S., "A model depth of 11 km for a single Mogi source for the inflation of Long Valley Caldera from 1992.5-1995.75 using InSAR", *Eos Trans. AGU*, 78, 818, 1997.

Modeling of Complex Structure in the Earth's Core (00-GS-010)

Principal Investigator: Barbara Romanowicz (UC Berkeley)
LLNL Collaborator: Shawn Larsen
Graduate Student: Ludovic Breger (UC Berkeley)
Postdoc: Hrvoje Tkalvcic (UC Berkeley

Core phases of the PKP type are the primary tool to study structure in the core and, in particular, put constraints on inner core anisotropy. While the first models of inner core anisotropy were simple, recent studies of PKP travel times indicate a large degree of spatial complexity. On the other hand, increased evidence for the existence of strong lateral heterogeneity and complexity in the D" region calls for a reevaluation of how PKP waves can be contaminated through the passage in D", how these effects can be corrected for, and how this affects our understanding of core structure.

In this study, we have complemented the existing collection of differential travel times of PKP(AB-DF) and PKP(BC-DF) as measured on high quality digital broadband records, and assembled a global dataset of differential PcP-P travel time data, also measured on broadband records. Our goal was to test how much of the PKP data could be explained by structure in the deep mantle (D") and whether complex inner core anisotropy was required. After correction for mantle structure using available tomographic models, the PKP(AB-DF) data were inverted jointly with PcP-P for structure in D", using PKP(BC-DF) as constraints. Various tests were performed to assess the stability of the models obtained with respect to subsets of data, and the allowance or not of inner core anisotropy. Our results show that over 80% of the variance in the PKP(AB-DF) data can be explained by D" structure. The very anomalous paths from the south Atlantic to Alaska are the only ones which remain to be explained. Allowing for a simple model of transverse isotropy in the inner core is one way to improve the fit to these data.

OBJECTIVES

Inner core anisotropy was proposed 15 years ago to explain two types of intriguing observations: (1) faster propagation of PKP phases traversing the inner core along paths quasi-parallel to the earth's rotation axis than along equatorial paths[10] and (2) anomalous splitting of inner core sensitive free oscillations.[14] Initially, simple models of transverse isotropy, with fast axis parallel to the earth's rotation axis were proposed, with strength of anisotropy between 1.5 and 3.5% on average, depending on the authors.

In recent years, with the accumulation of high quality global digital broadband data, increasing levels of complexity have been documented. The axis of anisotropy may not be aligned with the earth's rotation axis,[11,9] and only the western "quasi-hemisphere" may be anisotropic.[12,5] Furthermore, there is evidence for an isotropic layer 50-200 km thick at the top of the inner core.[5] To reconcile these complex observations, Creager and Garcia and Souriau have proposed the existence of a spatially asymmetric discontinuity between the top isotropic and the inner anisotropic part of the inner core.[5,6]

Further complexity has been documented from the study of PKP travel times by Bréger *et. al.* ,[2,3,4] who infer that the data require strong lateral variations of anisotropy on short spatial scales, or else the source of complexity must be sought elsewhere, most likely at the base of the earth's mantle.

On the other hand, recent results have shown that heterogeneity at the base of the mantle is stronger than described by tomographic models. In particular, our studies and those of other groups indicate that the borders of the African and Pacific "plumes" at the base of the mantle must be the sites of strong gradients and complex structure.[1]

This organized heterogeneity at the base of the mantle affects the travel times of PKP phases sensitive to core structure. In this project, we have investigated this issue, combining PKP and PcP travel time data measured on high quality broadband records.

PROGRESS

We have assembled a large dataset of high quality PKP(AB-DF), PKP(BC-DF) and PcP-P travel times measured on broadband records (Figure 1), from a variety of sources. We measured about half of the PKP(AB-DF) data ourselves, using cross-correlation between PKP(DF) and the Hilbert transformed PKP(AB). The uncertainty in the measurements is on the order of 0.1-0.2 sec. We complemented this dataset with data from other authors (Souriau, personal communication; Wysession, personal communication).[5,9] Whenever duplicate measurements existed for the same path, we checked them for consistency and removed suspicious ones. We also checked data for consistency by plotting trends for a given station or a given source region, as a function of azimuth or back azimuth, respectively. This was not possible for polar paths, for which the geographical distribution of data is not complete. Figure 2a shows the variation of PKP(AB-DF) residuals, computed with respect to model AK135 as a function of angle x of the path in the inner core with respect to the earth's rotation axis.[8] The very large residuals for angles around 30° correspond to paths from southern Atlantic (in particular, South Sandwich Islands) to stations in Alaska. A similar procedure was applied to assemble our global PKP(BC-DF) dataset, which also shows largest residuals for the same paths.

To complement the PKP dataset, and add independent constraints on mantle structure, we measured 1219 PcP-P differential travel times, by cross-correlation, in the epicentral distance 25° to 75°. While the global coverage with PcP-P is far from complete, in areas where there is good coverage, we note a high level of spatial coherency in the data (Figure 2b). An area of particular interest is middle America, where the alternation of positive and negative residuals indicates sharp lateral gradients on scale lengths of several hundred km in the deep mantle, in agreement with recent results based on ScS-S data.[15]

After correcting the different datasets for 3D mantle structure by testing different existing tomographic models and selecting the one which provides the best variance reduction,[7] when stripped of the last 300 km at the bottom of the mantle, we inverted jointly PKP(AB-DF) and PcP-P for heterogeneity in D", using PKP(BC-DF) as constraints to choose optimal damping parameters in the inversion. Figure 2a shows, superimposed on the observed residuals, the predicted residuals from our preferred model using the complete PKP(AB-DF) and PcP-P dataset. We compared models obtained using the complete dataset, with models without anomalous paths from the south Atlantic, and models in which only equatorial PKP(AB-DF) data were considered. We found that the resulting models were stable, in particular under Alaska and the south Atlantic, where they are therefore not artifacts of mapping inner core anisotropy signal into the mantle. Over 85% of the variance in the PKP(AB-DF) data can therefore be explained by structure in the mantle. Up to 2 sec of residual in the most anomalous paths from south-Atlantic to Alaska remain to be explained.

We also compared these models with models obtained by first correcting data for transverse isotropy in the inner core, using various inner core models. Accounting for inner core anisotropy can help explain up to 5% additional variance in the data. No complex inner core structure is however required.

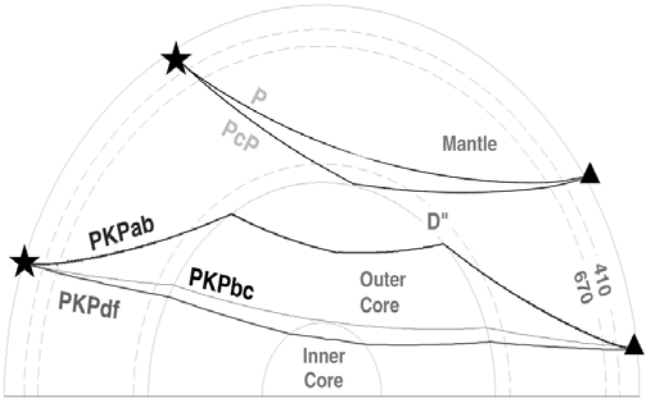

Figure 1. Cross section of the earth showing the paths of P, PcP, and the different branches of PKP phases.

a)

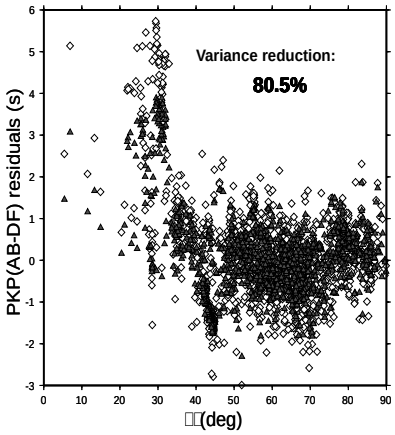

b)

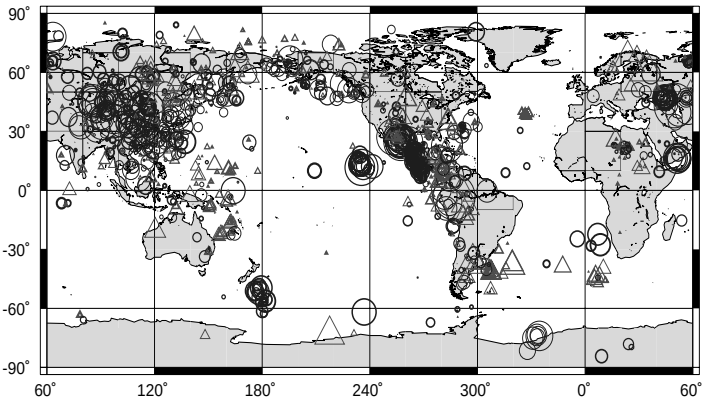

Figure 2 (a) PKP(AB-DF) travel time residuals with respect to AK135 (diamonds), and predictions from preferred mantle model (triangles) plotted as a function of angle x of the DF path in the inner core with respect to the earth's rotation axis. (b) Map showing the distribution of PcP-P travel time residuals, projected on the core-mantle boundary at the location of the PcP bouncepoint (from Tkalcic et al., 2001).

REFERENCES

1. Bréger, L., and B. Romanowicz (1998) "Three-Dimensional structure at the base of the mantle beneath the Central Pacific", *Science*, 382, 718-720.
2. Bréger, L., B. Romanowicz, and H. Tkalcic (1999) "PKP(BC-DF) travel times: New constraints on short scale heterogeneity in the deep earth", *Geophys. Res. Lett.*, 26, 3169-3172.
3. Bréger, L., B. Romanowicz and S. Rousset (2000a) "New constraints on the structure of the inner core from P'P'," *Geophys. Res. Lett.*, 27, 2781-2784.
4. Bréger, L., H. Tkalcic, and B. Romanowicz (2000b) "The effect of D" on PKP(AB-DF) travel time residuals and possible implications for inner core structure," *Earth Planet. Sci. Lett.*, 175, 133-143.
5. Creager, K.C. (1999) "Large-scale variations in inner core anistropy," *J. Geophys. Res.*, 104, 23,127-23,139.
6. Garcia, R., and A. Souriau (2000) "Inner core anisotropy and heterogeneity level," *Geophys. Res. Lett.*, 27, 3121-3124.
7. Karason, H., and R. van der Hilst (2000) "Improving global tomogaphy models of P wavespeed. I: incorporation of differnetial times for refracted and diffracted core phases (PKP, Pdiff)," *J. Geophys. Res.*, in press.
8. Kennett, B.L.N., E.R. Engdahl, and R. Buland (1995) "Constraints on seismic velocities in the Earth from travel times," *Geophys. J. Int.*, 122, 108-124.
9. McSweeney, T.J., K.C. Creager, and R.T. Merrill (1997) "Depth extent of inner core seismic anisotropy and implications for geomagnetism," *Phys. Earth Planet. Inter.*, 101, 131-156.
10. Morelli, A., A.M. Dziewonski, and J.H. Woodhouse (1986) "Anisotropy of the core inferred from PKIKP travel times," *Geophys. Res. Lett.*, 13, 1545-1548.
11. Su, W.J., and A.M. Dziewonski (1995) "Inner core anisotropy in three dimensions," *J. Geophys. Res.*, 100, 9831-9852.
12. Tanaka, S., and H. Hamaguchi (1997) "Degree one heterogeneity and hemispherical variation of anisotropy in the inner core from PKP(BC)-PKP(DF) times", *J. Geophys. Res.*, 102, 2925-2938.
13. Tkalcic, H., B. Romanowicz, and N. Houy (2001) "Constraints on D" structure using PKP(AB-DF), PKP(BC-DF) and PcP-P travel time data from broadband records", submitted to *Geophys. J. Int.*
14. Woodhouse, J.H., D. Giardini, and X.-D. Li (1986) "Evidence for inner core anisotropy from splitting in free oscillation data," *Geophys. Res. Lett.*, 13, 1549-1552.
15. Wysession, M.E., K.M. Fischer, G.I. Al-eqabi, and P.J. Shore (2000) "Using MOMA broadband array, ScS-S data to image smaller-scale structures at the base of the mantle", submitted to *Geophys. Res. Lett.*

X-Ray Tomography to Determine Moisture Distribution in a Soil Sample for Various Outflow Conditions (00-GS-012)

Principal Investigator: Jan W. Hopmans (UC Davis)
LLNL Collaborator: D. Wildenschild
Other Collaborator: C.M. Vaz, (Embrapa CMPDIA, Sao Carlos, Brazil)
Student: Wendy Acosta (UC Davis)

The fundamental understanding of transport mechanisms in porous media can be achieved only by studying pore-scale processes. However, these micro-scale mechanisms cannot be measured with traditional techniques that require insertion of a sensor at or near the region of interest. X-ray computed tomography (CT) overcomes this problem by providing non-destructive cross-sectional or three-dimensional object representations from the attenuation of electromagnetic radiation. CT uses projection views (radiographs) from different angles to mathematically reconstruct the complete three-dimensional image of the object. The physical basis for CT is the absorption or attenuation of the penetrating electromagnetic radiation by the object, which is proportional to the density profile of the object. Since CT allows non-invasively measurements of phase distribution and species concentration, x-ray CT offers significant advantages to study fundamental physical processes of water movement and contaminant transport in porous media. We present results obtained with a micro-tomography system based at the synchrotron facility of the Advanced Photon Source at Argonne National Laboratory providing spatial resolutions on the order of 10 mm. Using the synchrotron-based system we were able to detect individual pores and grains as well as phase distributions.

OBJECTIVES

The current understanding of water flow and contaminant transport in soils has been limited by the technology of the measurements. Also, studies on contaminant transport have shown repeatedly that water-soluble chemical constituents move through the soil much faster than the macroscopic flow theory predicts. To correctly describe transport of contaminant species it is essential to understand the interplay of advection, mechanical dispersion and diffusion, and their dependency on soil water distribution. As the relative importance of each transport component strongly depends on the soil water flow rate, the possibility of studying dynamic flow systems as proposed in this study becomes profoundly attractive. In all cases, an argument can be made that a fundamental understanding of transport mechanisms in porous media can be achieved only by studying pore-scale processes.

However, these mechanisms operating at the micro scale cannot be measured with traditional techniques, which generally require insertion of a sensor at or near the region of interest. X-ray tomography overcomes this problem via the non-invasive observation of changing fluid phase content and solution concentration while resolving increasingly smaller features of the pore space.[1,2,3,4] Our main objective of this study is to use the micro-tomography capabilities of beamline 13-BM , to observe spatial and temporal distribution of air and water phases during drainage experiments.

The goal was to perform outflow experiments on a soil sample while simultaneously observing the distribution of air and water phases in the sample using x-ray CT. Existing equipment was modified to fit on the mounting table of the x-ray facility.

Two different types of experiments were performed on the samples: (1) one-step experiments for which one relatively high pneumatic pressure was imposed on the sample to induce outflow and (2) multi-step outflow experiments where the procedure was the same as for the one-step experiments except that a varying number of smaller pressure increments were applied instead of one large pressure step.[5] Between each successively increasing pressure increment, time was allowed for the sample to equilibrate or at least for outflow to cease. During selected experiments, the flow cell with the draining soil was placed in the x-ray beam, and changes in water content were scanned in vertical cross sections from the top to the bottom of the flow cell. Spatial and temporal changes in water saturation can then be compared for cases with different water outflow rates.

PROGRESS

Outflow experiments have been carried out with two sizes of flow cells: 2.5 cm and 0.6 cm inner diameter with respective spatial resolutions of approximately 80 and 20 micrometer. Monochromatic x-ray beams were obtained by aligning a (water-cooled) silicon crystal such that a beam energy of about 33 keV was attained, corresponding to the characteristic energy level for specific photoelectric absorption, involving the K-shell of iodine that was used as a dopant. An example of the obtained images is illustrated in Figure 1a and 1b. The figure shows two slices through the center of a packed-sand core in identical position, but scanned after two different types of experiments were performed on the core. Figure 1a illustrates conditions after the core has been drained slowly to a final capillary pressure of 490 cm using a multi-step approach, whereas Figure 1b is a scan performed after the core has been drained very quickly using just one large pressure step of 490 cm. Clearly, there are major differences in overall amount of water retained in the core, but the distribution is also very different. For the material investigated in this study, microtomography has proven to be an extremely useful tool, and further evaluation of the large number of yet not analyzed images will without doubt provide us with new information on flow and transport behavior in porous materials.

In previous work by the authors it has become evident that the methods we use to measure the hydraulic properties can have a significant impact on the obtained results. In particular, a dependence on drainage outflow rate has been observed, suggesting interference from dynamic phenomena such as air entrapment, electrokinetic processes, non-Newtonian flow etc. X-ray computed tomography (CT) offers an advantageous possibility to non-invasively investigate these dynamic processes on the pore scale. The experiments carried out at the APS will open up the possibility of quantitatively explaining these flow-rate dependent phenomena. Moreover, it is suggested that the high spatial resolution measurements will provide a unique database that can be used for verification of Lattice Boltzmann numerical simulations of flow and transport in unsaturated porous media.

ACKNOWLEDGMENTS

We especially acknowledge the assistance of Dr. Mark Rivers of GSECARS (Argonne National Laboratory) to prepare the experimental setup for imaging.

REFERENCES

1. Clausnitzer, V., and J.W. Hopmans, "Estimation of phase-volume fractions from tomographic measurements in two-phase systems," *Advances in Water Resources*, 22:577-584 1999.

2. Clausnitzer, V., and J.W. Hopmans. 2000. "Pore-scale measurements of solute breakthrough using microfocus computed tomography." *Water Resources Research*, 36:2067-2079.

3. Hopmans, J. W., T. Vogel, and P. D. Koblik, "X-ray tomography of soil water distribution in one-step outflow experiments," *Soil Sc. Soc. Am. J.*, 56(2):355-362, 1992.

4. Hopmans, J. W., M. Cislerova and T. Vogel. 1994. "X-ray tomography of soil properties. In: Tomography of soil-water-root processes." Special Publication 36, *Soil Science Society of America*, pp. 17-28.

5. Wildenschild, D. and J.W. Hopmans, 1999. "Rate dependence of hydraulic properties for unsaturated porous media." In: *Proceedings of the International Workshop on Characterization and Measurement of the Hydraulic Properties of Unsaturated Porous Media*, Riverside, California, October 22-24, 1997. in press.

Crustal Stress Induced by Small-Scale Convection beneath California (00-GS-013)

Principal Investigator: Louise H. Kellogg (UC Davis)
LLNL Collaborator: William Bosl
Postgraduate Researcher: Fred Pollitz (UC Davis)
Graduate Research Assistant: Margaret Glasscoe (UC Davis)

Many physical processes contribute to stress in Earth's continental crust. The distribution of stress within the crust, the mechanism of stress transfer between zones of plastic deformation, and the relation between crustal stress and geologic regionaliza-tion all depend on the sources of stress. The best known contributors are those related to a crustal deformation cycle consisting of interseismic strain accumulation around major fault zones, coseismic stress release, and postseismic relaxation of the ductile lower lithosphere following earthquakes. The driving force invoked for this process is conventionally shear transmitted horizontally by motion of the bounding tectonic plates in conjunction with lateral flow beneath the upper crust. The contribution of vertical forces through small-scale mantle convection has received comparatively little attention. We have explored the importance of this stress source by performing research on two fronts: 1. Estimating the stresses imparted by a dense rift pillow which is possibly sinking beneath the New Madrid Seismic Zone (NMSZ). 2. Analyzing the topography and crustal stress patterns produced by small-scale mantle convection beneath northern California. We find that vertical forces may be the primary contributor to stress in the NMSZ, possibly explaining the predominance of thrust faulting in that region. Convection-induced crustal stress in northern California is a significant fraction of the stress pro-duced by recognized strain accumulation processes, and the corresponding dynamic topography is highly correlated with present topography.

OBJECTIVES

The idea that mantle flow can influence crustal stress has been investigated since the 19th century when geologists contemplated the mechanism of postglacial rebound. This idea evolved considerably in the 1960's when attention turned to the possible mechanisms driving plate motions. At a global scale, numerous characteristics of lithospheric properties and evolution are attributed to a vigorously convecting mantle, including the generation of hotspots; slab pull, basal drag, and ridge-push mechanisms driving plate motions; dynamic topography produced by upwelling mantle plumes or downgoing slab fragments.6 Numerical models of global mantle convection at a scale of 1000's of km are highly evolved and complement the efforts of seismologists and geochemists to understand the meaning of deeply-sunken slab fragments and global geochemical anomalies.[14]

Small scale convection, involving flow at much shallower depths at wavelengths of 10's to 100's of km, has received less attention. It is considered an important process at least beneath the ocean basins where it has been invoked as a mechanism to explain short wavelength geoid anomalies,[2] the budget of heat flow for older oceanic lithosphere,[5] variations in seismic velocity,[13] and the distribution of hotspots.[25] Other suspected consequences, such as segmentation of mid-oceanic axial rift valleys, could be quoted. Small scale convection beneath continents has received surprisingly little attention. The most prominent examples are the interaction of an upwelling thermal instability with continental lithosphere,[10]

uplift and/or thermal/mechanical coupling of continental lithosphere with a flowing mantle around subduction zones,[24,9] and dynamic support for the southern Sierra Nevada range.[16] The objective of this proposal is to understand the pattern of small scale convec-tion beneath selected continental regions and its influence on crustal stress patterns.

Our chosen study areas are the New Madrid Seismic Zone (NMSZ) and northern California. Both are highly tectonically active regions where subsurface structure is reasonably well constrained and capable of producing significant convective flow.

PROGRESS

New Madrid Seismic Zone In the interest of brevity, we omit here discussion of our results for the New Madrid Seismic Zone. These results are discussed in detail in our manuscript Pollitz *et. al.* (Bull. Seismol. Soc. Am., submitted). Northern California This region exhibits significant lateral and depth variation of mechanical properties as revealed by topography, petrology, and seismic tomography.[1,12,20] We are motivated by two basic observations:

(1) Low seismic velocities beneath the northern Coast Ranges are associated with high elevation of the mountain range, i.e. it is a dynamic topographic feature produced by the presence of a buoyant uppermost mantle.[1] Estimation of the crustal stresses associated with dynamic uplift may help clarify how much of Pacific - Sierra Nevada relative plate motion is accommodated across the mountain chain.[18]

(2) Most (but not all) of the Great Valley is situated above the remnants of the fossil subducted Farallon slab, which are presumably sinking and creating dynamic topography in their wake. East of our study area, the fossil Farallon slab has descended into the deeper upper mantle at about 2 cm/yr over the past 18 Myr,[23] suggesting a strong flow pattern beneath the shallower slab remnants of central California.

Crust and mantle density anomalies are generated using the v s (shear velocity) model of Pollitz (Figure 1) and the relation $d \ln\rho / d \ln v_s = 0.40$.[20] An additional contribution from laterally varying crustal thickness is added since the v_s model was derived after correction for such crustal structure. Mooney and Weaver provide variations in crustal thickness over the region.[17] Based on the recently estimated 35-40 km thickness of the crust beneath the southern Sierra Nevada,[21] we truncate Mooney and Weaver's crustal thickness distribution at a maximum of 40 km. The density contrast between the crust and mantle is assumed to be ~400-500 kg m ^{3} . The mass anomalies generated by the shear velocity model and crustal thickness variations are then placed in a coupled elastic-viscoelastic model, assumed to consist of an elastic upper crust overlying viscoelastic lower crust and mantle. As the model of Pollitz prescribes v_s variations from 16 to 200 km depth, most of the mass anomalies are within the ductile (viscoelastic) portion of the viscoelastic model, and their buoyancy generates a flow field which may be evaluated in the steady state.[20]

This yields steady state displacement and stress within the elastic crust and a velocity field in the underlying viscoelastic portion of the model. The steady state response of the viscoelastic system to point forces distributed in the defined volume underlying northern California is calculated using the VISCO1D algorithm of Pollitz,[19] presented at a workshop at Stanford University in 1999 (see "Papers and Presentations Supported by this Project"). The final calculations reported below required approxi-mately 12 hours computation time on a Sun Ultra80 workstation.

It is well known that the steady state response of the viscoelastic system does not depend on the absolute viscosity distribution but only on its relative depth variation.

Here we consider the response of a perfectly elastic crust underlain by an isoviscous mantle. Dynamic topography and vertical stress on this model is shown in Figure 2.

The contributions of laterally heterogeneous structure, crustal thickness variation, and their sum are shown separately. The effects of these two separate factors are anticorrelated with one another, suggesting that subcrustal density anomalies balance to some extent the mass variations of crustal columns. However, the contribution of the crustal thickness variation is dominant. We consider it likely that the region is in better isostatic equilibrium than the resultant dynamic topography would indicate, and the imperfect balancing shown here is due to inadequate knowledge of the shallowest mantle density structure. The northern Coast Ranges are best correlated with the heterogeneous structure component, whereas the southern Sierra Nevada is better correlated with the crustal thickness component. Since the elevated southern Sierra Nevada is thought to be supported mainly by mantle density sources,[16,21] the density anomaly distributions in the crust and mantle assigned here may require substantial revision. Underestimation of the mantle density anomalies due to underestimation of the shear velocity perturbations in the tomographic inversion, as suggested by Pollitz, is a strong possibility.

Dynamic topography of 1 km and stress of 1 MPa are robust features of this modeling. The generated dynamic deviatoric stresses are a substantial fraction of the yield strength of the upper crust. This could be interpreted as meaning that convective forces contribute to cycles of plastic deformation (i.e., faulting). A more detailed interpretation should include other sources of stress such as lateral compression transmitted by the convergent Sierra Nevada block and lateral shear stress transmitted by the San Andreas fault.[7] In future work we wish to factor in such additional sources of stress as well as test the implications of more complicated viscoelastic structures on dynamic stressing of the lithosphere.

Figure 1. Distribution of shear velocity structure at six depth slices in the crust and upper mantle.

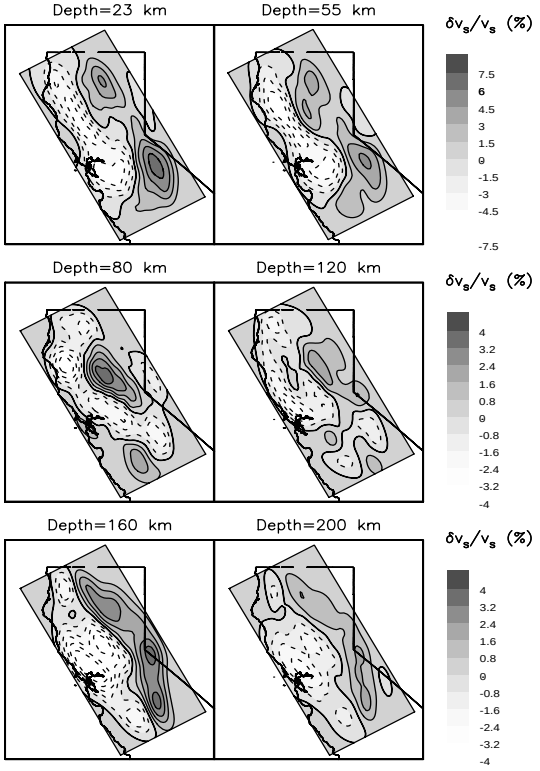

Figure 2. Dynamic topography at Earth's surface and dynamic vertical stress at depth 10 km resulting from 3D density anomalies with respect to a 1D background model plus crustal thickness variations. The rheological strucure consists of a purely elastic crust underlain by an isoviscous mantle. Contribution of crustal thickness variation is based on a density contrast of 500 kg m^{-3} between the crust and mantle .

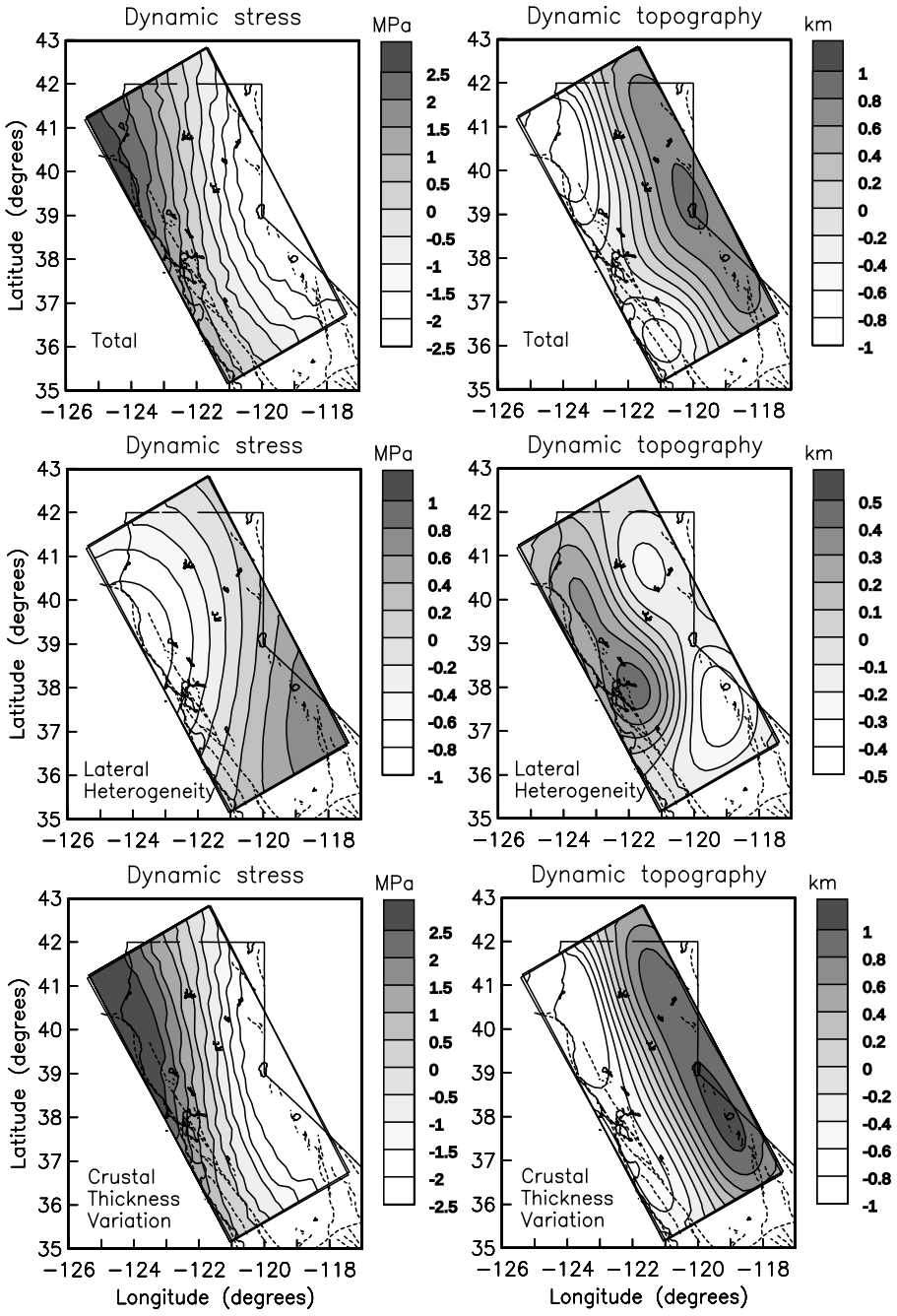

REFERENCES

1. Benz, H.M., G. Zandt, and D.H. Oppenheimer, "Lithospheric structure of northern California from teleseismic images of the upper mantle," *J. Geophys. Res*., 97, 4791- 4807, 1992.

2. Cazenave, A., B. Parsons, and P. Calcagno, "Geoid lineations of 1000 km wavelength over the Central Pacific", *Geophys. Res. Lett.*, 22, 97-100 (1995).

3. Cohen, S.C., "A multilayer model of time dependent deformation following an earthquake on a strike slip fault, " *J. Geophys. Res*. 87, 5409-5421 (1982).

4. Cox, R.T., and R.B. Van Arsdale, "Hotspot origin of the Mississippi embayment and its possible impact on contemporary seismicity," *Eng. Geol.*, 46, 5-12, 1997.

5. Davaille, A., and C. Jaupart, "Onset of thermal convection in fluids with temperature -dependent viscosity: Application to the oceanic mantle", *J. Geophys. Res*., 99, 19853-19866 ,1994.

6. Davies, G. F., and M. A. Richards, "Mantle convection", *J. Geology*, 100, 151-206, 1992.

7. Flesch, L.M., W.E. Holt, A.J. Haines, and B. Shen-Tu, "Dynamics of the Pacific-North American plate boundary zone in the western United States", *Science*, 287, 834-836, 2000.

8. Furlong, K. P., and C. A. Langston, "Geodynamic aspects of the Loma Prieta earthquake," *Geophys. Res. Lett.*, 17, 1457-1460, 1990.

9. Geist, E.L., "Relationship between the present-day stress field and plate boundary forces in the Pacific Northwest", *Geophys. Res. Lett.*, 23, 3381-3384, 1996.

10. Griffiths, R. W., and I. H. Campbell," Interaction of mantle plume heads with the Earth's surface and onset of small-scale convection," *J. Geophys. Res*., 96, 18295- 18310, 1991.

11. Hough, S.E., J.G. Armbruster, L. Seeber, and J.F. Hough, "On the modified Mercalli intensities and magnitudes of the 1811-1812 New Madrid earthquakes," *J. Geophys. Res*., 105, 23,839-23,864, 2000.

12. Humphreys, E.D., and K.G. Dueker, "Western U.S. upper mantle structure," *J. Geophys. Res*., 99, 9615-9634, 1994.

13. Katzman, R., L. Zhao, and T. H. Jordan, "High-resolution, two-dimensional vertical tomography of the Central Pacific mantle using ScS reverberations and frequency-dependent travel times," *J. Geophys. Res*., 103, 17933-17971, 1998.

14. Kellogg, L., B. Hager, and R. D. Van der Hilst, "Compositional stratification in the deep mantle", *Science*, 283, 1881-1884, 1999.

15. Kelson, K.I., G.D. Simpson, R.B. Arsdale, C.C. Haraden, and W.R. Lettis, "Multiple late Holocene earthquakes along the Reelfoot fault, central New Madrid seismic zone," *J. Geophys. Res*., 101, 6151-6170, 1996.

16. Liu, M., and Y. Shen, "Sierra Nevada uplift: A ductile flank to mantle upwelling under the Basin and Range province," *Geology*, 26, 299-302, 1998.

17. Mooney, W., and C.S. Weaver, "Regional crustal structure and tectonics of the Pacific coastal states: California, Oregon, and Waqshington", *Geol. Soc. Amer. Mem*., 172, 129-161, 1989.

18. Montgomery, D. R., "Compressional uplift in the Central California Coast Ranges," *Geology*, 21, 543-546, 1993.

19. Pollitz, F.F., "Gravitational-viscoelastic postseismic relaxation on a layered spherical Earth," *J. Geophys., Res.*, 102, 17921-17941, 1997.

20. Pollitz, F.F., "Regional velocity structure in northern California from inversion of scattered seismic surface waves," *J. Geophys. Res*., 104, 15,043-15,072, 1999.

21. Ruppert, S., M.M. Fliedner, and G. Zandt, "Thin crust and active upper mantle beneath the southern Sierra Nevada in the western United States," *Tectonophysic*s, 286, 237-252, 1998.

22. Stuart, W.D., T.G. Hildenbrand, and R.W. Simpson, "Stressing of the New Madrid Seismic Zone by a lower crust detachment fault", *J. Geophys. Res*., 102, 27,623- 27,633, 1997.

23. Van der Lee, S., and G. Nolet, "Seismic image of the subducted trailing fragments of the farallon plate," *Nature*, 386, 266-269, 1997.

24. Wdowinski, S., and Y. Bock, "The evolution of deformation and topography of high elevated plateaus; 2, Application to the Central Andes," *J. Geophys. Res*. 99, 7121- 7130, 1994.

25. Yamaji, A., "Periodic hotspot distribution and small-scale convection in the upper mantle", *Earth Planet. Sci. Lett.*, 109, 107-116, 1992.

Thermobarometry and Monazite Th-Pb Chronology of the Red River Shear Zone: Implications for Indo-Asian Extrusion

(00-GS-017)

Principal Investigators: T. Mark Harrison and An Yin (UCLA)
LLNL Collaborator: F.J. Ryerson
Graduate Student: Lisa Gilley (UCLA)

The Red River Shear Zone (RRSZ), the only known mid-crustal section exposed through a transform plate boundary, plays a central role in the hypothesis that strike-slip extrusion of Indo-China accommodated a significant portion of Indo-Asian convergence immediately following onset of collision. High-grade mid-crustal rocks exposed in the massifs that define the RRSZ exhibit evidence for left-lateral, ductile deformation. Interpretation of magnetic stripes in the South China Sea as a pull-apart basin formed at the SE termination of the RRSZ predicts that left-lateral slip occurred between 35-17 Ma at a rate of ~4 cm/a. While $^{40}Ar/^{39}Ar$ thermochronometry documents diachronous transtension along the RRSZ between 24-17 Ma in support of this interpretation, the timing of earlier high-temperature deformation has been only indirectly constrained from U-Pb ages of granitoids. By directly dating the prograde phase of metamorphism using Th-Pb ion microprobe analyses of monazite inclusions in garnets, we can potentially provide a direct link between the RRSZ and the chronology preserved in the South China seafloor. In the course of the past year, we 1) analyzed RRSZ gneiss samples curated at UCLA to assess the feasibility of establishing the thermobarometric history during shearing and 2) undertook a systematic sampling across the RRSZ at a previously inaccessible location to obtain a sample suite optimized for garnet inclusion dating.

OBJECTIVES

Our goal is to directly assess the deformation history of rocks sheared in a left-lateral sense in uplifted gneiss massifs in central Yunnan, China and northern Vietnam. We accomplish this by measuring *in situ* Th-Pb ages in monazites encompassed by syndeformational garnets, since monazite forms at similar temperatures to those over which garnet grows. X-ray maps were obtained to identify zoned garnets from which compositional data were collected to determine the pressure-temperature conditions of garnet growth. By coupling these two approaches, we can potentially obtain *P-T-t* histories. These results can, in turn, be interpreted in the context of a thermo-mechanical model permitting insights into a number of questions including: When did shear along the RRSZ begin? Is metamorphism diachronous along the RRSZ? Is the time lag between the onset of strike-slip faulting and midcrustal metamorphism consistent with shear heating at the Moho?

PROGRESS

In situ Th-Pb ion microprobe dating of monazite has been applied to samples collected on previous field excursions to the Diancang Shan, Ailao Shan and Day Nui Con Voi as well as on our April 2000 expedition during which we sampled extensively in the Ailao Shan and Diancang Shan and reached further north to the Xuelong Shan. A micaschist from the southern Xuelong Shan (YU-30-00) contains matrix monazites with Th-Pb ages between 25.5-18.9 Ma, while zircons from a nearby sample (YU-34-00) yield concordant U-Pb ages of 2.7 Ga, 740 Ma and 332 Ma. The fact that these zircons do not exhibit a Tertiary signal is not surprising in that temperature required to reset or recrystallize zircon were likely not achieved dur-

ing the Oligocene-Early Miocene event. Garnets from these rocks are skeletal, contain penetrating strings of Fe-oxides, and are otherwise unsuitable for thermobarometry.

In the southern Diancang Shan, near Xiaguan, a matrix monazite from a micaschist (DC-3) was dated at 22.7 Ma. Previous thermobarometry on this sample indicates an almost isothermal decompression from 550°C at 7 kbar to 570°C at 5 kbar.[5] Seven matrix monazites from a nearby pelitic schist (YU-27a-00) cluster between 27.7-24.6 Ma, while zircons from a cross-cutting leucogranite vein (YU-27b-00) yield concordant U-Pb ages of 1.2 Ga, 880 Ma and 516 Ma.

Results from the Ailao Shan are consistent with the above data. A garnet gneiss collected north of Gasa (YU86) contains monazite inclusions ranging from 34.3-31.5 Ma and matrix monazites from 30.9 to 21.6 Ma. One partially reset relict monazite yields a Paleocene age. Biotite and plagioclase inclusions in the core of the garnet were used to estimate metamorphic conditions during prograde garnet growth,[3,1] yielding temperatures between 750-780°C and pressures of 7-8 kbar. However, compositional zoning patterns in YU86 garnets indicate that original growth zoning has been destroyed by diffusional relaxation and retrograde net transfer reactions, which requires temperatures in excess of ~650° C (10° C/Ma cooling) or ~730° C (100° C/Ma cooling).[6] Two samples from west of Gasa (YX-47, YU-14-00) date garnet growth between 30.6-21.3 Ma. Matrix monazites overlap this range, yielding ages as young as 20.4 Ma. Monazite inclusions from a paragneiss (YX36e) from south of Gasa yield Th-Pb dates between 29.5-25.2 Ma while four matrix grains yield a weighted mean age of 25.3±0.5 Ma. These results plot on the extrapolation of the thermal history obtained for the Gasa region by Harrison *et. al*.[4] North of Mosha in the Ailao Shan (YX16d), garnet growth occurred from ~26-24 Ma with matrix monazites yielding ages between ~23-19 Ma. South of Mosha (YU82), matrix grains yield similar results but also record a Late Cretaceous signature, interpreted to represent partial resetting of an earlier metamorphic assemblage. Zircon separates from a leucogranite vein in gneiss near Yuanjiang (YU-4c-00) yield $^{206}Pb/^{238}U$ ages of ~580, 203, 37.3, and 30.7 Ma. Six zircons from a leucogranite (YU-4a-00) that cross-cuts this vein were dated at ~246 Ma. Th-Pb dating of five separated monazites from YU-4a-00 yield a mean age of 21.7±0.2 Ma (MSWD = 0.63), pointing to a metamorphic event of sufficient temperature to reset the isotopic system in any preexisting monazites but not hot enough to initiate diffusive Pb loss in zircon.

Monazites in a garnet gneiss (V220) from near Luc Yen, Day Nui Con Voi, Vietnam, yield ages ranging from 212 to 32 Ma. A second sample (V5) from north of Yen Bai yielded similar ages (170-25 Ma) and a third sample (V132) from Ninh Binh gave a more limited range (103-32 Ma). In general, the oldest monazites are located within the garnet cores while matrix and rim monazites tend toward Tertiary ages. We interpret the older monazites as remnants of the Triassic Indosinian metamorphic assemblage, partially reset during mid-Tertiary shearing along the RRSZ but armored against complete equilibration by their garnet hosts. Zircons from the Day Nui Con Voi do not record any Tertiary signal, indicating that temperatures were not as high as in the Ailao Shan during sinistral shearing. Zoning profiles in garnets (V5) show evidence for diffusional homogenization, indicating that temperatures were in excess of ~750 or ~825° C, for a cooling rate of 10 or 100° C/Ma, respectively .[6]

These results are the first to directly indicate that metamorphism and left-lateral shearing occurred along the RRSZ during the Late Oligocene. Thus the period of left-lateral deformation now documented along the RRSZ (i.e., 31-17 Ma) is almost completely coincident with the timing derived from the South China seafloor (i.e., 32-17 Ma;[2]). This linkage clearly supports the extrusion hypothesis and strengthens the view that continental deformation can be accommodated by shear localization on lithospheric-scale strike-slip faults.

REFERENCES

1. Berman, R.G., 1990. "Mixing properties of Ca-Mg-Fe-Mn garnets." *American Mineralogist*, 75: 328-344.

2. Briais, A., Patriat, P., and Tapponnier, P., 1993. "Updated interpretation of magnetic anomalies and seafloor spreading stages in the South China Sea: implications for the Tertiary tectonics of Southeast Asia." *J. of Geophys. Res.*, 98: 6299-6328.

3. Ferry, J.M., and Spear, F.S., 1978. "Experimental calibration of partitioning of Fe and Mg between biotite and garnet." Contributions to *Mineralogy and Petrology*, 66: 113-117.

4. Harrison, T.M., Leloup, P.H., Ryerson, F.J., Tapponier, P., Lacassin, R. and Chen Wenji, 1996. "Diachronous initiation of transtension along the Ailao Shan-Red River Shear Zone, Yunnan and Vietnam." *In The Tectonic Evolution of Asia* (Yin, A. and Harrison, T.M., editors) Cambridge University Press, 208-226.

5. Leloup, P.H., Lacassin, R., Tapponnier, P., Schärer, U., Dalai, Z., Xiaohan, L., Liangshang, Z., Shaocheng, J., and Trinh, P.T., 1995. "The Ailao Shan-Red River shear zone (Yunnan, China), Tertiary transform boundary of Indochina." *Tectonophysics*, 25: 3-84.

6. Spear, F.S., 1991. "On the interpretation of peak metamorphic temperatures in light of garnet diffusion during cooling." *Journal of Metamorphic Geology*, 9: 379-388.

Is North Tibet Extruding as a Rigid Block or Spreading as a Viscous Sheet during the Indo-Asian Collision? (00-GS-024)

Principal Investigator: An Yin (UC Los Angeles)
LLNL Collaborator: F.J. Ryerson
Graduate Student: M.H. Taylor (UC Los Angeles)

To evaluate the role of east-west extension within the Tibetan plateau, detailed geologic mapping was conducted to constrain the fault geometry and fault kinematics of active north-south trending rift systems spanning central Tibet. The results of this research indicate that north-south trending rifts in Tibet are linked via an east-west trending belt of conjugate strike-slip faults. In the Qiangtang terrane, active NE-striking left-slip faults are dominant in its southern region, which are in turn linked with NS-striking normal faults in its northern region. In the Lhasa terrane, NW-striking right-slip faults are dominant along its northern margin and interact with a series of north-south striking normal faults to the south. The strike-slip fault systems merge along the EW-trending Bangong-Nujiang suture zone, separating the Qiangtang and Lhasa terranes. Geologic mapping along two prominent rift systems spanning the Bangong-Nujiang suture indicates their magnitudes of strike-slip displacement (~11-17 km) and slip rates (1-3 mm/yr) are similar. This suggests the Qiangtang block is not a rigid block extruding eastward as a coherent block. Instead, Tibet has been deforming in a constrictional strain field through distributed eastward spreading and coeval north-south shortening via conjugate strike-slip fault systems during the Cenozoic. More accurate determination of slip rates and initiation ages of conjugate strike-slip faulting for both rift systems is being currently conducted at UCLA and LLNL.

OBJECTIVE

The salient feature observed in satellite images of Tibet is the topographically expressed N-S trending rift systems of the Lhasa block. These features are interpreted to have formed by the development of both strike-slip and extensional tectonics, which in turn assist eastward rigid block translation of the Qiangtang terrane. Recently however, the kinematic role of active fault systems within the Qiangtang and Lhasa blocks has been reevaluated, and thus, their geodynamic significance continues to be an issue of intense debate.

In contrast to our knowledge of E-W extension in the Lhasa block, the studies of N-S trending rifts in the Qiangtang (Fig. 1a) have been almost entirely based on fault-plane solutions of earthquakes and interpretation of Landsat images.[8,9,1] Due to the absence of surface geological investigations, the geometry, timing, and magnitude of deformation are poorly constrained. Without this knowledge of rift development in Tibet, it is not possible to test whether E-W extension is driven by local or regional boundary conditions. Once we understand the history of faulting in the Qiangtang and Lhasa terranes we can address the larger issue of whether strain has been distributed uniformly in time and space across Tibet, or instead has experienced diachronous initiation from south to north. For example, if Tibetan E-W extension has been driven by outward expansion of the Himalayan arc, one would expect little extension in Tibet north of the Karakorum-Jiali fault zone (Fig. 1b). This hypothesis would require that the Quaternary slip rates of strike-slip and normal faults be significantly less in the Qiangtang compared to those estimated for Lhasa rifts.

PROGRESS

Our field observations of interacting normal and strike-slip faults within the Qiangtang and Lhasa terranes suggests significant wholesale eastward rigid block extrusion of the Qiangtang may not be as complete a kinematic description as previously thought.[3] This report documents the geometry and fault kinematics of an active conjugate strike-slip system spanning ~ 450 km across the Qiangtang and Lhasa terranes. Additionally, a regional compilation of active fault systems in Tibet, based on satellite imagery, high resolution digital topography and previous mapping by UCLA and LLNL results in a minimum regional E-W elongation estimate of Tibet. The combined observations result in a regional kinematic model of Tibet that illustrates distributed E-W extension (i.e., strike-slip faults are spaced on the order of 100 km and slip for tens of km in the late Cenozoic) and coeval N-S shortening suggestive of a constrictional strain.

YIBUG CAKA RIFT: GEOMETRY AND FAULT KINEMATICS

Active faulting in the Qiangtang block

The Yibug Caka rift system (Fig. 2), beginning in the SW at the Bangong-Nujiang suture and continuing to the NE includes: (1) a ~120 km linear fault zone comprised of en echelon, left-stepping, left-slip faults producing an array of segmented pull-apart basins trending N65°E; (2) a ~130 x 50 km central dilatational stepover dominated by W-dipping normal faults striking N10°E, forming an E-dipping crustal section; and (3) a ~90 km left lateral fault striking N35°E, as indicated by left-slip kinematic indicators.

Southwest Segment

Estimates of fault offsets (separations) along the southwest segment of the left-slip Yibug Caka rift system (NE of Riganpei Co) (Fig. 2) are possible by correlating a system of south-directed thrusts which are offset by the rift-bounding strike-slip fault. South-directed thrusts are characterized by juxtaposition of massive Permian limestone in the hanging wall against Tertiary red beds in the footwall. Thrusts themselves are commonly tightly folded into E-W trending antiformal structures, with erosional windows exposing the thrust contacts. A correlation of similar stratigraphic relationships and the south-directed thrusts across the Yibug Caka fault yields an estimate of 11–16 km left-lateral separation. Kinematic indicators observed on the fault surfaces indicate left-slip with a slight normal component. The observed left-slip separation of the thrusts reflects the magnitude of motion along the southwest segment of the Yibug Caka fault system.

Central Segment

The central segment of the Yibug Caka rift system is characterized by a broad basin linking with left-slip faults of the northeast and southwest segments of the rift system. The basin formed as a dilational stepover between the two left-slip faults (Fig. 2). Kinematic indicators along the rift-bounding faults in this N-S trending segment indicate it is dominated by normal faulting and E-W extension. In particular, a system of W-dipping normal faults along its eastern margin has resulted in a broadly east-dipping inselburg in its hanging-wall.

Northeast Segment

A thrust juxtaposing Paleozoic carbonate strata in its hanging wall against shallow-dipping Tertiary red beds in its footwall is systematically offset left laterally by the fault system into three segments. On the east side of the rift-bounding fault, the thrust changes its strike westward, from N90°E in the east to N30°E in the west. The dip of the fault becomes subvertical as it approaches the active strike-slip fault due to oroclinal bending. The thrust is offset by the left-slip fault for ~ 5 km to the west. This central segment of the thrust is in turn offset left laterally by another left slip fault to the west for ~ 11 km (Fig. 2). Thus, a total amount of ~16 km left-lateral separation is

indicated by the offset of this distinctive thrust. Kinematic indicators observed on fault surfaces that truncate the thrust display subhorizontal striations. Left-slip along this rift segment is indicated by offsets of stream channels varying in magnitude from ~300 m to ~1500 m.

GYARING CO FAULT: GEOMETRY AND FAULT KINEMATICS

Active faulting in the Lhasa block

A previous geologic investigation along the Gyaring Co fault located in the Lhasa terrane was conducted near Xianza at its SE termination.[2] Our efforts focused on the NE segment of the Gyaring Co fault near its intersection with the Bangong-Nujiang suture to the north (Fig. 1c). The Gyaring Co fault system strikes ~N70°W and is a dextral slip structure. The main fault bounds the NE side of the rift valley and locally changes strike to N-NW. The change in fault geometry locally results in releasing structures controlling the location of the major lakes. The magnitude of right-slip is constrained by several offset relationships, (1) the offset of a Paleozoic/Mesozoic contact, (2) correlation of a north-dipping thrust belt and (3) an offset Tertiary basin. Neotectonic mapping at several localities along the Gyaring Co fault was also conducted to constrain the surface exposure ages of offset geomorphic landforms in order to calculate derivative slip-rates for the right-slip fault system.

The magnitude of strike-slip displacement along the Gyaring Co fault is indicated by the right-lateral separation of a Tertiary basin near Goman Co and Caibu Co (Fig. 1c). The Tertiary (?) basin on the west side of the Gyaring Co fault is bounded along its northern margin by a north-dipping thrust juxtaposing massive Mesozoic limestones in its hanging wall against interbedded volcaniclastics, red sandstones, and conglomerates in the footwall. Additionally, a series of S-directed Mesozoic thrusts located to the north can be correlated across the rift-bounding fault, systematically indicating right-separation.

Prominent geomorphic landforms including alluvial fans, stream channels and terrace risers indicate right-slip displacement along the fault. Where the main fault is exposed, fault zone fabrics indicate a right-oblique motion along the fault. Along-strike variability in the fault zone geometry is evident by anastomosing and right-stepping fault strands forming sag ponds and pull-apart basins. Locally, pressure ridges are observed along the main fault NW of Zigwi Co where the fault strikes nearly E-W (Fig. 1c). The active fault may become anastomosing near the western shore of Zigwi Co, as suggested by a recent earthquake event that ruptured the surface ~2 km south of the main fault (see Fig. 1c). Our observations from this location only documents structural damage to several homes and may only result from ground shaking.

INITIATION OF CONJUGATE STRIKE-SLIP FAULTS AND E-W ELONGATION OF TIBET

Yibug Caka rift system

Three topographic profiles were measured across a prominent SE-facing fault scarp to constrain the fault offset. Applying the linear diffusion model of Avouac and using the climatic parameters of Yin *et. al.* for fault scarp degradation yields a fault scarp age of ~10 ka.[3,12] If the width of the basin reflects the magnitude of extension along the rift-bounding fault, then a minimum offset of ~7 km is estimated for the total normal slip along the rift-bounding fault. The estimates on the fault scarp age and magnitude of slip imply an initiation age of normal faulting at ~2 Ma. Because extension is accomadated via several fault strands across the basin, an estimated slip rate would be a minimum for the fault system.

Gyaring Co fault system

Regressive shorelines of Zigwi Co are disrupted by the main fault. If the regressive shorelines can be correlated with a regional climate change then the age of the paleoshorelines is most likely ~8 ka.[3] We can qualitatively approximate a

fault slip rate. A maximum right-lateral offset of the oldest shoreline is ~7 m at this site. When averaged over 8 ka, this fault offset implies a minimum slip rate of ~1 mm yr^{-1} along this strand of the right-slip fault. However, the active fault zone is comprised of several strands at this locality and the slip rate is therefore a minimum.

East-west extensional strain across Tibet

The presence of conjugate strike-slip faults in central Tibet makes specific predictions regarding the magnitude of extension across Tibet. Therefore, we calculate the E-W extensional strain for north and south Tibet by restoring normal faulting across the major N-S trending rifts (Fig. 1a).

E-W profiles were chosen to sample elevation data (GTOPO30) normal to the major rift axis where extension is interpreted to be maximum. The following strain calculation is a minimum based on the following criteria: all rift-bounding faults have a planar geometry, dip 60° (lower dip values would result in greater amounts of slip along the faults), and the dip-slip along a rift-bounding fault is equal to the maximum topographic relief between the rift shoulder and the valley floor. Using topography as an offset marker requires negligible erosional denudation of the rift flanks and the basin fill to be thin. The assumption of negligible erosional denudation is probably justified for most of the rifts in north Tibet.[12] These geologic observations are consistent with results of (U-Th)/He analysis (Table 1.) of rocks along the Yibug Caka rift, which yields a low temperature cooling history of Late Mesozoic age. Three sites sampled over a vertical distance of ~800 m range in age from 187 to 136 Ma, suggesting little Tertiary He loss and fault displacements of less than 2 km. Based on the above assumptions the minimum amount of E-W extension is 71 km for the Qiangtang and 92 km for the Lhasa block. Corresponding to the minimum amount of E-W extension is the minimum E-W elongation estimate of 5% and 8% respectively.

SUMMARY

The widely distributed rifts in the Qiangtang suggest that rigid block eastward extrusion via the Karakoram-Jiali fault zone is an incomplete kinematic description of Late Cenozoic deformation within the Tibetan plateau.[2] Instead, the observation of an E-W trending belt of conjugate strike-slip faults is suggestive of distributed deformation over the entire region of Tibet and is characteristic of a contrictional strain with relatively uniform E-W extension and coeval N-S compression. The conjugate-strike-slip interpretation is consistent with similar slip magnitudes along the left-slip fault system in the Qiangtang and right-slip faults in the Lhasa block. The slip rates for both fault systems are currently being quantitatively evaluated via cosmogenic dating at LLNL.

Sample	raw age	+/- abs	age(Ma)	+/-abs	U (ppm)	Th (ppm)	He (ncc)/mg	Ft
99.5.26.1A	112	1.4	136.7	1.7	15.6	7.1	219.4	0.82
99.5.26.2A	132.6	1.6	181.7	2.2	35.7	14.1	638.8	0.73
99.5.26.3A	142.8	1.7	183.1	2.1	59.0	34.3	1092.1	.078

Table 1. Ft = Alpha ejection correction after Farley et al. (1996). The dimensions of the apatite grains in each sample (~10 grains) were measured to determine the alpha-emission correction (Farley et al., 1996). He ages were calculated based on absolute He and U-Th determinations on the same sample. For helium analyses, samples were first outgassed, then retrieved and dissolved in a doubly spiked (^{230}Th-^{235}U) HNO3 solution in preparation for U and Th determinations using isotope dilution ICP-MS (for analytical procedures see Stockli et al., 2000).

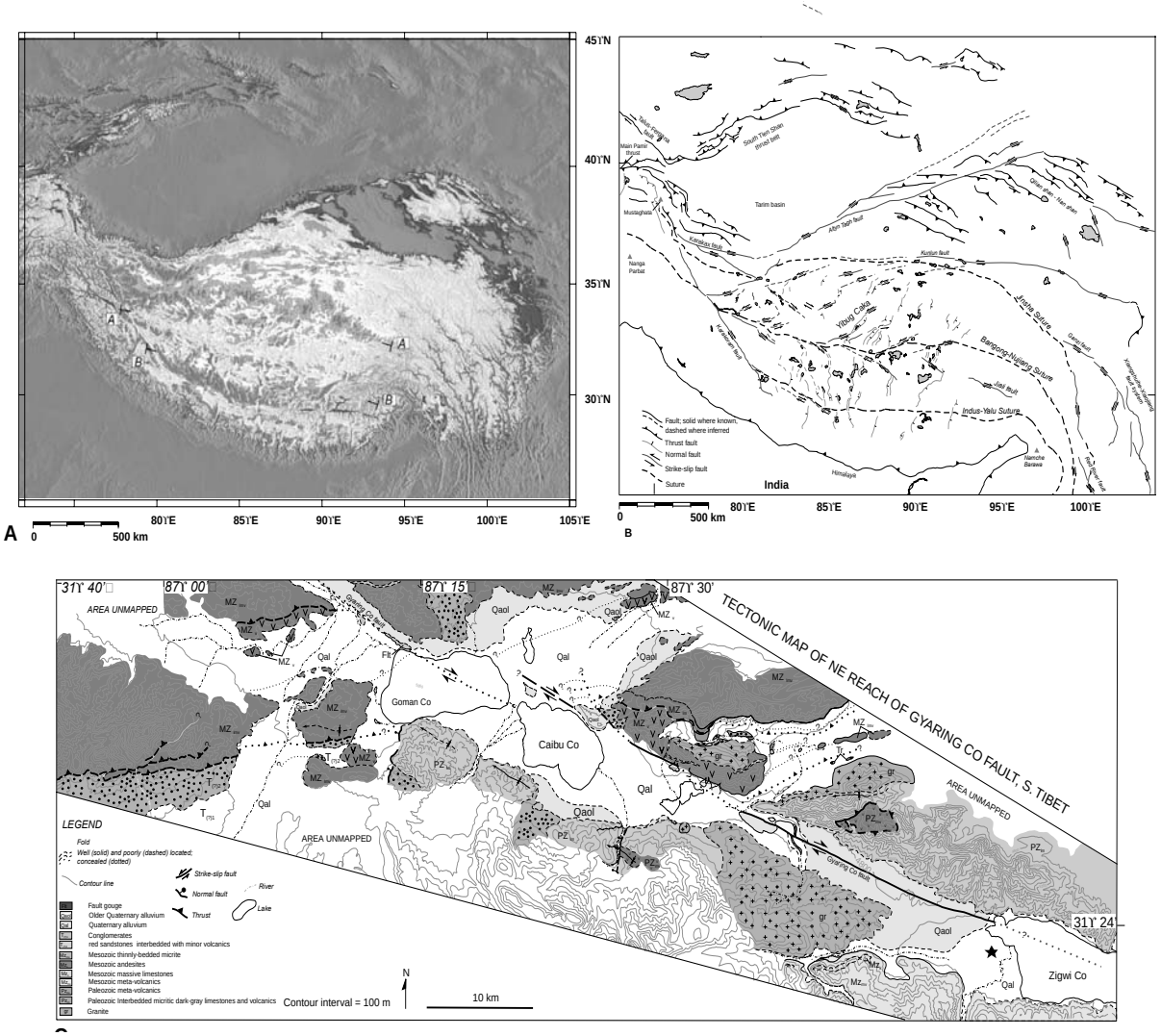

Figure 1a. Color shaded relief map of the Tibetan Plateau enhanced with artificial illumination from the east. Color palette designed to emphasize extensional structures in the interior of the plateau. Width of color on scale bar is proportional to elevation range associated with a given color. AA' and BB' are end points of topographic profiles used in regional strain calculation.

Figure 1b. Regional tectonic map of the Tibetan Plateau modified after Armijo et al. (1986, 1989). Note that an E-W trending belt of conjugate strike-slip faults is present along the Bangong-Nujiang suture zone (BNS) in central Tibet. IYS, Indus-Yalu suture; JS, Jinsha suture.

Figure 1c. (A) Simplified tectonic map of the Yibug Caka rift system and lower hemisphere stereographic projections of kinematic data collected from rift-bounding faults.

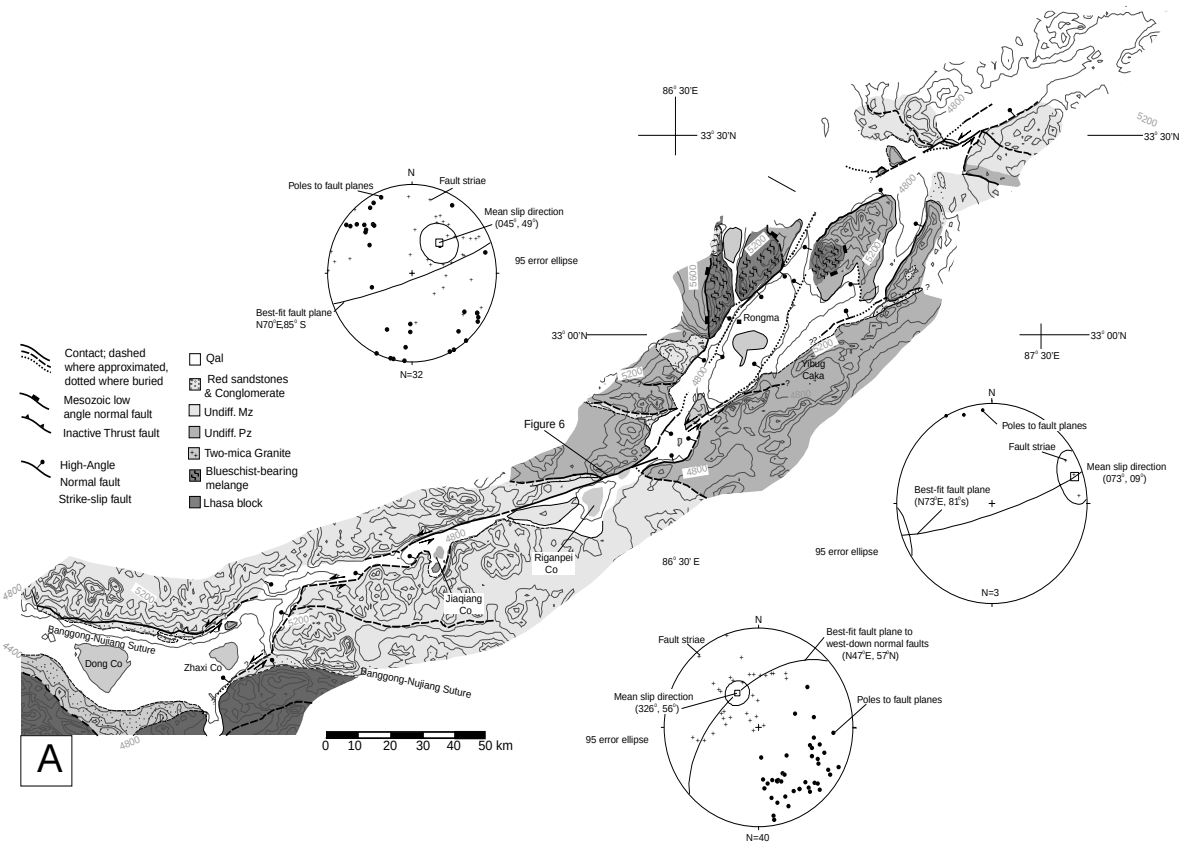

Figure 2. Simplified tectonic map of the NE reach of the Gyaring Co fault.

REFERENCES

1. Armijo, R., Tapponnier, P., Mercier, J. L., and Han, T.-L., 1986, "Quaternary extension in southern Tibet: Field observations and tectonic implications: *Journal of Geophysical Research*, 91, 13803-13872.

2. Armijo, R., Tapponnier, P., and Tonglin, H., 1989, "Late Cenozoic right-lateral strike-slip faulting in southern Tibet," *J. Geophys. Res.*, 94, p. 2787-2838.

3. Avouac, J. P., and Peltzer, G., 1993, "Active tectonics of the southern Xinjiang, China: Analysis of terrace risers and normal fault scarp degradation along the Hotan-Qira fault system," *J. Geophys. Res*, 98, 21,773-21,807.

4. Blisniuk, P. M., Siwen, S., Kuchel, O., and Ratschbacher, L., 1998, "Late Neogene extension in the Shuang Hu graben, central Tibet," *EOS Trans. AGU)*, 79, 794.

5. Farley, K.A., Wolf, R.A., and Silver, L.T., 1996, "The effects of long alpha-stopping distances on (U-Th)/He ages," *Geochimica et Cosmochimica Acta*, 60, 4223–4229.

6. Kapp, P., Yin, A., Manning, C. E., Murphy, M., Harrison, T. M., and Spurlin, M., 2000, "Blueschist-bearing metamorphic core complexes in the Qiangtang block reveal deep crustal structure of northern Tibet," *Geology.*

7. Liao, K., 1990, "Atlas of the Qinghai-Xizang Plateau: Beijing," Institute of Geography, Science Publishing House, 237 p.

8. Molnar, P., and Lyon-Caen, H., 1989. "Fault plane solutions of earthquakes and active tectonics of the Tibetan plateau and its margins," *Geophys. J. I.*, 99, p. 123-153.

9. Rothery, D. A., and Drury, S. A., 1984. "The neotectonics of the Tibetan plateau," *Tectonics*, 3, 19-26.

10. Siwen, B., Blisniuk, P., Hacker, B., Glodny, J., Ryerson, R., and L., R., 1999, "Timing of Late Neogene extension in central Tibet," *EOS, trans. AGU*, 80, no. 46, p. F1015.

11. Stockli, D. F., Farley, K. A., and Dumitru, T. A., 2000. "Calibration of the apatite U-Th)/He thermochronometer on an exhumed fault block, White Mountains, California." *Geology*, 28, 983-986.

12. Yin, A., Kapp, P. A., Murphy, M. A., Harrison, T. M., Grove, M., Ding, L., Deng, X., and Wu, C., 1999, Significant late Neogene east-west extension in northern Tibet: *Geology*, 27, no. 9, p. 787-790.

Timing of Late Quaternary Glaciation in the Mountains Bordering the Northeastern and Southeastern Margins of Tibet (00-GS-025)

Principal Investigator: Lewis A. Owen (UC Riverside)
LLNL Collaborators: Robert C. Finkel and Marc W. Caffee
Postdoctoral Researcher: Joel Q. Spencer (UC Riverside)
Graduate Student: Patrick Barnard (UC Riverside)

This project aims to constrain and compare the timing of late Quaternary glaciation along northeastern (Qilian Shan) and southeastern Tibet (Khumbu Himal) using geomorphic, sedimentalogical and geochronological techniques. These data will be compared with data sets from regions an the western end of the Himalayan and the Tibetan Plateau to test if glaciation was synchronous across the Tibetan Plateau. These data will help assess the relative importance of different climatic systems, namely the mid-latitude westerlies and the Indian summer monsoon, in driving climate change in central Asia. Such work is essential for developing and testing general circulation models that are used to predict future global and regional environmental change.

OBJECTIVE

The first component of this project involved fieldwork in the Lenglong Ling (Qilian Shan), La Ji and Anyemaqen Mountains, during June 1999. The Tibetan fieldwork was funded by the National Geographic Society and allowed Owen, Spencer, Derbyshire, Haizhou, Sha, Zeng and Cao to work in three mountain ranges in NE Tibet. Originally, we had only planned to examine the Lenglong Ling mountains in the Qilian Shan, however, because of the excellent logistical support provided by colleagues in Quinghai Normal University, we were able to add two extra mountain ranges to our study and widen the extent of this project. In September 1999, this fieldwork was followed by a study of the Khumbu Himal along the southeastern margin of Tibet. Finkel, Barnard and Owen undertook three weeks fieldwork and concentrated their efforts on the areas around the Khumbu and Lhotse Glaciers in Nepal.

Detailed mapping was undertaken to reconstruct the extent of former glaciers in all the field areas. Rock and sediment samples were collected for cosmogenic radionuclide and optically stimulated luminescence (OSL) dating to constrain the timing of glaciation. Radiocarbon dating was also used ho help constrain the age of terrace formation and glaciation and as a test of the reliability of OSL and cosmogenic dating. The cosmogenic dating is being undertaken by Barnard, Finkel and Coffee at LLNL. Barnard, a graduate student of Owen's, has been working closely with Finkel and Coffee at LLNL since October 1999 and will remain on this project the LLNL until April 2000.

Appendix 1 shows the results of the cosmogenic dating to date. By April 2000, we will have >100 cosmogenic radionuclide dates on the moraines in NE and SE margins of Tibet. Furthermore, Barnard has also been able to utilize his funding to date rock samples from terraces in the Khumbu and Garhwal Himalayas. This is part of his Ph.D. thesis. He currently has about 40 dates on these terraces, and believes that these terraces can be directly related to deglaciation. Therefore, our main project on timing of glaciation will help Barnard test his hypothesis for his doctoral work. Spencer at UCR is undertaking the OSL dating. All the chemical preparation has been completed and Spencer in currently staging the luminescence mnnonmmenrn on each sample. Several radiocarbon dates have bean obtained and me are still awaiting the results of six more dates. Our initial

results show that we have had three major glaciations in NE Tibet that ended ~50 ka, 14 ka and 10 ka. This is very similar to the timing of glaciation in the western Himalayas that was determined in previous projects. In the Khumbu Himal, we have been able to identify a glacial advance that ended as about 26-20 ka, ~10 ka ~6 ka and 2-1.5 ka. This seems to suggest that glaciation in the Khumbu Himal is asynchronous with NE Tibet and the western Himalaya. Furthermore, the terrace work in the Khumbu suggests that the main river terraces and fans formed very rapidly upon deglaciation.

During the first six months of this project we have had four meetings between researchers at LLNL and UCR, and have presented some of our work at the Geological Society of America's Annual Meeting in Denver and at the IGCP4I5 meeting in the Rockies during October 1999. We will also present a paper at the International Quaternary Association's meeting on glaciation in Chengdu, China in June (see below).

By the end of April 2000, all the dating will have been completed and we will begin to work on writing research pagers. This will include papers on: i) the glacial history of Anyemaqen Mountains; ii) the timing of glaciation in the Khumbu Himal; iii) a comparison of the glacial histories, of the Lenglong Ling, La Ji, Anyemaqen Mountains and the Khumbu Himal; iv) the relationship between glaciation and terraceformation is the Khumbu Himal; v) the timing terrace formation and rates of incision in the Khumbu Himal.

Development of a New Method for Determining Chemical Weathering Rates using Geochemical Tracer Ages and Spring Chemistry (00-GS-031)

Principal Investigator: Jordan F. Clark (UC Santa Barbara)
LLNL Collaborator: G. Bryant Hudson
Graduate Student: Laura Rademacher (UC Santa Barbara)

Chemical weathering rates were determined for several springs in the Sierra Nevada, California using geochemical tracer ages and mass balance calculations. Conductivity and chemical weathering rates correlate with spring water age. The majority of solutes in both young and old springs are acquired during the first few years of the water's evolution. This relationship suggests a strong influence of soils on the chemistry of shallow groundwater. This study provides evidence for the relationship developed by Garrels and Mackenzie in which higher conductivity springs have longer contact times with the surrounding rock.

OBJECTIVES

The objectives of this project are to:11) Develop a new approach for studying chemical weathering rates in field settings by combining geochemical tracer ages of groundwater flow with chemical mass balance calculations. 2) Understand chemical weathering rates, how they evolve through time, and how they vary with rock type. This will provide valuable information about how chemical weathering influences global biogeochemical cycling by providing a sink for CO_2 and by releasing base cations. 3) Determine spring water chemistry (major cations and anions), DIC, pH, alkalinity, and CFC and tritium/^{3}He concentrations in springs from Sagehen Creek Basin, CA.

Understanding chemical weathering rates can provide valuable insight into the global processes controlling biogeochemical cycling of CO_2 and base cations. Additionally, the products of chemical weathering reactions are involved in many processes on a local scale, such as neutralizing acid deposition, providing essential nutrients for biota, and controlling soil fertility. It is essential to include an understanding of chemical weathering rates in predictions of the long-term changes in source and sink terms of these components and their rate of interaction in biogeochemical cycles.

Field-based weathering rates are often estimated from catchment studies focusing on variations in the chemical composition of streams.[9,10] However, streams integrate water from many different flow paths and sources within a catchment. These pathways include direct interception of precipitation by the stream channel, overland flow, subsurface flow through the soil zone, and groundwater discharge.[1] These pathways differ in length and as a result, waters traveling through them have different residence and mineral reaction times before reaching the stream. The time scale of water-rock reactions ranges from hours to minutes for overland flow to hundreds of years for groundwater flow.

Using mass balance calculations, local lithology, and spring chemistry from the Sierra Nevada, Garrels and Mackenzie determined the primary weathering reactions occurring in the subsurface,[4] thus establishing a fundamental approach for studying the chemical evolution of waters. However, at the time of this study, shallow groundwater residence times were unknown. Hence, Garrels and Mackenzie (1967) were unable to combine a chronology with their mass balance calculations to calculate chemical weathering rates.

The goal of this study is to further develop the approach of Garrels and Mackenzie (1967) by dat-

ing spring water using geochemical techniques developed during the last decade. In this manner, rates of chemical weathering in the shallow groundwater zone can be estimated. For this study, we returned to the Sierra Nevada to sample springs from the Sagehen basin. For a more detailed description of the results see Rademacher et al. (submitted).

The springs in the Sagehen basin (elevation: 1900 to 2400 m) emerge on the north and south sides of Sagehen Creek and exist predominantly in glacial till. The mean annual air temperature of Sagehen basin at 1932 meters is 5.2°C, and the mean annual precipitation is 88.5 cm per year. These springs have been under study because of their importance to invertebrate diversity.[3] Through their studies, Erman and Erman have found evidence for a relationship between spring permanence, invertebrate diversity, and conductivity.

Eleven springs in the Sagehen basin were sampled in August 1997 and again in November 1999. Care was taken to collect samples as near to the source as possible to avoid sampling water from a mixed source. A copper tube was inserted into the ground at the source of the spring to minimize air contamination. Samples were collected for analysis of cations, anions, chlorofluorocarbons (CFCs), tritium, He isotopes, neon, and argon.

Chemical weathering rates are determined with mass balance calculations using NETPATH, a geochemical mass balance model developed by the USGS and geochemically determined residence times of spring waters.[5] Precipitation chemistry data corrected for evapotranspiration using chloride are used to establish the initial (pre-chemical weathering) chemistry of the water,[9] and chemistry of the spring water is used as the end-point of the chemical evolution of the groundwater (post-chemical weathering). The residence time of the spring water is calculated utilizing geochemical tracer ages of the sampled spring waters determined with both CFCs and tritium/^{3}He.[2] The tracer age represents the time it has taken groundwater to flow from the water table (recharge location) to the sampling point (spring discharge zone). Both tracer methods estimate groundwater ages with uncertainties of ±2 years.

PROGRESS

The CFC-11 and CFC-12 tracer ages calculated for eleven springs sampled in the Sagehen basin range from 10 years to almost 40 years and are in excellent agreement . Tritium/^{3}He tracer ages show a strong correlation with the CFC ages (R2=0.83). However, a slight offset exists between the CFC and T/^{3}He ages such that the CFC ages are slightly older (10-15 years). Additionally, with only two exceptions, CFC-11 ages from the same springs collected in 1997 and 1999 agree within the limits of the dating technique.

Mixing of flowpaths from waters of different ages is a common explanation for disagreement among tracer ages. A number of tests can be performed with tracer data to determine the degree of mixing. First, little or no excess ^{4}He, which can exist in deeply circulating groundwaters as a result of alpha decay of U and Th series nuclides,[8] was found in the spring samples after accounting for excess air using argon and neon. Therefore, it is unlikely that a very old source (greater than 50 years) is mixing with younger spring waters. Second, spring waters of similar ages have similar conductivities despite geographical spacing. This correlation is unlikely if mixing of water of very different ages is significant, as it would require distant springs of similar tracer ages and conductivity to be mixing similar proportions of old and young waters. Third, tritium/^{3}He measurements for the springs reproduce the tritium input function well with only one exception, S7. These tests suggest a scenario where little mixing in the spring waters has occurred between old (> 50 year) and young (< 50 years) groundwaters. However, this evidence does not exclude mixing of flow paths of similar groundwater ages.

Assuming mixing is minor in the springs, possible explanations for the offset between the two tracer ages include a thick vadose zone, which forces CFC ages to appear older than the T/^{3}He

ages or poor He confinement,[2] causing the tritium/^{3}He ages to appear younger.[7]

Conductivity, Ca and Na of the spring water samples increases with increasing spring water age. This increase is indicative of a chemically evolving groundwater system. Water with longer residence times has more time to interact with the surrounding material and weather primary minerals. The increase of pH with increasing spring water age and conductivity indicates that more evolved groundwaters have less acid remaining to continue weathering primary minerals and suggest that the weathering rate will slow.

The chemical composition of spring water varies significantly throughout Sagehen basin and correlates well with spring water ages. This suggests that water discharging in the Sagehen springs is recording a complex history of rock weathering and changes in the recharge conditions. By sampling the springs, the groundwater component was separated from the other flow components contributing to the chemical composition of a stream. This isolation provides a means of directly studying the chemical evolution of shallow groundwaters and the influence of chemical weathering rates and potential land use changes on their chemical composition and contribution to catchment hydrochemistry.

REFERENCES

1. Church, M.R., 1997, "Hydrochemistry of forested catchments," *Annual Review of Earth and Planetary Science*, 23, p. 23-59.

2. Cook, P.G. and Solomon, D. K., 1997, "Recent advances in dating young groundwater: Chlorofluorocarbons, ^{3}H/^{3}He and ^{85}Kr," *Journal of Hydrology*, 191, 245-265.

3. Erman, N.A., and Erman, D. C., 1995, "Spring permanence, Trichoptera species richness, and the role of drought," *Journal of the Kansas Entomological Society*, 68, 50-64.

4. Garrels, R.M. and Mackenzie, F. T., 1967, "Origin of the chemical compositions of some springs and lakes, in Gould, R.F., ed., Equilibrium Concepts in Natural Water Systems," Washington D. C., *American Chemical Society Publication*, 222-242.

5. Plummer, L.N., E. C. Prestemon, and Parkhurst, D. L., 1994, "An interactive code (NETPATH) for modeling NET geochemical reactions along a flow PATH-Version 2.0," *U. S. Geological Survey Water-Resource Investigation Report* 94-4169.

6. Rademacher, L. K., J. F., Hudson, G. B., Erman, D. C., and Erman, N. A., "Chemical evolution of shallow groundwater as recorded by spring waters, Sagehen basin, California", Submitted to: *Chemical Geology.*

7. Schlosser, P., M. Stute, C. Sonntag, and Munnich, K. O., 1989, "Tritiogenic 3He in shallow groundwater," *Earth and Planetary Science Letters*, 94, 245-256.

8. Solomon, D.K., A. Hunt, and Poreda, R. J., 1996, "Source of radiogenic helium 4 in shallow aquifers: Implications for dating young groundwater," *Water Resources Research,* 32, 1805-1813.

9. Stallard, R.F. and Edmond, J. M., 1983, "Geochemistry of the Amazon 2. The influence of geology and weathering environment on the dissolved load," *J. Geophys. Res.*, 88, 9671-9688.

10. Velbel, M.A., 1985, "Geochemical mass balances and weathering rates in forested watersheds of the southern Blue Ridge," *American Journal of Science*, 285, 904-930.

Hyperspectral Remote Sensing in an Active Caldera, Long Valley, Califonia (00-GS-040)

Principal Investigator: Eli A. Silver (UC Santa Cruz)
LLNL Collaborator: William L. Pickles
Graduate Student: Brigette A. Martini (UC Santa Cruz)

We have imaged Long Valley caldera hyperspectrally, using the high spatial and spectral resolution of the HyMap instrument (3-5m pixel size). We obtained improved fault mapping in the caldera via the spectral identification of linearly distributed hydrothermal alteration minerals such as kaolinite and alunite. The presence of northeast-trending structures in the western caldera is confirmed with this method and supported by independent lines of evidence including local stress calculations and models and intrusion orientation determination. The presence of such faults and their interaction with faults of other orientations will serve to fine tune models of the Mono-Inyo volcanic chain as well as the caldera formation itself. We also performed geobotanical mapping of the CO_2-induced tree-kill at Horseshoe Lake.

OBJECTIVES

As one of the more active and well-studied calderas in the world, Long Valley Caldera serves as a prime choice for hyperspectral imaging validation studies. The relatively new technology of hyperspectral imaging (or imaging spectroscopy)[1] and it's uses, strengths, and weaknesses for active volcanic monitoring and assessment, have not been fully determined. Recent and future launches of space-based hyperspectral imagers make baselining efforts with higher resolution, air-based imagers critical. Our primary goal in this study was to gain a more fundamental understanding of the geothermal and tectonic processes acting in Long Valley Caldera utilizing high resolution airborne hyperspectral imagery. Mapping utilized spectral signatures in various computer driven algorithms to create spectral-based geology and vegetation distribution maps. The processed hyperspectral data are then integrated with previous geophysical and geochemical studies which may provide insights into the caldera's hydrothermal and structural systems. We have produced improved fault maps, improved local and regional tectonic models, hydrothermal system characterization, volcanic hazard monitoring techniques and geothermal ecosystem mapping. We find hyperspectral imagery to be a viable and useful addition to the tool kit of volcanologists, resource scientists and engineers.

PROGRESS

On September 7, 1999, seven LLNL-funded lines of hyperspectral data were flown of the caldera with the HyMap instrument (Integrated Spectronics, Ltd.), satisfying our initial objective to acquire higher spatial resolution imagery than previously available (Figure 1). The Long Valley dataset samples reflectances from 400 to 2500 nm, in 126 separate but contiguous bands. Each pixel is from 3-5 m in dimension and the signal-to-noise is reportedly greater than 1000:1. The atmospherically corrected images were processed spectrally using an algorithm called the Minimum Noise Fraction (MNF), and spatially using the Purest Pixel Index (PPI) algorithm contained within the software program ENVI. The goal in this processing is to isolate spectrally pure endmembers of earth materials for use in an array of supervised classifications and unmixing algorithms.

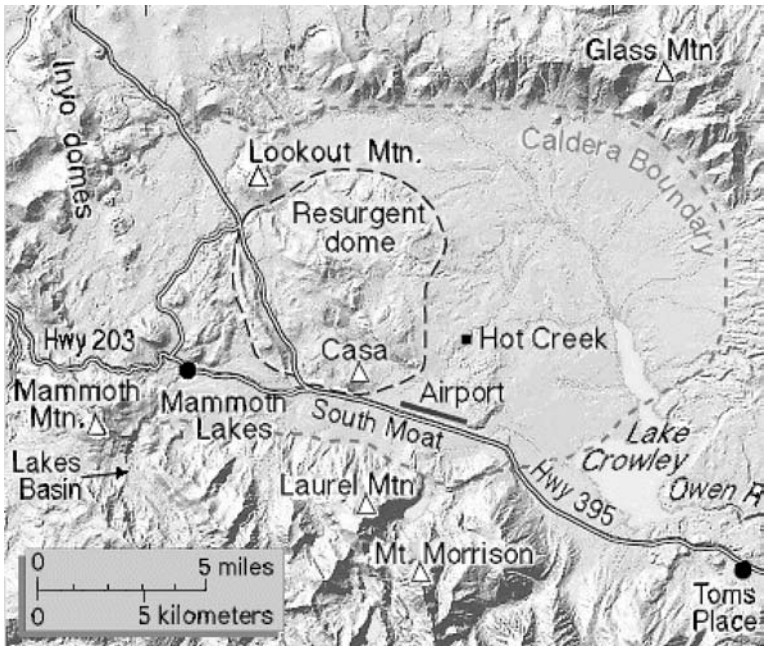

Figure 1. Location map of the Long valley caldera. Light rectangle shows approximate boundary of September 7, 1999 acquisition. Darker rectangles are the subsets dicussed in this study. Modified from http://quake.wr.usgs.gov/VOLCANOES/LongValley.

Figure 2 shows spectral-based mapping on a small subset of the HyMap imagery from the southwestern flank of Mammoth Mountain, a small strato volcano located on the southwestern rim of the caldera (location in Fig. 1). By comparing previously constructed geologic maps with spectroscopic-based maps, it is possible to ascertain both that spectroscopy can produce comparable fault maps to those created by traditional field methods, and that spectroscopic maps can reveal faulting previously unrecognized. Linear distributions of hydrothermal alteration minerals are used as proxies for fault and fracture locations. Figure 2 highlights a northeast-trending lineament mapped out by kaolinite and alunite distributions, as well as several northwest-trending lineaments. The pattern seen in the processed image of higher temperature minerals (alunite) surrounded by lower temperature clays (kaolinite) is very common in hydrothermal environments. Though not currently discharging gasses or hydrothermal fluids, the northeast-trending zone seems to be a paleo-fumarolic zone. The presence of alunite in particular, indicates a high acid-sulfate temperature and low pH, in agreement with the hypothesis that a high temperature hydrothermal reservoir exists beneath Mammoth Mountain.[6]

The northeast-trending fault that we see spectroscopically on the southwestern flank, is consistent with faults mapped just to the northeast of Mammoth Mountain in the Discovery Fault Zone.[7] In addition, regional northeast-trending structures can be found to the south in the Deep Springs Fault Zone, to the northeast in the Excelsior mountains, and to the north in the Bodie Hills. Local minimum compressive stress in the western caldera is orientated NW-SE4 and the 1989 dike intrusion beneath Mammoth was orientated approximately N20E and lay beneath the southwestern flank.[2] We interpret these NE-trending faults as part of a rotational fault system slipping left-laterally in a larger NW-trending system of right shear. This kinematic pattern results in local extension along the NE-trending faults and easier egress of both magma and geothermal fluids in the Long Valley caldera and in other geothermal systems associated with the Eastern California Shear zone.[4]

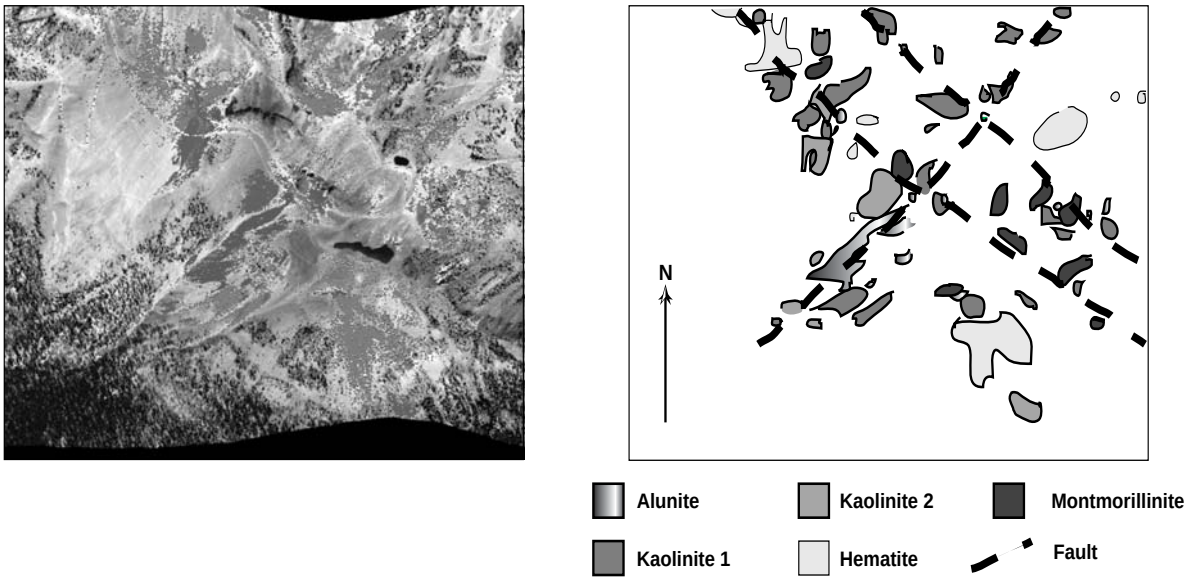

Figure 2. Classification results from the southwestern flank of Mammoth Mountain. The image on the left is a grey-scale (2.2um) subset with overlayed alteration distributions. The image on the right shows these distributions with more clarity. Also plotted on the right-hand image are faults that coincide with these linearly distributed alteration minerals.

The effect of volcanic phenomena on caldera ecosystems is also studied. Biological-geological interactions can be identified and mapped such as the spectral-based tree-kill map shown in Figure 2. Massive magmatic CO_2-induced tree kills were initiated in 1989 after the dike intrusion event mentioned previously.[2] Since 1989, over 50 hectares of trees have died surrounding the volcano. The Horseshoe Lake Tree-kill shown in Figure 2 is the site of highest flux on the mountain with approximately 100 tons/day fluxing diffusively out of the ground.[5] Spectral signatures of healthy robust trees, dead trees, and physiologically stressed trees were extracted from the imagery and used in several mapping schemes. The kill itself is mapped in Figure 2b, including transitional zones of sub-morbid populations. Figure 2c shows the comparison of the kill boundaries as mapped by traditional field methods and via hyperspectral data analysis. Such maps are available for other kill regions on the volcano.

The examples above suggest that hyperspectral data can provide geological and biological information about a system quickly, synoptically and without a host of other ground-based monitoring programs. This makes it an attractive tool for studying other calderas around the world which often lack basic maps as well as dense seismic, GPS, and geochemical monitoring programs. The expense of hyperspectral data will likely decrease once such instruments are spaceborne and the computational size and time required for analysis is increasingly attainable.

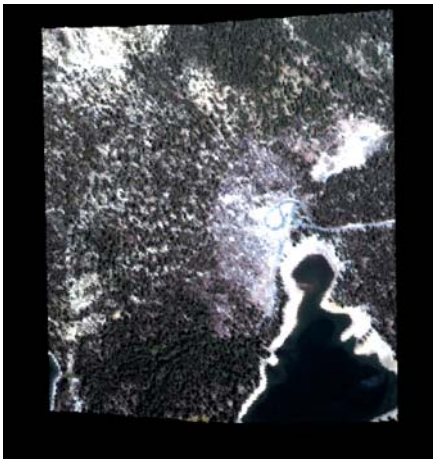

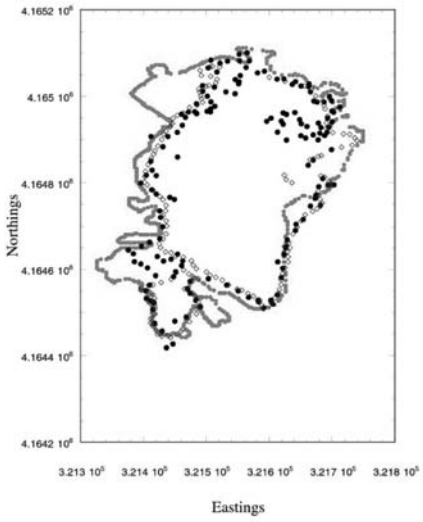

Figure 3. The image on the left shows Horseshoe Lake tree-kill mapping results. The lightest shades represent transitional zones (sub-lethal tree populations), while the darker shades show the present boundaries of dead populations. On the right is a comparison of hyperspectral based size estimates of kills with previous estimates via more traditional means.

REFERENCES

1. Goetz A.F.H., G. Vane, J.E. Solomon, B.N. Rock, "Imaging Spectrometry for Earth Remote Sensing," *Science* 228, 1147-1153 (1985).

2. Hill, D.P., et al., "The 1989 earthquake swarm beneath Mammoth Mountain, California: An intial look at the 4 May through 30 September activity," *Bul. Seis. Soc. Am,.* 80, 325-339 (1990).

3. Moos, D. and M.D Zoback, "State of stress in the Long Valley caldera, California," *Geology,* 21, 837-840 (1993).

4. Reheis, M.C., T.H. Dixon, "Kinematics of the Eastern California shear zone: Evidence for slip transfer from Owens and Saline Valley fault zones to Fish Lake Valley fault zone" *Geology,* 24, (339-342).

5. Rogie, J.D., "Dynamics of carbon dioxide emission at Mammoth Mountain, California," in prep

6. Sorey, M.L., G.A. Suemnicht, N.C. Sturchio, G.A. Nordquist, "New evidence on the hydrothermal system in Long Valley caldera, California, from wells, fluid sampling, electrical geophysics, and age determinations of hot-spring deposits," *Journal of Volcanology and Geothermal Research,* 48, 229-263 (1991).

7. Suemnicht, G.A. and R.J. Varga, "Basement structure and implications for hydrothermal circulation patterns in the western moat of Long Valley Caldera, California," *J. Geophys. Res.* 93 13,191-13,207 (1988).

Trace Element Partitioning between Clinopyroxene, Feldspar, and CO_2-H_2O fluids: Constraints on Mantle Metasomatism and the Formation of Granulites (00-GS-041)

Principal Investigator: Donald J. Depaolo (UC Berkeley)
LLNL Collaborators: F. J. Ryerson and Ian Hutcheon
Graduate Student: Maureen Feineman (UC Berkeley)

Fluids in the upper mantle, subduction zones, and the lower crust are believed to play a major role in transporting chemical constituents, and consequently in determining the fluxes in the large scale geochemical cycles of the solid earth. This fluid exchange affects the composition of continents, the composition and isotopic evolution of the mantle, the composition and volume of the oceans, and the generation of magma in subduction zones; all major aspects of the planetary scale evolution of the earth.

Fluids released during the dehydration of subducting oceanic crust carry a geochemical message regarding the compositions of materials hidden deep within subduction zones, and the processes by which subducted material is altered. Mineral-fluid partition coefficients for the major minerals in the residual slab (clinopyroxene, garnet) have been determined in previous studies.[3] However, trace element partitioning by accessory phases, for which partitioning data may not be known, has been shown to be significant.

Experiments have been performed to determine the partitioning of various trace elements (Ba, Sr, Pb, U, Th, Nb, Ta, Rb, Cs, B, Be, Li) between hydrous phases in the upper mantle and aqueous fluid over a range of pressures and temperatures (1.0-2.0 GPa, 700-900°C). The results of this study suggest that very strong partitioning of barium relative to thorium into phlogopite mica limits the amount of phlogopite in the dehydrated slab residuum in order to allow for Ba/Th enrichment at island arcs. The higher compatibility of the large ion lithophile elements (LILE) relative to high field strength elements (HFSE) in phlogopite suggest that it is not a likely phase for retaining HFSE in the slab region, thereby generating the characteristc HFSE/LILE enrichment observed in island arc magmas.

OBJECTIVE

Understanding of the major chemical fluxes, and interpretation of the many clues provided by the isotopic and trace element characteristics of crustal and mantle rocks and fluids, is still limited by the paucity of experimental data on the partitioning of elements between minerals and aqueous fluids at high temperature and pressure. The objective of this work is to expand the database of mineral-aqueous fluid partition coefficients at upper mantle conditions.

PROGRESS

The goal of these experiments was to equilibrate phlogopite with aqueous fluids at high P and T in order to characterize the distribution of trace elements between phlogopite and fluid under upper mantle conditions. This information would help to determine the importance of phlogopite as an accessory phase that may contribute to the trace element characteristics of subduction zone lavas. The experiments were performed using the large-volume capsule technique of Ayers *et. al.*[1] A thick-walled transition metal (Ni) cylinder is lined

with a noble metal (Pt) sleeve and topped on the open end by first a thin noble metal, then a thicker transition metal disc. The capsule is then loaded with sample and pressurized in a piston-cylinder apparatus, first to 0.5 GPa and 300°C, which cold-seals the noble metal inner capsule, and then the pressure and temperature are raised simultaneously to run conditions (800-900°C and 1.0-2.0 GPa). The capsule is loaded first with trace elements, then the starting material and other solutes, and finally filled with H_2O immediately prior to sealing the capsule. The starting material used in these experiments was a natural phlogopite. Other solutes added to the experiments were silica and albite glasses, in order to approximate natural mantle fluid compositions. The run products typically consist of a combination of well-formed crystals up to 1 mm in size, and glassy, bead-like quench products ("fish roe"). Following an experiment, the major element compositions of the crystalline run products were measured on the JEOL-733 electron microprobe, and trace element concentrations were determined on the Cameca IMS-3f ion microprobe. The trace element concentrations in the fluid are calculated by mass balance.

In order to assure that our data would be consistent with previously obtained mineral-fluid partition coefficients, we began by duplicating an experiment performed by Brenan *et. al.* (1995) in the same laboratory, using the same technique. The experiment chosen for this purpose was partitioning of Ba, Sr, Pb, U, and Th between diopside and aqueous fluid at 900°C and 2.0 GPa. Once we reproduced the results of Brenan et al within a reasonable margin of error, a series of new experiments was performed.

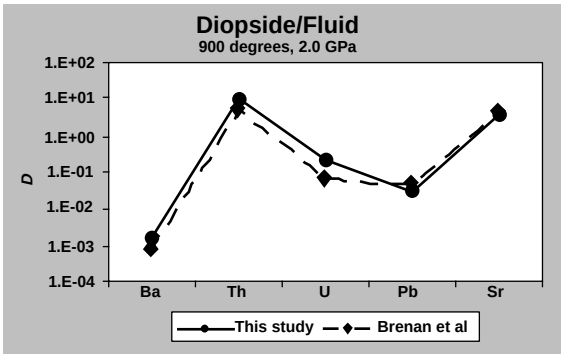

Our experiments have focused primarily on the partitioning of Ba, Pb, Sr, Rb, U, Th, Nb, and Ta into natural phlogopite. The most successful runs have been performed at 900°C, 2.0 GPa. With the exception of uranium, phlogopite/fluid partition coefficients (Dphlog/fluid) were found to be relatively high (~1 or greater). In contrast to previously studied upper mantle minerals such as clinopyroxene and garnet,[3] partition coefficients for barium were notably high (~100). The extreme compatibility of Ba relative to Th in phlogopite indicates that the total Ba/Th ratio of an upper mantle fluid is likely to be strongly affected by the presence of phlogopite, even as an accessory phase. However, island arc magmas are characterized by enrichment in Ba relative to Th,[6] the opposite of what would be expected if phlogopite were a residual phase in the slab region. In fact, the high partition coefficients of many trace elements traditionally believed to be fluid-mobile counterindicate phlogopite as a residual phase in the source regions of mantle-derived fluids.

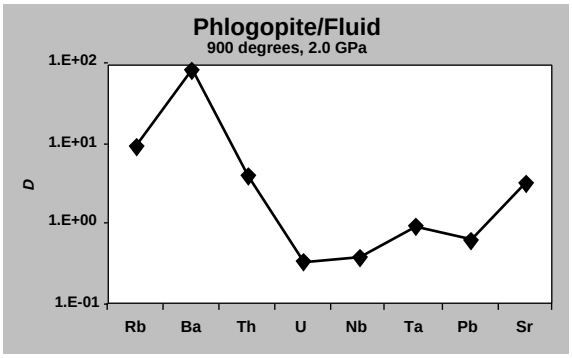

Relative depletion in high field strength elements such as Nb and Ta is a characteristic geochemical feature of island arcs. Researchers have attempted to find a suitable mechanism for generating this particular trace element signature. Based on the high amphibole/clinopyroxene and phlogopite/clinopyroxene ratios measured for Nb and Ta, some researchers have suggested that amphibole and phlogopite may be significant host minerals for these elements.[4] However, although D_{Nb} and D_{Ta} are much higher for phlogopite than cpx (~40x and 100x, respectively), they still do not exceed ~1, which makes them unlikely as

accessory minerals to store enough of these elements to be responsible for the HFSE depletion observed in island arcs. Furthermore, any effect phlogopite may have on drawing down HFSE abundances would be overwhelmed by the higher compatibility of the LILE such as K, Rb, Ba, and Sr.

If we assume that the trace element enrichments characteristic of subduction zone magmas are attributable to fluids transported away from the dehydrating slab, then we can use experimentally determined mineral-fluid partition coefficients to determine the enrichments to be expected in such fluids, and thus in subduction zone magmas.

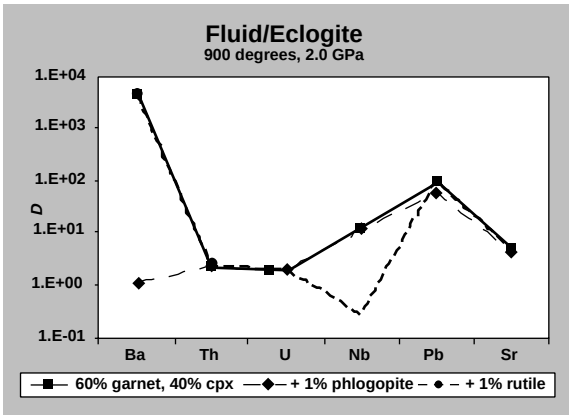

The fluid-rock partitioning demonstrates the effect of adding one percent phlogopite or rutile to an eclogitic residuum following slab dehydration. The fluid-rock partition coefficients are bulk partition coefficients based on a model eclogite mineralogy of 60% garnet and 40% clinopyroxene, and partition coefficients for these minerals taken from Brenan *et. al.* (1995). The addition of a small amount of phlogopite has little effect on inter-element fractionation, with the exception of barium, which is strongly depleted. Furthermore, the results support the idea that a small amount of rutile is required in the residual slab in order to account for the HFSE depletion associated with subduction zones – such a signature cannot be accomplished by the addition of phlogopite alone.

Theoretical Model

Blundy and Wood have shown that mineral-melt partition coefficients depend on ionic radius and charge of the substituent cation,[2] and the Young's Modulus and lattice dimensions of the host mineral. The mineral-melt partition coefficient for trace element substitution can be predicted by

$$D = D_0 \cdot \exp\left(\frac{4\pi N_A E\left[\frac{r_0}{2}\left(r_i - r_0\right)^2 + \frac{1}{3}\left(r_i - r_0\right)^3\right]}{RT}\right)$$

where D_0 is a constant representing the partition coefficient for a cation substitution that does not strain the crystal lattice, NA is Avogadro's number, E is the Young's Modulus, ri is the ionic radius of the trace element, r_0 is the ideal ionic radius for the lattice site, R is the gas constant, and T is the temperature in degrees Kelvin. The values of E, D_0, and r_0, can be determined by regression of the data. The data should plot as a parabola, with D_0 at the apex, corresponding to r_0 on the x-axis. The Young's Modulus of the site will determine the width of the parabola. The applicability of this method to mineral-aqueous fluid partitioning, however, remains to be shown.

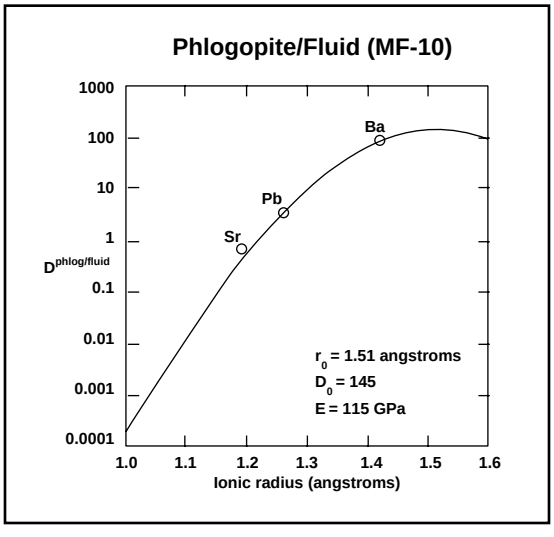

The D(phlog/fluid) determined in this study for the divalent cations Ba, Pb, and Sr have been plotted against the ionic radii for these elements

and fit to the above equation. The value of Young's Modulus determined by this method was 115 GPa. This value is comparable to the value of 165 GPa determined by LaTourrette *et. al.* for phlogopite-melt partitioning using the same method,[5] under similar conditions (2.0 GPa, 1165°C). The value of Do was determined to be 145 for divalent substitution, considerably higher than the value of 3.67 determined by LaTourette et al for a similar substitution between phlogopite and melt. The difference in Do is to be expected due to the greater capacity of silicate melt to accommodate trace element cations than aqueous fluid. To a first approximation, the Blundy Wood method appears to be suitable for application to mineral-fluid as well as mineral-melt partitioning.

High mineral-fluid partition coefficients for certain elements in accessory phases enable us to constrain the quantities of these phases allowable in the source region. In the case of phlogopite, the extreme compatibility of barium relative to thorium limits the amount of phlogopite residual in a subducting slab if one is to account for enrichment in barium relative to thorium in the associated arc magma. Furthermore, the high LILE/HFSE compatibility ratios in phlogopite counter-indicate this phase as a likely receptacle for HFSE's in subduction zones.

REFERENCES

1. Ayers, J., Brenan, J., Watson, E., Wark, D., Minarik, W. (1992), "A new capsule technique for hydrothermal experiments using the piston-cylinder apparatus," *American Mineralogist* 77, 1080-1086.

2. Blundy, J., Wood, B. (1994), "Prediction of crystal-melt partition coefficients from elastic moduli," *Nature*, 372, 452-454.

3. Brenan, J., Shaw, H., Ryerson, F., Phinney, D. (1995), "Mineral-aqueous fluid partitioning of trace elements at 900°C and 2.0 GPa: Constraints on the trace element chemistry of mantle and deep crustal fluids," *Geochimica et Cosmochimica Acta*, 59, 3331-3350.

4. Ionov, D., Hofmann, A. (1995), "Nb-Ta-rich mantle amphiboles and micas: Implications for subduction-related metasomatic trace element fractionations," *Earth and Planetary Science Letters*, 131, 341-356.

5. LaTourrette, T., Hervig, R., Holloway, J. (1995), "Trace element partitioning between amphibole, phlogopite, and basanite melt," *Earth and Planetary Science Letters*, 135, 13-30.

6. Tatsumi, Y., Eggins, S. (1995), "Subduction Zone Magmatism," *Blackwell Science*.

Section IV. IGPP–LLNL Seminars

January 15, 1999
"Building the Microwave Anisitropy Probe"
Mark Halpern, University of British Columbia

January 22, 1999
"Blazars and Their Host Galaxies"
Meg Urry, Space Telescope Science Institute

January 29, 1999
"An Accelerating Universe and Other Cosmological Implications from SNe Ia"
Adam Riess, University of California at Berkeley

February 5, 1999
"Probing the Universe with Quasars"
Chris Impey, Steward Observatory/The University of Arizona

February 12, 1999
"The Hubble Deep Fields: North and South, Optical and Infrared"
Mark Dickinson, Space Telescope Science Institute

February 19, 1999
IGPP Colloquium Series
Ray Weymann, The Observatories of the Institution of Washington

February 26, 1999
"The Cosmological Origin of Disk Galaxy Scaling Laws"
Julio Navarro, University of Victoria

March 5, 1999
"Magnetic Fields in Nascent Neutron Stars"
Norm Murray, Canadian Institute for Theoretical Astrophysics

March 12, 1999
"Optical Gravitational Lensing Experiment - Current Work and Future Plans"
Bohdan Paczynski, Princeton University

March 19, 1999
IGPP Colloquium Series
Pierro Madau, Space Telescope Science Institute

March 26, 1999
IGPP Colloquium Series
Reinhard Genzel, Max-Planck-Institut fur Astrophysik

April 2, 1999
IGPP Colloquium Series
Robert Antonucci, University of California at Santa Barbara

April 9, 1999
"Some Proposed Precision Measurements"
Andy Gould, Ohio State University

April 16, 1999
IGPP Colloquium Series
Arieh Konigl, University of Chicago

April 23, 1999
"The Relative Star Formation Histories of Cluster Galaxies"
Michael Balogh, University of Colorado

April 30, 1999
"Brown Dwarfs: The New Frontier"
Jonathan Lunine, University of Arizona

May 7, 1999
"The Propinquity of Very Massive Black Holes"
Doug Richstone, University of Michigan

May 21, 1999
"The Search for Planets"
David Latham, Harvard-Smithsonian

May 28, 1999
"The Baldwin Effect... Quasars, Massive Galaxies, & Cosmology"
Kirk Korista, Western Michigan University

June 11, 1999
"Gravitational Collapse and Fragmentation in Molecular Clouds: The Formation of Binary and Multiple Stars"
Richard Klein, LLNL

September 10, 1999
"Delivery of asteroids and meteoroids to the inner solar system."
Dr. William Bottke, Cornell University

September 17, 1999
"What does acceleration of the Universe today have to do with the Planck scale?"
Dr. Andreas Albrecht, University of California at Davis

September 24, 1999
"WFPC2 Astrometry, a New HST Gold Mine".
Professor Ivan King, University of California at Berkeley

October 1, 1999
"3D Spectroscopy in Astronomy using a ground-based Imaging FTS"
Dr. Jean-Pierre Maillard, Institut d'Astrophysique de Paris

October 8, 1999
"extra-solar planets with photometric and astro metric microlensing"
Dr. Kim Griest, University of California at San Diego

October 15, 1999
"The ionization history of the IGM"
Dr. Jordi Miralda-Escude, University of Pennsylvania

October 22, 1999
"Sunyaev-Zeldovich decrements with no clusters?"
Professor Priya Natarajan IoA, Cambridge and Yale University

October 29, 1999
"Recent Observations of Pulsar Plants"
Professor Alex Wolszczan Penn State University

November 5, 1999
"Stardust - Laboratory analysis of cometary materials"
Don Brownlee, University of Washington

November 12, 199
"Quasar environments at z=1"
Joanne Baker, University of California at Berkeley

December 3, 1999
"Fixing the lower rungs of the cosmological distance ladder"
Stanek Krzysztof, Harvard University

December 10, 1999
"NICMOS Imaging of Dramatic Disks around Gen-X Stars"
Alycia Weinberger, U.C.L.A.

December 17, 1999
"The DEEP View of the Distant Universe"
Marc Davis, University of California at Berkeley

January 14, 2000
"The physics of dense objects: from the micro-physics to the Galactic implications"
Gilles Chabrier, Ecole Normale Superieure de Lyon

January 21, 2000
"Ages of Globular Clusters and Field Halo Stars"
Dr. Don A. VandenBerg, University of Victoria

January 28, 2000
"Size, Mass and Shape of the Galaxy The Case for a Leaner Milky Way"
Robert Olling, Rutgers University

February 4, 2000
"The Hamburg/ESO survey for bright quasars"
Lutz Wisotzki, Massachusetts Institute of Technology

February 11, 2000
"The X-ray Emission of Dwarf Novae"
Peter Wheatley, University of Leicester

February 18, 2000
"Resonances, Drag Forces, and the Jacobi Constan"
Douglas P. Hamilton, University of Maryland

March 3, 2000
"The distant galaxy content of the Universe as revealed from first observations from the DEEP Survey"
Sandra M. Faber, University of California at Santa Cruz/Lick Observatory

March 10, 2000
"Infrared Spectroscopy of Molecular Supernova Remnants"
William Reach, California Institute of Technology

March 24, 2000
"New Insights on the Angular Momentum Evolution of Low-Mass Pre-Main Sequence Stars"
Keivan Stassun, University of Wisconsin

March 31, 2000
"Dwarf galaxies in the Local Group and Local Volume"
Eva Grebel, University of Washington

April 7, 2000
"Studies of M31's Stellar Halo".
Puragra Guhathakurta, University of California at Santa Cruz

April 7, 2000
"Ultraprecise Photometry From Space: Exploring Pulsations and Planets with the "Hubble Space Telescope"
Jaymie Matthews, University of British Columbia

April 17, 2000
"Cygnus X-3 - a turbo charged swan?".
Jocelyn Burnell, Princeton University

April 19, 2000
"Models of the X-Ray background: Optical and far infrared identifications"
Marco Salvati, Osservatorio Astrofisico di Arcetri, Firenze

April 28, 2000
"StrUniversity of California atture and Formation of Galaxies and Galaxy Systems: An X-Ray Perspective"
David Buote, University of California at Santa Cruz

May 5, 2000
"TES detectors: Pulsars and other recent results, Cosmology and other future potential"
Roger W. Romani, Stanford University

May 11, 2000
"HST and VLBA Observations of FRI Radio Galaxies"
Christopher O'Dea, NASA Space Telescope Institute

May 12, 2000
"A Large Eddy Simulation of Turbulent Compressible Convection: Differential Rotation in the Solar Convection Zone"
Francis Robinson, Yale University

May 19, 2000
"Evolution of the Magnetic Field of a Neutron Star During Polar-Cap Accretion"
Andrew Melatos, University of California at Berkeley

June 23, 2000 "Formation and evolution of early-type galaxies"
Pieter van Dokkum, California Institute of Technology

July 14, 2000
"REM: an automatic IR telescope for GRB follow-up"
Filippo Zerbi, MarOsservatorio di Brera, Italy

August 29, 2000
`Theoretical Modeling of HII regions and Warm Infrared Galaxies'
Lisa Kewley, Mount Stromlo Observatory

September 8, 2000
"Stellar Abundances from K band Spectroscopy: The Abundance Gradient in the Inner Galactic Bulge"
Jay Frogel, The Ohio State University

September 15, 2000
"High-Redshift Observations of Supernovae: Understanding Cosmology and the Physics of Supernovae"
Peter Nugent, Lawrence Berkeley Laboratory

September 22, 2000
“Chandra, the X-ray Background and Black Holes”
Richard Mushotzky, NASA / GFSFC

Section V. Bibliography

Publications 1999-2000

Afonso, C., Alard, C., Albert, J. N., Andersen, J., Ansari, R., Aubourg, É., Bareyre, P., Bauer, F., Beaulieu, J. P., Bouquet, A., Char, S., Charlot, X., Couchot, F., Coutures, C., Derue, F., Ferlet, R., Glicenstein, J. F., Goldman, B., Gould, A., Graff, D., Gros, M., Haissinski, J., Hamilton, J. C., Hardin, D., de Kat, J., Kim, A., Lasserre, T., Lesquoy, É., Loup, C., Magneville, C., Marquette, J. B., Maurice, É., Milsztaj, A., Moniez, M., Palanque-Delabrouille, N., Perdereau, O., Prévot, L., Regnault, N., Rich, J., Spiro, M., Vidal-Madjar, A., Vigroux, L., Zylberajch, S., Alcock, C., Allsman, R. A., Alves, D., Axelrod, T. S., Becker, A. C., Cook, K. H., Drake, A. J., Freeman, K. C., Griest, K., King, L. J., Lehner, M. J., Marshall, S. L., Minniti, D., Peterson, B. A., Pratt, M. R., Quinn, P. J., Rodgers, A. W., Stetson, P. B., Stubbs, C. W., Sutherland, W., Tomaney, A., Vandehei, T., Rhie, S. H., Bennett, D. P., Fragile, P. C., Johnson, B. R., Quinn, J., Udalski, A., Kubiak, M., Szymanski, M., Pietrzynski, G., Wozniak, P., Zebrun, K., Albrow, M. D., Caldwell, J. A. R., DePoy, D. L., Dominik, M., Gaudi, B. S., Greenhill, J., Hill, K., Kane, S., Martin, R., Menzies, J., Naber, R. M., Pogge, R. W., Pollard, K. R., Sackett, P. D., Sahu, K. C., Vermajk, P., Watson, R., Williams, A., "Combined Analysis of the Binary-Lens Caustic-Crossing Event MACHO 98-SMC-1," *Astrophys. J.*, 532, 340 (2000).

Akerlof, C., Balsano, R., Barthelmy, S., Bloch, J., Butterworth, P., Casperson, D., Cline, T., Fletcher, S., Frontera, F., Gisler, G., Heise, J., Hills, J., Hurley, K., Kehoe, R., Lee, B., Marshall, S., McKay, T., Pawl, A., Piro, L., Szymanski, J., Wren, J., "Prompt Optical Observations of Gamma-Ray Bursts, " *Astrophys. J. Lett.*, 532, L25 (2000).

Akerlof, C., Balsano, R., Barthelemy, S., Bloch, J., Butterworth, P., Casperson, D., Cline, T., Fletcher, S., Frontera, F., Gisler, G., Heise, J., Hills, J., Kehoe, R., Lee, B., Marshall, S., McKay, T., Miller, R., Piro, L., Priedhorsky, W., Szymanski, J., Wren, J., "Observation of Contemporaneous Optical Radiation from a Gamma-Ray Burst," *Nature*, 398, 400 (1999).

Alcock, C. Allsman, R.A., Alves, D.R., Axelrod, T.S., "Halo Lensing or LMC Self Lensing? Insights From the HST CMD of MACHO Microlensing Source Stars," *Astrophys. J.*, submitted (2000).

Alcock, C., Allsman, R. A., Alves, D. R., Axelrod, T. S., Becker, A. C., Bennett, D. P., Cook, K. H., Drake, A. J., Freeman, K. C., Geha, M., Griest, K., Lehner, M. J., Marshall, S. L., Minniti, D., Peterson, B. A., Popowski, P., Pratt, M. R., Nelson, C. A., Quinn, P. J., Stubbs, C. W., Sutherland, W., Tomaney, A. B., Vandehei, T., Welch, D. L., The MACHO Collaboration, "The MACHO Project Large Magellanic Cloud Variable-Star Inventory. IX. Frequency Analysis of the First-Overtone RR Lyrae Stars and the Indication for Nonradial Pulsations," *Astrophys. J.*, 542, 257, (2000).

Alcock, C., Allsman, R. A., Alves, D. R., Axelrod, T. S., Basu, A., Becker, A. C., Bennett, D. P., Cook, K. H., Drake, A. J., Freeman, K. C., Geha, M., Griest, K., King, L., Lehner, M. J., Marshall, S. L., Minniti, D., Nelson, C. A., Peterson, B. A., Popowski, P., Pratt, M. R., Quinn, P. J., Stubbs, C. W., Sutherland, W., Tomaney, A. B., Vandehei, T., Welch, D. L., "The MACHO Project 9 Million Star Color-Magnitude Diagram of the Large Magellanic Cloud," *Astron. J.*, 119, 2194, (2000).

Alcock, C., Allsman, R. A., Alves, D. R., Axelrod, T. S., Becker, A. C., Bennett, D. P., Cook, K. H., Freeman, K. C., Geha, M., Griest, K., Lehner, M. J., Marshall, S. L., McNamara, B. J., Minniti, D., Nelson, C., Peterson, B. A., Popowski, P., Pratt, M. R., Quinn, P. J., Rodgers, A. W., Sutherland, W., Templeton, M. R., Vandehei, T., Welch, D. L., "The MACHO Project Sample of Galactic Bulge High-Amplitude Delta Scuti Stars: Pulsation Behavior and Stellar Properties," *Astrophys. J.*, 536, 798, (2000).

Alcock, C., Allsman, R. A., Alves, D., Axelrod, T. S., Baines, D., Becker, A. C., Bennett, D. P., Bourke, A., Brakel, A., Cook, K. H., Crook, B., Crouch, A., Dan, J., Drake, A. J., Fragile, P. C., Freeman, K. C., Gal-Yam, A., Geha, M., Gray, J., Griest, K., Gurtierrez, A., Heller, A., Howard, J., Johnson, B. R., Kaspi, S., Keane, M., Kovo, O., Leach, C., Leach, T., Leibowitz, E. M., Lehner, M. J., Lipkin, Y., Maoz, D., Marshall, S. L., McDowell, D., McKeown, S., Mendelson, H., Messenger, B., Minniti, D., Nelson, C., Peterson, B. A., Popowski, P., Pozza, E., Purcell, P., Pratt, M. R., Quinn, J., Quinn, P. J., Rhie, S. H., Rodgers, A. W., Salmon, A., Shemmer, O., Stetson, P., Stubbs, C. W., Sutherland, W., Thomson, S., Tomaney, A., Vandehei, T., Walker, A., Ward, K., Wyper, G., "Binary Microlensing Events from the MACHO Project," *Astrophys. J.*, 541, 270, (2000).

Alcock, C., Allsman, R. A., Alves, D. R., Axelrod, T. S., Becker, A. C., Bennett, D. P., Charles, P. A., Cook, K. H., Drake, A. J., Freeman, K. C., Geha, M., Griest, K., Groot, P., Lehner, M. J., Marshall, S. L., McGowan, K. E., Minniti, D., Nelson, C. A., Peterson, B. A., Popowski, P., Pratt, M. R., Quinn, P. J., Sutherland, W., Tomaney, A. B., Vandehei, T., van Paradijs, J., "Searching for periodicities in the MACHO light curve of LMC X-2," *Mon. Not. R. Astron. Soc.*, 316, 729, (2000).

Alcock, C., Allsman, R. A., Alves, D., Axelrod, T. S., Becker, A. C., Bennett, D. P., Cook, K. H., Drake, A. J., Freeman, K. C., Griest, K., Lehner, M. J., Marshall, S. L., Minniti, D., Peterson, B. A., Pratt, M. R., Quinn, P. J., Stubbs, C. W., Sutherland, W., Tomaney, A., Vandehei, T., Welch, D. L., The MACHO Collaboration, "Difference Image Analysis of Galactic Microlensing. I. Data Analysis," *Astrophys. J.*, 521, 602A, (1999).

Alcock, C., Allsman, R. A., Alves, D., Axelrod, T. S., Becker, A. C., Bennett, D. P., Cook, K. H., Drake, A. J., Freeman, K. C., Griest, K., Lehner, M. J., Marshall, S. L., Minniti, D., Peterson, B. A., Pratt, M. R., Quinn, P. J., Stubbs, C. W., Sutherland, W., Tomaney, A., Vandehei, T., Welch, D. L., "Difference Image Analysis of Galactic Microlensing. II. Microlensing Events," *Astrophys. J. Suppl.*, 124, 171A, (1999).

Alcock, C., Allsman, R. A., Alves, D., Axelrod, T. S., Becker, A. C., Bennett, D. P., Cook, K. H., Drake, A. J., Freeman, K. C., Griest, K., King, L. J., Lehner, M. J., Marshall, S. L., Minniti, D., Peterson, B. A., Pratt, M. R., Quinn, P. J., Rhie, S. H., Rodgers, A. W., Stetson, P. B., Stubbs, C. W., Sutherland, W., Tomaney, A., Vandehei, T., "Discovery and Characterization of a Caustic Crossing Microlensing Event in the Small Magellanic Cloud," *Astrophys. J.*, 518, 44A, (1999).

Alcock, C., Allsman, R. A., Alves, D. R., Axelrod, T. S., Becker, A. C., Bennett, D. P., Bersier, D. F., Cook, K. H., Freeman, K. C., Griest, K., Guern, J. A., Lehner, M., Marshall, S. L., Minniti, D., Peterson, B. A., Pratt, M. R., Quinn, P. J., Rodgers, A. W., Stubbs, C. W., Sutherland, W., Tomaney, A., Vandehei, T., Welch, D. L., "The MACHO Project LMC Variable Star Inventory. VIII. The Recent Star Formation History of the Large Magellanic Cloud from the Cepheid Period Distribution," *Astron. J.*, 117, 920A, (1999).

Alcock, C., Allsman, R. A., Alves, D., Axelrod, T. S., Becker, A. C., Bennett, D. P., Cook, K. H., Freeman, K. C., Griest, K., Lehner, M. J.,

Marshall, S. L., Minniti, D., Peterson, B. A., Pratt, M. R., Quinn, P. J., Rodgers, A. W., Rorabeck, A., Sutherland, W., Tomaney, A., Vandehei, T., Welch, D. L., The MACHO Collaboration, "The MACHO Project LMC Variable Star Inventory. VI. The Second Overtone Mode of Cepheid Pulsation from First/Second Overtone Beat Cepheids," *Astrophys. J.*, 511, 185A, (1999).

Alcock, C., Allsman, R. A., Alves, D. R., Axelrod, T. S., Becker, A. C., Bennett, D. P., Cook, K. H., Drake, A. J., Freeman, K. C., Geha, M., Griest, K., Lehner, M. J., Marshall, S. L., Minniti, D., Peterson, B. A., Popowski, P., Pratt, M. R., Nelson, C. A., Quinn, P. J., Stubbs, C. W., Sutherland, W., Tomaney, A. B., Vandehei, T., Welch, D. L., The MACHO Collaboration, "Calibration of the MACHO Photometry Database," *Pubs. Astron.Soc. Pac.*, 111, 1539, (1999).

Alcock, C., Allsman, R. A., Alves, D., Axelrod, T. S., Becker, A. C., Bennett, D., Cook, K. H., Drake, A. J., Freeman, K. C., Griest, K., Lehner, M., Marshall, S., Minniti, D., Peterson, B., Pratt, M., Quinn, P., Rodgers, A., Stubbs, C., Sutherland, W., Tomaney, A., Vandehei, T., Welch, D. L., "Baryonic Dark Matter: The Results from Microlensing Surveys," *ASP Conf. Series*, 165, 362, "In The Third Stromlo Symposium: The Galactic Halo," eds. Gibson, B.K., Axelrod, T.S. & Putman, M.E., (1999).

C. Alcock, R.A. Allsman, D.R. Alves, T.S. Axelrod, A.C. Becker, D.P. Bennett, K.H. Cook, N. Dalal, A.J. Drake, K.C. Freeman, M. Geha, K. Griest, M.J. Lehner, S.L. Marshall, D. Minniti, C.A. Nelson, B.A. Peterson, P. Popowski, M.R. Pratt, P.J. Quinn, C.W. Stubbs, W. Sutherland, A.B. Tomaney, T. Vandehei, D. Welch, The MACHO collaboration, "The MACHO Project: Microlensing Results from 5.7 Years of LMC Observations," *Asrophys. J.*, 542, 281A (2000).

Alcock, C., Allsman, R. A., Alves, D. R., Axelrod, T. S., Becker, A. C., Bennett, D. P., Cook, K. H., Drake, A. J., Freeman, K. C., Geha, M., Griest, K., Lehner, M. J., Marshall, S. L., Minniti, D., Nelson, C. A., Peterson, B. A., Popowski, P., Pratt, M. R., Quinn, P. J., Stubbs, C. W., Sutherland, W., Tomaney, A. B., Vandehei, T., Welch, D., "The MACHO Project: Microlensing Detection Efficiency ," *Astrophys. J. Supp.*, 136, 439A (2001).

Alonso, M. V., Minniti, D., Zijlstra, A., Tolstoy, E., "Infrared photometry of the inner regions of the dwarf irregular galaxy NGC 3109," *Astron. Astrophys.*, 346, 33A, (1999).

Alves, D.R., Nelson, C.A., "The Rotation Curve of the Large Magellanic Cloud and the Implications for Microlensing," *Astrophys. J.*, 542, 798, (2000).

Alves, D. R., Basu, A., Cook, K. H., Welch, D. L., The MACHO Collaboration "The MACHO Project LMC Variable Star Inventory: Classical Cepheids AGB Variables, and the Nine Million Star Color-Magnitude Diagram," *IAU Symp. 190*, 517, "New Views of the Magellanic Clouds," eds. Y.-H. Chu, N. Suntzeff, J. Hesser, & D. Bohlender (1999).

Alves, D., "The 9 Million Star Color-Magnitude Diagram of the Large Magellanic Cloud," Thesis (PHD). University of California, Davis, Source DAI-B 60/02, p. 681, Aug 1999, 176 pages, (1999).

Arav, N., Becker, R.H., Laurent-Muehleisen, S.A., Gregg, M.D., White, R.L., Brotherton, M.S., de Kool, M. "What Determines the Depth of BALs? Keck HIRES Observations of BALQSO 1603+3002," *Astrophys. J.*, 524, 566, (1999).

Arav, N., Korista, K.T., de Kool, M., Junkkarinen, V. T., Begelman, M. C., "Hubble Space Telescope Observations of the Broad Absorption Line QuasarPG 0946+301," *Astrophys. J.*, 516, 27A, (1999).

Arav, N., "Are There Clouds in the BLR? Keck Observations of NGC 4151," Structure and

Kinematics of Quasar Broad Line Regions, *ASP Conf. Series*, 175, 9, eds. C. M. Gaskell, W. N. Brandt, M. Dietrich, D. Dultzin-Hacyan, and M. Eracleous. (1999).

Arav, N., "PG 0946+301: the Rossetta Stone of BALQSOs?" *ASP Conf. Series*, 175, 119, "Structure and Kinematics of Quasar Broad Line Regions," eds. C. M. Gaskell, W. N. Brandt, M. Dietrich, D. Dultzin-Hacyan, and M. Eracleous. (1999).

Arav, N., Shlosman, I., Weymann, R. J., "Book Review: Mass ejection from AGN / Astronomical Society of the Pacific, 1997," *The Observatory*, 118, 1147, 373 (1998).

Barth, A. J., Tran, H. D., Brotherton, M. S., Filippenko, A. V., Ho, L. C., van Breugel, W., Antonucci, R., Goodrich, R. W., "Polarized Narrow-Line Emission from the Nucleus of NGC 4258," *Astron. J.*, 118, 1609, (1999).

Becker, A. C., Alcock, C., Allsman, R. A., Alves, D., Axelrod, T. S., Bennett, D. P., Cook, K. H., Drake, A. J., Freeman, K. C., Geha, M., Griest, K., Lehner, M. J., Marshall, S. L., Minniti, D., Nelson, C. A., Peterson, B. A., Popowski, P., Pratt, M. R., Quinn, P. J., Rodgers, A. W., Stubbs, C. W., Sutherland, W., Tomaney, A. B., Vandehei, T., Welch, D. L., MACHO Collaboration, "The MACHO Project: Microlensing Results from 5.7 Years of Large Magellanic Cloud Observations," *Astrophys. J.*, 542, 281, (2000).

Becker, R.H., White, R.L., Gregg, M.D., Brotherton, M.S., Laurent-Muehleisen, S.A., Arav, N., "Properties of Radio-selected Broad Absorption Line Quasars from the First Bright Quasar Survey," *Astrophys. J.* 538, 72, (2000).

Becker, R., White, R. L., Gregg, M. D., Brotherton, M. S., Laurent-Muehleisen, S., Arav, N., "Properties of Radio-Selected Broad Absorption-Line Quasars From The First Bright Quasar Survey," *Astron. Astrophys.*, submitted (1999).

Becker, R., Gregg, M., Schecthter, P. L., Morgan, N. D., White, R. L., "The Gravitational Lens Candidate FBQ 1633 + 3134," *Astrophys. J.*, submitted (1999).

Bicknell, G. V., Sutherland, R. S., van Breugel, W., Dopita, M., Dey, A., Miley, G. K., "Jet-Induced Emission-Line Nebulosity and Star Formation in the High-Redshift Radio Galaxy 4C41.17," *Astrophys. J.*, 540, 678 (2000).

Blais-Ouellette, S., Carignan, C., Amram, P. "Fabry-Perot Observations of Spiral Galaxies: The Impact on Mass Distribution (Poster)," *ASP Conf. Series*, 195, "Imaging the Universe in Three Dimensions," W. van Breugel and J. Bland-Hawthorn, Eds. (2000).

Blais-Ouellette, S., Carignan, C., Amram, Ph., Côté, S., "Accurate Parameters of the Mass Distribution in Spiral Galaxies. I. Fabry-Perot Observations of NGC 5585," *Astron. J.*, 118, 2123 (1999).

Blanton, E., Gregg, M., Helfand, D., Becker, R., and White, R., "Bent-Double Radio Sources: Tracers of High Redshift Clusters," *Astron. J.*, in press, (2000).

Blanton, E.L., Gregg, M.D., Helfand, D.J., Becker, R.H., White, R.L., "FIRST Bent-Double Radio Sources: Tracers of High-Redshift Clusters," *Astrophys. J.*, 531, 118 (2000).

Brinkmann, W., Laurent-Muehleisen, S. A., Voges, W., Siebert, J., Becker, R.H., Brotherton, M.S., White, R.L., Gregg, M.D., "Radio and X-ray bright AGN: the ROSAT - FIRST correlation," *Astron. Astrophys.*, 356, 445 (2000).

Brinkmann, W., Laurent-Muehleisen, S. A., Voges, W., Siebert, J., Becker, R. H., Brotherton, M. S., White, R. L., Gregg, M. D., "ROSAT-FIRST AGN correlation (Brinkmann+, 2000)," *Astron. Astrophys.*, 356, 445B (2000).

Brotherton, M. S., van Breugel, Wil, Stanford, S. A., Smith, R. J., Boyle, B. J., Miller, Lance,

Shanks, T., Croom, S. M., Filippenko, Alexei V., "A Spectacular Poststarburst Quasar," *Astrophys. J. Lett.*, .520, L87 (1999).

Brotherton, M. S., Gregg, M. D., Becker, R. H., Laurent-Muehleisen, S. A., White, R. L., Stanford, S. A., "Discovery of a Radio-Loud/Radio-Quiet Binary Quasar," *Astrophys. J. Lett.*, 514, L61 (1999).

Brotherton, M. S., P. J. Francis, "The Intermediate Line Region and the Baldwin Effect Quasars as Cosmological Probes," *ASP Conf. Ser.*, 162, 395, "Quasars and Cosmology," eds. Gary Ferland and Jack Baldwin. (1999).

Brotherton, M.S., van Breugel, W., Smith, R.J., Shanks, T., Croom, S.M., Miller, L. and Becker, R.H., "Discovery of Radio-Loud Broad Absorption Line Quasars using Ultraviolet Excess and Deep Radio Selection," *Astrophys. J. Lett.*, 505, L7 (1998).

Brotherton, M. S., van Breugel, W., Dey, A., Antonucci, R., "Spectropolarimetry of FIRST 0840+3633," *ASP Conf. Ser.*, 128, 84, "Mass Ejection from Active Galactic Nuclei," eds. N. Arav, I. Shlosman and R. J. Weymann (1997).

Bunker, A. J., van Breugel, W. "THE HY-REDSHIFT UNIVERSE: Galaxy Formation and Evolution at High Redshift," *ASP Conf. Series*, 193, Andrew J. Bunker and Wil J. M. van Breugel, Eds. (1999).

Canalizo, G., Stockton, A., Brotherton, M.S., van Breugel, W., "A Companion Galaxy to the Post-starburst Quasar UN J1025-0040," *Astron. J.*, 119, 59, (2000).

Cohen, M. H., Ogle, P. M., Tran, H. D., Goodrich, R. W., Miller, J. S., "Polarimetry and Unification of Low-redshift Radio Galaxies," *Astron. J.*, 118,1963 (1999).

Cook, K., Alcock, C., Marshall, S., "Asteroids & Comets - Completing the Inventory of the Solar System," Outer Limits of the Solar Syste

Cook, K. (Ed.), "1999 Observatory Report," *Bul. Amer. Astron. Soc.* (2000).

Cook, K. (Ed.), "1998 Observatory Report," *Bul. Amer. Astron. Soc.* (1999).

Cook, K. H., Mateo, M., Olszewski, E. W., Vogt, S. S., Stubbs, C., Diercks, A. "The Systemic Velocity and Internal Kinematics of the Dwarf Galaxy LGS 3: an Optical Foray beyond the Milky Way," *Pubs. Astron. Soc. Pac.*, 111 (1999).

Côté, P., Mateo, M., Olszewski, E. W., Cook, K. H., "Internal Kinematics of the Andromeda II Dwarf Spheroidal Galaxy," *Astrophys. J.*, .526, 147, (1999).

de Breuck, C., van Breugel, W., Rottgering, H., Miley, G., "A Sample of 669 Ultra Steep Spectrum Radio Sources to find High Redshift Radio Galaxies," *Astron. Astrophys.*Suppl., 143, 303 (2000).

de Breuck, C., van Breugel, W., Rottgering, H., Miley, G., "ATCA Search for the Most Distant Radio Galaxies in the Southern Hemisphere," *ATNF Newsletter*

de Breuck, C., van Breugel, W., Rottgering, H., Miley, G., "Ultra steep spectrum radio sources catalog (De Breuck+ 2000)," *VizieR On-line Data Catalog*: J/A+AS/143/303.

de Breuck, C., van Breugel, W., Rottgering, H., Miley, G., "Thomson Thick X-ray Absorption in a Broad Absorption Line Quasar PG0946+301," *Astron. Astrophys.*, submitted

de Breuck, C., van Breugel, W., Minniti, D., Miley, G., Rottgering, H., Stanford, S. A., Carilli, C., "VLT Spectroscopy of the z=4.11 Radio Galaxy TN J1338-1942*," *Astrophys. J.*, submitted (1999).

de Breuck, C., van Breugel, W., Minniti, D., Miley, G., Rottgering, H., Stanford, S.A., Carilli, C., "VLT spectroscopy of the z=4.11 Radio Galaxy TN J1338-1942, " *Astron. Astrophys.*, 352, L51 (1999).

de Pater, I., Macintosh, B., Roe, H., Gavel, D., Gibbard, S., Max, C., "Keck Adaptive Optics Images of Uranus and its Rings," *Icarus*, submitted.

de Pater, I., Hogerheijde, M. R., Wright, M. C. H., Forster, R., Hoffman, W., Snyder, L. E., Remijan, A., Woodney, L. M., A'Hearn, M. F., Palmer, P., Kuan, Y.-J., Huang, H.-C., Blake, G. A., Qi, C., Kessler, J., Liu, S.-Y., "Comet C/1999 S4 (LINEAR), *IAU Circ.*, 7467, 1. Green, D. W. E., Eds. (2000).

de Pater, I., Showalter, M., Burns, J., Nicholson, P., Liu, M., Hamilton, D. P., Graham, J., "Keck Infrared Observations of Jupiter's Ring System near Earth's 1997 Ring Plane Crossing," *Icarus*, 138, 214D (1999).

de Propris, R., Stanford, S. A., Eisenhardt, P. R., Dickinson, M. E., Elston, R., "The K-band Luminosity Function in Galaxy Clusters to z ~ 1," *Astron. J.*, 118, 719D (1999).

de Vries, W.H., O'Dea, C.P., Barthel, P.D., \& Thompson, D.J., "Identifications and spectroscopy of Gigahertz Peaked Spectrum sources. II.," *Astron. Astrophys.Suppl.*,143, 181 (2000).

de Vries, W.H., O'Dea, C.P., Barthel, P.D., Fanti, C., Fanti, R., \& Lehnert, M.D., "HST/NICMOS Observations of the Host Galaxies of Powerful Radio Sources: Does Size Matter?" *Astron. J.*, in press (2000).

de Vries, W. H., O'Dea, C. P., Baum, S. A., Barthel, P. D., "Optical-Radio Alignment in Compact Steep-Spectrum Radio Sources," *Astrophys. J.*, 526, 27D (1999).

de Vries, W.H., O'Dea, C.P., Baum, S.A., Barthel, P.D., "Optical -- Radio Alignment in Compact Steep Spectrum Radio Sources," *Astrophys. J.*, 526, 27 (1999).

de Kool, M., Arav, N., Becker, R., Gregg, M., White, R., Laurent-Muehleisen, S., Price, T., and Korista, K., "The Size of the Broad Absorption Line Region: Keck Hires Observations of BALQSO FIRST J104459.6+365605," *Astrophys. J.*, submitted. (2000).

della Ceca, R., Griffiths, R. E., Heckman, T. M., Lehnert, M. D., Weaver, K. A., "ASCA Observations of the Starburst-driven Superwind Galaxy NGC 2146: Broadband (0.6-9 KEV) Spectral Properties," *Astrophys. J.*, 514, 772D (1999).

Dickinson, M., Hanley, C., Elston, R., Eisenhardt, P. R., Stanford, S. A., Adelberger, K.L., Shapley, A., Steidel, C. C., Papovich, C., Szalay, A. S., Bershady, M. A., Conselice, C. J., Ferguson, H. C., Fruchter, A. S., "The Unusual Infrared Object HDF-N J123656.3+621322," *Astrophys. J.*, 531, 624D (2000).

Drake, A., Alcock, C., Cook, K.H., Marshall, S.L., Nelson, C. A., Allsman, R.A., Alves, D.R.,. Axelrod, T.S., Freeman, K.C., Peterson, B.A., Becker, A.C., Tomaney, A.B., Bennett, D.P., Geha, M., Griest, K., Lehner, M.J., Minniti, D., Popowski, P., Pratt, M.R., Quinn, P.J., "The MACHO Project: Microlensing Optical Depth towards the Galactic Bulge from Difference Image Analysis," *Astrophys. J.*, 541, 734 (2000).

Drake, R.P., Smith, T.B., Carroll, J.J.~III, Yan, Y., Glendinning, S.G., Estabrook, K., Ryutov, D.D., Remington, B.A., Wallace, R.J., McCray, R. "Progress toward the Laboratory Simulation of Young Supernova Remnants," *Astrophys. J.Supp.*, 127, 305 (2000).

Drake, A. J., Minniti, D., Alcock, C., Allsman, R. A., Alves, D., Axelrod, T. S., Becker, A. C., Bennett, D., Cook, K. H., Freeman, K. C., Griest, K., Lehner, M., Marshall, S., Peterson, B., Pratt, M., Quinn, P., Rodgers, A., Stubbs, C., Sutherland, W., Tomaney, A., Vandehei, T., Welch, D. L., "Results from the MACHO Galactic Pixel Lensing Search," *ASP Conf. Ser.*, 165, 382, "In The Third Stromlo Symposium: The Galactic Halo," eds. Gibson, B.K., Axelrod, T.S. & Putman, M.E. (1999).

Drinkwater M., Jones, J. B., Gregg, M. D., Phillips, S., "Compact Stellar Systems in the Fornax Cluster: Super-massive Star Clusters or Extremely Compact Dwarf Galaxies?" *Pubs Astron. Soc. Australia,* 17 (3), 227 (2000).

Drinkwater, M. J., Phillipps, S., Gregg, M. D., Davies, J. I., Deady, J. H., Jones, J. B., Parker, Q. A., Sadler, E. M., Smith, R. M., "The Fornax Spectroscopic Survey -- I. Design and Aims," *Mon. Not. R. Astron. Soc.*, submitted

Drinkwater, M. J., Phillipps, S., Gregg, M. D., Davies, J. I., Deady, J. H., Jones, J. B., Parker, Q. A., Sadler, E. M., Smith, R. M.,"The Fornax Spectroscopic Survey: Survey Strategy and Preliminary Results on the Redshift Distribution of a Complete Sample of Stars and Galaxies," *Astron. Astrophys.*, 355, 900 (2000).

Drinkwater, M. J., Phillipps, S., Gregg, M. D., Parker, Q. A., Smith, R. M., Davies, J. I., Jones, J. B., Sadler, E. M., "The Fornax Spectroscopic Survey: The Number of Unresolved Compact Galaxies," *Astrophys. J.* Lett., 511, 97D (1999).

Drinkwater, M. J., Waugh, M., Webster, R. L., Barnes, D. G., Gregg, M. D., Phillipps, S., Jones, J. B., "Hidden Galaxies in the Fornax Cluster'" *ASP Conf. Proc.*, 218, 239, "Mapping the Hidden Universe: The Universe behind the Milky Way - The Universe in HI." eds. Renée C. Kraan-Korteweg, Patricia A. Henning, and Heinz Andernach.

Drinkwater, M. J.; Phillipps, S.; Jones, J. B., "The Fornax spectroscopic survey - Low Surface Brightness galaxies in Fornax," *ASP Conf. Proc.*, 170, "Low Surface Brightness Universe," eds.J.I. Davies, C. Impey, and S. Phillipps (1999).

Drinkwater, M. J.; Phillipps, S.; Jones, J. B.; Gregg, M. D.; Parker, Q. A.; Smith, R. M., Davies, J. I.; Sadler, E. M., "Found: High Surface Brightness compact galaxies," *ASP Conf. Proc.*, 170, 128, "Low Surface Brightness Universe," eds. J.I. Davies, C. Impey, and S. Phillipps (1999).

Fan, X., White, R. L., Davis, M., Becker, R. H., Strauss, Mi. A., Haiman, Z., Schneider, D. P., Gregg, M. D., Gunn, J. E., Knapp, G. R., Lupton, R. H., Anderson, J. E., Jr., Anderson, S. F., Annis, J., Bahcall, N.a A., Boroski, W. N., Brunner, R. J., Chen, B., Connolly, A. J., Csabai, I., Doi, M., Fukugita, M., Hennessy, G. S., Hindsley, R. B., Ichikawa, T., Ivezic, Z., Loveday, J., Meiksin, A., McKay, T. A., Munn, J. A., Newberg, H. Jo, Nichol, R., Okamura, S., Pier, J. R., Sekiguchi, M., Shimasaku, K., Stoughton, C, Szalay, A. S., Szokoly, G. P., Thakar, A. R., Vogeley, M. S., York, D. G. "The Discovery of a Luminous Z=5.80 Quasar from the Sloan Digital Sky Survey," *Astron. J.*, 120, 1167 (2000).

Garnero, E. J., Vidale, J. E., "ScP: A probe of ultralow velocity zones at the base of the mantle," *Geophs. Rev. L.ett*, 26, 377G (1999).

Gavel, D. T., Olivier, S. S., Bauman, B. J., Max, C. E., Macintosh, B. A., "Progress with the Lick adaptive optics system," Proc. SPIE Vol. 4007, "Adaptive Optical Systems Technology," Wizinowich; Ed. (2000).

Ge, Ciarlo, D., Kuzmenko, P., Macintosh, B., Alcock, C., Cook, K., "Etched Silicon Gratings for NGST," *ASP Conf. Ser.*, 207, 457, "Next Generation Space Telescope Science and Technology," eds. Eric Smith and Knox Long (2000).

Ge, J., Ciarlo, D., Kuzmenko, P., Alcock, C., Macintosh, B., Cook, K., Max, C., Angel, R., Woolf, N., Lloyd-Hart, M., Najita, J., "Adaptive Optics High Resolution Spectroscopy: Present Status and Future Direction (Poster) ," *ASP Conf. Ser.*, 195, 568, "Imaging the Universe in Three Dimensions," eds. W. van Breugel and J. Bland-Hawthorn (2000).

Ge, J., Bechtold, J., "H_2 and C I in Damped LY alpha Quasar Absorbers at Intermediate and High Redshifts," *ASP Conf. Ser.*,156, 121,

"Highly Redshifted Radio Lines," eds. C. L. Carilli, S. J. E. Radford, K. M. Menten, & G. I. Langston (1999).

Ge, J., Ciarlo, D. R., Kuzmenko, P. J., Alcock, C. R., Macintosh, B. A., Angel, J. R. P., Woolf, N.J., Lloyd-Hart, M., Fugate, R. Q., Najita, J., "Adaptive optics high-resolution spectroscopy: present status and future direction," *Proc. SPIE*, 3762, 174, "Adaptive Optics Systems and Technology," eds. Robert K. Tyson; Robert Q. Fugate (1999).

Gibbard, S. G., Levy, E. H., Lunine, J. I., de Pater, I., "Lightning on Neptune," *Icarus*, 139, 227G (1999).

Gibbard, S. G., Macintosh, B., Gavel, D., Max, C. E., de Pater, I., Ghez, A. M., Young, E. F., McKay, C. P., "Titan: High-Resolution Speckle Images from the Keck Telescope," *Icarus*, 139, 189G (1999).

Gibbard, S.G., de Pater, I., Roe, H., Macintosh, B., Gavel, D., Max, C.E., Baines, K. H., Ghez, A., "High-resolution infrared imaging of Neptune from the Keck telescope," *Icarus*, submitted.

Gliozzi , M., Brinkmann, W., Laurent-Muehleisen, S. A., Takalo, L. O., Sillanpaa, A., "ROSAT HRI observations of radio-loud AGN," *Astron. Astrophys.*, 352, 437 (1999).

Gould, A., Popowski, P., "Systematics of RR Lyrae Statistical Parallax. III. Apparent Magnitudes and Extinctions," *Astrophys. J.*, 508, 844G (1998).

Graham, James R., Abrams, Mark, Bennett, C., Carr, J., Cook, K., Dey, A., Najita, J., Wishnow, E., "The Performance and Scientific Rationale for an Infrared Imaging Fourier Transform Spectrograph on a Large Space Telescope," *Pubs. Astron. Soc. Pac.*, 110, 1205G (1998).

Gregg, M. D., Becker, R. H., Laurent-Muehleisen, S., White, R. L., Brotherton, M., Helfand, D. J., "The Discovery of a FIRST FR II Radio-Loud Broad Absorption Line Quasar," *Astrophys. J.*, submitted.

Gregg, M.D., Wisotzki, L., Becker, R.H., Maza, J., Schechter, P.L., White, R.L., Brotherton, M.S., Winn, J.N., "A Close-Separation Double Quasar Lensed by a Gas-rich Galaxy," *Astron. J.*, 115, 2535 (2000).

Gregg, M. C., Özsoy, E., Latif, M. A., "Quasi-steady exchange flow in the Bosphorus," *Geophs. Res. Lett.*, 26, 83G (1999).

Grupe, D., Leighly, K.M., Thomas, H.-C., Laurent-Muehleisen, S.A., "The enigmatic Soft X-ray AGN RX J0134.2-4258," *Astron. Astrophys.*, 356, 11 (2000).

Helfand, D. J., Schnee, S., Becker, R. H., White, R. L., McMahon, R. G., "The FIRST Unbiased Survey for Radio Stars," *Astron. J.*, 117, 1568H (1999).

Hwang, D. Q., Ryutova, M., Mclean, H., "Penetration of a Compressible Magnetized Plasma Object into a Low Beta Target Plasma," *Physics of Plasmas*, submitted

Johansson, E. M., Acton, D. S., An, J. R., Avicola, K., Beeman, B. V., Brase, J. M., Carrano, C. J., Gathright, J., Gavel, D. T., Hurd, R. L., Lai, O., Lupton, W., Macintosh, B. A., Max, C. E., Olivier, S. S., Shelton, J. C., Stomski, P. J., Tsubota, K., Waltjen, K. E., Watson, J. A., Wizinowich, P. L., "Initial performance of the Keck AO wavefront controller system," *Proc. SPIE*, 4007, "Adaptive Optical Systems Technology," Wizinowich, Ed. (2000).

Kapahi, V, K., Athreya, R, M., van Breugel, W,, McCarthy, P, J., Subrahmanya, C. R., "The Molonglo Reference Catalog 1 Jy Radio Source Survey. II. Radio Structures of Galaxy Identifications," *Astrophys. J. Supp.*, 118, 275K (1998).

Kapahi, V. K., Athreya, R. M., Subrahmanya, C. R., Baker, J. C., Hunstead, R. W., McCarthy, P. J., van Breugel, W., "The Molonglo Reference Catalog 1 Jy Radio Source Survey. III. Identi-

fication of a Complete Quasar Sample," *Astrophys. J. Supp*., 118, 327K (1998).

Kapp, P., Yin, A., Manning, C. E., Murphy, M., Harrison, T. M., Spurlin, M., "Blueschist-bearing metamorphic core complexes in the Qiangtang block reveal deep crustal structure of northern Tibet," *Geology*, 28, 19 (2000).

Kishimoto, T., Antonucci, R., Cimatti, A., Hurt, T., Dey, A., van Breugel, W., Spinrad, H., "UV Spectropolarimetry of Narrow-line Radio Galaxies," *Astrophys. J*., submitted

Kissler-Patig, M., Grillmair, C. J., Meylan, G., Brodie, J. P., Minniti, D., Goudfrooij, P., "Toward an Understanding of the Globular Cluster Overabundance around the Central Giant Elliptical Galaxy NGC 1399," *Astron. J.*, 117, 1206K (1999).

Kovács, G., Alcock, C., Allsman, R., Alves, D., Axelrod, T., Becker, A., Bennett, D., Clement, C., Cook, K. H., Drake, A., Freeman, K., Geha, M., Griest, K., Kurtz, D. W., Lehner, M., Marshall, S., Minniti, D., Nelson, C., Peterson, B., Popowski, P., Pratt, M., Quinn, P., Rodgers, A., Rowe, J., Stubbs, C., Sutherland, W., Tomaney, A., Vandehei, T., Welch, D. L., The MACHO Collaboration, "Frequency Analysis of the RRc Variables of the MACHO Database for the LMC," *ASP Conf. Series*, Vol. 203, "The Impact of Large-Scale Surveys on Pulsating Star Research," Szabados and Kurtz Eds. (2000).

Kovács, G., Alcock, C., Allsman, R., Alves, D., Axelrod, T., Becker, A., Bennett, D., Clement, C., Cook, K. H., Drake, A., Freeman, K., Geha, M., Griest, K., Kurtz, D. W., Lehner, M., Marshall, S., Minniti, D., Nelson, C., Peterson, B., Popowski, P., Pratt, M., Quinn, P., Rodgers, A., Rowe, J., Stubbs, C., Sutherland, W., Tomaney, A., Vandehei, T., Welch, D. L., The MACHO Collaboration, "Frequency Analysis of the RRc Variables of the MACHO Database for the LMC," *ASP Conf. Ser.*, 203, "The Impact of Large-Scale Surveys on Pulsating Star Research," eds. Szabados and Kurtz (2000).

Kurk, J. D., Röttgering, H. J. A., Pentericci, L., Miley, G. K., van Breugel, W., Carilli, C. L., Ford, H., Heckman, T., McCarthy, P., Moorwood, A., "A Search for Clusters at High Redshift. I. Candidate Ly--alpha emitters near 1138-262 at z=2.2," *Astron. Astrophys.*, 358, L1 (2000).

Kurtz, D. W., Alcock, C., Allsman, R. A., Alves, D., Axelrod, T. S., Becker, A. C., Bennett, D. P., Cook, K. H., Freeman, K. C., Griest, K., Lehner, M. J., Marshall, S. L., Minniti, D., Peterson, B. A., Pratt, M. R., Quinn, P. J., Rodgers, A. W., Stubbs, C. W., Sutherland, W., Tomaney, A., Welch, D. L., The MACHO Collaboration, *ASP Conf. Ser.*, 203, "A New Look at the Blazhko Effect in RR Lyrae Stars with High-Quality Data from the MACHO Project ," (2000).

Lacy, M., "Radio Galaxy Clustering at Z ~ 0.3," *Astrophys. J. Lett*., 536, 1 (2000).

Lacy, M., Bunker, A.J., Ridgway, S.E., "The Evolution of the Stellar Hosts of Radio Galaxies," *Astron. J.*,120, 68 (2000).

Lacy, Mark D., Becker, Andrew J., Ridgway, S. E., "The evolution of the stellar hosts of radio galaxies," *Astrophys. J*., 120, 68 (2000).

Lacy, M., Kaiser, M.E., Hill, G.J., Rawlings, S., "A Complete Sample of Radio Sources in the North Ecliptic Cap, Selected at 38 MHz -- III. Further Imaging Observations and the Photometric Properties of the Sample," *Mon. Not. R. Astron. Soc*., 308, 1087(1999).

Lacy, M., "HST Imaging of Two z > 4 Radio Galaxies," *ASP Conf. Proc.*, 193, "The Hy-Redshift Universe: Galaxy Formation and Evolution at High Redshift," eds. Andrew J. Bunker and Wil J. M. van Breugel (1999).

Laurent-Muehleisen, S. A., Kollgaard, R. I., Feigelson, E. D., Brinkmann, W., Siebert, J.,

"The RGB Sample of Intermediate BL Lacertae Objects," *Astrophys. J.*, 525, 127L (1999).

Lehnert, M. D., van Breugel, W. J. M., Heckman, T. M., Miley, G. K., "HUBBLE SPACE TELESCOPE Imaging of the Host Galaxies of High-RedshiftRadio-loud Quasars," *Astrophys. J. Supp.*, 124, 11L (1999).

Lloyd, J. P., Liu, M. C., Macintosh, Be A., Severson, S. A., Deich, W. T., Graham, J. R., "IRCAL: the infrared camera for adaptive optics at Lick Observatory," *Proc. SPIE*, 4008, p. 814-821, "Optical and IR Telescope Instrumentation and Detectors," Masanori Iye, Alan F. Moorwood, Eds. (2000).

Macintosh, B., Gavel, D., Gibbard, S., Max, C., Eckart, M., dePater, I., Ghez, A., Spencer, R., "Speckle Imaging of Volcanic Hotspots on Io with the Keck Telescope," *Icarus*, submitted (2000).

Macintosh, B., Gavel, D., Gibbard, S., Max, C.E., de Pater, I., Ghez, A., Spencer, J., "Infrared speckle imaging of the July/August 1998 transient volcano on Io," *Icarus*, submitted (1999).

Martini, B.A., Cochran, S.A., Silver, E.A., Pickles, W.L., Potts, D.C., "Geological and geobotanical characterization of a geothermal system sing hyperspectral imagery analysis, Long Valley Caldera, CA.," *Proc. of the Thirteenth International Conf. on Applied Remote Sensing.* Vol. 1., 337-341 (1999).

Max, C. E., Macintosh, B. A., Gibbard, S., Gavel, D. T., Roe, H., de Pater, I., Ghez, A. M., Acton, S., Wizinowich, P. L., Lai, O., "Neptune and Titan observed with the Keck telescope adaptive optics," *Proc. SPIE*, 4007, p. 803-810, Adaptive Optical Systems Technology, Peter L. Wizinowich, Ed. (2000).

Max, C. E., "Laser Guide Star Operational Issues," *Laser Guide Star Adaptive Optics for Astronomy,* eds. N. Ageorges, and C. Dainty (2000).

Max, C., Baines, K. H., Ghez, A., "High-resolution infrared imaging of Neptune from the Keck telescope," *Icarus*, submitted (1999).

McMahon, R.G., White, R.L., Helfand, D.J., Becker, R.H., "Optical Counterparts for 70,000 Radio Sources: APM Identifications for the First RAdio Survey," *Astron. Astrophys.* submitted.

Minniti, D., Alcock, C., Alves, D. R., Axelrod, T. S., Becker, A. C., Bennett, D. P., Cook, K. H., Freeman, K. C., Griest, K., Lehner, M. J., Marshall, S. L., Peterson, B. A., Quinn, P. J., Pratt, M. R., Rodgers, A. W., Stubbs, C. W., Sutherland, W., Tomaney, A., Vandehei, T., Welch, D., "Bulge Delta Scuti Stars in the MACHO Database," *Proc. of IAU Symp.* 189, "Fundamental Stellar Properties: Confrontation between Theory and Observations," eds. T. R. Bedding, A. J. Booth and J. Davis (1999).

Minniti, D., Alcock, C., Allsman, R. A., Alves, D., Axelrod, T. S., Becker, A. C., Bennett, D., Cook, K. H., Drake, A. J., Freeman, K. C., Griest, K., Lehner, M., Marshall, S., Peterson, B., Pratt, M., Quinn, P., Rodgers, A., Stubbs, C., Sutherland, W., Tomaney, A., Vandehei, T., Welch, D. L., "MACHO RR Lyrae in the Inner Halo and Bulge," *ASP Conf. Ser.*, 165, 284, In The Third Stromlo Symposium: The Galactic Halo, eds. Gibson, B.K., Axelrod, T.S., Putman, M.E., Nelson, C. A. (1999).

Minniti, D., Bedding, T.R., Soria, R., Dey, A., Marleau, F. R., Graham, J., Liu, M., Charlot, S., "Old metal-rich stars in the halo of the giant elliptical galaxy NGC 5128," *Nature*, submitted.

Minniti, D., Zijlstra, A. A., Alonso, M. V., "The Stellar Populations of NGC 3109: Another Dwarf Irregular Galaxy with a Population II Stellar Hal," *Astron. J.*, 117, 881M (1999).

Mirabal, N., Halpern, J.P., Eracleous, M., Becker, R.H., "Search for the Identification of 3EG J1835+5918: Evidence for a New Type of

High-Energy Gamma-Ray Source," *Astrophys. J.*, 541, 180 (2000).

Moran, E. C., Lehnert, M. D., Helfand, D. J., "X-Rays from NGC 3256: High-Energy Emission in Starburst Galaxies and Their Contribution to the Cosmic X-Ray Background," *Astrophys. J.*, .526., 649M (1999).

Nelson, C.A., Cook, K.H., Popowski, P, Alves, D.R., "The Distance to the Large Magellanic Cloud via the Eclipsing Binary HV 2274," *Astron. J.*, 119, 1205 (2000).

Nilsson, K., Takalo, L. O., Pursimo, T., Sillanpää, A., Heidt, J., Wagner, S. J., Laurent-Muehleisen, S. A., Brinkmann, W., "Discovery of a blue arc near the BL Lacertae object RGB 1745+398," *Astron. Astrophys.*, 343, 81N (1999).

O'Dea, C.P., de Vries, W.H., Worrall, D.M., Baum, S.A., Koekemoer, A., "ASCA observations of the Gigahertz Peaked Spectrum Radio Galaxies 1345+125 and 2352+495," *Astron. J.*, 119, 478 (2000).

Ogle, P. M., Cohen, M. H., Miller, J. S., Tran, H. D., Goodrich, R. W., Martel, A. R., "Polarization of Broad Absorption Line QSOs I. A Spectropolarimetrick Atlas," *Astrophys. J.* Suppl., 125, 1 (1999).

Olivier, S. S., Gavel, D. T., Friedman, H. W., Max, C. E., An, J. R., Avicola, K., Bauman, B. J., Brase, J. M., Campbell, E. W., Carrano, C. J., Cooke, J. B., Freeze, G. J., Gates, E. L., Kanz, V. K., Kuklo, T. C., Macintosh, B. A., Newman, M. J., Pierce, E. L., Waltjen, K. E., Watson, J. A., "Improved performance of the laser guide star adaptive optics system at Lick Observatory," *Proc. SPIE*, 3762, 2, Adaptive Optics Systems and Technology, eds. Robert K. Tyson; Robert Q. Fugate (1999).

Owen, T., Mahaffy, P., Niemann, H. B., Atreya, S., Donahue, T., Bar-Nun, A., de Pater, I. "A low-temperature origin for the planetesimals that formed Jupiter, " *Nature*, 402, 269O (1999).

Papadopoulos, P. P., Rottgering, H. J. A., van der Werf, P. P., Guilloteau, S., Omont, A., van Breugel, W. J. M. , Tilanus, R. P. J., "CO (4-3) and Dust Emission in Two Powerful High-Z Radio Galaxies, and CO Lines at High Redshifts," *Astrophys. J.*, 528, 626 (2000).

Pentericci, L., Kurk, J.D., Rottgering, H.J.A., Miley, J.K., van Breugel, W., Carilli, C.L., Ford, H., Heckman, T., McCarthy, P., Moorwood, A., "A Search for Clusters at High Redshift - II. A Proto Cluster around a Radio Galaxy at z = 2.16," *Astron. Astrophys.*, 361, L25-L28 (2000).

Pentericci, L., Röttgering, H. J. A., Miley, G. K., McCarthy, P., Spinrad, H., van Breugel, W. J. M., Macchetto, F. "HST images and properties of the most distant radio galaxies," *Astron. Astrophys.*, 341, 329P (1999).

Pollard, K. R., Alcock, C., Allsman, R. A., Alves, D., Axelrod, T. S., Becker, A. C., Bennett, D. P., Cook, K. H., Freeman, K. C., Griest, K., Lehner, M. J., Marshall, S. L., Peterson, B. A., Pratt, M. R., Quinn, P. J., Sutherland, W., Tomaney, A., Welch, D. L., The MACHO Collaboration, "RV Tauri Stars and Type II Cepheids in the Magellanic Clouds -- Results from the MACHO Database," *ASP Conf. Series*, Vol. 203, " The Impact of Large-Scale Surveys on Pulsating Star Research," Edited by L. Szabados and D. Kurtz. (2000).

Pollitz, F.F., R. Burgmann, and L. Kellogg, "Sinking mafic body in a reactivated lower crust: A mechanism for stress concentration at the New Madrid Seismic zone," *Bull. Seismol. Soc. Am.*, submitted (2000).

Popowski, P., "Clump Giant Distance to the Magellanic Clouds and Anomalous Colors in the Galactic Bulge," *Astrophys. J.*, 528L., 9P (2000).

Popowski, P., "The Distance to the Large Magellanic Cloud," *ASP Conf. Ser.*, 203, "The Impact of Large-Scale Surveys on Pulsating

Star Research," p.203-207, Eds. L. Szabados and D. Kurtz. (2000).

Popowski, P., "Harmonizing the RR Lyrae and Clump Distance Scales - Stretching the Short Distance Scale to Intermediate Ranges?" *Mon. Not. R. Astron. Soc.*, submitted, (2000).

Popowski, P., Alcock, C., "Correcting Parameters of Events Based on the Entropy of Microlensing Ensemble," *Astrophys. J.*, submitted (2000).

Popowski, P., "The Distance to the Large Magellanic Cloud," *ASP Conf. Ser.*, 203. "The Impact of Large-Scale Surveys on Pulsating Star Research, eds. L. Szabados and D. Kurtz. (2000).

Popowski, P., Gould, A., "The RR Lyrae Distance Scale," *Post-Hipparcos cosmic candles*, 237, 53, eds. A. Heck and F. Caputo (1999).

Popowski, P., Gould, A., "Systematics of RR Lyrae Statistical Parallax. I. Mathematics," *Astrophys. J.*, .506, 259P (1998).

Popowski, P., Gould, A., "Systematics of RR Lyrae Statistical Parallax. II. Proper Motions and Radial Velocities," *Astrophys. J.*, .506, 271P, (1998).

Proctor, D., "Low Resolution Pattern Recognition - Sorting the FIRST Data - Part I. The Triples," *Journal of Electronic Imaging*

Pursimo, T., Smith, P.S., Nilsson, K., Heinamaki, P., Laurent-Muehleisen, S.A., Takalo, L.O., Sillanpaa, A., Schmidt, Brinkmann, W., Katajainen, S., "Optical polarization of ROSAT Green Bank BL Lacs," *Astron. Astrophys.*, submitted

Rejkuba, M., Minniti, D., Gregg, M.l D., Zijlstra, A. A., Alonso, M. V., Goudfrooij, P., "Deep Hubble Space Telescope STIS Color-Magnitude Diagrams of the Dwarf Irregular Galaxy WLM: Detection of the Horizontal Branch," *Astron. J.*, 120, 801-809 (2000).

Richards, G. T., York, D. G., Yanny, B., Kollgaard, R. I., Laurent-Muehleisen, S. A., vanden Berk, D.E., "Determining the Fraction of Intrinsic C IV Absorption in Quasi-stellar Object Absorption-Line Systems," *Astrophys. J.*, .513, 576R (1999).

Roe, H., Gavel, D., Max, C. E., de Pater, I., Gibbard, S., Macintosh, B., Baines, K. , "Observations of Neptune's Tropospheric Cloud Layer with the Lick Observatory Adaptive Optics System," *Astrophys. J.*, submitted.

Roe, H., Gavel, D., Max, C., de Pater, I., Gibbard, S., Macintosh, B., "Observations of Neptune's tropospheric cloud layer with the Lick Adaptive Optics system," *Astron. J.*, submitted.

Roe, H.G., de Pater, I., Gibbard, S., Macintosh, B., Max, C., McKay, C., "Near and mid-infrared resolved imaging of Titan's atmosphere," *EOS Trans. Am. Geophys. Union*, 81, 797 (2000).

Roe, H.G., Graham, J.R., McLean, I.A., de Pater, I., Becklin, E.E., Figer, D.F., Gilbert, A.M., Larkin, J.E., Levenson, N.A., Teplitz, H.I., Wilcox, M.K., "The altitude of an infrared bight cloud feature on Neptune from near-infrared spectroscopy," *Astron. J.*, Submitted (2000).

Rosati, P., Stanford, S. A., Eisenhardt, P. R., Elston, R., Spinrad, H., Stern, D., Dey, A., "An X-ray Selected Galaxy Cluster at z = 1.26," *Astron. J.*, 123, 619 (2000).

Ryutova, M. P., Tarbell, T. D., "On the Transition Region Explosive Events," *Astrophys. J.*, 541, L29 (2000).

Ryutova, M., Habbal, S., Woo, R., Tarbell, T.D., "Quiet Photospheric Network as the Base of the Fast Solar Wind," *Solar Physics*, submitted (2000).

Savine, C., Adami, C., Mazure, A., West, M., Gregg, M., Ulmer, M. P., Conselice, C., Picat, J. P., Cuillandre, J. C., McCraken, H., Mathez, G., Pello, R., van Waerbeke, L., Gallagher, J., "A deep wide multicolor and spec-

troscopic survey of the Coma cluster," *Bull. CFH*, 42, (2000).

Siebert, J., Brinkmann, W., Gliozzi, M., Laurent-Muehleisen, S. A., Matsuoka, M., "Recent ASCA and SAX observations of intermediate BL Lac objects," *Astronomische Nachrichten*, 320, 315 (1999).

Siebert, J., Leighly, K. M., Laurent-Muehleisen, S. A., Brinkmann, W., Boller, Th., Matsuoka, M. "An ASCA observation of the radio-loud narrow-line Seyfert 1 galaxy RGB J0044+193," *Astron. Astrophys.*, 348, 678S (1999).

Silva, A.V. R., Lin, R. P., de Pater, I., White, S. M., Shibasaki, K., Nakajima, H., "Images of Gradual Millimeter Emission and Multi-Wavelength Observations of the 17august 1994 Solar Flare," *Solar Physics*, 183, 389S (1998).

Stanford, S. A., Stern, D., van Breugel, W., De Breuck, C., "The FIRST Sample of Ultraluminous Infrared Galaxies at High Redshift," *Astrophys. J.* S., 131, 185 (2000).

Stanford, S. A., "Morphological Evolution in High Redshift Galaxy Clusters," *ASP Conf. Proc.*, 193, The Hy-Redshift Universe: Galaxy Formation and Evolution at High Redshift, eds. Andrew J. Bunker, Wil J. M. van Breugel (1999).

Stern, D., Spinrad, H., Eisenhardt, P., Bunker, A.J., Dawson, S., Stanford, S.A., Elston, R., "Discovery of a Color-Selected Quasar at z=5.50," *Astrophys. J. Lett.*, 533, L75 (2000).

Stockton, A., Canalizo, G., "Recent Spectroscopy of the 3C 48 Host Galaxy and a Simple Image Slicer Design," *ASP Conf. Ser.*, 195, 385, Imaging the Universe in Three Dimensions. eds. W. van Breugel and J. Bland-Hawthorn (2000).

Stutz, A., Popowski, P., Gould, A., "Anomalous RR Lyrae (V-I)_0 Colors in Baade's Window," *Astrophys. J.*, .521, 206S (1999).

Tarbell, T., Ryutova M., Shine, R., "Electro-Mechanical Coupling Between the Photosphere and Transition Region," *Solar Physics*, 193, 195, (2000).

Taylor, M.H., "Distributed Eastward Extrusion of the Tibetan Plateau: A Perspective from Rift-Bounding Faults in Central Tibet ," [*MS thesis*]: University of California, Los Angeles, 65 p. (2000).

Taylor, M.H., An Yin, Kapp, P., Ryerson, F.J., Zou Yong and Din Ling, Distributed eastward extension of the Qiangtang and Lhasa terranes: A Perspective from a conjugate strike-slip fault system in central Tibet, *Journal of Structural Geology*, submitted (2000).

Tran, H. D., Brotherton, M. S., Stanford, S. A., van Breugel, W., Dey, A., Stern, D., Antonucci, R., "A Polarimetric Search for Hidden Quasars in the Three Radio Selected Ultraluminous Infrared Galaxies," *Astrophys. J.* 516, 85 (1999).

Tran, H. D., Brotherton, M. S., Stanford, S. A., van Breugel, W., Dey, A., Stern, D., Antonucci, R. "A Polarimetric Search for Hidden Quasars in Three Radio-selected Ultraluminous Infrared Galaxies," *Astrophys. J.*, 516, 85T (1999).

van Breugel, Stern, D., Eisenhardt, P., Spinrad, H., Dawson, S., Dey, A., deVries, W., Stanford, S.A., "No Longer the Most Distant Known Galaxy," *Nature*, submitted.

van Breugel, W. J., "Highest redshift radio galaxies," *Proc. SPIE*, 4005, 83-94, "Discoveries and Research Prospects from 8- to 10-Meter-Class Telescopes," Jacqueline Bergeron, Ed. (2000).

van Breugel, W. , de Breuck, C. , Stanford, S.A. , Stern, D. , Rottgering, H., Miley, G., "A Radio Galaxy at Z = 5.19," *Astrophys. J. Lett.*, 518, L61 (1999).

van Breugel, W., "Monsters and babies from the FIRST / IRAS survey," *Astrophys. and Space Science*, 266, 23 (1999).

van der Tak, F., de Pater, I., Silva, A., Millan, R., " Variability in the Radio Brightness Distribution of Saturn," *Icarus*, 142, 125V (1999).

Veal, J. M., Snyder, L. E., Wright, M., Woodney, L. M., Palmer, P., Forster, J. R., de Pater, I., A'Hearn, M. F., Kuan, Y.-J., "An Interferometric Study of HCN in Comet Hale-Bopp (C/1995 O1)," *Astron. J.*,119, 1498V (2000).

Vidale, J.E., Dodge, D.A., Earle, P.S., "Slow differential rotation of the Earth's inner core indicated by temporal changes in scattering," *Nature*, 405, 445 (2000).

Wang, J., Heckman, T. M., Lehnert, M. D., "On the Structure and Morphology of the 'Diffuse Ionized Medium' in Star-forming Galaxies," *Astrophys. J.*, .515, 97W (1999).

Wang, J., Heckman, T. M., Lehnert, M. D., "Toward a Unified Model for the 'Diffuse Ionized Medium' in Normal and Starburst Galaxies," *Astrophys. J.*, .509, 93W (1998).

White, R. L., Becker, R. H., Gregg, M. D., Laurent-Muehleisen, S. A., Brotherton, M. S., Impey, C. D., Petry, C. E., Foltz, C. B., Chaffee, F. H., Richards, G. T., Oegerle, W. R., Helfand, D. J., McMahon, R. G., Cabanela, J. E., "The FIRST Bright Quasar Survey. II. 60 Nights and 1200 Spectra Later," *Astrophys. J. S.*, 126, 133 (2000).

White, R. L., Becker, R. H., Helfand, D. J., Gregg, M. D., "The FIRST Survey, version 1999 Jul (White+ 1999)," *VizieR On-line Data Catalog*: VIII/59

White, R.L., Becker, R.H., Helfand, D.J., and Gregg, M.D., "A Catalog of 1.4 GHz Radio Sources from the FIRST Survey," *Astrophys. J.*, 475, 479 (1997).

Willott, C. J., Rawlings, S., Blundell, K. M., Lacy, M.,, "The quasar fraction in low-frequency-selected complete samples and implications for unified schemes," *Mon. Not. R. Astron. Soc.*, 316, 449 (2000).

Wills, B. J., Laor, A., Brotherton, M. S., Wills, D., Wilkes, B. J., Ferland, G. J., Shang, Z., "The PG X-Ray QSO Sample: Links between the Ultraviolet-X-Ray Continuum and Emission Lines," *Astrophys. J.*, 515L, 53W (1999).

Wills, B. J., Brotherton, M. S., Laor, A., Wills, D., Wilkes, B. J., Ferland, G. J., "The PG X-ray QSO Sample: Links among X-ray, UV & Optical Spectra," *ASP Conf. Ser.*, 175, 241, Structure and Kinematics of Quasar Broad Line Regions, eds. C. M. Gaskell, W. N. Brandt, M. Dietrich, D. Dultzin-Hacyan, and M. Eracleous (1999).

Wizinowich, PActon, D. S., Shelton, C., Stomski, P., Gathright, J., Ho, K., Lupton, W., Tsubota, K., Lai, O., Max, C., Brase, J., An, J., Avicola, K., Olivier, S., Gavel, D., Macintosh, B., Ghez, A., Larkin, J., "First Light Adaptive Optics Images from the Keck II Telescope: A New Era of High Angular Resolution Imagery," *Pubs. Astron. Soc. Pac.*, 112, 315 (2000).

Wold, M., Lacy, M., Lilje, P. B., Serjeant, S., "Clustering of galaxies around radio quasars at 0.5<=z<=0.8," *Mon. Not. R. Astron. Soc.*, 316, 267 (2000).

Wold, M., Lacy, M., Lilje, P., Serjeant, S., "Cluster Environments around Quasars at 0. 5 <= z <= 0. 8," *ASP Conf. Ser.*, 200, 464, Clustering at High Redshift, eds. A. Mazure, O. Le Fèvre, and V. Le Brun (2000).

Yin, A., Harrison, T.M., "Geologic Evolution of the Himalayan-Tibetan orogen," *Journal of Annual Review of Earth and Planetary Sciences*, 28, 211 (2000).

Yin, An.. "Mode of Cenozoic east-west extension in Tibet suggests a common origin of rifts in Asia during the Indo-Asian collision," *Journal of Geophysical Research*,105, 745 (2000).

Yin, A., Kapp, P. A., Murphy, M. A., Harrison, T. M., Grove, M., Ding, L., Deng, X., and Wu, C., "Significant late Neogene east-west exten-

sion in northern Tibet:," *Geology*, 27, 787 (1999).

Zheng, W., Tsvetanov, Z. I., Schneider, D. P., Fan, X., Becker, R.H., Davis, M., White, R. L., Strauss, M. A., Anderson, J. E., Jr., Annis, J., Bahcall, N. A., Connolly, A. J., Csabai, I., Davidsen, A. F., Fukugita, M., Gunn, J. E., Heckman, T. M., Hennessy, G. S., Ivezic, Z., Knapp, G. R., Lupton, R. H., Peng, E., Szalay, A. S., Thakar, A. R., Yanny, B., York, D. G., "Five High-Redshift Quasars Discovered in Commissioning Imaging Data of the Sloan Digital Sky Survey," *Astron. J.*, 120, 1607 (2000).

Zijlstra, A. A., Minniti, D., "A Dwarf Irregular Galaxy at the Edge of the Local Group: Stellar Populations and Distance of IC 5152," *Astron. J.*, 117, 1743Z (1999).

Presentations 1999-2000

Alcock, C., Allsman, R.A., Alves, D.R., Axelrod, T.S., Becker, A.C., Bennett, D.P., Cook, K.H., Freeman, K.C., Geha, M., Griest, K., Lehner, M.J., Marshall, S.L., McNamara, B.J., Minniti, D., Nelson, C., Peterson, B.A., Popowski, P., Pratt, M.R., Quinn, P.J., Rodg, A.W., "The MACHO Project Sample of Galactic Bulge High-Amplitude Scuti Stars," *Pulsation Behavior and Stellar Properties Summit Conference*, Seattle, WA, July 29-31, 1999.

Alcock, C., Cook, K., Geha, M., Marshall, S. L., Popowski, P., Welch, D. L., Becker, A. C., Pratt, M., Stubbs, C. W., Tomaney, A. B., Axelrod, T. S., Drake, A. J., Freeman, K. C., Peterson, B. A., Griest, K., Vandehei, T., Allsman, R. A., Alves, D. R., Bennett, D. P., Lehner, M. J., Minniti, D., Sutherland, W., Quinn, P. J., MACHO Collaboration, "Identifying Microlensing Source Stars with HST and Difference Imaging," *Am. Astron. Soc. #195*, 48.03 (1999).

Alcock, C., Allsman, R., Alves, D., Axelrod, T., Becker, A. C., Bennett, D., Cook, K., Drake, A., Freeman, K., Griest, K., Lehner, M., Marshall, S., Minniti, D., Peterson, B., Pratt, M., Quinn, P., Rodgers, A., Stubbs, C., Sutherland, W., Tomaney, A., Vandehei, T., Welch, D., "Baryonic Dark Matter: The Results from Microlensing Surveys," *MACHO Summit Meeting*, Canberra, AUSTRALIA, August 21-28, 1998.

Alcock, C., Allsman, R., Alves, D., Axelrod, T., Becker, A. C., Bennett, D., Cook, K., Drake, A., Freeman, K., Griest, K., Lehner, M., Marshall, S., Minniti, D., Peterson, B., Pratt, M., Quinn, P., Rodgers, A., Stubbs, C., Sutherland, W., Tomaney, A., Vandehei, T., Welch, D., "Baryonic Dark Matter," I*nternational Conference on Neutrino Physics and Astrophysics*, Sudbury, Canada, June 2000.

Alves, D. R., Alcock, C., Allsman, R. A., Axelrod, T. S., Basu, A., Becker, A. C., Bennett, D. P., Cook, K. H., Drake, A. J., Freeman, K. C., Geha, M., Griest, K., King, L. J., Lehner, M. J., Marshall, S. L., Minniti, D., Peterson, B. A., Popowski, P., Pratt, M. R., Quinn, P. J., Rodgers, A. W., Stubbs, C. W., Sutherland, W., Tomaney, A., Vandehei, T., Welch, D. L., MACHO Collaboration, "The MACHO Project 9 Million Star Color-Magnitude Diagram of the Large Magellanic Cloud: Probing the LMC Disk," *Am. Astron. Soc. #193*, 108.01; Bull. Am. Astron. Soc., 30, 1414 (1998).

Arav, N., de Kool, M., Becker, R. H., Laurent-Muehleisen, S. A., White, R. L., Price, T., Gregg, M. D., "The Size of the Broad Absorption Line Region: Keck HIRES Observations of BALQSO FIRST J104459.6+365605," *Am. Astron. Soc. #195*, 18.05; Bull. Am. Astron. Soc., 31, 1400 (1999).

Becker, A. C., Alcock, C., Allsman, R. A., Alves, D., Axelrod, T. S., Bennett, D. P., Cook, K. H., Drake, A. J., Freeman, K. C., Geha, M., Griest, K., Lehner, M. J., Marshall, S. L., Minniti, D., Nelson, C. A., Peterson, B. A., Popowski, P., Pratt, M. R., Quinn, P. J., Rodgers, A. W., Stubbs, C. W., Sutherland, W., Tomaney, A. B., Vandehei, T., Welch, D. L., MACHO Collaboration, "The MACHO Project: Microlensing Results from 5.7 Years of LMC Observations," *Am. Astron. Soc. #195*, 48.02; Bull. Am. Astron. Soc., 31,1444 (1999).

Becker, R. H., Gregg, M. D., Laurent-Muehleisen, S., White, R. L., Brotherton, M., Helfand, D. J., "The Discovery of a FIRST Radio-loud FRII BAL Quasar," *Am. Astron. Soc. #195*, 17.02; Bull. Am. Astron. Soc., 31,1398 (1999).

Becker, R. H.; White, R. L.; Gregg, M. D.; Laurent-Muehleisen, S. A.; Brotherton, M. S.; Impey, C. D.; Petry, C. E.; Chaffee, F.; Richards, G.; Oegerle, W. R.; Helfand, D. J.; McMahon, R. G.; Cabanela, J. E.,"The FIRST Bright Quasar Survey. II. 60 Nights and 1200 Spectra Later," *Am. Astron. Soc. #193*, 107.02; Bull. Am. Astron. Soc., 30,1410 (1998).

Becker, A. C., Alcock, C., Allsman, R. A., Alves, D. R., Axelrod, T. S., Bennett, D. P., Cook, K. H., Drake, A. J., Freeman, K. C., Griest, K., King, L. J., Lehner, M. J., Marshall, S. L., Minniti, D., Peterson, B. A., Popowski, P., Pratt, M. R., Quinn, P. J., Rodgers, A. W., Stubbs, C. W., Sutherland, W., Tomaney, A., Vandehei, T., Welch, D. L., Baines, D., Brakel, A., Crook, B., Howard, J., Leach, T., McDowell, D., McKeown, S., Mitchell, J., Moreland, J., Pozza, E., Purcell, P., Ring, S., Salmon, A., Ward, K., Wyper, G., Heller, A., Kaspi, S., Kovo, O., Maoz, D., Retter, A., Rhie, S. H., Stetson, P., Walker, A., MACHO Collaboration, "Candidate Binary Microlensing Events from the MACHO Project," *Am. Astron. Soc. #193*, 108.02; Bull. Am. Astron. Soc., 30,1415 (1998).

Bennett, D. P., Alcock, C., Allsman, R. A., Alves, D., Axelrod, T. S., Becker, D., Cook, K. H., Crouch, A., Drake, A. D., Fragile, P. C., Freeman, K. C., Geha, M., Gray, J., Griest, K., Johnson, B. R., Lehner, M. J., Marshall, S. L., Messenger, B., Minniti, D., Nelson, C. A., Peterson, B. A., Popowski, P., Quinn, J. L., Quinn, P. J., Rhie, S. H., Stetson, P., Stubbs, C. W., Sutherland, W., Thomson, S., Tomaney, A. B., Vandehei, T., Welch, D., "Gravitational Microlensing Parallax Events: Evidence for Isolated Black Hole Stellar Remnants and White Dwarf MACHOs," *Am. Astron. Soc. #195*, 37.07; Bull. Am. Astron. Soc., 31,1422 (1999).

Bloch, J. J., Akerlof, C., Balsano, R., Barthelmy, S., Butterworth, P., Casperson, D., Cline, T., Fletcher, S., Frontera, F., Gisler, G., Heise, J., Hills, J., Kehoe, R., Lee, B., Marshall, S., McKay, T., Miller, R. S., Piro, L., Priedhorsky, W., Szymanski, J., Wren, J., ROTSE Team, "A Robotic System Discovers Contemporaneous Optical Radiation from a Gamma-Ray Burst, " *Am. Astron. Soc. #196*, 19.02 (2000).

Brotherton, M. S., van Breugel, W., Stanford, S. A., Smith, R. J., Boyle, B. J., Shanks, T., Croom, S. M., Miller, L., Filippenko, A. V., "A Spectacular Post-Starburst Quasar," *Am. Astron. Soc. #193*, 20.06; Bull. Am. Astron. Soc., 30,1280 (1998).

Bunker, A. J.; van Breugel, W. J. M., "The Hy-Redshift Universe: Galaxy Formation and Evolution at High Redshift," *Proc. of a conference held in Berkeley, CA*, June 21-24,1999.

Connaughton, V., Robinson, C. R., McCollough, M. L., Laurent-Muehleisen, S. A., "BATSE Observations of BL Lac Objects," BL Lac Phenomenon Conference, Turku, Finland, June 22-26, 1998.

Conselice, C., Bershady, M. A., Dickinson, M., Ferguson, H. C., Fruchter, A. S., Hanley, C., Lucas, R. A., Mack, J., Madau, P., Postman, M., Connolly, A., Papovich, C., Szalay, A., Eisenhardt, P., Elston, R. J., Giavalisco, M., Hook, R. N., Stanford, S. A., Steidel, C. C. , "Quantitative Morphology of the NICMOS Hubble Deep

Field," *Am. Astron. Soc. #193*, 75.12; Bull. Am. Astron. Soc., 30,1368 (1998).

Cote, P., West, M. J., Marzke, R. O., Minniti, D., "Globular Cluster Metallicity Distribution Functions: Multimodality as a Consequence of Intrinsic Processes and Capture," *Am. Astron. Soc. #194*, 14.06; Bull. Am. Astron. Soc., 31, 880 (1999).

de Breuck, C., van Breugel, W., Röttgering, H., Miley, G., Carilli, C. "The Highest Redshift Radio Galaxy Known in the Southern Hemisphere," *Proc. of the ESO/Australia Workshop*, "Looking Deep in the Southern Sky, " eds. Faffaella Morganti and Warrick J. Couch, held at Sydney, Australia, December 10-12, 1997.

de Breuck, C., van Breugel, W., Röttgering, H., Miley, G., Stanford, A. "Searches for High Redshift Radio Galaxies," *Proc. of the colloq., "The Most Distant Radio Galaxies*," Royal Netherlands Academy of Arts and Sciences, eds. H. J. A. Röttgering, P. N. Best, and M. D. Lehnert, held in Amsterdam, October 15-17, 1997.

de Pater, I., Roe, H., Macintosh, B., Gibbard, S., Max, C., Gavel, D., "Keck Adaptive Optics Imaging of Uranus and its Rings," *Am. Astron. Soc., DPS meeting #32*, 48.01 (2000).

de Pater, I., Brecht, S. H., "SL9 Impacts: Microwave Observations and Diffusive Shock Acceleration Models," *Am. Astron. Soc., DPS meeting #31*, 73.03 (1999).

Dey, A., Najita, J. R., Graham, J. R., Bennett, C. L., Cook, K. H., Wurtz, R., Macoy, N. H., Wickham, D. R., Hertel, R. J., Abrams, M. C., Carr, J., Morris, S. L., Villemaire, A., Wishnow, E., "Simulating the Performance of a Fourier Transform Imaging Spectrometer on NGST," *Am. Astron. Soc. #193*, 35.08; Bull. Am. Astron. Soc., 30, 1296 (1998).

Dickinson, M,, "A Complete NICMOS Map of the Hubble Deep Field North," *9th Annual October Astrophysics Conf.*, "After the Dark Ages: When Galaxies were Young (the Universe at $2 < z < 5$). eds. S. Holt and E. Smith, held in College Park, Maryland, October 12-14, 1998.

Dickinson, M., Ferguson, H. C., Fruchter, A. S., Hanley, C., Lucas, R. A., Mack, J., Madau, P., Postman, M., Connolly, A., Papovich, C., Szalay, A., Bershady, M. A., Conselice, C., Eisenhardt, P., Elston, R. J., Giavalisco, M., Hook, R. N., Stanford, S. A., Steidel, C. C., "A Complete NICMOS Map of the Hubble Deep Field (North)," *Am. Astron. Soc. #193*, 75.11; Bull. Am. Astron. Soc., 30, 1367 (1998).

Drake, A. J., Allsman, R. A., Axelrod, T. S., Freeman, K. C., Peterson, B. A., Alcock, C., Cook, K. H., Marshall, S. L., Minniti, D., Popowski, P., Becker, A. C., Stubbs, C. W., Tomaney, A., Bennett, D. P., King, L. J., Alves, D. R., Griest, K., Vandehei, T., Lehner, M. J., Pratt, M. R., Quinn, P. J., Sutherland, W., Welch, D. L., MACHO Collaboration, "Results from Difference Image Analysis of Galactic Microlensing by the MACHO Collaboration," *Am. Astron. Soc. #193*, 108.04 (1998).

Drinkwater, M. J., Phillipps, S. J., Gregg, M. D., Jones, J. B.,"Dwarf Remains Found in Fornax," *IAP 2000 meeting*, "Constructing the Universe with Clusters of Galaxies," eds.Florence Durret and Daniel Gerbal , Paris, France, July 2000.

Drinkwater, M. J., Sadler, E. M., Davies, J. I., Dickens, R. J., Gregg, M. D., Parker, Q. A., Phillipps, S., Smith, R. M., "A Complete 2dF Survey of Fornax," *Proc. of the ESO/Australia Workshop* "Looking Deep in the Southern Sky," eds. Faffaella Morganti and Warrick J. Couch held at Sydney, Australia, December 10-12, 1997.

Edmonds, P. D., Gilliland, R. L., Livio, M., Petro, L. D., van Hamme, W. V., Meylan, G., Minniti, D., Pryor, C., Phinney, E. S., Sams, B., Tinney, C. G., "HST observations of Cataclysmic Variables in the Globular Cluster 47 Tucanae," *Am. Astron. Soc. #193*, 101.04; Bull. Am. Astron. Soc., 30, 1399 (1998).

Erskine, D., Ge, J., "A Prototype Fringing Spectrograph for Sensitive Extra-solar Planet Searches and Astroseismology studies," *Am. Astron. Soc. #194*, 9.02; Bull. Am. Astron. Soc., 31, 837 (1999).

Fan, X., Strauss, M. A., Schneider, D. P., Gunn, J. E., Lupton, R. H., Anderson, S. F., Becker, R. H., Davis, M., Newman, J. A., Richards, G. T., White, R. L., SDSS Collaboration, "High-redshift Quasars from the Sloan Digital Sky Survey," *Am. Astron. Soc. #195*, 98.04; Bull. Am. Astron. Soc., 31, 1517 (1999).

Fux, R., Axelrod, T., Popowski, P., "The 3D structure of the Galactic bulge from the MACHO red clump stars," *IAU Symp. 205*, "Galaxies and their Constituents at the Highest Angular Resolution," Manchester, England, August 2000.

Ge, J., "World's first anisotropically etched silicon grisms at LLNL," *Colloquium at Pennsylvania State Astronomy & Astrophysics Dept*., University Park, Pennsylvania , December 6, 1999.

Ge, J., Erskine, D., "Searches for low mass extrasolar planets," *Signal and Imaging Sciences Workshop*, Livermore, CA November 11-12, 1999.

Ge, J., Ciarlo, D., Kuzmenko, P., Macintosh, B., Alcock, C., Cook, K., "Etched Silicon Gratings for NGST," *Proceedings of a conference held at Hyannis, MA*, September 13-16, 1999.

Ge, J., Ciarlo, D., Kuzmenko, P., Macintosh, B., Alcock, C., Cook, K., Gavel, D., Max, C., Lloyd, J., Graham, J., Liu M., Severson, S., "The first light of the world's first silicon grisms," *Am. Astron. Soc. #195*, 87.15; Bull. Am. Astron. Soc., 31, 1504 (1999).

Ge, J., Ciarlo, D., Kuzmenko, P., Alcock, C., Macintosh, B., Max, C., van Breugel, W., Cook, K., Gavel, D., Olivier, S., Friedman, H., Angel, R., Woolf, N., Lloyd-Hart, M., McCarthy, D., Fugate, R., Najita, J., Graham, J. R., "Next Generation Ground-based Very High Resolution Optical and Infrared Spectrographs for Extra-solar Planet Searches," *Am. Astron. Soc. #195*, 87.15; Bull. Am. Astron. Soc., 31, 1504 (1999).

Geha, M., Axelrod, T., Cook, K., Zaritsky, Z., Kobulnicky, H., MACHO Collaboration, "A Search for Quasars Behind the Magellanic Clouds," *Am. Astron. Soc. #194*, 73.13; Bull. Am. Astron. Soc., 31, 952 (1999).

Gibbard, S. G., Macintosh, B., Max, C., Roe, H., de Pater, I., Young, E. F., McKay, C. P., "The Surface of Titan from Adaptive Optics Observations," *24th meeting of the IAU*, Joint Discussion 12, "Highlights of Planetary Exploration from Space and from Earth," Manchester, England, August 2000.

Gibbard, S. G., Macintosh, B., Max, C.E., Roe, H., de Pater, I., Young, E. F., McKay, C.P., "Adaptive Optics Observations of Titan from the W.M. Keck Telescope," *Am. Astron. Soc., DPS Meeting #32*, 18.01 (2000).

Gibbard, S. G., Macintosh, B., Max, C. E., Gavel, D., de Pater, I., Roe, H., Young, E. F., McKay, C. P., "High-Resolution Infrared Speckle Imaging of Titan: Haze and Surface Properties," *Am. Astron. Soc., DPS Meeting #31*, 41.04 (1999).

Gibbard, S.G., Macintosh, B., Max, C.E., Gavel, D.,de Pater, I., "High-resolution speckle images of Neptune from the Kecktelescope," *Bull. Am. Astron. Soc.*, 30, 1099 (1998).

Gibson, B. K., T. S. Axelrod, M. E. Putman, "The Third Stromlo Symposium: The Galactic Halo," *ASP Conf. Ser.*, Australian Academy of Science, Canberra, AUSTRALIA, August 17-21, 1998.

Gilley, L., Harrison, T.M., Ryerson, F.J., Leloup, P.H., Wang, J., "Direct dating of left-lateral slip along the Red River Shear Zone," *15th Himalaya-Karakorum-Tibet Workshop*, Chengdu, China, 2000.

Gilley, L., Harrison, T.M., Yin, A., Leloup, P.H., Ryerson, F.J., and Wang, J., "Direct evidence for Late Oligocene sinistral slip along the Red River Shear Zone: further confirmation of the extrusion hypothesis," *EOS, Trans. Am. Geophys. Un. Fall meeting Supplement* (2000).

Graham, J. R., Macoy, N. H., Wickham, D. R., Hertel, R. J., Abrams, M. C., Bennett, C. L., Cook, K. H., Wurtz, R., Carr, J., Dey, A., Najita, J. R., Morris, S. L., Villemaire, A., Wishnow, E., "IFIRS: an Imaging Fourier Transform Spec-

trometer for NGST," *Am. Astron. Soc. #194*, 91.08; Bull. Am. Astron. Soc., 31, 984 (1999).

Goudfrooij, P., Alonso, M. V., Minniti, D., "The Globular Cluster System of NGC 1399," *IAU Symp. #186*, held at Kyoto, Japan, August 26-30, 1997. "Galaxy Interactions at Low and High Redshift," eds. J. E. Barnes, and D. B. Sanders, 1999.

Halpern, J. P., Mirabal, N., Eracleous, M., Becker, R. H., "Search for the Identification of 3EG J1835+5918: Evidence for a New Type of High-Energy Gamma-Ray Source?" *Am. Astron. Soc. #195*, 26.01; Bull. Am. Astron. Soc., 31, 1410 (1999).

Helfand, D. J., Becker, R. H., Gregg, M. D., Laurent-Muehleisen, S., Brotherton, M., White, R. L., "The FIRST Quasar Survey: Where's the Bimodality in Radio Loudness?" *Am. Astron. Soc. #195*, 17.01; Bull. Am. Astron. Soc., 31, 1398 (1999).

Helfand, D. J., Yadigaroglu, I. A., Berger, R., Postman, M., White, R. L., Lauer, T. R., Oegerle, W. R., Becker, R. H.,"Optical Identification of 700 Radio Sources in Sixteen Square Degrees of the FIRST Survey," *Am. Astron. Soc. #193*, 40.02; Bull. Am. Astron. Soc., 30, 1307 (1998).

Hjorth, J., Courbin, F., Cuadra, J., Minniti, D., "GRB 990712 optical decay: indication of bright host galaxy," *GRB Circular Network*, 389, 1 (1999).

King, I. R., Liebert, J. W., de Pater, I., "Observations of Hyron Spinrad," *ASP Conf. Proc.*, 193, "The Hy-Redshift Universe: Galaxy Formation and Evolution at High Redshift," eds. Andrew J. Bunker and Wil J. M. van Breugel Berkeley, CA, June 21-24, 1999.

King, L. J., Alcock, C., Allsman, R. A., Alves, D. R., Axelrod, T. S., Becker, A. C., Bennett, D. P., Cook, K. H., Drake, A. J., Freeman, K. C., Griest, K., Lehner, M. J., Marshall, S. L., Minniti, D., Peterson, B. A., Popowski, P., Pratt, M. R., Quinn, P. J., Rodgers, A. W., Stubbs, C. W., Sutherland, W., Tomaney, A., Vandehei, T., Welch, D. L., MACHO Collaboration "Identification on HST Images of Microlensed Stars from the MACHO Project," Am. *Astron. Soc. #193*; Bull. Am. Astron. Soc., 30, 1415 (1998).

Kong, Nishiizumi, K., Finkel, R. C. Caffee, M. W., "In situ cosmogenic 10Be and 26Al in olivine," *EOS, Trans. Am. Geophys. Union*, 80, F1166 (1999).

Kriss, G., Green, R., Brotherton, M., Davidsen, A., Friedman, S., Oegerle, W., Kaiser, M. E., Zheng, W., Hutchings, J., Shull, M., Woodgate, B., Koratkar, A., FUSE Science Team, "Initial FUSE Results on Active Galactic Nuclei," *Am. Astron. Soc. #195*, 6.07; Bull. Am. Astron. Soc., 31, 1376 (1999).

Kovács, G., Alcock, C., Allsman, R., Alves, D., Axelrod, T., Becker, A., Bennett, D., Clement, C., Cook, K. H., Drake, A., Freeman, K., Geha, M., Griest, K., Kurtz, D. W., Lehner, M., Marshall, S., Minniti, D., Nelson, C., Peterson, B., Popowski, P., Pratt, M., Quinn, P., Rodgers, A., Rowe, J., Stubbs, C., Sutherland, W., Tomaney, A., Vandehei, T., Welch, D. L., The MACHO Collaboration, "Frequency Analysis of the RRc Variables of the MACHO Database for the LMC," *IAU Colloq. #176*, "The Impact of Large-Scale Surveys on Pulsating Star Research," (2000)

Kulkarni, Varsha P., Bechtold, Jill, Ge, Jian, "Element Abundances in Damped Lyman-Alpha Quasar Absorbers," *Proc. of the ESO Workshop* "Chemical Evolution from Zero to High Redshift," eds. Jeremy R. Walsh, Michael R. Rosa held at Garching, Germany, October 14-16, 1998.

Kurtz, D. W., Alcock, C., Allsman, R. A., Alves, D., Axelrod, T. S., Becker, A. C., Bennett, D. P., Cook, K. H., Freeman, K. C., Griest, K., Lehner, M. J., Marshall, S. L., Minniti, D., Peterson, B. A., Pratt, M. R., Quinn, P. J., Rodgers, A. W., Stubbs, C. W., Sutherland, W., Tomaney, A., Welch, D. L., The MACHO Collaboration, "A New Look at the Blazhko Effect in RR Lyrae Stars with High-Quality Data from the MACHO Project," *IAU Colloq. #176*, "The

Impact of Large-Scale Surveys on Pulsating Star Research," (2000).

Lacy, M., "HST Imaging of Two z > 4 Radio Galaxies," *Proc. of a conference held in Berkeley, CA*, "The Hy-Redshift Universe: Galaxy Formation and Evolution at High Redshift," June 21-24,1999.

Laurent-Muehleisen, S. A., Becker, R. H., Gregg, M. D., Brotherton, M. S., White, R. L., Helfand, D. J. "The FBQS BL Lac Sample," *Am. Astron. Soc. #193*, 27.01; Bull. Am. Astron. Soc., 30, 1286 (1998).

Laurent-Muehleisen, S. A., Becker, R. H., Brinkmann, W., Seibert, J., Feigelson, E. D., Kollgaard, R. I., Schmidt, G., Smith, P., "Four new BL Lac Surveys: Sampling New Populations," *BL Lac Phenomenon Conference*, Turku, Finland, June 22-26, 1998.

Lehnert, M. D., "Superwinds and the nature of starburst galaxies," *IAU Colloq. #193* "Wolf-Rayet Phenomena in Massive Stars and Starburst Galaxies." eds. Karel A. van der Hucht, Gloria Koenigsberger, and Philippe R. J. Eenens held in Puerto Vallarta, Mexico, November 3-7, 1998.

Lehnert, M. D., "Host Galaxies of High Redshift Quasars and Their Relationship with Radio Galaxies," Proc. of the colloq.held at Royal Netherlands Academy of Arts and Sciences "The Most Distant Radio Galaxies," eds. H. J. A. Röttgering, P. N. Best, and M. D. Lehnert, held in Amsterdam, October 15-17, 1997.

Li, W. D., Modjaz, M., Halderson, E., Shefler, T., King, J. Y., Papenkova, M., Treffers, R. R., Filippenko, A. V., De Breuck, C. "Supernova 1998ef in UGC 646," *IAU Circ.*, 7032, 1 (1998).

Macintosh , B., "Practical Adaptive Optics," CFAO Workshop, Berkeley, CA (1999).

Macintosh, B., Max, C. E., Roe, H., Gibbard, S., Gavel, D., Acton, S., Lai, O., Wizinowich, P., de Pater, I., Ghez, A., Baines, K,., "Adaptive optics imaging of Neptune with the W.M. Keck telescope," *Am. Astron. Soc., DPS meeting #31*, 65.06; Bull. Am. Astron. Soc., 31, 1175 (1999).

Macintosh, B.,Gavel, D., Gibbard, S., Max, C.E., de Pater, I., Ghez, A., Eckart, M., "Infrared speckle imaging of Io's volcanoes with 60 km/pixel resolution," *EOS*, 79, F539 (1998).

Martin, S. C., Roe, H., de Pater, I., Macintosh, B., Gibbard, S., Max, C.E., Gavel, D., Brown, M., Ghez, A., "The Evolution of Cloud Features on Neptune over a 20-day time period," *Am. Astron. Soc., DPS meeting #32*, 10.17 (2000).

Martini, B.A., Silver, E.A., Potts, D.C., Pickles, W.L., "Geological and Geobotanical Studies of Long Valley Caldera, CA, USA Utilizing New 5m Hyperspectral Imagery," *Proc. of the IEEE International Geoscience and Remote Sensing Symposium*. July 2000.

Martini, B.A., Silver, E.A., Pickles, W.L., Potts, D.C., "Geological and geobotanical studies of Long Valley Caldera and Mammoth Mountain, CA utilizing new high-resolution hyperspectral imagery," *EOS, Trans. Am. Geophys. Union*. Fall 1999.

Martini, B.A., Cochran, S.A., Silver, E.A., Pickles, W.L., Potts, D.C., "Geological and geobotanical characterization of a hydrothermal system using hyperspectral imagery analysis, Long Valley Caldera, CA," *EOS, Trans. Am. Geophys. Union*, Fall 1998.

Mathur, S., Green, P., Otani, C., Shields, J., Hamann, F., Korista, K., Arav, N., DeKool, M., Elvis, M., Peterson, B., Crenshaw, M., Foltz, C., Goodrich, R., Hines, D., Mushotzky, R., Shlosman, I., van Breugel, W., Voit, M., Brotherton, M., "Deep ASCA Observation of a Typical BALQSO PG0946+301," *Am. Astron. Soc. #195*, 98.01; Bull. Am. Astron. Soc., 31, 1516 (1999).

Max, C., Macintosh, B., Gibbard, S., Roe, H., de Pater, I., Ghez, A., Acton, S., Wizinowich, P., Lai, O., "Adaptive Optics Imaging of Neptune and Titan with the W.M. Keck Telescope," *Am. Astron. Soc. #195*, 93.02; Bull. Am. Astron. Soc., 31, 1512 (1999).

McCarthy, D. W., Ge, J., Hinz, J. L., Finn, R. A., Low, F. J., Cheselka, M., Salvestrini, K., "A

Wide-Field Camera for 1-2.5mu M Imaging at the 2.3 and 6.5m Telescopes," *Am. Astron. Soc. #193*, 11.09; Bull. Am. Astron. Soc., 30, 1265 (1998).

Minniti, D., Alcock, C., Alves, D. R., Axelrod, T. S., Becker, A. C., Bennett, D. P., Cook, K. H., Freeman, K. C., Griest, K., Lehner, M. J., Marshall, S. L., Peterson, B. A., Quinn, P. J., Pratt, M. R., Rodgers, A. W., Stubbs, C. W., Sutherland, W., Tomaney, A., Vandehei, T., Welch, D., "Bulge Delta Scuti Stars in the MACHO Database," *IAU Symp. #189*, "Fundamental Stellar Properties: Confrontation between Theory and Observations," eds. T. R. Bedding, A. J. Booth and J. Davis, Kluwer, Dordrecht (1999).

Minniti, D., Rejkuba, M., Zijlstra, A. A., Alonso, M. V., Gregg, M., "Old Stars in Dwarf Irregular Galaxies: WLM and NGC3109," *Proc. of the ESO Symp., From Extrasolar Planets to Cosmology: The VLT Opening Symposium*, eds. Jacqueline Bergeron and Alvio Renzini.held at Antofagasta, Chile, March1-4, 1999.

Minniti, D. "Stellar Populations in Galaxies," IX *Latin American Regional IAU Meeting*, "Focal Points in Latin American Astronomy", held in Tonantzintla, Mexico, November 9-13, 1998.

Minniti, D., Alcock, C., Allsman, R., Alves, D., Axelrod, T., Becker, A. C., Bennett, D., Cook, K., Drake, A., Freeman, K., Griest, K., Lehner, M., Marshall, S., Peterson, B., Pratt, M., Quinn, P., Rodgers, A., Stubbs, C., Sutherland, W., Tomaney, A., Vandehei, T., Welch, D., "MACHO RR Lyrae in the Inner Halo and Bulge," M*ACHO Summit Meeting*, Canberra, AUSTRALIA, August 21-28, 1998.

Minniti, D., Alcock, C., Allsman, R., Alves, D., Axelrod, T., Becker, A. C., Bennett, D., Cook, K., Drake, A., Freeman, K., Griest, K., Lehner, M., Marshall, S., Peterson, B., Pratt, M., Quinn, P., Rodgers, A., Stubbs, C., Sutherland, W., Tomaney, A., Vandehei, T., Welch, D., "Variable Stars in the MACHO Bulge Database," *International Symp. on Astrophysics, Research and Science Education*, Castel Gandolfo, ITALY, June 13-21, 1998.

Nelson, C., Eggleton, P., "Conservative Case A Binaries," *Binary and Mulitiple Star Systems*, held in Bormio, Italy on June 2000.

Newberg, H. J., Richards, G. T., Fan, X., Laurent-Muehleisen, S. A., "Automated Selection of QSO Candidates from Multicolor Photometry in SDSS Passbands," *Am. Astron. Soc. #193*, 107.09; Bull. Am. Astron. Soc., 30, 1412 (1998).

Nilsson, K., Takalo, L. O., Pursimo, T., Sillanpää, A., Heidt, J., Wagner, S. J., Laurent-Muehleisen, S. A., Brinkmann, W. "Discovery of a blue arc near the BL Lacertae object RGB 1745+398 (poster)," *Proc. of the conference held in Turku, Astrophysics with the NOT*, held in Turku, Finland, August 12-15, 1998.

Owen, T. C., Mahaffy, P., Niemann, H. B., Atreya, S., Donahue, T., Bar-Nun, A., de Pater, I., "Low Temperature Condensates Brought Heavy Elements to Jupiter," *Am. Astron. Soc., DPS meeting #31*, 36.09 (1999).

Papovich, C., Dickinson, M., Ferguson, H. C., Fruchter, A. S., Hanley, C., Lucas, R. A., Mack, J., Madau, Piero, Postman, M., Connolly, A., Szalay, A., Bershady, M. A., Conselice, C., Eisenhardt, P., Elston, R. J., Giavalisco, M., Hook, R. N., Stanford, S. A., Steidel, C. C., "Galaxy Photometry in the HDF-0North from Combined NICMOS, WFPC2 and Ground-based data," *Am. Astron. Soc. #193*, 75.13; Bull. Am. Astron. Soc., 30, 1368 (1998).

Patience, J., Ghez, A. M., White, R. J., McCabe, C., Macintosh, B., Liu, M. C., Graham, J. R., Max, C. E., Gavel, D., Olivier, S., Rudy, R., Puetter, R., Matthews, K., Weinberger, A. J., "A High-Resolution Search for Stellar Companions to Stars with Planets," *Am. Astron. Soc. #193*, 97.08; Bull. Am. Astron. Soc., 30, 1392 (1998).

Pollard, K. R., Alcock, C., Allsman, R. A., Alves, D., Axelrod, T. S., Becker, A. C., Bennett, D. P., Cook, K. H., Freeman, K. C., Griest, K., Lehner, M. J., Marshall, S. L., Peterson, B. A., Pratt, M. R., Quinn, P. J., Sutherland, W., Tomaney, A., Welch, D. L., The MACHO Collaboration,

"RV Tauri Stars and Type II Cepheids in the Magellanic Clouds -- Results from the MACHO Database," *IAU Colloq. #176*, The Impact of Large-Scale Surveys on Pulsating Star Research (2000).

Pollitz, F.F., "VISCO1D Deformation Program," *SCEC Stress Triggering and Deformation Software Workshop*, Stanford University, California, September 8, 1999.

Pollitz, F.F., Burgmann, R., Kellogg, L., "Sinking mafic body in a reactivated lower crust: A mechanism for stress concentration at the New Madrid Seismic zone," *EOS, Trans. Am. Geophys. Union*, San Francisco, CA, December 7, 1999.

Popowski, P., "The Distance to the Large Magellanic Cloud," *IAU Colloq. #176*, The Impact of Large-Scale Surveys on Pulsating Star Research, (2000),

Proctor, D., "Use of Morphological Operators and Pattern Recognition Techniques for sorting the First Data," *Center for Advanced Signal and Image Sciences, 1999 Signal and Imaging Sciences Workshop*, LLNL, Livermore, CA, November 11-12, 1999.

Pursimo, T., Takalo, L. O., Sillanpää, A., Nilsson, K., Laurent-Muehleisen, S. A., Brinkmann, W., "RGB BL Lacs, a new sample of BL Lac objects," *Proc. of the OJ-94 Annual Meeting 1999*, Blazar Monitoring towards the Third Millennium, eds. C.M. Raiteri, M. Villata, L.O. Takalo, held in Torino, Italy, May 19-21, 1999.

Pursimo, T., Nilsson, K., Heinamaki, P., Katajainen, S., Sillanpaa, A., Takalo, L.O., Smith, P. S., Schmidt, G., Laurent-Muehleisen, S. A., Brinkmann, W., "Polarimetry on RGB BL Lacs," *Proc. of the conference held in Turku, Astrophysics with the NOT*, held in Turku, Finland, July 7-10, 1998.

Quinn, J. L., Alcock, C., Allsman, R. A., Alves, D., Axelrod, T. S., Becker, D., Bennett, D. P., Cook, K. H., Drake, A. D., Freeman, K. C., Geha, M., Griest, K., Lehner, M. J., Marshall, S. L., Minniti, D., Nelson, C. A., Peterson, B. A., Popowski, P., Quinn, P. J., Rhie, S. H., Stubbs, C. W., Sutherland, W., Tomaney, A. B., Vandehei, T., Welch, D. "Constraining the Parameters of Microlensing Black Hole Candidate MACHO-96-BLG-5," *Am. Astron. Soc. #195*, 37.08 (1999).

Rhie, S., Becker, A., Bennett, D., Calitz, J., Cook, K., Fragile, P., Johnson, B., Gurovich, S., Han, C., Hoffman, M., Laws, C., Martinez, P., Meintjes, P., Minniti, D., Park, S., Peterson, B., Quinn, J., "Microlensing Planet Search Project," *IAU Symp. #202*, Planetary Systems in the Universe, Manchester, England, August 2000.

Roe, H. G., de Pater, I., Gibbard, S.G., Macintosh, B., Max, C.E., McKay, C.P., "Near- and mid-Infrared Resolved Imaging of Titan's Atmosphere," *Bull. Am. Astron. Soc*, 32, 17.03 (2000).

Roe, H., Graham, J. R., de Pater, I., Gibbard, S., Macintosh, B., Max, C., Baines, K., Gilbert, A. M., McLean, I. S., Becklin, E. E., Figer, D. F., Larkin, J. E., Levenson, N. A., Teplitz, H. I., Wilcox, M. K., NIRSPEC Team, "Near-Infrared Spectroscopic Investigation of Neptune's Hazes and Storms at the Keck Telescope," *Am. Astron. Soc., DPS meeting #31*, 31.51 (1999).

Roe, H., Graham, J.R., de Pater, I., Baines, K., Gibbard, S., Macintosh, B., Max, C., NIRSPEC team, "Near-infrared spectroscopic investigation of Neptune's hazes and storms at the keck telescope," *Bull. Am. Astron. Soc*., 31, 1153 (1999).

Röttgering, H. J. A., Best, P. N., Lehnert, M. D., "The Most Distant Radio Galaxies," *Proc. of the Colloq., Royal Netherlands Academy of Arts and Science*s, The Most Distant Radio Galaxies,.Amsterdam, October 15-17, 1997.

Russell, S.A., Rodgers, A.J., Schwartz, S.Y., "Lithospheric structure of the Red Sea rift zone from complete waveform modeling," *EOS, Trans. Am. Geophys. Union*, 81, 834 (2000).

Ryutova, M. P., Tarbell, T. D., "Observation of Shocks in the Chromosphere and Transition

Region," *Am. Astron. Soc., SPD meeting #32*, 01.41 (2000).

Schilizzi, R. T., Gurvits, L. I., Miley, G. K., Bremer, M. A. R., Röttgering, H. J. A., Nan, R., Chambers, K. C., van Breugel, W. J. M., "VLBI observations of galaxies at high redshift," *Proc. of the colloq., "The Most Distant Radio Galaxies,"* Royal Netherlands Academy of Arts and Sciences, eds. H. J. A. Röttgering, P. N. Best, and M. D. Lehnert, held in Amsterdam, October 15-17, 1997.

Stanford, S. A., "Chandra Observations of z > 1 Clusters," *IAP 2000 meeting*, Constructing the Universe with Clusters of Galaxies, Paris, France, July 2000.

Stanford, S. A., "Galaxy Populations in High Redshift Clusters," *Proc. of the ESO Symp., From Extrasolar Planets to Cosmology: The VLT Opening Symposium*, held at Antofagasta, Chile, March 1-4, 1999.

Stanford, S. A., "Morphological Evolution in High Redshift Galaxy Clusters," *Proc. of a conference held in Berkeley,*The Hy-Redshift Universe: Galaxy Formation and Evolution at High Redshift, held in Berkeley, CA, June 21-24, 1999.

Stanford, S. A., "Elliptical Galaxies in High -z Clusters: How old are they?" The Birth of Galaxies, held in Blois, FRANCE, June 29-July 3, 1998.

Taylor, M.H., Yin, A., Kapp, P., D'Andrea, J., Harrison, T.M., Ryerson, F.J., Yong, Z., "The Mayer Kangri Rift and Transform System: Kinematics and Magnitude of Extension in Central Tibet," *AGU Fall Meeting*, 1999.

Tran, H. D., Brotherton, M. S., Stanford, S. A., van Breugel, W., "Hidden Quasars in Ultraluminous Infrared Galaxies," *IAU Symp. #194*, Byurakan, ARMENIA, August 17-21, 1998.

Tran, H. D., Brotherton, M. S., Stanford, S. A., van Breugel, W., Dey, A., Stern, D., Antonucci, R., "Hidden Quasars in Radio-Selected Ultraluminous Infrared Galaxies," *Am. Astron. Soc. #193*, 107.04; *Bull. Am. Astron. Soc*., 30, 1410 (1998).

van Breugel, W. J. M., De Breuck, C., Stanford, S. A., Stern, D., Rottgering, H., Miley, G. K., "The Most Distant AGN: A Radio Galaxy at Z = 5.19," *Am. Astron. Soc. #194*, 110.07 (1999).

van Breugel, W., Bland-Hawthorn, J. "Imaging the Universe in Three Dimensions: Astrophysics with Advanced Multi-Wavelength Imaging Devices," *An International Conference held under the Auspices of the Lawrence Livermore National Laboratory*, Walnut Creek, CA, March 29 - May 1, 1999.

van Breugel, W., "Monsters and Babies from the FIRST / IRAS Survey," *Ultraluminous Galaxies: Monsters or Babies?* held in Munich, GERMANY, Sept 20-25, 1998.

van Breugel, W., De Breuck, C., Stanford, S. A., Röttgering, H., Miley, G., Stern, D., Minniti, D., Carilli, C., "Ultra-Steep Spectrum Radio Galaxies at Hy Redshifts," *ASP Conf. Proc.*, 193, "The Hy-Redshift Universe: Galaxy Formation and Evolution at High Redshift," eds. Andrew J. Bunker and Wil J. M. van Breugel Berkeley, CA, June 21-24, 1999.

van Breugel, W., de Breuck, C., Röttgering, H., Miley, G., Stanford, A., "Very High Redshift Radio Galaxies," *Proc. of the ESO/Australia Workshop*, "Looking Deep in the Southern Sky, " eds. Faffaella Morganti and Warrick J. Couch, held in Sydney, Australia, December 10-12, 1997.

van Breugel, W., Stanford, A., Dey, A., Miley, G., Stern, D., Spinrad, H., Graham, J., McCarthy, P., "Induced star formation and morphological evolution in very high redshift radio galaxies," *Proc. of the colloq., "The Most Distant Radio Galaxies,"* Royal Netherlands Academy of Arts and Sciences, eds. H. J. A. Röttgering, P. N. Best, and M. D. Lehnert, held in Amsterdam, October 15-17, 1997.

Vidale, J., Dodge, D., Earle, "Inner-core scattering: a seismic phase that reveals fine-scale

structure and inner core rotation at roughly 0.1° per year," *AGU Fall Meeting*, 1999.

Wold, M., Lacy, M., Lilje, P. B., Serjeants, S., "Quasar environments at 0. 5 < z < 0. 8," *Proc. of the workshop held on La Palma*, The NOT in the 2000's, April 12-15, 2000.

Wood, P. R., Alcock, C., Allsman, R. A., Alves, D., Axelrod, T. S., Becker, A. C., Bennett, D. P., Cook, K. H., Drake, A. J., Freeman, K. C., Griest, K., King, L. J., Lehner, M. J., Marshall, S. L., Minniti, D., Peterson, B. A., Pratt, M. R., Quinn, P. J., Stubbs, C. W., Sutherland, W., Tomaney, A., Vandehei, T., Welch, D. L., "MACHO observations of LMC red giants: Mira and semi-regular pulsators, and contact and semi-detached binaries," *IAU Symp. 191*, Asymptotic Giant Branch Stars (1999).

Woodney, L. M., A'Hearn, M. F., de Pater, I., Forster, J. R., Kuan, Y.-J., Meier, R., Palmer, Patrick, Snyder, L. E., Veal, J. M., Wright, M. C. H., "Sulfur Chemistry in Comets Hale-Bopp and Hyakutake," *Am. Astron. Soc., DPS meeting #31*, 17.22 (1999).

Wurtz, R., Cook, K. H., Bennett, C. L., Bixler, J., Carr, D., Wishnow, E. H., "Ground-Based Demonstration of Imaging Fourier Transform Spectrometry and Techniques," *ASP Conf. Proc.*, 207, Next Generation Space Telescope Science and Technology, held at Hyannis, MA, September 13-16, 1999.

Wurtz, R., Abrams, M. C., Bennett, C. L., Bixler, J. V., Carr, D. J., Carr, J., Cook, K. H., Dey, A., Graham, J. R., Hertel, R. J., Macoy, N. H., Morris, S. L., NAstron. J.ita, J. R., Villemaire, A., Wickham, D. R., Wishnow, E., "First Observations with the LLNL Optical Imaging Fourier Transform Spectrometer," *Am. Astron. Soc. #194*, 91.01; *Bull. Am. Astron. Soc.*, 31, 983 (1999).

Yadigaroglu, I. A., Buchalter, A., Helfand, D. J., Becker, R. H., White, R. L, "Faint Optical Counterparts for Millijansky Radio Sources from the FIRST Survey," Am. Astron. Soc. #193, 40.01; *Bull. Am. Astron. Soc.*, 30, 1307 (1998).

Yanny, B., Newberg, H., Becker, R. H., Laurent-Muehleisen, S., Pier, J. R., Richards, G., Sloan Digital Sky Survey Collaboration, "Faint A stars as tracers of the structure of the Galactic Halo," *Am. Astron. Soc. #194*, 84.05; *Bull. Am. Astron. Soc.*, 31, 970 (1999).

Zirm, A., Dey, A., Dickinson, M., McCarthy, P. J., Eisenhardt, P., Djorgovski, S. G., Spinrad, H., Stanford, A., van Breugel, W., "NICMOS Imaging of High-Redshift Radio Galaxies," *Am. Astron. Soc. #193*, 107.10; *Bull. Am. Astron. Soc.*, 30, 1412 (1998).

Zirm, A., Dey, A., Dickinson, M., McCarthy, P. J., Eisenhardt, P., Djorgovski, S. G., Spinrad, H., Stanford, S. A., van Breugel, W., "NICMOS Imaging of High-Redshift Radio Galaxies," *ASP Conf. Proc.*, 193, "The Hy-Redshift Universe: Galaxy Formation and Evolution at High Redshift," eds. Andrew J. Bunker and Wil J. M. van Breugel Berkeley, CA, June 21-24, 1999.

Section VI. Fiscal Year 2001 IGPP–LLNL University Collaborative Research Program

Project No.	UC Campus	Campus Investigators	LLNL Collaborators	Project Title
01-AP006	Berkeley	I. De Pater J. Rice C. Liang	S. Marshall	Detection of Occultations
01-AP009	Berkeley	I. De Pater S. Martin H. Roe	S. Gibbard B. Macintosh	High Resolution Imaging and Spectroscopy of Neptune and Titan
01-AP014	Berkeley	J. Graham D. Ciarlo P. Kuzmenko J. Lloyd	B. Macintosh J. Ge	Development, Testing, and Application of Silicon Grisms for Infrared Astronomical Spectroscopy
01-AP015	Berkeley	H. Spinrad S. Dawson	W. van Breugel W. de Vries M. Lacy	A Census of Massive Galaxies at High Redshift
01-GS007	Berkeley	M. Richards J. Lynch	R. Ferencz	Finite Element Models of Crustal Stress in Strike slip Fault Zones: Applications to the San Andreas and Hayward Faults in N. California
01-GS008	Berkeley	B. Romanowicz L. Breger	S. Larsen	Seismic Modeling of Lateral Heterogeneity in the Vicinity of the CMB
01-GS016	Berkeley	J. Kirchner L. Glaser C. Riebe	R. Finkel	Rates of physical erosion and chemical weathering over 10-year and 10,000-year timescales
01-GS037	Berkeley	B. Ingram K. McKeagan J. Moran P. Weber	I. Hutcheon	Microchemical Determination of Isotopic Composition in Otoliths
01-GS038	Berkeley	R. Jeanloz W. Panero	I. Hutcheon	Metal-Silicate Partitioning at High Pressures
01-GS041	Berkeley	D. Depaolo M. Feineman	F. Ryerson I. Hutcheon	Trace element partitioning between clinopyroxene, feldspar, high pressure hydrous minerals and CO_2-H_2O fluids: Constraints on mantle and deep crustal metasomatism
01-AP011	Davis	R. Becker	W. van Breugel M. Gregg M. Lacy	A Radio Selected Sample of Active Galactic Nuclei

Project No.	UC Campus	Campus Investigators	LLNL Collaborators	Project Title
01-AP019	Los Angeles	B. Zuckerman D. Kaisler	B. Macintosh	Direct Detection of Massive Planetary Companions to Young Stars
01-GS017	Los Angeles	T. Harrison L. Gilley	F. Ryerson	Thermobarometry and Monazite Th-Pb Chronology of the Red River Zone: Implications for Indo-Asian Extrusion
01-GS022	Los Angeles	J. Vidale P. Earle F. Xu	D. Dodge	Inner-Core Scattering and Rotation
01-GS024	Los Angeles	A. Yin M. Taylor	F. Ryerson	Did Tibet Extrude Eastward Via Distributed Conjugate Strike-Slip Faulting During the Cenozoic Indo-Asian Collision?
01-GS001	Riverside	L. Owen P. Barnard J. Spencer	M. Caffee R. Finkel	Rates of landscape evolution in an active Himalayan valley: Gangotri, Garhwal Himalaya, Northern India
01-GS003	San Diego	P. Shearer H. Scott	J. Bhattacharyya	Investigation of Upper Mantle Seismic Attenuation Structure
01-GS020	San Diego	G. Masters C. Reif	M. Flanagan	Crust and Lithosphere Models for Global Monitoring of Regional Phases
01-GS025	Santa Barbara	R. Antonucci D. Whyssong	C. Max G. Canalizo W. de Vries	Adaptive Optics Obeservations of Active Galactic Nuclei and Quasars
01-GS021	Santa Barbara	J. Clark L. Rademacher	G. Hudson	The Impact of Chemical Weathering in Soils and Shallow Groundwater on Catchment Hydrochemistry
01-AP026	Santa Cruz	P. Guhathakurta M. Geha	K. Cook	Searching for Quasars in the MACHO Database
01-GS010	Santa Cruz	R. Anderson L. Perg	R. Finkel	Testing a provacative new age model of the Santa Cruz marine terraces: Is ^{10}Be and ^{26}Al dating of regressive marine sediments a valid technique?
01-GS036	Santa Cruz	Q. Williams H. Scott	F. Ryerson	Experimental Constraints on the Chemical Evolution of Icy Satellites: A renewal Proposal